PHOTOCHEMICAL AND PHOTOPHYSICAL STUDIES OF

DIBENZOYLMETHANATOBORON DIFLUORIDE

by

Shisen Wang

B.Sc., Jilin University (China), 1982

M.Sc., Dalian Institute of Chemical Physics, Chinese Academy of Sciences, 1985

THESIS SUBMITTED IN PARTIAL FULFILMENT OF THE REQUIREMENTS FOR THE

DEGREE OF DOCTOR OF PHILOSOPHY

in the Department

of

Chemistry

© Shisen Wang 1996

Simon Fraser University

November 1996

ISBN 0-612-17164-7

Canada

APPROVAL

Name: Shisen Wang

Degree: Ph.D. Chemistry

Title of Thesis: Photochemical and Photophysical Studies of
                 Dibenzoylmethanatoboron Difluoride

Examining Committee:

Chairperson: Dr. Fred Einstein

Dr. Y. L. Chow, Professor
Senior Supervisor

Dr. S. Wolfe, Professor

Dr. S. Holdcroft, Associate Professor

Dr. A. Bennet, Assistant Professor
Internal Examiner

Dr. Cornelia Bohne, Assistant Professor
External Examiner
Department of Chemistry
University of Victoria

Date Approved: Nov 5, 1996

ii

PARTIAL COPYRIGHT LICENSE

I hereby grant to Simon Fraser University the right to lend my thesis, project or extended essay (the title of which is shown below) to users of the Simon Fraser University Library, and to make partial or single copies only for such users or in response to a request from the library of any other university, or other educational institution, on its own behalf or for one of its users. I further agree that permission for multiple copying of this work for scholarly purposes may be granted by me or the Dean of Graduate Studies. It is understood that copying or publication of this work for financial gain shall not be allowed without my written permission.

Title of Thesis/Project/Extended Essay

Photochemical and Photophysical Studies of

Dibenzoylmethanatoboron Difluoride.

Author:_
(signature)

SHISEN WANG.

(name)

Nov. 5, 1996

(date)

Abstract

Dibenzoylmethanatoboron difluoride (DBMBF$_2$), as an electron acceptor sensitizer, exhibits a variety of photoreactions from its singlet excited state.

Studies were undertaken on the photoreactions of DBMBF$_2$ with electron-rich cyclic dienes or vinyl ethers and with electron-deficient α,β-unsaturated ketones or esters. In most cases, photocycloaddition of DBMBF$_2$ to the olefin was regioselective to yield the head-to-head orientation, and stereoselective to give the stereoisomer having a *cis*-configuration for its side chains. In the quenching of DBMBF$_2$ fluorescence, the reactivities of olefins increase with electron donating ability and follow: simple olefin $\leq$ non-conjugated cyclic diene < conjugated cyclic diene. However in acetonitrile, the adduct quantum yield of DBMBF$_2$ photoreactions decreases along the same sequence: cyclooctene ($\Phi_A = 0.4$) > 1,5-cyclooctadiene ($\Phi_A \sim 0.2$) >> 1,3-cyclooctadiene ($\Phi_A \sim 0$). This order is attributed to the increased charge transfer (CT) character of DBMBF$_2$-olefin exciplexes, proposed as the precursor of the cycloaddition product.

Solvent effects on the photoreaction of DBMBF$_2$ with electron-rich olefins were examined to test for the formation of exciplex and its polar nature. In the polar solvent acetonitrile, the singlet excited DBMBF$_2$ reacted with 1,3-cyclohexadiene or phenyl vinyl ether to generate cation radicals which then dimerized. With solvents of decreasing polarity, the dimerization was gradually superseded by the cycloaddition reaction of DBMBF$_2$ with the olefin. A smooth correlation of the adduct quantum yield was found with the empirical solvent polarity E$_T$(30), through the solvent range from acetonitrile to xylene. As an interpretation, the DBMBF$_2$-olefin exciplex would respond to the changes in

the solvent polarity by differentially partitioning among ionic dissociation, adduct formation, and decay to starting materials.

The formation of DBMBF$_2$ excimer promotes photocycloaddition of DBMBF$_2$ to electron-rich olefins, which showed a DBMBF$_2$ concentration effect in non-aromatic solvents. With cyclic dienes, the reaction follows a dual pathway involving both excited DBMBF$_2$ monomer and excimer. With vinyl ethers, the excimer reaction predominates. However in aromatic solvents, the singlet excited DBMBF$_2$ converts to an emissive exciplex with the ground state solvent molecule. In benzene for example, the DBMBF$_2$-benzene exciplex is the principal species which reacts with olefins to form adducts. A very efficient Diels-Alder dimerization of 1,3-cyclohexadiene ($\Phi_D = 0.6$) was found to be cosensitized by the DBMBF$_2$-xylene exciplex in acetonitrile. Two pathways are proposed for the diene radical cation initiation: (1) an ionic dissociation of the DBMBF$_2$-xylene exciplex, followed by an exothermic electron transfer from the diene to the xylene radical cation; or (2) an electron transfer mediated by a triplex intermediate, *(DBMBF$_2$-xylene-diene).

To

my parents

ACKNOWLEDGEMENT

CONTENTS

LIST OF TABLES

LIST OF FIGURES

Abbreviations and Symbols

*A	excited state acceptor
AAH	acetylacetone
$AABF_2$	acetylacetonatoboron difluoride
$BABF_2$	benzoylacetonatoboron difluoride
CD	2-cyclododecenone
CHD	1,3-cyclohexadiene
CH	2-cyclohexenone
CI	chemical ionization (in mass spectrometry)
CIDNP	chemically induced dynamic nuclear polarization
CIP	contact ion radical pair
CO	2-cyclooctenone
COD	cyclooctadiene
COSY	two-dimensional correlation NMR spectroscopy
CP	2-cyclopentenone
CT	charge transfer
D	ground state electron donor
DBM	dibenzoylmethane
$DBMBF_2$	dibenzoylmethanatoboron difluoride
DEPT	distortionless enhancement by polarization transfer (in ^{13}C NMR spectroscopy)
DHP	3,4-dihydro-2H-pyran
DMSO	dimethyl sulfoxide
EA	electron affinity

EI	electron impact ionization (in mass spectrometry)
E_{ox}	oxidation potential
E_{red}	reduction potential
E_S	singlet excited state energy
E_T	triplet excited state energy
$E_T(30)$	an empirical parameter of solvent polarity
EVE	ethyl vinyl ether
FID	flame ionization detector (for GC)
FI	free ion radical
HH	head-to-head
HT	head-to-tail
I	intensity of fluorescence emission
IP	ionization potential
IVE	isobutyl vinyl ether
k_q	quenching rate constant
K_{SV}	Stern-Volmer quenching constant with the superscript:

      m   for quenching excited monomer species,

      ex   for quenching excimer or exciplex species,

      y   for monitoring product quantum yield.

MMA	methyl methacrylate
$MBDBF_2$	4-*tert*-butyl-4'-methoxydibenzoylmethanatoboron difluoride
MO	mesityl oxide
NBD	norbornadiene
PET	photoinduced electron transfer
PVE	phenyl vinyl ether

Q	quencher
QC	quadricyclane
R	arene compound
R_f	the "ratic-to-front" constant or "retention factor" in Thin - Layer Chromatography
RT	retention time (on GC analysis)
SCE	saturated calomel electrode
SSIP	solvent separated ion radical pair
THF	tetrahydrofuran
THP	tetrahydropyran
ε	dielectric constant of solvent
ε_A	molar absorption coefficient
ΔG_{ET}	free energy change for an electron transfer process
δ	chemical shift in NMR spectroscopy
μ	dipole moment
τ	lifetime of an excited species
λ_{ex}	wavelength of excitation light beam
λ_{moni}	wavelength where to monitor the emission intensity
Φ	quantum yield with the subscript:

A	for addition product formation,
D	for dimer formation,
f	for fluorescence emission,
isc	for intersystem crossing.

Compound Catalog

1

2

3

4

5

6

7

8

9

10

11

12

13   OPh

14   OPh / OPh

15   OPh / OPh

16   PhO, O, Ph, Ph, O

17

18

19

20

21

22

23

24

25

26

27

28

29

30

31

32

33

34

35

36 CH₃CH=CHCN

37

38 CN
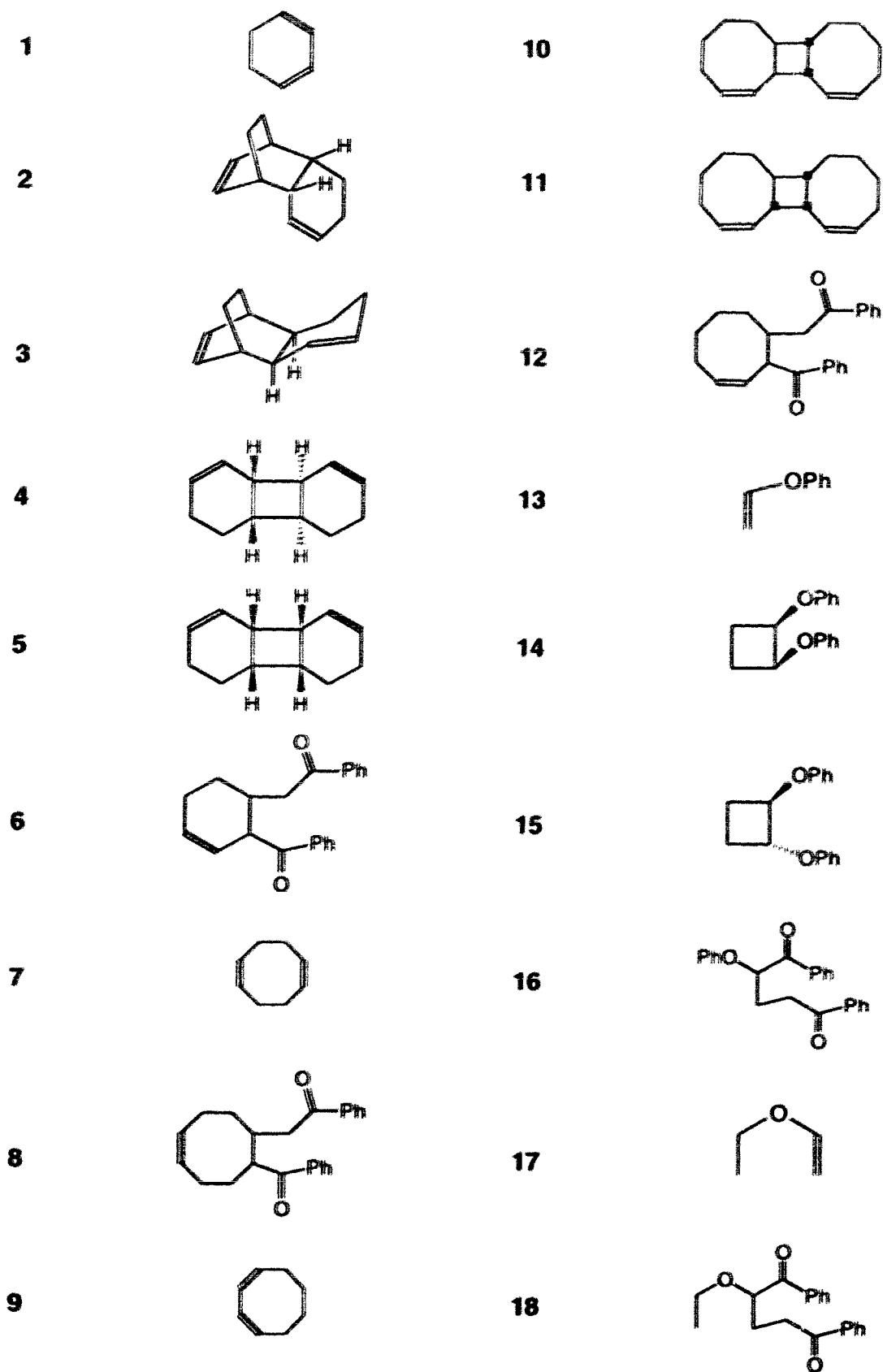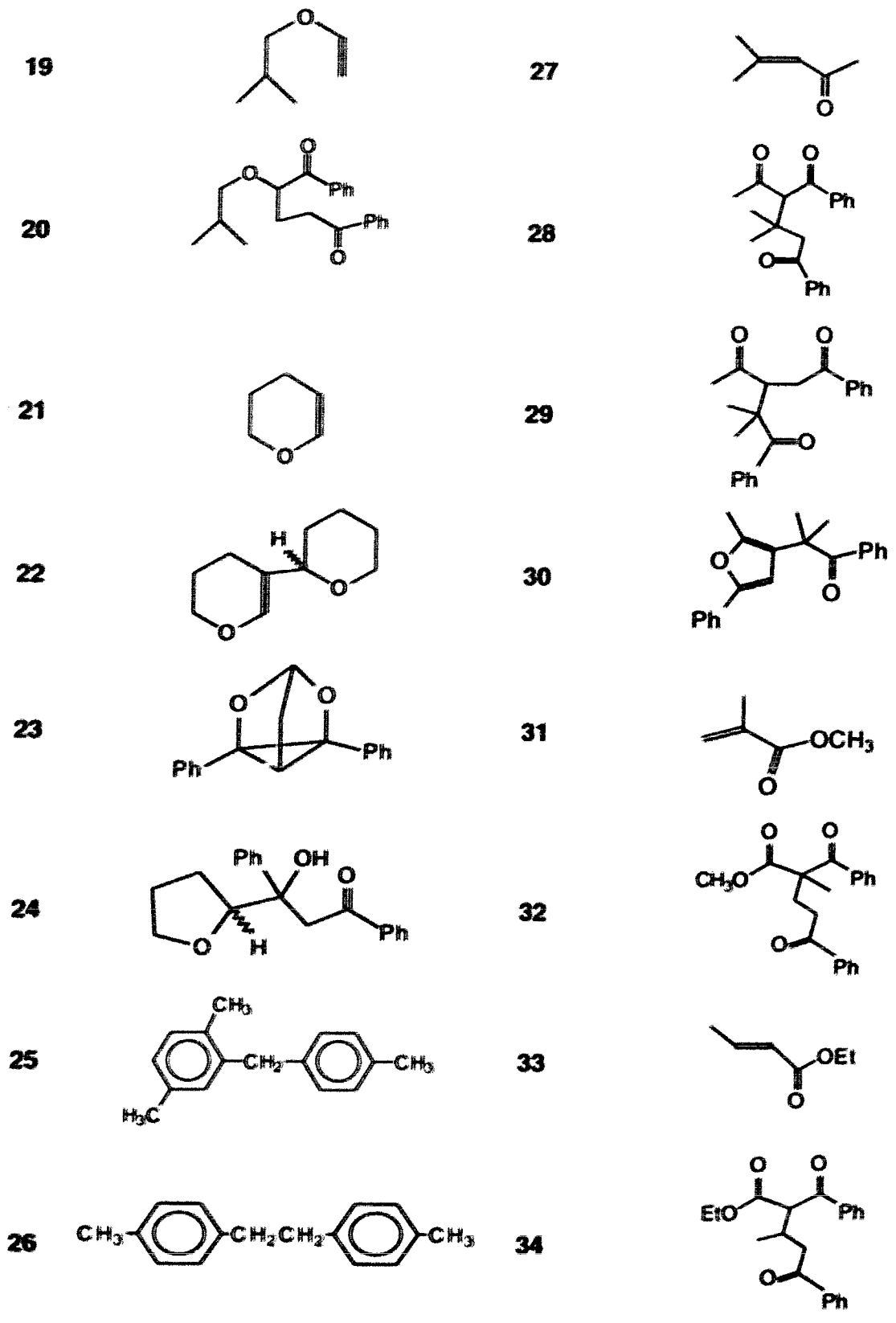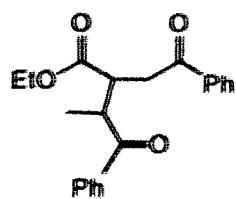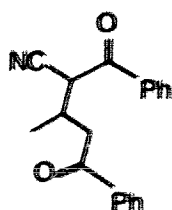
39
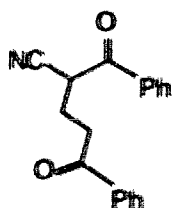
40
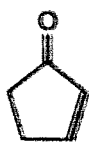
41
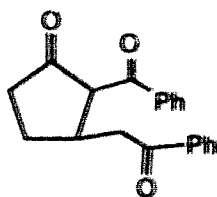
42

43
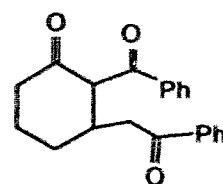
44
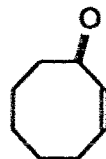
45
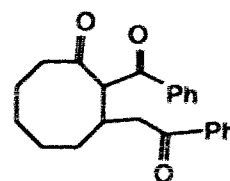
46
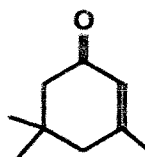
47
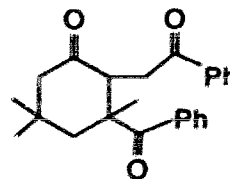
48
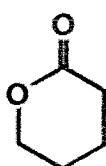
49
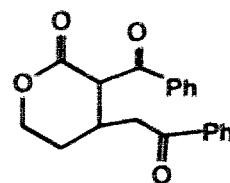
50
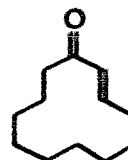
51
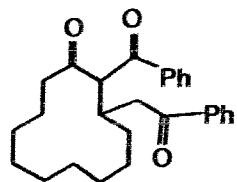
52
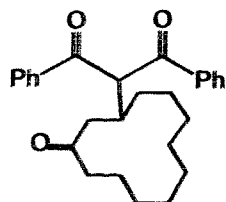
53
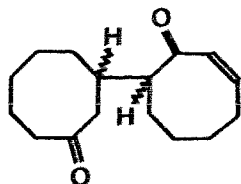
54
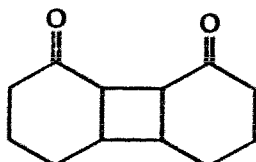
55
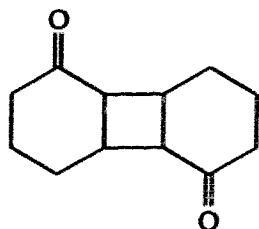
56
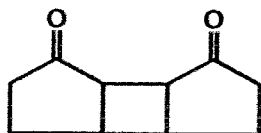
57
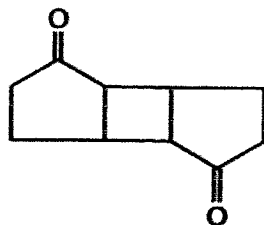
CHAPTER ONE

INTRODUCTION

1.1 Photoinduced Electron Transfer

Photoinduced electron transfer (PET) is well recognized as a fundamental process in chemistry and has attracted tremendous interest of chemists from many fields.[1] Photoexcitation of either an acceptor or a donor molecule will promote an electron transition from a HOMO to a LUMO orbital. The electronically excited molecule thus formed has an enhanced redox reactivity as both a better donor and acceptor, which can be visualized in the HOMO - LUMO picture shown in Fig. 1.1.[2] In the ground state, electron transfer from the $HOMO_D$ of a donor to the $LUMO_A$ of an acceptor is an endothermic process. However, when the acceptor molecule is in an excited state, electron transfer from the $HOMO_D$ to the half-filled $HOMO_A$ is energetically feasible (Fig. 1.1). Therefore, upon photoexcitation, electron transfer between donor and acceptor molecules occurs more easily than in their ground states. The driving force for the electron transfer is provided by light absorption.

For a bimolecular electron transfer between two ground state molecules in the gas phase, the free energy change is estimated by:

$$\Delta G_{ET} = IP_D - EA_A \qquad \text{(Eq. 1.1)}$$

where IP_D is the ionization potential of the donor and EA_A is the electron affinity of the acceptor molecule. When the acceptor molecule is an excited state species, the free energy change of electron transfer can be estimated based on the simplified MO diagram (Fig. 1.1),[2, 3] where $\Delta G_{ET} = IP_D - EA_{A^*}$ and $EA_{A^*} = EA_A + E_{A^*}$

thus we have: $\qquad \Delta G_{ET} = (IP_D - EA_A) - E_{A^*} \qquad \text{(Eq. 1.2)}$

In Eq. 1.2, E_{A^*} is the transition energy from $HOMO_A$ to $LUMO_A$ of the acceptor, and
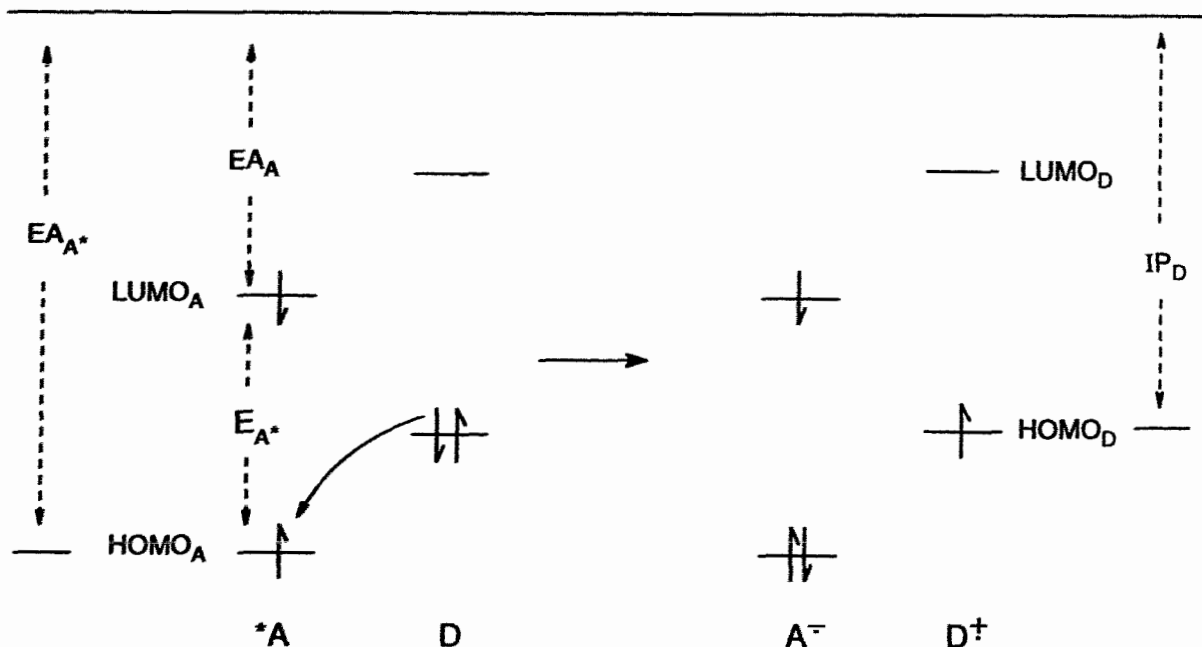
Fig. 1.1 A simple MO diagram for electron transfer from a donor (D)
to a singlet excited acceptor (*A)

the term $(IP_D - EA_A)$ is the energy stored in the radical ions $A^{-\cdot}$ and $D^{+\cdot}$. If the excitation

energy of the acceptor molecule $(E_{A\cdot})$ exceeds the energy stored in the radical ions, then

the electron transfer from D to A* should occur.

In solution, the free energy for the bimolecular PET process must include the

solvation energies $(\Delta G_{D^+}^{sol} + \Delta G_{A^-}^{sol})$ and the energy of Coulombic interaction $(e^2/\varepsilon r)$

between the cation $(D^{+\cdot})$ and the anion $(A^{-\cdot})$ as shown in Eq. 1.2a:[2]

$$\Delta G_{ET} = (IP_D - EA_A) + (\Delta G_{D^+}^{sol} + \Delta G_{A^-}^{sol}) - E_{A\cdot} - e^2/\varepsilon r \qquad \text{(Eq. 1.2a)}$$

$$E_D^{ox} - E_A^{red} = (IP_D - EA_A) + (\Delta G_{D^+}^{sol} + \Delta G_{A^-}^{sol}) \qquad \text{(Eq. 1.3)}$$

As the ionization potential and electron affinity are related to the redox potential

according to Eq. 1.3,[4] combining Eq. 1.3 into Eq. 1.2a gives the Rehm - Weller equation

for the free energy ΔG_{ET} of solvent separated radical ion pair formation in a solvent of

$$A + D \xrightarrow{\ h\nu\ } A^{-\cdot} \cdots\cdots D^{+\cdot}$$

$$\Delta G_{ET} = (E_D^{ox} - E_A^{red}) - E_{A\cdot} - e^2/\varepsilon r \qquad\qquad (Eq.\ 1.4)$$
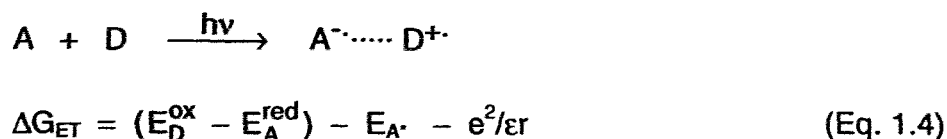
dielectric constant ε (Eq. 1.4).[5] Using the redox potentials determined in acetonitrile as

a reference, the free energy ΔG_{ET} of a PET process in various solvents can also be

estimated by Eq. 1.5:[6, 4, 7]

$$\Delta G_{ET}\ (eV) = (E_D^{ox} - E_A^{red})_{CH_3CN} - E_{A\cdot} + \Delta E_{coul} \qquad\qquad (Eq.\ 1.5)$$

$$\text{where:}\quad \Delta E_{coul}\ (eV) = \frac{e^2 N}{4\pi\varepsilon_o r}\left(\frac{1}{\varepsilon} - \frac{2}{37.5}\right)\frac{1}{F} = 2.058\left(\frac{1}{\varepsilon} - \frac{2}{37.5}\right)$$

In Eq. 1.5, $(E_D^{ox} - E_A^{red})_{CH_3CN}$ is the difference between the oxidation potential of the

donor and the reduction potential of the acceptor measured in acetonitrile; ΔE_{coul} is the

free energy of solvation and Coulombic interaction for bringing the cation and anion to

the encounter distance $r = 7$ Å in a solvent with dielectric constant ε,[4, 6] $\varepsilon_o = 8.854 \times 10^{-12}$

$CV^{-1}m^{-1}$, $N = 6.023 \times 10^{23}$ mole^{-1}, $F = 96489$ C and $e = 1.602 \times 10^{-19}$ C. Based on Rehm

- Weller equation, the direction and energetics of electron transfer, from a ground state

donor molecule to an excited state acceptor, can be predicted from their redox

potentials, excitation energy and solvent polarity.

1.2 Radical Ion Pair and Exciplex

There are a variety of reactive intermediates involved in the course of a

photoinduced bimolecular electron transfer reaction. A complete electron transfer will

lead to the formation of radical ion pairs, but when a partial electron transfer occurs, an

excited molecular complex, or exciplex, can be formed. The first observed exciplex was

reported in 1963 by Leonhardt and Weller,[8] in the fluorescence quenching of excited

arenes by arylamines. Since then, many other exciplexes have been found and shown

to be key intermediates in PET processes.[9]

An exciplex is defined as an excited molecular complex of definite stoichiometry

that is dissociated or weakly associated in its ground state.[3] Experimentally, the

spectroscopic evidence of exciplex formation is the observation of a structureless

emission spectrum which (i) occurs at the long wavelength side of the absorption spectra

from both acceptor (A) and donor (D), (ii) does not correspond to the individual emission

spectrum of either A or D, and (iii) is concentration dependent. If an exciplex is

dominated by its locally excited configuration (*AD), then the vibrational structure of *A

does appear in the exciplex emission spectrum.[10]

The driving force of exciplex formation arises from a net stabilization upon the

MO interactions between the excited state acceptor (*A) and the ground state donor (D)

as shown in Fig. 1.2. The exciplex is symbolized as $A^{\delta-}D^{\delta+}$, which indicates that the
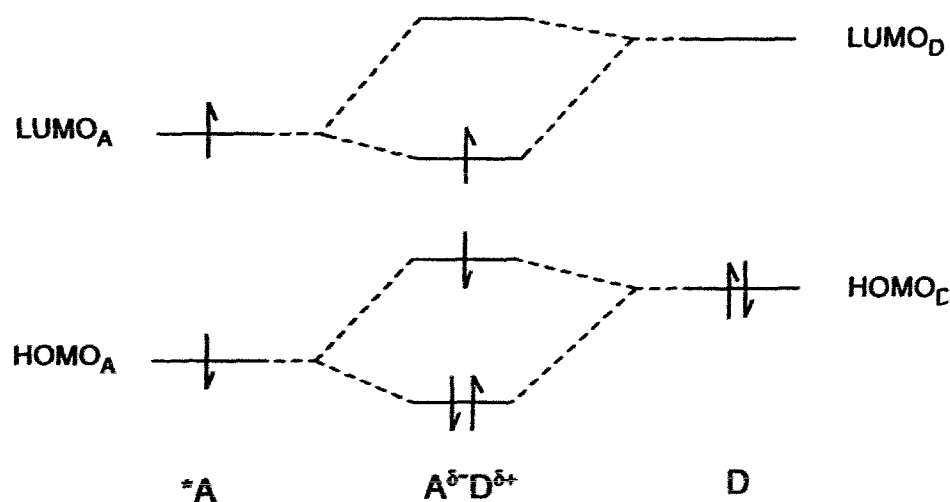
Fig. 1.2 A simple MO diagram for the exciplex formation between the singlet
excited electron acceptor (*A) and the ground state donor (D).

acceptor component in the exciplex has gained more electron density. The stability of the exciplex can also be briefly described in the resonance formulation:[11]

$$^*AD \longleftrightarrow A^-D^+$$
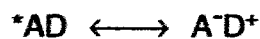
$$\Psi = c_1 \Psi(^*AD) + c_2 \Psi(A^-D^+) \qquad (Eq. 1.6)$$

In Eq. 1.6, $^*AD$ refers to the locally excited configuration and A^-D^+ represents the charge transfer configuration. The weighting of the charge transfer (CT) configuration should determine the CT character of the exciplex. Thus the wave function of Eq. 1.6 will correspond to a non-polar exciplex for $c_1 > c_2$, a polar exciplex for $c_1 < c_2$, and in the extreme case $c_1 \ll c_2$, the exciplex becomes a contact ion pair. The extent of CT character can be affected by solvent polarity.[12] For example, when the polarity of solvent is increased, the exciplex CT character should be promoted, causing the fluorescence quantum yield and lifetime of a polar exciplex to decrease.[13] The emission maximum of an exciplex also shifts to longer wavelength from nonpolar to polar solvents. By measuring these red-shifts of exciplex emission, the dipole moment of the exciplex can be estimated.[14, 15]

The intermediacy of an exciplex in photoreactions was first demonstrated by Caldwell.[16] It was observed that the exciplex emission of 9-cyanophenathrene-anethole and their corresponding photocycloaddition were equally quenched by added quenchers. This clearly demonstrated that the emitting exciplex is indeed the precursor for the related cycloadduct formation.

Further studies on photoreactions of donor-acceptor cycloaddition via an exciplex showed that an increase in the exciplex CT extent generally impedes the process of cycloaddition.[12] For example, observations of the decrease in adduct quantum yields were reported when either a stronger acceptor or stronger donor was used in the

photocycloaddition.[17] The decrease of adduct quantum yields with increasing solvent polarity was also observed where a polar exciplex was involved.[18] These phenomena suggest that the donor-acceptor cycloaddition is inherently a non-ionic process,[12] largely attributed to the local excited configuration (*AD) of the exciplex.

In studying the PET reactions of cyanoarenes with alkylbenzenes, Gould and Farid have proposed an overall mechanistic scheme covering radical ion pairs and exciplex intermediates (Scheme 1.1).[19] In Scheme 1.1, *A(S)D is the encounter

Scheme 1.1:

$$R_{DA} \sim 3.5 \, \text{Å} \qquad 6 \sim 8 \, \text{Å} \qquad > 8 \, \text{Å}$$
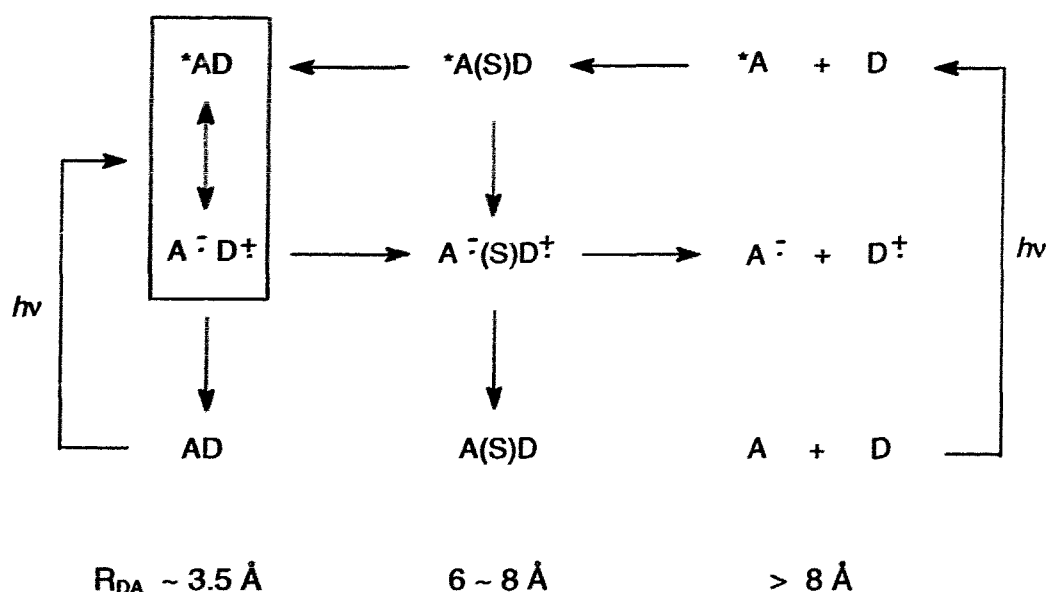
complex, $A^{-}D^{+\cdot}$ is the contact radical ion pair, $A^{-\cdot}(S)D^{+\cdot}$ is the solvent separated ion pair (SSIP), AD is the ground state complex and R_{DA} is the separation distance between molecules A and D which increases from left to right. According to this scheme, diffusional quenching of excited state acceptor (*A) by a donor molecule (D) primarily forms *A(S)D. Electron transfer then occurs by two pathways: (i) the exciplex formation and (ii) the formation of $A^{-\cdot}(S)D^{+\cdot}$ directly from *A(S)D. The importance of each pathway was evaluated by determining efficiencies of exciplex formation. The results suggested

that, for a complete mechanism of these PET reactions, the intermediacy of exciplex must be taken into account even in polar solvents.[10]

Since the electronic structure of an exciplex can be described by charge transfer and locally excited configurations, the extent of charge transfer determines the type of intermediates, and the intermediate in turn determines the pathways of reactions.[20] In defining the mechanism of PET reactions, one of the challenges is to determine what intermediates are involved and which pathways they proceed. Searching for answers to these questions is essential for elucidation of the electron transfer mechanism of excited state molecules.

1.3 Photocycloadditions of Electron-Rich Olefins via Radical Ion Pairs and Exciplexes

One of the earliest photoreactions of olefins is the alkene-enone [2+2]-cycloaddition, and this type of photoreaction is best known now in the synthesis of cyclobutane rings.[21] The relevant mechanistic aspects and synthetic applications have been widely reviewed in literature.[21, 22] Between the 1950's to the 1970's, the discovery of excited molecular complexes (excimer / exciplex) stimulated extensive research on those excited species for photophysics and photochemistry.[8, 23] As a result of those efforts, PET induced reactions of olefins have emerged to be a new field in organic photochemistry.[12]

The PET reactions of olefins can be grouped in two categories according to the chemical role of the excited state molecule.[12, 24] The first group comprises the PET reactions, such as photoisomerization,[25] cation radical [2+2] dimerization[26] and Diels-Alder dimerization,[27] which often use an electron acceptor sensitizer. The excited acceptor molecule initiates the electron transfer reaction of ground state olefins, and the

7

acceptor itself is not consumed in the course of reactions. In the second group, the

excited molecule undergoes bimolecular chemical reactions via an exciplex to give a

donor - acceptor addition.[16]

In section 1.3.1, the [2+2] cyclodimerization of N-vinylcarbazole and phenyl vinyl

ether will be introduced first, followed by Diels-Alder dimerization of 1,3-cyclohexadiene.

The radical cation intermediacy in these reactions will be the focus of discussion. The

photocycloaddition of electron-rich olefins, which proceeds via an exciplex intermediate,

will be briefly reviewed in section 1.3.2.

1.3.1 The Sensitized Dimerization of Electron-Rich Olefins

The [2+2] dimerization of electron-rich olefins under PET conditions is often

found to involve a radical cation as intermediate. A general mechanism for the cation

radical reactions has been proposed as follow:[28, 20, 24b]

Scheme 1.2:
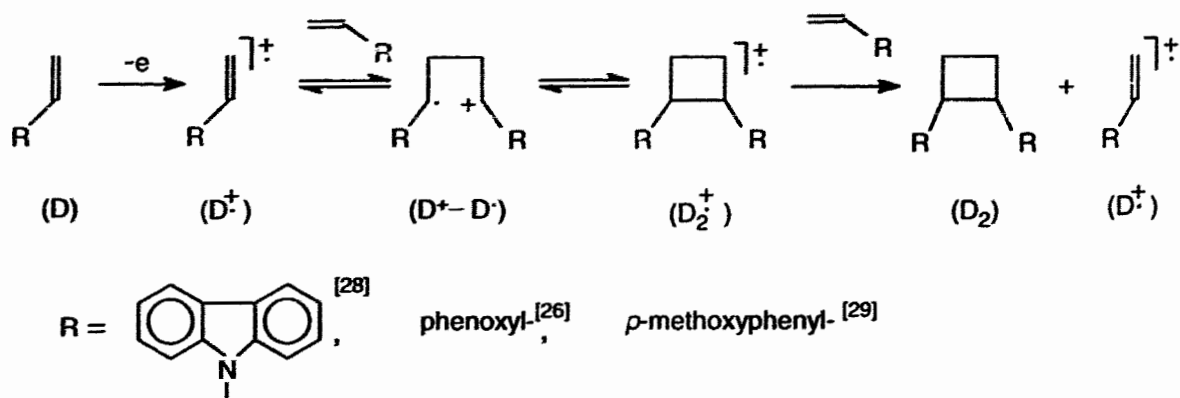
The first example of PET induced dimerizations is the photoreaction of N-vinyl-

carbazole (NVC) in methanol,[20, 24b, 30] which gives the *trans*-head-to-head cyclodimer of

NVC. Chloranil was used as the electron acceptor sensitizer. Ledwith thoroughly

investigated the PET dimerization of NVC by using a wide range of sensitizers and

proposed that the dimerization followed a radical cation chain mechanism (Scheme

8

1.2).[28, 31] The chain nature of this reaction is supported by the observation that the

dimer quantum yield is in excess of unity ($\Phi_{max} = 66$[31]). The dimerization can be

initiated photochemically either by the reaction of NVC with an excited acceptor

sensitizer or by the direct excitation of the ground state complex of NVC with the

acceptor molecule. The electron transfer nature of this reaction is also reflected by its

solvent dependence: the dimerization is very fast in polar solvents methanol and

acetonitrile, but no reaction occurs in cyclohexane.

The photocyclodimerization of phenyl vinyl ether (PVE) was reported by

Shigemitsu postulating an exciplex intermediate (Eq. 1.7).[32] Further studies by Evans

and Farid suggested that the dimerization was a radical cation reaction.[33, 26b,c]

$$cis\text{-} : trans\text{-} = 60 : 40$$
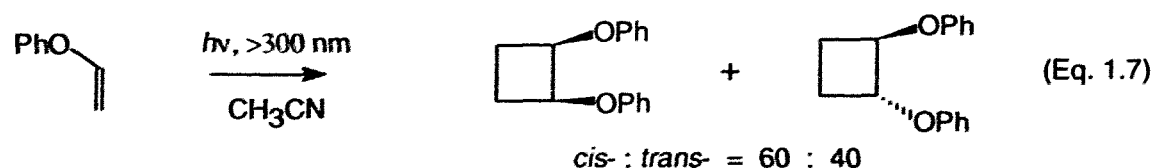
(Sensitizer: 9,10-dicyanoanthracene,[26] benzonitrile or dimethyl terephthalate[32])

Quenching of 9,10-dicyanoanthracene (DCA) fluorescence by PVE showed that a weak

exciplex emission appeared at -40 °C in methylcyclohexane, and the quenching rate

constants were found to correlate linearly with solvent polarity. The interpretation of

these results is that the singlet excited DCA reacts with PVE to form an exciplex which

then dissociates in polar solvents to give radical cation of PVE. As a support for this,

CIDNP effects on the ^{1}HNMR spectrum of PVE was observed in the sensitized

dimerization of PVE in acetonitrile-d_3.[34]

The radical cation of PVE was suggested as a chain carrier since the DCA

sensitized dimerization of PVE gave a limiting quantum yield of 1.7.[26c] The dimer

formation was quenched by 1,5-dimethoxynaphthalene (DMN), a better electron donor

than PVE. On the basis of a chain mechanism (Scheme 1.2), kinetic studies revealed two quenching patterns at different concentrations of DMN. At low concentrations, the quenching of dimerization is caused by the selective interception of chain propagating step by DMN, *i.e.*, $D_2^{+\cdot}$ + DMN $\rightarrow$ D_2 + $DMN^{+\cdot}$. At relatively high concentrations, the secondary electron transfer from DMN to $D^{+\cdot}$ dominates the quenching event, *i.e.*, $D^{+\cdot}$ + DMN $\rightarrow$ D + $DMN^{+\cdot}$.[26c] Other studies on PVE cyclodimerizations were also reported in which a polymeric electron acceptor sensitizer[35a, 26a] or an optically active sensitizer was used. [35b]

Table 1.1 Reaction conditions and product ratio of CHD dimerization

(Eq. 1.8)
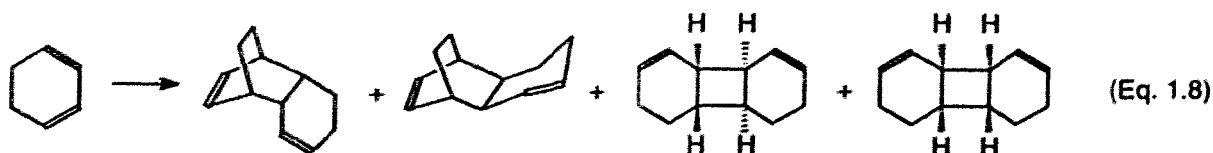
| No. | Conditions and sensitizer | Yield% | [4+2] dimer | | [2+2] dimer | | Ref. |
			endo-	exo-	anti-	syn-	
1	Δ, 200 °C, neat	32	80	20			37a
2	$Ar_3N^{+}SbCl_6^{-}$, in CH_2Cl_2, at 0 °C	70	83	17			37b
3	hv, > 330 nm, in CH_2Cl_2, DCA	60	77	23			27a
4	hv, > 330 nm, in CH_2Cl_2, DCN	41	80	10	7	3	37c
5	hv, > 330 nm, in benzene, DCN [CHD] = 0.11 M [CHD] = 2.1 M	 -- --	 3.4 28.3	 21.6 21.7	 75 50		37d & 24c
6	hv, > 330 nm, neat	--	--	37	41	22	37e
7	hv, triplet, β-acetonaphthone	92	--	20	60	20	37a

Note: $Ar_3N^{+}SbCl_6^{-}$ is *tris(p-bromophenyl)aminium* hexachloroantimonate. The sensitizer DCA is 9,10-dicyanoanthracene and DCN is 1,4-dicyanonaphthalene.

Table 1.1 summarized results of some typical experiments in the dimerization of 1,3-cyclohexadiene (CHD) under a variety of conditions.[24c, 20, 36] The [4+2] dimerization predominates either under thermal reactions (by heating or by oxidation), or under PET conditions (Table 1.1, No. 1 ~ 4). Direct irradiation and triplet sensitization produce mainly [2+2] dimers with a minor amount of *exo*-[4+2] dimer (Table 1.1, No. 6 and 7).

A chain mechanism (Scheme 1.3A) was established by Bauld for the thermal radical cation reaction of CHD (Table 1.1, No. 2).[37b, 28b, 38] This scheme is consistent with the reported chain reaction of the CHD radical cation initiated by γ-irradiation.[39]

Scheme 1.3:

(A) Chain mechanism

$$Ar_3N^{+\bullet} + CHD \atop or \atop A + CHD \xrightarrow{h\nu} CHD^{+\bullet} \xrightarrow{CHD} (CHD)_2^{+\bullet} \xrightarrow{CHD} [4+2]\text{-}(CHD)_2$$

(B) Electron transfer sensitization

$$A \xrightarrow{h\nu} {}^{*}A \xrightarrow{CHD} CHD^{+\bullet} \xrightarrow{CHD} (CHD)_2^{+\bullet} \xrightarrow{A^{-\bullet}} [4+2]\text{-}(CHD)_2$$
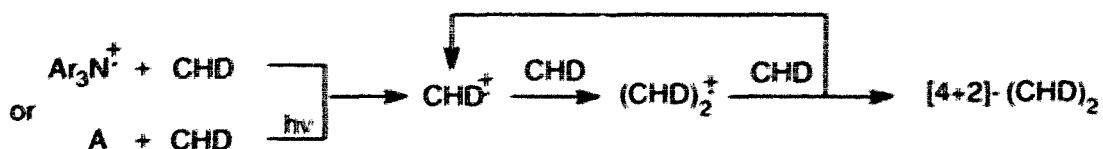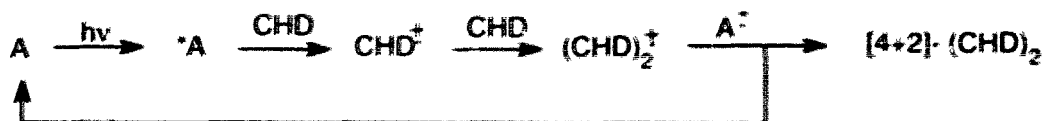
A: electron acceptor sensitizer

The photochemically induced Diels-Alder reaction of CHD was observed when a methylene chloride solution of 9,10-dicyanoanthracene (DCA) and CHD was irradiated at > 330 nm (Table 1.1, No. 3). Having examined the CHD dimerization sensitized by 1,4-dicyanonaphthalene (DCN) in acetonitrile, Schuster suggested a radical cation chain mechanism for this photochemical CHD dimerization (Scheme 1.3A).[37a] The radical anion DCN$^{-\bullet}$ was observed in laser flash photolysis, and the *endo*-[4+2] dimer was selectively quenched by the added 1,3,5-trimethoxybenzene (TMB), an electron donor

for intercepting CHD$^{+\cdot}$.[37d] Steckhan also postulated the chain-reaction mechanism for the CHD dimerization using pyrylium salt as sensitizer in CH$_2$Cl$_2$.[40]

The electron transfer sensitization, shown in scheme 1.3B, is a parallel mechanism which explains the photochemical Diels-Alder reaction of CHD.[20, 36b] This scheme is different from scheme 1.3A in that the sensitizer (A) is regenerated through a back electron transfer from its radical anion (A$^-$) to the dimeric cation (CHD)$_2^+$. Eberson and Olofsson disputed scheme 1.3A regarding the role of triarylamine radical cation (Ar$_3$N$^+$), and they suggested that the cation Ar$_3$N$^+$ should be regenerated by:

$$(CHD)_2^+ + Ar_3N \rightarrow [4+2]\text{-}(CHD)_2 + Ar_3N^+$$

Thus a conventional catalytic mechanism can be an alternative to scheme 1.3A.[41] To what extent, Scheme 1.3A or 1.3B is involved in the photochemical Diels-Alder dimerization of CHD is still not clear.[26a, 36a]

A non-ionic pathway of [4+2]-photodimerization of CHD was reported by Schuster for the 1,4-dicyanonaphthalene (DCN) sensitized reaction of CHD in benzene.[37d] Consistent with the general finding that the formation of radical ions is not favorable in nonpolar solvents, no ionic species were detected in the laser flash photolysis of DCN with CHD in benzene. The quencher 1,3,5-trimethoxybenzene (TMB) for intercepting CHD$^{+\cdot}$ showed no effects on this dimerization. Based on these observations, the non-ionic pathway involving the formation of triplex was suggested:

$$^*DCN\text{--}CHD + CHD \rightarrow {}^*(DCN\text{-}CHD\text{-}CHD) \qquad \text{(Eq. 1.9)}$$

In Eq. 1.9, the exciplex *DCN--CHD is intercepted by another CHD molecule to form a triplex *(DCN-CHD-CHD), and this triplex is suggested to give the endo-[4+2] dimer of CHD.[37d] This explained that the increased CHD concentration in benzene resulted in more endo-[4+2] dimer formation (Table 1.1, No. 5).[37d, 42]

1.3.2 The Cycloaddition of Electron-Rich Olefins via Exciplexes

The photocycloaddition of anthracenes to 1,3-cyclohexadiene (CHD, Eq. 1.10) and 2,5-dimethyl-2,4-hexadiene (DMHD) has been reported to proceed via exciplex intermediates.[43a,b] As the exciplexes are fluorescent for most diene-arene pairs,[43c]

Eq. 1.10:

$$X = H, \ Cl, \ Br, \ CN, \ CN$$
$$Y = H, \ Cl, \ Br, \ H, \ CN \qquad [4+4] \qquad\qquad [4+2]$$
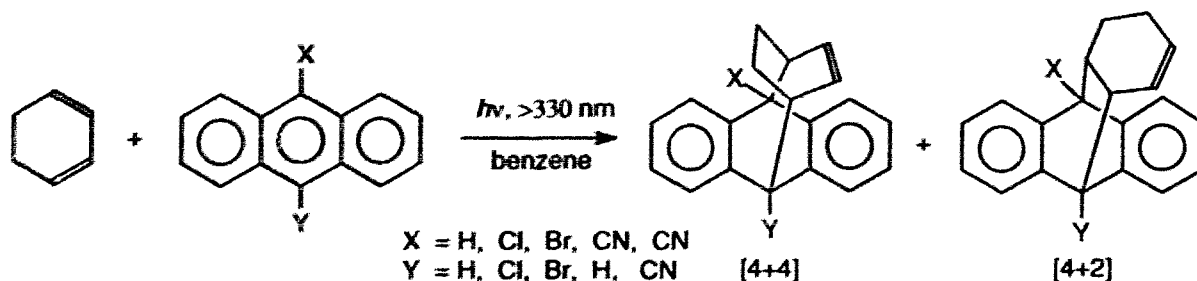
this allows the exciplex polarity to be measured qualitatively simply by comparing the red-shifts of exciplex fluorescence maxima in various solvents. Using this method, the distribution of [4+2] and [4+4] adducts was found to be related to the polarity of exciplexes: nonpolar exciplexes from anthracene and naphthalene undergo the concerted [4+4] cycloaddition, but polar exciplexes of substituted anthracenes undergo mainly the stepwise [4+2] additions.[43a] Similar work on the relationship between the exciplex CT nature and the orientation of photocycloaddition were also reported by Albini,[44] for the photocycloaddition of 1- or 2-cyanonaphthalene and 1,4-dicyanonaphthalene to 1,3-dienes (CHD, DMHD and 2,3-dimethyl-1,3-butadiene) in benzene, where nonemissive exciplexes were postulated as the intermediate.

Pac's group has studied the photoreactions of 1- and 2-cyanonaphthalene with vinyl ethers (Eq. 1.11), such as ethyl vinyl ether and phenyl vinyl ether.[45] Since the postulated exciplexes in the reaction systems are nonemissive, solvent effects were examined on the quenching of cyanoarene fluorescence by vinyl ethers and on the cycloaddition of the donor-acceptor pairs. The charge transfer (CT) nature of the exciplex is expected to change with solvent polarity and so is the chemical reactivity

Eq. 1.11:

R = ethyl, phenyl

exo-
(minor)

endo-adduct
(major)
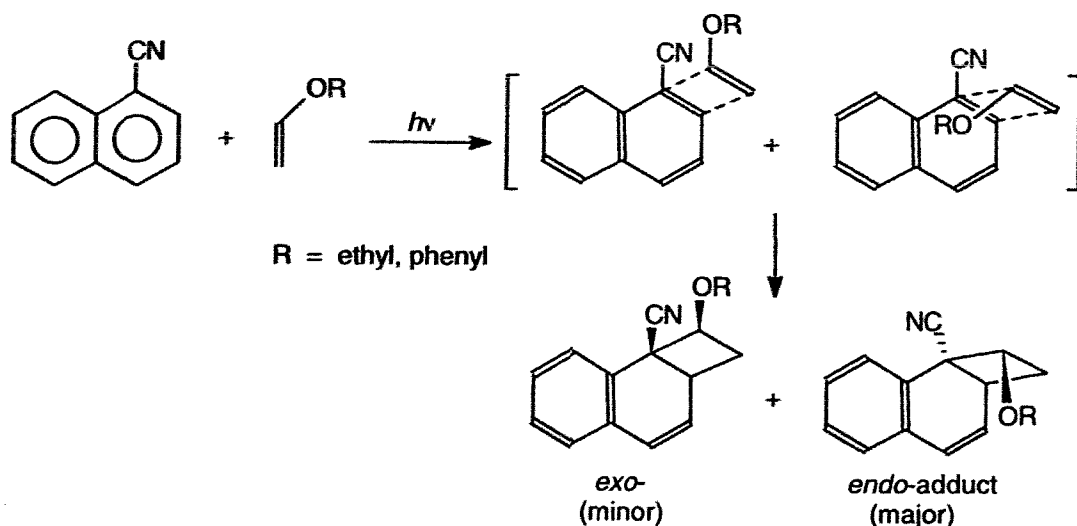
of the exciplex towards cycloadduct formation. The reported results are consistent with the general understanding of a polar exciplex mediated reaction: an efficient arene-vinyl ether addition occurs in less polar solvents, corresponding to an exciplex with low CT contributions; but in polar solvents, the extent of CT contributions can be induced significantly so that the ionic dissociation of the exciplex dominates over the adduct formation.[45, 46]

The majority of PET reactions reviewed in literature involve electron acceptor sensitizers.[47] Among them, cyanoarenes are most common (Table 1.2). Besides the listed chloranil, a few other carbonyl compounds, such as fluorenone, biacetyl and benzil, were also reported in literature as electron acceptor sensitizers.[20, 24c] However, 1,3-diketones have received little attention as being the PET reagents. Although the BF_2-complexation of 1,3-diketones led to some findings in the emission properties of 1,3-diketonatoboron difluorides,[48a,b] no publications were found in studying their PET reactions until the work done by Chow's group in the photochemistry and photophysics of 1,3-diketonatoboron difluorides.[49]

Table 1.2 Reduction potential ($E^{red}_{1/2}$) and singlet excitation energy (E_S) of commonly used electron acceptor sensitizers [24b]

Sensitizer	$E^{red}_{1/2}$ (eV) in CH_3CN vs. SCE	E_S (eV) in CH_3CN
chloranil	0.02	--
2,4,6-triphenylpyrylium tetrafluoroborate	-0.29	2.80
2,6,9,10-tetracyanoanthracene	-0.45	2.82
1,2,4,5-tetracyanobenzene	-0.65	3.83
9,10-dicyanoanthracene	-0.89	2.88
1,4-dicyanonaphthalene	-1.28	3.45
1,4-dicyanobenzene	-1.60	4.27
9-cyanoanthracene	-1.70	2.96
1-cyanonaphthalene	-1.98	3.75
2-cyanonaphthalene	-2.13	3.68

1.4 Our Research Interests in 1,3-Diketonatoboron Difluorides

Our attention to 1,3-diketonatoboron difluorides stems from the investigations on acid promoted photocycloaddition of 1,3-diketones. It was found that the de Mayo reaction of acetylacetone (AAH) with cyclohexene[48c,d] was greatly enhanced in the presence of boron trifluoride (BF_3).[49] Subsequently it was found that the Lewis acid BF_3 actually reacted with AAH to form a BF_2-chelated compound, acetylacetonatoboron difluoride ($AABF_2$). It was soon realized that the BF_3-promoted photocycloaddition was a PET reaction between the singlet excited $AABF_2$ and the ground state donor olefin.[49]

1.4.1 1,3-Diketonatoboron Difluorides

It has been found that 1,3-Diketonatoboron difluorides have the potential to be a new type of electron acceptor in PET reactions.[49, 50] They are thermally stable[51] and easily prepared by the reaction of 1,3-diketones with boron trifluoride etherate in ether,[51c] acetonitrile[49] or benzene.[52]

The first synthesis of 1,3-diketonatoboron compounds was reported in 1906.[53] Since then, many analogues have been synthesized [51b, 52, 54] and their structures have been demonstrated by physical methods. The IR spectra of the boron difluoride chelates generally show pronounced C=O and C=C shifts to lower frequency without any indication of a free carbonyl group.[51b, c] The symmetrical chelate structure of AABF$_2$ (or DBMBF$_2$) is clearly supported by the identical chemical shift for the methyl (or phenyl) groups in ^{1}H and ^{13}C NMR spectra.[51c, 55] Further confirmation of the structure comes

Scheme 1.4:

R$_1$	R$_2$	R$_3$	
CH$_3$	H	CH$_3$	AABF$_2$
CH$_3$	H	C$_6$H$_5$	BABF$_2$
C$_6$H$_5$	H	C$_6$H$_5$	DBMBF$_2$
p-t-BuC$_6$H$_4$	H	p-MeOC$_6$H$_4$	MBDBF$_2$
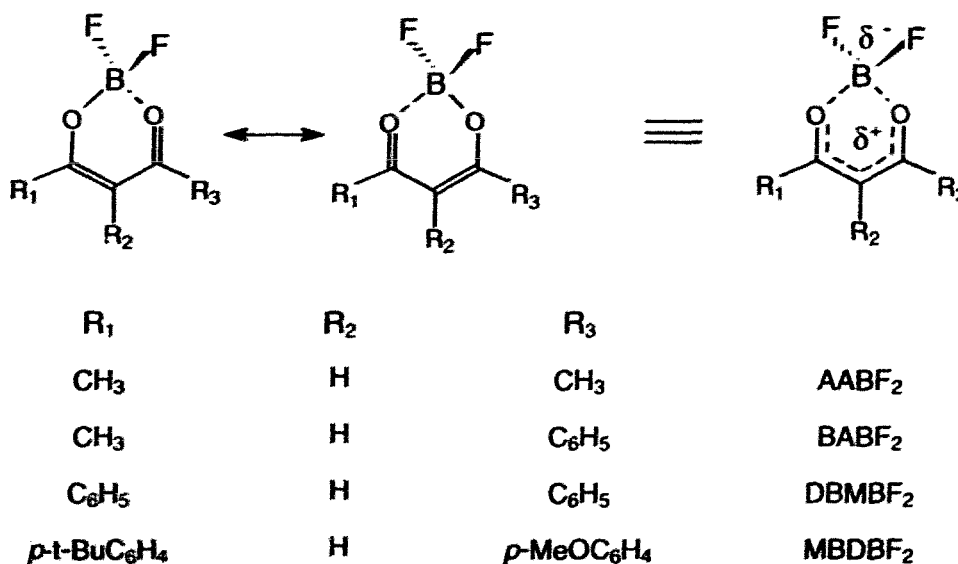
from the X-ray crystallography, which demonstrated that the two B–O (1.488 Å) and two C–O (1.304 Å) bonds in BABF$_2$ have the same lengths.[54f, 56] Finally, the electropositive

nature of the diketonate chelates (Scheme 1.4) is consistent with the observation of a significant downfield shift of the methine proton signal, as well as the large increase in the dipole moment after BF_2-complexation (Table 1.3).

The photophysical and photochemical properties have been examined in Chow's group for those difluoroborane chelates in Scheme 1.4.[64] Table 1.3 lists physical data of DBM and $DBMBF_2$, as typical examples, to illustrate the effects of BF_2-complexation on some photophysical properties. Chelating to BF_2-group leads to a 4.7 Debye

Table 1.3 Physical constants of dibenzoylmethane (DBM) and dibenzoylmethanatoboron difluoride ($DBMBF_2$)

	mp (^{o}C)	μ (Debye)	UV[c] λ_{max} (nm), log ε_A	E_{ox} (V)[e]	E_{red} (V)[e]	δ[g] (ppm)
DBM	77.5 - 79[a]	3.0[b]	342, 4.38	~1.6[b]	-1.38[b,f]	6.78[h]
$DBMBF_2$	194 - 197	6.7[b]	360, 4.48 (365, 4.61)[d]	2.45	-0.91	7.20

	E_S[j] (kcal/mol)	E_T[j] (kcal/mol)	τ_a[k] (ns)	τ_{AA}[l] (ns)	Φ_f[m]	Φ_{isc}[n]
DBM	74.4[b]	59.5,[b] 63.8[i]	--	--	0	--
$DBMBF_2$	73.5[b]	62.0[b]	0.30, 0.34	50	0.1	0.01

Notes: [a] From Ref. 57; [b] From Ref. 58a and references therein; [c] In chloroform solution (Ref. 51c); [d] In acetonitrile; [e] vs. SCE in acetonitrile (Ref. 58a); [f] vs. SCE in DMSO solvent from Ref. 59; [g] Chemical shift of the methine proton in ^{1}H NMR in $CDCl_3$; [h] From Ref. 60a; [i] From Ref. 61; [j] Singlet and triplet energies; [k] Lifetime of singlet excited state, in acetonitrile: 0.3 ns (Ref. 62a) and 0.34 ns (Ref. 54a, 58b); [l] Lifetime of excimer in acetonitrile (Ref. 62a); [m] Fluorescence quantum yield in acetonitrile at room temperature; [n] Triplet quantum yield (Ref. 63).

increase in dipole moment and 0.47 V increase in the reduction potential which makes DBMBF$_2$ an electron acceptor sensitizer comparable to 9,10-dicyanoanthracene.[24b] Indeed, DBMBF$_2$ and other 1,3-diketonatoboron difluorides have been patented for use as electron acceptors in the fabrication of photoconductive materials.[65]

1.4.2 Dibenzoylmethane (DBM) and Dibenzoylmethanatoboron Difluoride (DBMBF$_2$)

Dibenzoylmethane (DBM), like acetylacetone,[66] exists mainly as a chelated enol (> 90%) in non-hydroxylic organic solvents.[67] The principal UV absorption of DBM can be assigned to the $\pi \rightarrow \pi^*$ transition, characterized by a large molar absorption coefficient (ε_A) and long wavelength (λ_{max}).[51c] The lowest singlet excited state of DBM is mostly $\pi\pi^*$ in nature.[68] This is rationalized by that the $\pi\pi^*$ state is lower in energy than the $n\pi^*$ state,[68] because conjugation reduces the HOMO - LUMO gap of the π-orbitals, and the intramolecular hydrogen bonding increases the $n \rightarrow \pi^*$ gap.

Upon photolysis, the enol-form of DBM undergoes isomerization to its keto-form (Scheme 1.5).[69] This isomerization is believed to be the main radiationless route that results in undetectable DBM fluorescence at room temperature.[69a] In contrast, at 77 K in a glass matrix, the isomerization is inhibited and a strong fluorescence is observed

Scheme 1.5:
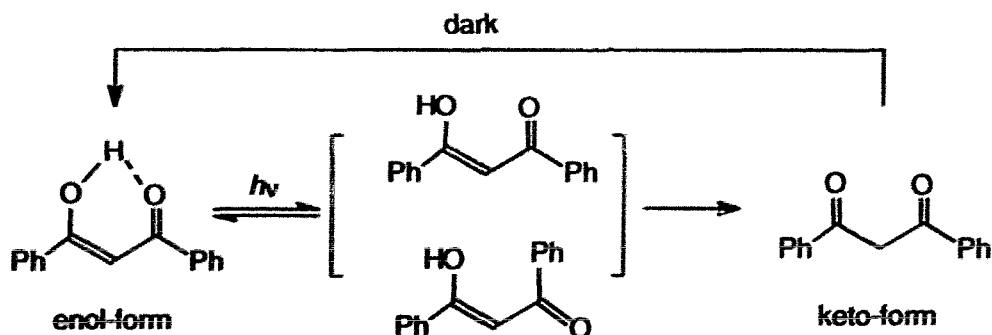
from the singlet excited DBM.[68] The reversibility of the keto-enol tautomerism has

shown industrial applications.[70]

Dibenzoylmethane undergoes photoaddition to styrenes, following the pattern of

the de Mayo reaction,[48c, d] to yield regioselectively the head-to-tail cycloadduct shown in

Scheme 1.6:[71]
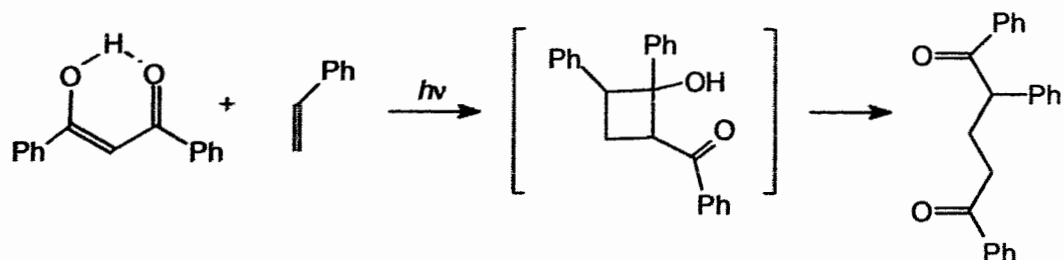
Compared to DBM, DBMBF$_2$ has a more rigid, electron delocalized, ring structure

(Scheme 1.7). This is evident from the different chemical shifts of the *ipso* and *para*

carbon atoms in DBMBF$_2$ (Table 1.4). The *para*-aromatic carbons are more deshielded

than the *ipso*-carbons.[55]

Scheme 1.7:
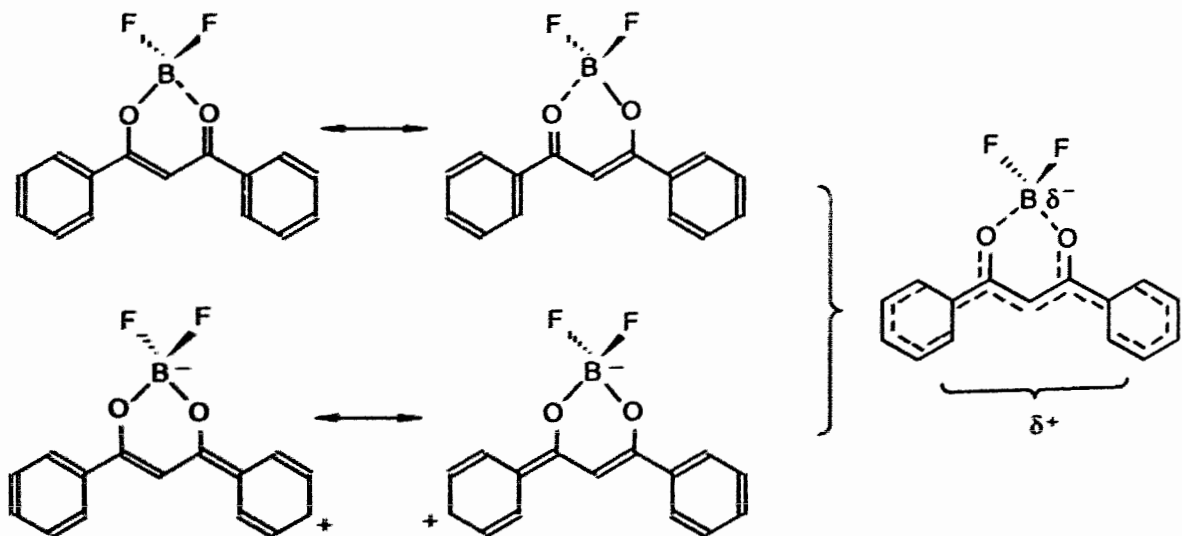
Table 1.4 Chemical shifts of phenyl carbon atoms (ppm)

in CDCl$_3$	para-phenyl carbon	ipso-phenyl carbon
DBM^a	132.3	135.5
DBMBF$_2$^{b}	135.2	132.1

Notes: ^{a} Ref. 60b; ^{b} Ref. 55b.

The BF$_2$- complexation also stabilizes the non-bonding electrons in DBM and increases energy of the n → π* transition, so that mixing of nπ* and ππ* states in DBMBF$_2$ is smaller than in DBM. Because of the rigidity of the system and the ππ* nature of the singlet excited state, DBMBF$_2$ exhibits strong fluorescence, even at room temperature.

1.4.3 The Reported Photochemistry and Photophysics of DBMBF$_2$

While the photochemistry and photophysics of 1,3-diketonatoboron compounds have received relatively little attention, the photoreactions of 1,3-diketones with alkenes, known as the de Mayo reaction,[48c,d] have been investigated extensively and it has been established that the reactive species is the triplet excited diketone.[71] Although DBM itself does not add to simple olefins,[49, 72] its BF$_2$ complex, DBMBF$_2$, undergoes efficient, regioselective and stereoselective [2 + 2] photocycloaddition to simple olefins from its singlet excited state (Scheme 1.8).[50a, c]

Compared to the photoaddition of acetylacetone (AAH) to cyclohexene, the BF$_2$-complexation of AAH not only changes the reaction species from triplet to singlet, but also accelerates and improves the selectivity of adduct formation.[50c]

$$R = CH_3(CH_2)_3, (CH_3)_3C, CH_2=CH(CH_2)_2$$
$$n = 1, 2, 3, 4$$
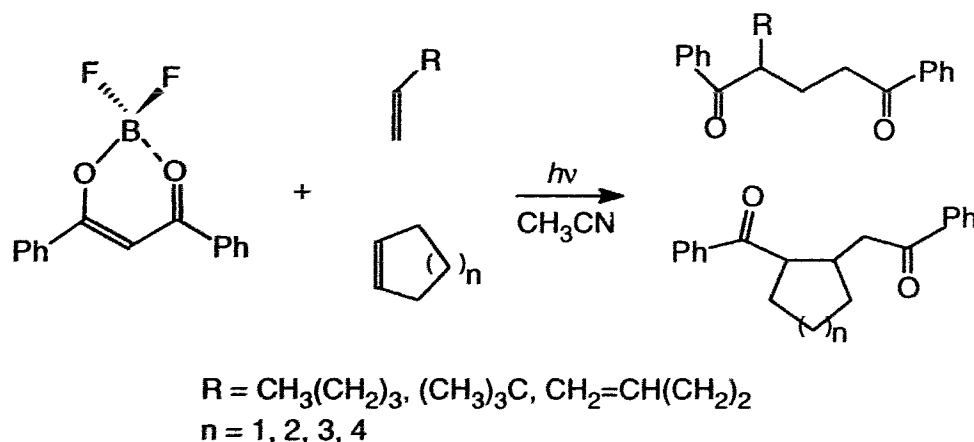
As a singlet excited acceptor, $DBMBF_2$ sensitizes electron-rich olefins towards radical cation reactions in acetonitrile (Scheme 1.9). Examples include Diels-Alder dimerization of 1,3-cyclohexadiene (CHD),[50a] [2+2] dimerization of *trans*-anethole[50b] and photoisomerization of quadricyclane (QC) to norbornadiene (NBD).[50b]

Scheme 1.9:

hv, 350 nm

$DBMBF_2$
in CH_3CN

endo / exo = 7 / 1

$DBMBF_2$ /*hv*

$DBMBF_2$/Arene/*hv*
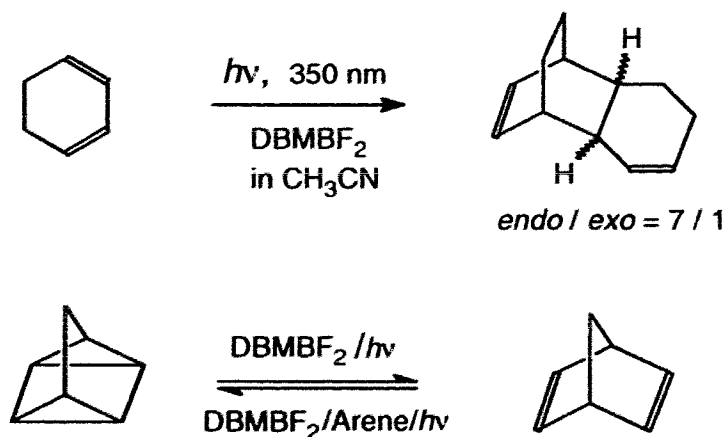
An electron transfer mechanism has been suggested for the reaction of singlet excited $DBMBF_2$ with donor olefins, on the basis of a semi-logarithmic correlation of the quenching rate constant of $DBMBF_2$ fluorescence with the ionization potentials of the quencher olefins.[50a, 49] This allows the photoreactions of $DBMBF_2$ to be rationalized in terms of two pathways: cycloaddition via an exciplex precursor, and alkene dimerization

via radical cations. Photocycloaddition predominates when the donor olefins has an IP > 8.4 eV; but with olefins of IP < 8.4 eV, the radical cation reaction dominates.[50a,49] The radical cation is thought to form from an encounter complex (an outer-sphere electron transfer [73]), and this is seen in the $DBMBF_2$ sensitized Diels-Alder dimerization of CHD in acetonitrile.[50a] On the other hand, CIDNP studies on $DBMBF_2$ sensitized photoisomerization of QC to NBD suggest that the radical ion $QC^{+\cdot}$ is generated by dissociation of its precursor, a $^*DBMBF_2$-QC exciplex or an in-cage contact ion pair.[74]

Photophysical studies of $DBMBF_2$ suggest that the singlet excited $DBMBF_2$ interacts with a ground state $DBMBF_2$ molecule to form its excimer, showing a strong fluorescence emission at 522 nm.[64a] $DBMBF_2$ in ground state can interact with alkyl substituted benzenes to form electron donor-acceptor (EDA) complexes.[58a] Among the EDA pairs of $DBMBF_2$ with xylene, toluene and benzene, only the $DBMBF_2$-p-xylene complex showed a CT band in acetonitrile significant enough for measuring the association constant, $K_a = 0.07 \pm 0.02$ M^{-1}.[58a] Upon excitation, the EDA complex leads to an emissive $DBMBF_2$-arene exciplex that can be also generated by excitation of $DBMBF_2$ alone.[58a, 63, 64a] The exciplexes of $DBMBF_2$ with arenes have been studied systematically for their photophysical properties.[58]

1.4.4 Research Proposals

The versatility of $DBMBF_2$ photochemistry and photophysics offers several aspects for further investigations. One major task is to further explore the $DBMBF_2$ photochemistry. This project is designed on the basis of following considerations:

Photoreactions of DBMBF₂ with electron-rich olefins

The reported photocycloadditions of $DBMBF_2$ to olefins are mostly limited to simple alkenes.[50a,c] It has not been successful to extend those reactions to electron-

rich olefins, such as conjugated cyclic dienes and vinyl ethers. For example, no photo-cycloaddition of DBMBF$_2$ was observed to either 1,3-cyclooctadiene (1,3-COD) or 1,3-cyclohexadiene (CHD) in acetonitrile, while only the dimers of CHD were obtained.[49] Our first aspect is to study the photoreactions of DBMBF$_2$ with electron-rich olefins and to examine whether the reactions involve the formation of a DBMBF$_2$ exciplex with those olefins.

One approach is the fluorescence quenching, which can provide the direct spectroscopic evidence for the intermediacy of an exciplex if it is emissive. Therefore, extensive experiments should be done in the quenching of DBMBF$_2$ fluorescence by conjugated cyclic dienes and vinyl ethers.

An alternative way of searching for the DBMBF$_2$ exciplex is to study the solvent effects on DBMBF$_2$ photoreactions with electron-rich olefins. If the electronic structure of the DBMBF$_2$ exciplex is sensitive to the solvent polarity, then the structure change in this exciplex may lead to different chemical reactions in solvents of different polarities. For example, when the free energy change is estimated using the Rehm-Weller equation (Eq. 1.5) for interactions of singlet excited DBMBF$_2$ with 1,3-COD and CHD, it predicts that the postulated DBMBF$_2$-diene exciplex should have a high CT extent. In polar solvents, this polar exciplex is expected to undergo a complete electron transfer, whereas in nonpolar solvents, electron transfer becomes endothermic and the exciplex is expected to lead to cycloadduct formation.

Photochemical properties of DBMBF$_2$-benzene exciplexes

The first DBMBF$_2$-benzene exciplex was found by Cheng in this group.[64a] The detailed studies on the photophysics of DBMBF$_2$-benzene exciplexes have been reported in Johansson's Ph.D. thesis.[58a] However, the chemical properties of these

DBMBF$_2$-arene exciplexes have not received much attention. The second aspect of this thesis is to examine the chemical reactions of DBMBF$_2$-arene exciplexes.

It is expected that the photocycloaddition of DBMBF$_2$ to electron-rich olefins may occur in a nonpolar solvent like benzene. Two excited species should be present in benzene, the singlet excited DBMBF$_2$ and its exciplex with a solvent molecule, but it is not known which principal species reacts with the olefins and what intermediates might be formed in the course of the reactions. To answer these questions, the fluorescence quenching and the photoreaction of DBMBF$_2$ with the cyclic diene in aromatic solvents were studied.

It is also expected that the CT extent of DBMBF$_2$-arene exciplexes can be promoted by increasing solvent polarity. In the extreme case, the exciplex could dissociate into radical ion pairs. Could DBMBF$_2$-benzene exciplexes dissociate in the polar solvent acetonitrile? What subsequent reactions might happen between the ion pair and the arene or the electron-rich olefin? To answer these questions, the photolysis of DBMBF$_2$ in acetonitrile-xylene solvent mixtures was examined.

The intermediacy of DBMBF$_2$ excimer

The formation of DBMBF$_2$ excimer is concentration dependent. Such DBMBF$_2$ concentration effects in the photoreaction have been used to indicate the intermediacy of DBMBF$_2$ excimer.[50c] For example, the photocycloaddition of DBMBF$_2$ to cyclic alkenes gave a higher adduct quantum yield when the concentration of DBMBF$_2$ was higher, whereas the quantum yield of DBMBF$_2$ reaction with an acyclic alkene showed a decrease.[50c] This result suggests that DBMBF$_2$ excimer has a selectivity to react with cyclic alkenes. However, it is not known whether this selectivity is controlled by an electronic effect or controlled by a geometric requirement relating to the olefin ring structures.

24

The third aspect of this project is to study the chemical reactivities of the DBMBF$_2$ excimer. Under this aspect, a variety of substrate olefins (electron-rich, electron-deficient, cyclic and acyclic) were selected and their photoreactions with DBMBF$_2$ were examined. The quenching of DBMBF$_2$ excimer fluorescence, using the selected substrate olefins as the quencher, was also studied in order to determine the intermediacy of DBMBF$_2$ excimer in those photoreaction systems. An important question is whether or not the product formation is actually a chemical consequence of the fluorescence quenching. Kinetic analyses were thus performed to establish the correlation of the fluorescence quenching with the chemical product formation.

Photoreactions of DBMBF$_2$ with electron-deficient olefins

The fourth aspect of this study is to examine the photoreactions of DBMBF$_2$ with α,β-unsaturated ketones and esters based on the following analyses:

(i) Photocycloadditions of DBMBF$_2$ to methyl vinyl ketone and ethyl acrylate have been reported.[49] This warranted an examination of new photoreactions of DBMBF$_2$ with electron-deficient olefins.

(ii) Despite their poorer electron-donating capability than simple alkenes, 2-cyclohexenone and methyl vinyl ketone showed abnormally higher efficiencies in quenching DBMBF$_2$ fluorescence. The Stern-Volmer quenching constant K_{SV} is 18 M^{-1} for 2-cyclohexenone and 8.3 M^{-1} for methyl vinyl ketone.[49] However, efficient quenching led to a rather slow photocycloaddition of 2-cyclohexenone to DBMBF$_2$. The isolation of cycloadducts was reported to be unsuccessful.[49] A detailed study on the abnormal behaviour of the enones was carried out in this thesis.

(iii) DBMBF$_2$ sensitized dimerization of cyclic enones was postulated,[49] but the possible dimer formation due to the direct enone irradiation was not considered. A few points thus needed clarification: How efficient are the DBMBF$_2$ sensitized dimerizations?

Do the enones absorb light in the presence of DBMBF$_2$? How does the light absorption affect dimer formation? To examine the efficiencies of the sensitized and the directly irradiated dimer formation, the photolysis of cyclic enones was performed with and without the presence of DBMBF$_2$.

(iv) Cyclic and acyclic alkenes have different patterns for their reactions with DBMBF$_2$ excimer.[50c] It is not known whether cyclic and acyclic enones might show the same reaction patterns as the alkenes. Thus the effect of DBMBF$_2$ concentrations on the photocycloaddition of DBMBF$_2$ to the enones was investigated.

As a summary of this section, the research project was designed as follows:

(1) study the photoreactions of DBMBF$_2$ with electron-rich olefins in nonpolar solvents and characterize structures of the products;

(2) examine the fluorescence quenching of the excited DBMBF$_2$ monomer, excimer and DBMBF$_2$-benzene exciplexes with various quencher olefins;

(3) examine solvent effects on the photoreactions of DBMBF$_2$ with electron-rich olefins and determine product quantum yields in various solvents;

(4) correlate DBMBF$_2$ fluorescence quenching with DBMBF$_2$ photoreaction;

(5) investigate the chemical reactions of DBMBF$_2$-arene exciplexes and examine how the reactions could be affected by solvent polarity, arene concentrations and diene concentrations;

(6) study the photoreactions of DBMBF$_2$ with α,β-unsaturated ketones and esters;

(7) search for the triplex which may be formed in the reaction of DBMBF$_2$ excimer or DBMBF$_2$-arene exciplexes with electron donor olefins.

1.5 Thesis Overview

Chapter two presents the photoreactions of DBMBF$_2$ with cyclic dienes and vinyl ethers, including the product studies, the fluorescence quenchings and the mechanistic studies. The stereochemistry of cycloadduct formation is discussed being consistent with the properties of an exciplex intermediate. The product patterns are given in various solvents ranging from acetonitrile to xylene. This leads to a full discussion of solvent effects on the exciplex reactions. On the basis of a mechanistic scheme, the intermediacy of DBMBF$_2$ excimer or DBMBF$_2$-arene exciplex is explored by correlating the fluorescence quenching with the photocycloaddition.

Chapter three presents the photoreactions of DBMBF$_2$ with cyclic dienes in binary solvent mixtures. The quantum yield studies on DBMBF$_2$-diene photoreactions in a group of binary solvent mixtures are first introduced. With the finding of a cosensitized Diels-Alder dimerization of CHD, the emphasis then shifts to the chemical properties of DBMBF$_2$-arene exciplexes. Two reactions of the DBMBF$_2$-xylene exciplex in acetonitrile are discussed: the coupling reaction of p-xylene and the dimerization of CHD. Several mechanistic points are also discussed: (i) the correlation of the DBMBF$_2$-xylene exciplex dissociation with its radiative decay, (ii) the competition of exciplex formation between DBMBF$_2$-arene and DBMBF$_2$-diene pairs, and finally (iii) two possible pathways for the initiation of CHD radical cation.

Chapter four presents the photocycloaddition of DBMBF$_2$ to twelve α,β-unsaturated enones and esters. Descriptions of the photoreactions include: the structural characterization of addition products, the stereochemistry of the photoadditions, and the reinvestigation of cyclic enone dimerizations. Mechanistic

studies, through fluorescence quenchings and quantum yield determinations, are motivated by searching for the intermediacy of DBMBF$_2$ excimer.

Chapter five presents the experimental detail, including steady-state fluorescence quenchings, photocycloadditions and quantum yield determinations.

1.6 Theoretical Aspects

1.6.1 Stern-Volmer Equations in DBMBF$_2$ Fluorescence Quenching

There are a variety ways of deactivation for an excited state molecule. A very important bimolecular deactivation process is the fluorescence quenching, which can be further classified into dynamic quenching and static quenching depending on whether or not diffusion of quencher molecules is involved during the lifetime of the excited state.

In dynamic quenching, the quencher molecule must diffuse to the excited species before deactivation of the excited state. Stern-Volmer equation is used to describe this diffusional quenching.[75a] In Eq. 1.12, I^o and I are the fluorescence

$$\frac{I^o}{I} = 1 + K_{SV}[D] = 1 + k_q \tau_o[D] \qquad \text{(Eq. 1.12)}$$

intensity in the absence and presence of quencher respectively, $K_{SV} = k_q \tau_o$ is the Stern-Volmer quenching constant whose kinetic expression should depend on the reaction mechanism, k_q is the quenching rate constant, τ_o is the lifetime of excited species in the absence of quencher D.

Static quenching occurs when the fluorophore and quencher molecules associate to form a ground state complex before light absorption. In this case, Stern-Volmer equation is no longer valid. The static quenching of fluorescence is described by Eq.

1.13,[75a] where K_a is the association equilibrium constant of ground state complex formation.

$$A \;+\; D \;\underset{}{\overset{K_a}{\rightleftharpoons}}\; AD$$

$$\frac{I^\circ}{I} \;=\; 1 \;+\; K_a[D] \tag{Eq. 1.13}$$

When the fluorescence quenching involves both diffusional collision and complex formation between excited species and quencher molecules, a modified Stern-Volmer equation can be used:[75a]

$$\frac{I^\circ}{I} \;=\; (1 \;+\; K_{SV}[D])\,(1 \;+\; K_a[D]) \tag{Eq. 1.14}$$

The following Scheme 1.10 serves as a provisional mechanism that describes the diffusional quenching of DBMBF$_2$ fluorescence. In this scheme, I_a is the absorbed light intensity. The rate constant of each process is defined as follows: k_m is for DBMBF$_2$ excimer formation; k_f (k_f^{ex}) is for fluorescence emission from *A (*AA); k_d (k_d^{ex}) is for

Scheme 1.10:
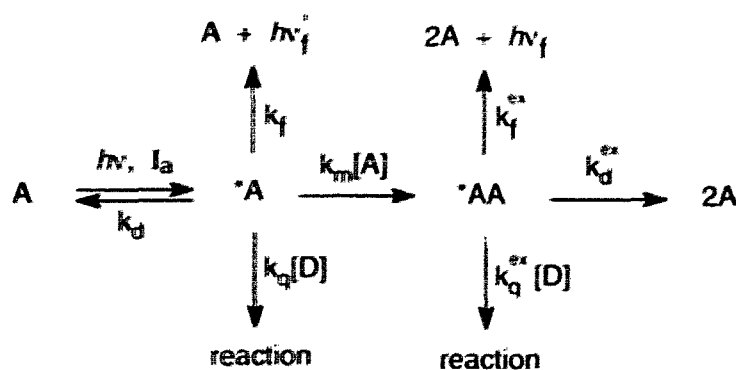
A = DBMBF$_2$, *A = excited DBMBF$_2$ monomer, *AA = DBMBF$_2$ excimer

nonradiative decay of *A (*AA); k_q (k_q^{ex}) is for the quenching of *A (*AA) by D.

For DBMBF$_2$ monomer fluorescence quenching, the steady-state treatment of Scheme 1.10 provides the following relationships in terms of the constant population of *A:

$$I_a = [^*A]_o (k_d + k_f + k_m[A])$$ in the absence of quencher D,

$$I_a = [^*A] (k_d + k_f + k_m[A] + k_q[D])$$ in the presence of quencher D.

Dividing the first equation by the second one gives Eq. 1.15:

$$\frac{[^*A]_o}{[^*A]} = \frac{k_d + k_f + k_m[A] + k_q[D]}{k_d + k_f + k_m[A]} = 1 + \frac{k_q}{k_d + k_f + k_m[A]}[D] \qquad (Eq. 1.15)$$

Because the fluorescence intensity (I) is proportional to the concentration of *A, we can obtain the Stern-Volmer equation for DBMBF$_2$ monomer fluorescence quenching as:

$$\frac{I^o}{I} = 1 + \frac{k_q}{\tau_a^{-1} + k_m[A]}[D] = 1 + K_{SV}^m [D] \qquad (Eq. 1.16)$$

In Eq. 1.16, $\tau_a = 1/(k_d + k_f)$ is the lifetime of singlet excited DBMBF$_2$ in the absence of quencher.

For DBMBF$_2$ excimer fluorescence quenching, a similar steady-state treatment provides relationships of the constant population for DBMBF$_2$ excimer (*AA):

$$k_m[^*A]_o[A] = (k_f^{ex} + k_d^{ex})[^*AA]_o$$ in the absence of quencher D,

$$k_m[^*A][A] = (k_f^{ex} + k_d^{ex} + k_q^{ex}[D])[^*AA]$$ in the presence of quencher D.

Dividing the top equation by the bottom one affords Eq. 1.17:

$$\frac{[^*AA]_o}{[^*AA]} \div \frac{[^*A]_o}{[^*A]} = \frac{k_f^{ex} + k_d^{ex} + k_q^{ex}[D]}{k_f^{ex} + k_d^{ex}} \qquad (Eq. 1.17)$$

Thus, by replacing the concentration ratio of the excited species with the ratio of fluorescence intensity, a modified Stern-Volmer equation for DBMBF$_2$ excimer fluorescence quenching is obtained:

$$\left(\frac{I^o}{I}\right)_{ex} \div \left(\frac{I^o}{I}\right)_{mon} = 1 + k_q^{ex} \tau_{AA}[D] = 1 + K_{SV}^{ex}[D] \qquad \text{(Eq. 1.18)}$$

In Eq. 1.18, $\tau_{AA} = 1/(k_f^{ex} + k_d^{ex})$ is the lifetime of DBMBF$_2$ excimer in the absence of

quencher D. K_{SV}^{ex} is the Stern-Volmer constant for quenching DBMBF$_2$ excimer.

Eq. 1.18 is the modified Stern-Volmer equation established by Caldwell.[75b] This

equation does not apply when the monomer fluorescence quenching dominates over the

quenching of excimer / exciplex. Also according to Caldwell's observations, Eq. 1.18 will

show a plot of downward curvature when the monomer spectrum is not well resolved

from the excimer (exciplex) spectrum. In such a case, it was suggested to take initial

slope as the quenching constant K_{SV}^{ex}.[75c]

Scheme 1.10 does not include the fluorescence quenching of DBMBF$_2$ in

aromatic solvents. Due to the formation of DBMBF$_2$ ground state complex with solvent

molecules, the static quenching may become significant. However, both the static and

the dynamic quenching lead to the same DBMBF$_2$-arene exciplex.[58a] Essentially, the

quencher D (alkenes) in aromatic solvents is actually quenching the DBMBF$_2$-arene

exciplex. In such cases, Eq. 1.12 should be applicable where the lifetime τ_o corresponds

to DBMBF$_2$-arene exciplex in the absence of quencher D.

1.6.2 Cyclic Voltammetry

Cyclic voltammetry is one of the popular electrochemical techniques, which can

be employed to determine redox potentials of various compounds and to examine their

electrochemical behaviour.[76] In this technique, the electrode potential is scanned

linearly from an initial value (E_i) to a final value (E_f), and then the direction of scan is

reversed from E_f to E_i to finish a cycle. During the potential scan, the current response

signal is recorded as a function of the applied potential, and the obtained current -
voltage curve is called voltammogram. A typical cyclic voltammogram for a reversible
redox couple is shown in Fig. 1.3, where the arrows are designated to indicate the scan
direction. For an electrochemically reversible couple, its oxidized- and reduced-forms
exchange electrons with the electrode rapidly enough to maintain the concentrations of
both species in equilibrium with each other at the electrode surface.[76]

Cathodic (i_c)

Current 0

Anodic (i_a)

Positive   Negative

Potential
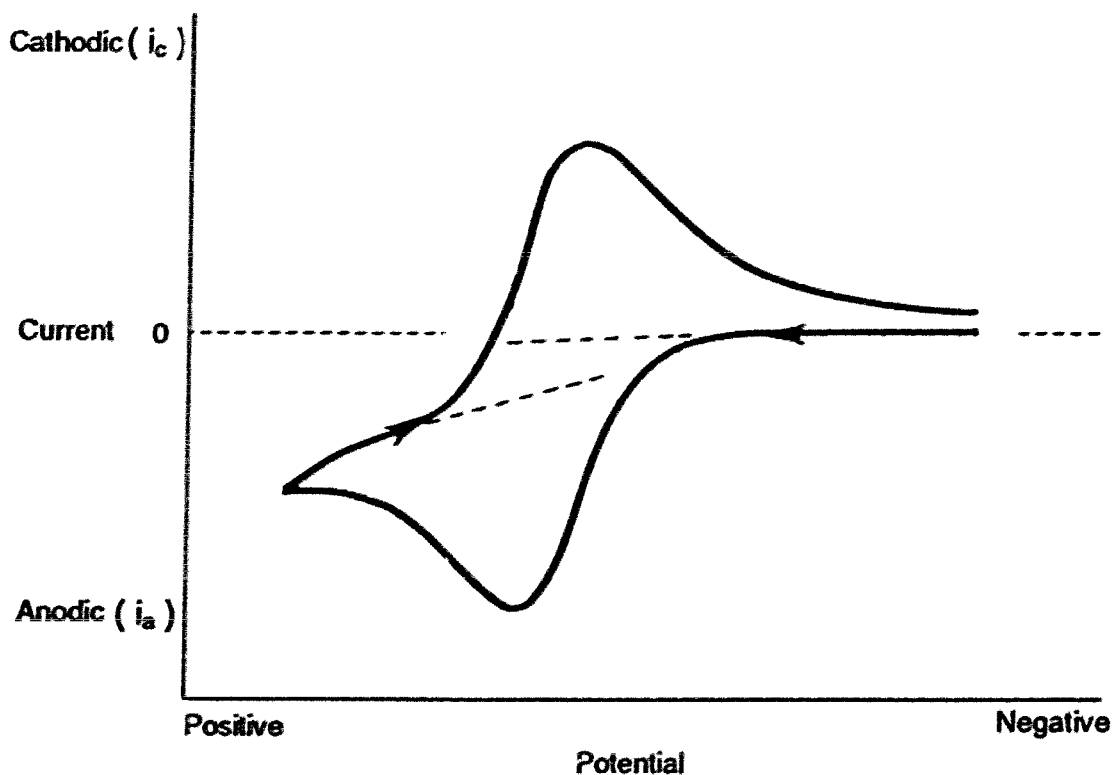
Fig. 1.3 The cyclic voltammogram of a reversible redox couple

The variation of current in Fig. 1.3 is affected by (1) the diffusion of electroactive
species to the electrode surface, and (2) the electron transfer reaction between the
species and the electrode.[76b] While the rate of latter process is accelerated by
increasing potentials, a sharp increase of current occurs, and correspondingly the
concentration of the reactant species at the electrode surface will rapidly decrease. This

reactant depletion generates a concentration gradient near the electrode surface; a diffusion layer appears between the electrode surface and the bulk solution. Since the solution is unstirred, the diffusion layer becomes thicker as the reaction proceeds. As a result, the reactant species must travel further to reach the electrode surface. At the point where the diffusion of reactant species becomes rate determining, a maximum of anodic current (i_{pa}, Fig. 1.3) is observed. After this peak, the further potential increase is no longer important to the diffusion controlled current. The current continues to decay owing to the decrease of reactant concentration gradient with the diffusion layer thickening. In the reverse scan (Fig. 1.3), the electrode quickly switches its role from an oxidant to reductant. The oxidized-form of the redox couple, which is still concentrated near the electrode surface, is converted back to the initial reduced-form. The formation of a cathodic current peak (i_{pc}) in reverse scan can be similarly rationalized.

Several parameters in Fig. 1.3 should be mentioned which characterize a redox couple: the anodic peak current (i_{pa}) and cathodic peak current (i_{pc}), and the peak potentials at which the peaks occur (E_{pc} and E_{pa}). For a reversible redox couple, the peak currents are proportional to the square root of scan rate, and the ratio of i_{pc} to i_{pa} is approximately unity.[76] The peak potentials are independent on the scan rate and related to the formal electrode potential ($E^{\circ'}$):

$$E^{\circ'} = \frac{E_{pa} + E_{pc}}{2} \approx E_{1/2} \qquad\qquad \Delta E_p = E_{pa} - E_{pc} \approx \frac{0.059}{n}$$

The half-wave potential ($E_{1/2}$) is a term from polarography, defined as the potential corresponding to one-half of the diffusion current on the polarographic wave. The equation $E^{\circ'} \approx E_{1/2}$ is valid when the differences of diffusion coefficients for the oxidized and reduced species are negligible.[76] The separation between the peak potentials

(ΔE_p) can be used for determining the number (n) of electrons transferred in the electrode reaction.

For an irreversible redox system, above equations are not applicable. The irreversibility is characterized by more separated peaks $\Delta E_p > 0.059 / n$. In this case, the electron exchange of redox species with the electrode is slow so that the concentrations of the species are unable to maintain their equilibrium during the potential scan. When there are chemical reactions following the electron exchange process, the current peak on the reverse scan is often absent. Because of the irreversibility, precautions are needed if the redox potentials determined from an irreversible couple are used as thermodynamic parameter.

In the calculation of free energy change (ΔG_{ET}) for a PET process, Rehm-Weller equation (Eq. 1.4) requires the redox potentials determined from electrochemically reversible couples. However, in using an oxidation potential from the irreversible couple, the quantitative evaluation of ΔG_{ET} was achieved after examining the thermodynamic significance of the value by electrochemical techniques in combination with spectroscopic studies; for example, the relationship between the UV-VIS absorption maximum of a charge transfer complex and the oxidation potential of a donor was applied.[77a] For qualitative evaluation of ΔG_{ET}, the peak or half-peak oxidation potentials of irreversible couples have been used in Rehm-Weller equation if those values are comparable and determined under nearly identical experimental conditions.[12, 77b,c] Other examples include the application of the potential values that are interpolated from a correlation of ionization potentials with the literature oxidation potentials.[14, 77d]

CHAPTER TWO

THE PHOTOREACTIONS OF DBMBF₂ WITH ELECTRON-RICH OLEFINS
CYCLIC DIENES AND VINYL ETHERS

2.1 Results

2.1.1 Photoreactions of DBMBF₂ with Cyclic Dienes

2.1.1.1 The Reaction Profile

The photolysis of DBMBF$_2$ and 1,3-cyclohexadiene (1, CHD) in acetonitrile led to rapid dimerization of the diene, proposed via a cation radical intermediate.[50a, 49] The product consists mainly of the [4+2] dimers **2** and **3**, with traces of [2+2] dimers **4** and **5**.

Eq. 2.1:

0.5 M	$h\nu$, 350 nm	48%
(1)	6 hr., CH$_3$CN	cis-endo
	0.05 M DBMBF$_2$	(2)

5%
cis-exo
(3)

trace
cis-anti-cis
(4)

trace
cis-syn-cis
(5)
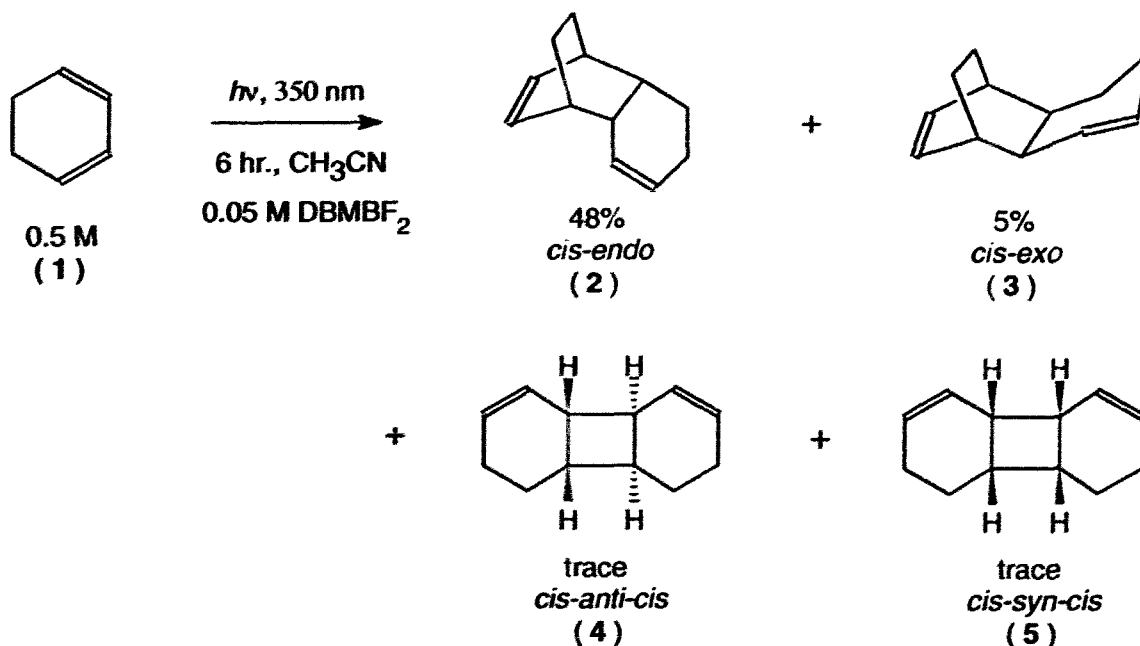
There was no addition of DBMBF$_2$ to CHD found in acetonitrile, and the DBMBF$_2$ was mostly recovered. However, the irradiation of an ether solution of DBMBF$_2$ (0.05 M) and CHD (0.5 M) yielded two adducts of DBMBF$_2$ to CHD in the ratio 9 : 1. GC analysis

showed that the adduct peaks had longer retention time than DBMBF$_2$ and increased

with the gradual disappearance of DBMBF$_2$. Diene dimers were also observed as a

mixture of the isomers **2 / 3 /4 / 5** (31 : 23 : 35 : 11), in a total GC yield of 3%, based on

the internal standard dodecane.

Eq. 2.2:

Head-to-Head
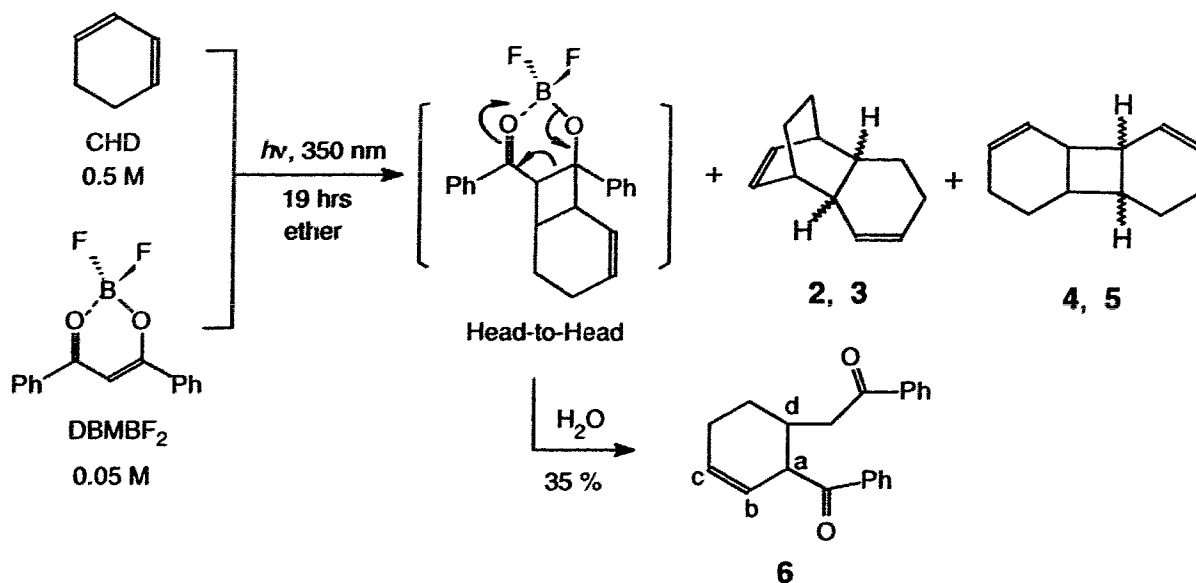
Column chromatography yielded a major and a minor cycloaddition product in

35% yield. Both products exhibited parent ion peaks at m/z = 304 (EI) and 305 (M+1,

CI), corresponding to dibenzoylmethane plus CHD. The products displayed similar

fragmentation patterns. However, the structure of the minor product was not

determined. The major product was determined to be **6** on the basis of spectroscopic

data (Table 5.6). In the MS spectrum, the parent ion produced two main fragments: (1)

the base peak was the benzoyl side chain (m/z = 105), which lost a carbon monoxide to

give the phenyl ion (m/z = 77); (2) the fragment having m/z = 185 from loss of a

phenacyl side chain. The presence of benzoyl and phenacyl side chains was indicated

by a broad IR absorption at 1682 cm^{-1} and by ^{13}C NMR peaks at 199.64 and 201.26 ppm

for the two carbonyls, and 127.98, 128.44, 128.56, 128.72, 132.87, 132.99, 137.16 and

137.27 ppm for the two sets of phenyl carbons. The C=C double bond was identified by

^{13}C NMR peaks of 124.13 and 129.91 ppm, and ^{1}H NMR peaks at 5.77 and 5.93 ppm

(H_b, H_c and J_{bc} = 9.7 Hz). A multiplet at 4.43 ppm in ^{1}H NMR was assigned to the

methine proton (H_a) adjacent to C=C and C=O groups. The coupling pattern of H_a was

traced with 2D-COSY and decoupling experiments, leading to J_{ab} = 4.0 Hz and J_{ad} = 5.1

Hz. The latter coupling is consistent with the *axial - equatorial* coupling in the

cyclohexene ring,[78a] and suggests that the adduct 6 has a *cis*-configuration of its side

chains. The above analysis suggests that DBMBF$_2$ approaches CHD (1) in a head-to-

head orientation, as shown in Eq. 2.2.

Eq. 2.3:
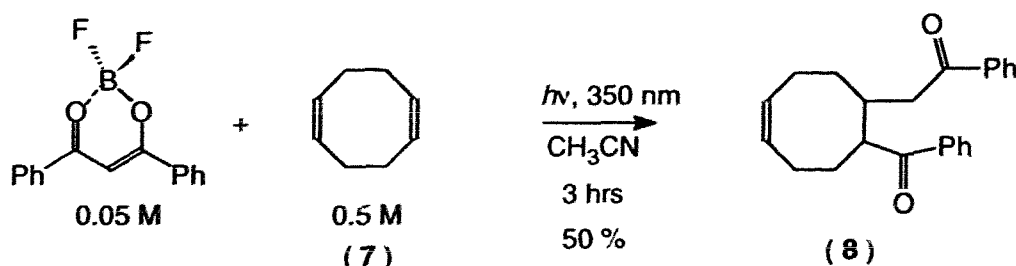
It has been reported that DBMBF$_2$ undergoes efficient photoaddition to 1,5-

cyclooctadiene (7, 1,5-COD) in acetonitrile (Eq. 2.3), but that, in the same solvent, no

photocycloadduct is detected from the photolysis of DBMBF$_2$ and 1,3-cyclooctadiene (9,

1,3-COD).[50c] In the present work, the latter reaction was found to produce a complex

mixture of 1,3-COD dimers in poor yield. The two major dimers were identified as the

cis-anti-cis (10) and *trans-anti-cis* (11) fused cyclobutanes, assigned by GC coinjections

with authentic samples and by comparing the mass spectra.[78b, 79]

The irradiation of a benzene solution of DBMBF$_2$ and 1,3-COD (9) gave a 1:1 *cis*-adduct in 47% isolated yield, together with a small amount of the *trans*-isomer and less than 1% of a mixture of 1,3-COD dimers (Eq. 2.4). The reaction was accompanied by the formation of a polymer which coated the inside surface of the photocell and hindered further irradiation.

Eq. 2.4:
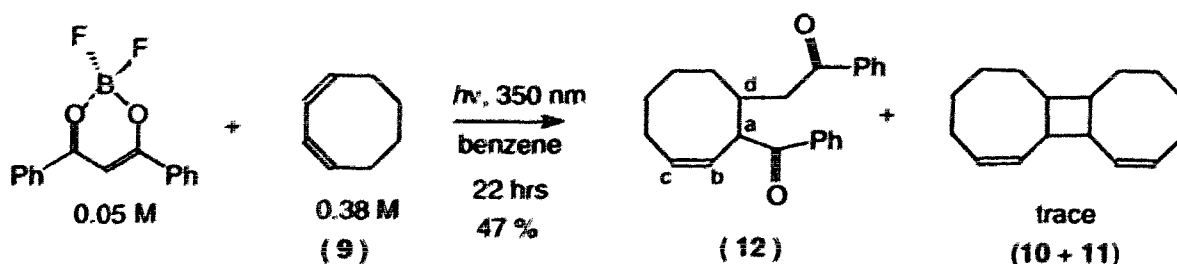
The structure of adduct 12 was assigned on the basis of the following analyses. The molecular ion peak in MS was found at m/z = 332 (EI) and at m/z = 333 (M+1, CI), corresponding to the addition of dibenzoylmethane (DBM) to 1,3-COD. Fragmentation occurred by loss of the benzoyl and phenacyl side chains. The two side chains of the major adduct (*cis*-12) were revealed by two carbonyl peaks (199.56, 201.36 ppm) and two sets of phenyl peaks (128.10, 128.44 (2C), 128.72, 132.78, 133.03, 136.72, 137.17 ppm) in the ^{13}C NMR. Similarly for the minor adduct *trans*-12, the carbonyl absorptions were found at 199.96 and 202.04 ppm, and the phenyl peaks at 128.41, 128.51 (2C), 128.67, 133.21, 133.52, 136.94 and 137.63 ppm. This serves as a diagnostic pattern for most DBMBF$_2$ addition products. The C=C bond was identified firstly by two olefinic carbon absorptions (132.25 and 125.83 ppm for the *cis*-12; 132.88 and 128.96 ppm for the *trans*-12 in Table 5.6), and secondly by two vinyl protons (in *cis*-12: 6.05 (H$_b$, dd) and 5.97 (H$_c$, ddd) ppm as well as in *trans*-12: 5.92 (H$_c$, ddd) and 5.38 (H$_b$, dd) ppm). The

38

connections of the benzoyl and phenacyl chains to the ring skeletons were assigned on the basis of the chemical shifts and coupling patterns of the methine protons H_a and H_d. The proton H_a in *cis*- and *trans*-12 was deshielded by neighbouring C=C and C=O groups, showing a downfield chemical shift of > 4.4 ppm. The proton H_a also had vicinal coupling to the vinyl proton H_b (J_{ab} = 9.3 Hz for *cis*-12 and 10.5 Hz for *trans*-12), indicating that the benzoyl side chain is allylic to the double bond. In *cis*-12, the proton H_a was found at 4.73 ppm, having a vicinal coupling to H_d (J_{ad} = 3.9 Hz), consistent with a *cis*-configuration of the two side chains as in the analogue *cis*-8.[50c, 49] In *trans*-12, the proton H_a appeared at 4.43 ppm with a vicinal coupling J_{ad} = 10.5 Hz (Table 5.6) consistent with a *trans*-configuration of the side chains as in *trans*-8.[50c] The structural assignment of *cis*- and *trans*-12 was also consistent with the general trends summarized in Table 4.3, namely, a *cis*-adduct of DBMBF$_2$ to a cyclic substrate has a larger chemical shift of H_a and a smaller coupling constant J_{ad} than a *trans*-adduct.

In summary, the products of DBMBF$_2$ photoreactions with cyclic dienes change significantly from the polar solvent acetonitrile to the less polar solvents ether and benzene. Dimerization of CHD dominates in the polar solvent, but photoaddition of DBMBF$_2$ to the diene dominates in the less polar solvents. Adduct formation is regioselective and stereoselective.

2.1.1.2 Steady State Fluorescence Quenching Studies

Three types of DBMBF$_2$ fluorescent species have been reported: (1) The singlet excited state of DBMBF$_2$ shows a fluorescence emission in acetonitrile with maxima at 398, 417 and 440 nm.[84a] (2) At high concentrations of DBMBF$_2$, the singlet excited state interacts with a second DBMBF$_2$ molecule to form an emissive excimer with a

maximum at 522 nm.[64a] (3) In the presence of benzene, a strong exciplex fluorescence is observed at 420 - 430 nm in acetonitrile. This is a result of association of the singlet excited $DBMBF_2$ with the ground state benzene.[64a, 58, 63] Since the three different excited species could act differently upon an electron donor such as a cyclic diene, it is necessary to examine the fluorescence quenching by cyclic dienes.

(a) Monomeric Fluorescence Quenching

At room temperature, the quenching of $DBMBF_2$ (5×10^{-6} M) fluorescence by cyclic dienes in THF and dioxane was carried out using the right-angle illumination technique (section 5.2). The sample solution was freshly prepared and excited at 365 nm where $DBMBF_2$ has strong absorbance. The fluorescence intensity was then monitored at 417 nm. The totally added quencher was less than 25 μL (method one, section 5.2.1), therefore the dilution effect on the $DBMBF_2$ concentration was insignificant ($\leq$ 1%). The difference between the corrected and the uncorrected fluorescence intensity was within the experimental errors (< 1%, Table 5.1).

The relationship between the relative emission intensity (I^o/I) and the concentration of the quencher cyclic diene [D] can be analysed according to the Stern-Volmer equation derived in section 1.6.1:

$$I^o/I = 1 + K_{SV}^m [D] = 1 + k_q \tau_A [D] \qquad \text{(Eq. 1.16)}$$

$$\tau_A = (\tau_a^{-1} + k_m[A])^{-1} \qquad \text{(Eq. 1.16a)}$$

In Eq. 1.16, I^o and I are the fluorescence intensity respectively in the absence and the presence of a quencher diene (D); K_{SV}^m is the Stern-Volmer quenching constant (unit: M^{-1}) characterising the quenching efficiency of $DBMBF_2$ (A) monomer fluorescence by a quencher (D); k_q is the quenching rate constant ($M^{-1}s^{-1}$); k_m is the rate constant of the

DBMBF$_2$ excimer formation (M^{-1}s^{-1}); τ_A is the actual lifetime and τ_a is the intrinsic lifetime of the singlet excited DBMBF$_2$ monomer (ns).

A typical fluorescence quenching of the singlet excited DBMBF$_2$ in THF solvent is shown in Figure 2.1, using 1,3-COD (9) as the quencher. The fluorescence intensity ratio I^o/I at 417 nm was determined as a function of 1,3-COD concentration. The corresponding Stern-Volmer plot of I^o/I against [1,3-COD] produced a line with the slope K$^m_{SV}$ = 8.1M^{-1} (Figure 2.1A).

The quenching of DBMBF$_2$ fluorescence by 1,3-COD (9) in dioxane was examined at two concentrations of DBMBF$_2$. For the sample of [DBMBF$_2$] = 5 x 10^{-6} M, measurements were performed using the right-angle illumination technique, while the front-face illumination method was used for measurements with [DBMBF$_2$] = 0.03M. In the case of [DBMBF$_2$] = 5 x 10^{-6} M, a plot of I^o/I at 417 nm against [1,3-COD] was linear, with slope K$^m_{SV}$ = 3.7 M^{-1} (Figure 2.1B). At [DBMBF$_2$] = 0.03 M, the spectrum of excited DBMBF$_2$ monomer was accompanied by a faint shoulder peak caused by excimer emission. The plot of I^o/I at 432 nm vs. [1,3-COD] was linear with slope K$^m_{SV}$ = 3.8 M^{-1} for the monomer fluorescence quenching (Figure 2.2A). The similarity of the K$^m_{SV}$-values, despite the large differences in DBMBF$_2$ concentrations, suggests that 1,3-COD may quench the same excited species in each case.

(b) Excimer Fluorescence Quenching

The irradiation of a DBMBF$_2$ (0.20 M) solution in THF exhibited a monomeric fluorescence peak at 440 nm and a broad fluorescence band at 524 nm, assigned to the emission of the DBMBF$_2$ excimer. The quenching of the excimer fluorescence with a cyclic diene was carried out in THF solvent using the front-face illumination technique.
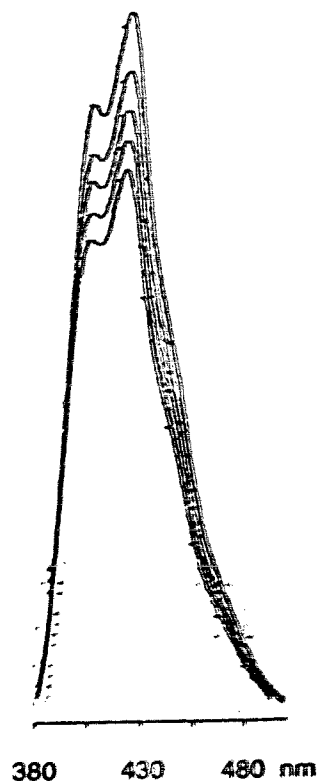
A: in THF, $K_{SV}^m = 8.1 \pm 0.3$ M^{-1}
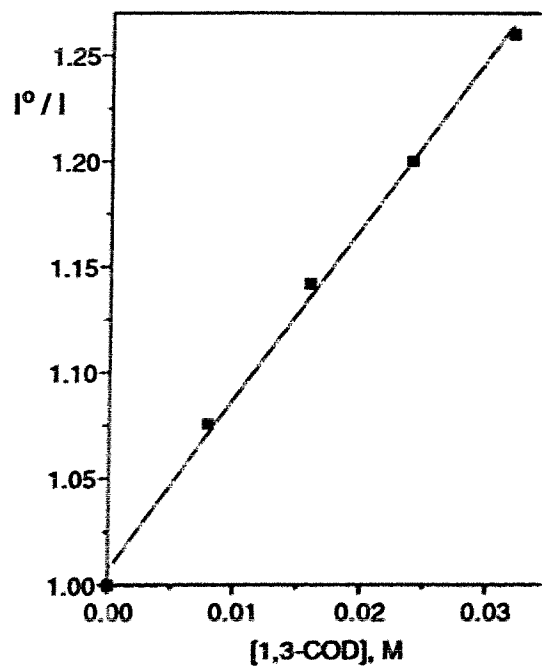
B: in dioxane, $K_{SV}^m = 3.7 \pm 0.2$ M^{-1}
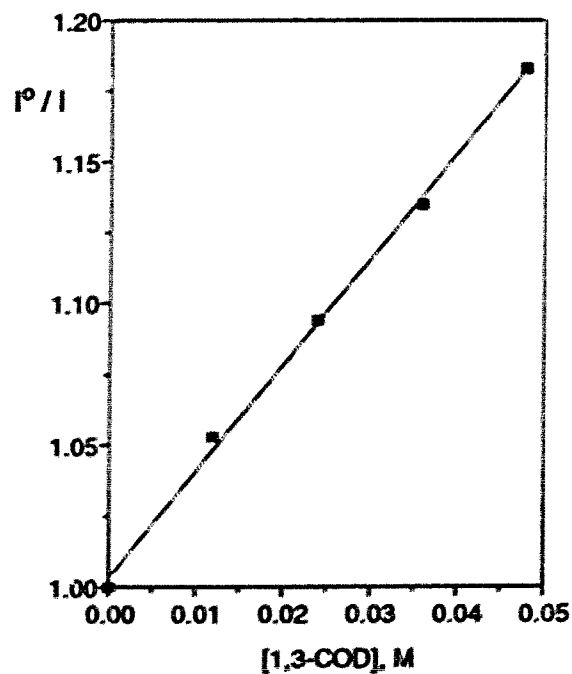
Fig. 2.1 The quenching of DBMBF$_2$ (5×10^{-6} M) fluorescence by 1,3-COD and the related Stern-Volmer plots: (A) in THF $K_{SV}^m = 8.1$ M^{-1}; (B) in dioxane $K_{SV}^m = 3.7$ M^{-1} excited at $\lambda_{ex} = 365$ nm and monitored at $\lambda_{moni} = 417$ nm.

A: $K_{SV}^m = 3.8 \pm 0.2 \ M^{-1}$

B: $K_{SV}^{ex} = 155 \pm 5 \ M^{-1}$

Fig. 2.2 The quenching of DBMBF$_2$ fluorescence by cyclic dienes ($\lambda_{ex} = 365$ nm):

(A) by 1,3-COD at [DBMBF$_2$] = 0.03 M in dioxane, $K_{SV}^m = 3.8 \ M^{-1}$ at $\lambda_{moni} = 432$ nm;

(B) by CHD at [DBMBF$_2$] = 0.20 M in THF, $K_{SV}^{ex} = 155 \ M^{-1}$ at $\lambda_{moni} = 524$ nm.
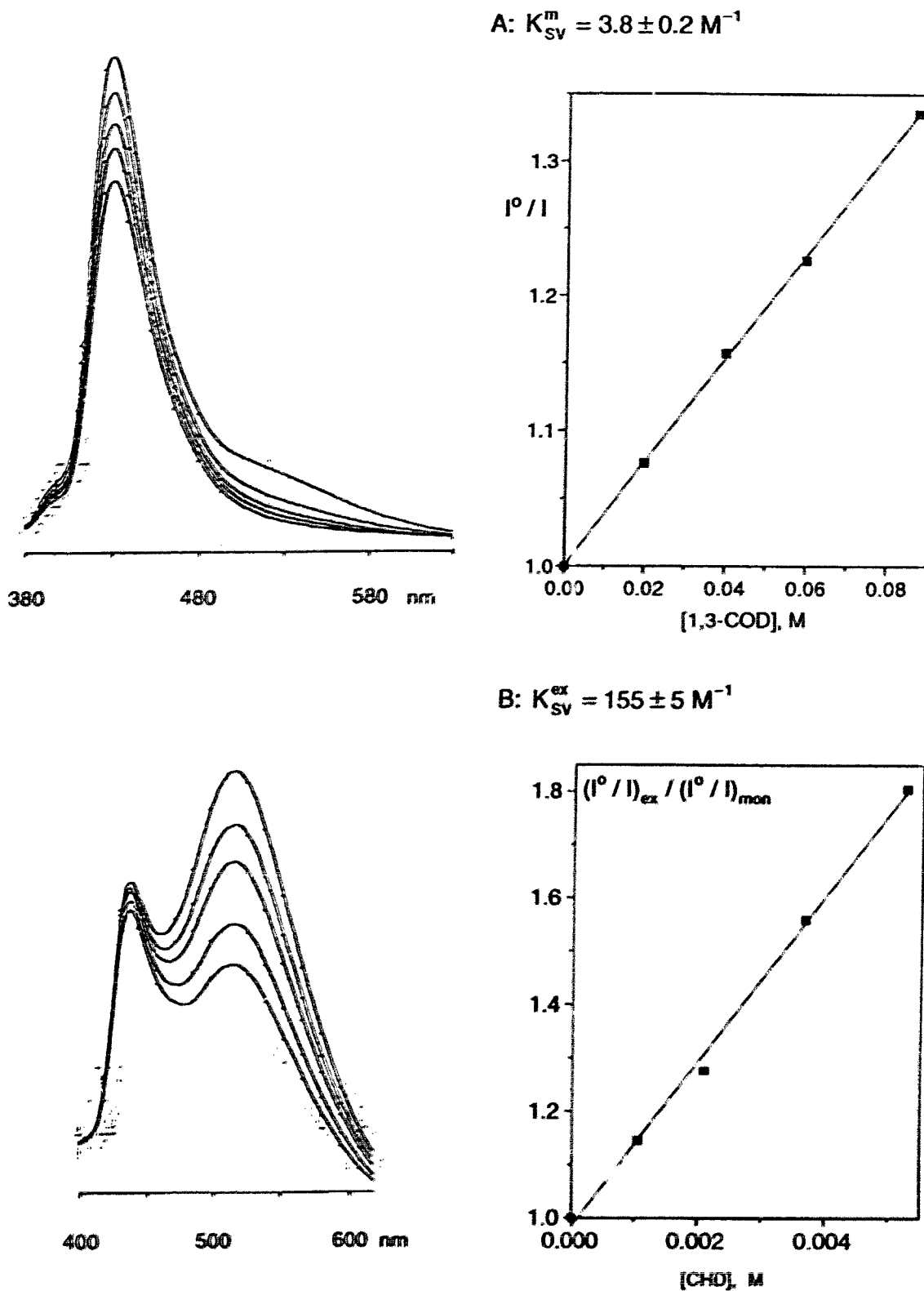
A modified Stern-Volmer equation was developed by Caldwell[75b] to analyse steady-state excimer quenching (section 1.6):

$$(I^o/I)_{ex} \div (I^o/I)_{mon} = 1 + K_{SV}^{ex}[D] = 1 + k_q^{ex}\tau_{AA}[D] \qquad \text{(Eq. 1.18)}$$

In Eq. 1.18, $(I^o/I)_{ex}$ is the intensity ratio of quenching the excimer at 522 nm; $(I^o/I)_{mon}$ is the ratio for quenching the monomer at 440 nm; K_{SV}^{ex} is the Stern-Volmer quenching constant of excimer; k_q^{ex} is the quenching rate constant and τ_{AA} is the lifetime of the DBMBF$_2$ excimer. In the excimer fluorescence quenching, spectrum overlap corrections were made. These are described in the experimental section 5.2.3.2.

Figure 2.2B shows the fluorescence quenching of DBMBF$_2$ (0.2 M) by CHD (1) in THF solvent, in which a monotonic decrease of fluorescence intensity was observed with addition of CHD. The excimer quenching at 524 nm was much faster than that of the DBMBF$_2$ monomer at 440 nm. The Stern-Volmer plot of $(I^o/I)_{ex} \div (I^o/I)_{mon}$ versus the CHD concentration was linear line with slope $K_{SV}^{ex} = 155$ M^{-1} (Fig. 2.2B). Similarly, the quenching of DBMBF$_2$ (0.20 M) fluorescence by 1,3-COD in THF gave $K_{SV}^{ex} = 56.0$ M^{-1} (Fig. 5.5). The obtained Stern-Volmer quenching constants (K_{SV}) are listed in Table 2.1.

Table 2.1 Quenching efficiency (K_{SV}) of DBMBF$_2$ fluorescence
by cyclic dienes in THF and in doxane

[DBMBF$_2$] M	Solvent	K_{SV} (M^{-1})		
			Q = CHD	1,3-COD
5×10^{-6} M^a	THF	K_{SV}^m	11.6 ± 0.3	8.1 ± 0.3 7.9 ± 0.3
0.20 M^b	THF	K_{SV}^{ex}	155 ± 5	56 ± 1
0.03 M^c	Dioxane	K_{SV}^m	10.6 ± 0.4	3.8 ± 0.2 3.6 ± 0.2

Notes: ^{a} Excited at λ_{ex} = 365 nm and monitored at λ_{moni} = 417 nm;

^{b} λ_{ex} = 365 nm and λ_{moni} = 524 nm; ^{c} λ_{ex} = 365 nm and λ_{moni} = 432 nm.

$$K_{SV}^{ex} = 10.2 \pm 0.5 \ M^{-1} \text{ in benzene}$$
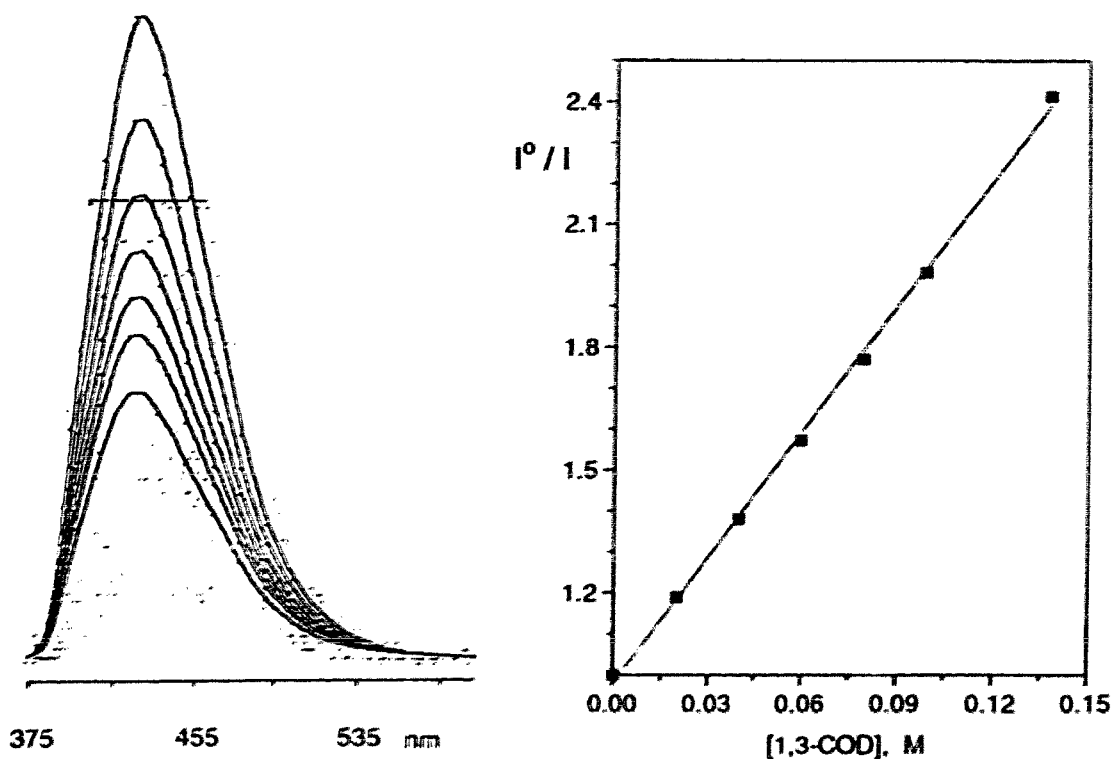
Fig. 2.3 The quenching of $DBMBF_2$ (5×10^{-6} M) fluorescence by 1,3-COD

in benzene and the related Stern-Volmer plot: $K_{SV}^{ex} = 10.2 \ M^{-1}$

excited at $\lambda_{ex} = 365$ nm and monitored at $\lambda_{moni} = 424$ nm.

Table 2.2 Quenching efficiency (K_{SV}) of $DBMBF_2$ fluorescence
by cyclic dienes in benzene [a]

[DBMBF$_2$] M, in benzene	K_{SV} (M^{-1})	
	Q = CHD	1,3-COD
5×10^{-6} M	20.6 ± 1.0	10.2 ± 0.5
		$10.0 \pm 0.\mathbb{C}$
0.03 M	21.4 ± 1.1	8.8 ± 0.4
		8.7 ± 0.3

Note: [a] excited at $\lambda_{ex} = 365$ nm and monitored at $\lambda_{moni} = 424$ nm

(c) Exciplex Fluorescence Quenching

In neat benzene, a structureless fluorescence peak of the $DBMBF_2$-benzene exciplex is observed at 424 nm showing a much longer lifetime (2.1 ns) than the excited $DBMBF_2$ monomer.[63] Addition of 1,3-COD (9) to $DBMBF_2$ (5×10^{-6} or 0.03 M) in benzene caused a monotonic decrease of the emission intensity (Figure 2.3). The corresponding Stern-Volmer plots of I^o/I against 1,3-COD concentration, monitored at 424 nm, were linear with slopes (K_{SV}) of 10.2 M^{-1} for $[DBMBF_2] = 5 \times 10^{-6}$ M and 8.8 M^{-1} for $[DBMBF_2] = 0.03$ M (Table 2.2).

Quenching of the exciplex emission by CHD (1) was determined similarly and summarized in Table 2.2.

The results in Table 2.2 suggest that an increase in $DBMBF_2$ concentrations does not significantly affect the quenching rate in benzene. Therefore, the principal species that is quenched is probably the $DBMBF_2$-benzene exciplex. This conclusion is consistent with the observation that the $DBMBF_2$ photocycloaddition quantum yield does not depend on the $DBMBF_2$ concentration in benzene solvent (see Table 2.4).

2.1.1.3 Studies of the Photoreaction Quantum Yield

(a) Solvent Effect

Because of its charge transfer nature, an exciplex is generally sensitive to solvent polarity. Experimentally, it is often observed that the emission of an exciplex shifts with changes in the solvent. If the exciplex acts as a precursor of a photoadduct, then the quantum yield of the photoaddition should change with the solvent polarity.[9a] The quantum yield of $DBMBF_2$ photoreactions with cyclic dienes was determined in different solvents using a Rayonet Photoreactor equipped with a 350 nm light source.

The incident light intensity was determined using the benzophenone-benzhydrol actinometer, which has a reported quantum yield of 0.74 in benzene.[80]

A relatively long irradiation time was employed to measure the quantum yields of the $DBMBF_2$ photoreactions with conjugated cyclic dienes (0.6 - 2 hours). In contrast, only 10 minutes of photolysis was needed for the reaction of $DBMBF_2$ with 1,5-COD (7) due to high efficiencies of the photocycloaddition. The quantum yields of adduct (Φ_A) and of dimer formation (Φ_D), from the $DBMBF_2$ photoreaction with cyclic dienes, are summarized in Table 2.3 together with the dielectric constant (ε) for each solvent used.

Examination of the data in Table 2.3 suggests the following:

(1) The photoreaction of $DBMBF_2$ with CHD and 1,3-COD depends on the solvent polarity, yielding mainly diene dimers in polar solvents and cycloadducts of $DBMBF_2$ to the diene in nonpolar solvents. A decrease of the solvent polarity from acetonitrile to p-xylene leads to a two orders of magnitude increase in the addition quantum yield (Φ_A) of $DBMBF_2$.

(2) The total dimer quantum yield (Φ_D) of CHD varies from 0.07 in CH_3CN to 0.003 in ether, mainly because of a decrease in the endo-[4+2] dimer 2. The quantum yield of [2+2] dimers (4 + 5) remains constant (0.002 - 0.004) throughout the solvent polarity range.

(3) The photoaddition of $DBMBF_2$ to 1,5-cyclooctadiene is less sensitive to solvent.

Table 2.3 Quantum yields of the photoreaction of $DBMBF_2$ with CHD, 1,3- and 1,5-COD in different solvents[a]

Solvent	ε^c	$10^3 \Phi_D$ of CHD dimer			Quantum yield of $DBMBF_2$ adduct		
		[4+2]	[2+2]	endo/exo	to: CHD, $(10^3 \Phi_A)$	1,3-COD, $(10^3 \Phi_A)$	1,5-COD (Φ_A)
CH_3CN	37.5	69.8	3.2	7.4	0.28	~0.09	0.18
acetone	20.7	7.9	3.1	4.9	0.60	0.65	--
CH_2Cl_2	8.93	55.6	3.4	3.9	1.66	0.78	0.40
THF	7.58	1.8	4.2	0.3	1.88	1.08	0.23
THP^b	5.60^d	1.2	2.3	0.4	4.52	5.20	--
dioxane	2.21	1.4	2.7	0.6	3.02	3.22	0.30
ether	4.34	1.5	1.8	1.0	11.5	26.2	0.41
benzene	2.27	13.5	2.5	2.7	14.7	28.3	0.44
toluene	2.40	8.9	2.1	2.5	22.3	39.2	0.40
p-xylene	2.27	10.7	3.3	2.1	25.9	48.1	0.19

Notes: [a] A 3 mL solution of $DBMBF_2$ (0.03 M) and CHD (0.3 M) or 1,3-COD (0.5 M) was purged with N_2 for 4 min and irradiated at 350 nm for 2 hrs in a non-aromatic solvent, and for 0.6 hr in an aromatic solvent. The conversion of $DBMBF_2$ was controlled to less than 15%. Irradiation was performed in the presence of an actinometer solution of benzophenone-benzhydrol (3 mL), and adduct formation was determined by GC analysis using an internal standard. Under the photolysis conditions, no dimerization of 1,5-COD (7) was detected in any solvents, and only trace amounts of dimers was found with 1,3-COD (9).

[b] Tetrahydropyran (THP).

[c] Ref. 81a; [d] Ref. 81b, c.

(b) Effect of DBMBF₂ Concentration

Formation of the $DBMBF_2$ excimer is concentration dependent. When $DBMBF_2$ concentration increases, the fluorescence intensity of the excited $DBMBF_2$ monomer decreases and a new broad emission peak of $DBMBF_2$ excimer appears at a longer wavelength than the $DBMBF_2$ monomer emission.[64a] The $DBMBF_2$ excimer has a longer lifetime (50 ns under N_2[62a] and 36 ns in aerated solution[62b]) than the excited monomer (0.34,[54a] 0.3 ns[62a]) in acetonitrile, and consequently the excimer has greater probability in reaction. If the excimer is involved in the photoaddition of $DBMBF_2$ to an electron-rich cyclic diene or vinyl ether, then the adduct formation should increase as the $DBMBF_2$ concentration is raised.

The quantum yield of the $DBMBF_2$ photocycloaddition to cyclic dienes was examined as a function of $DBMBF_2$ concentrations in dioxane, methylene chloride and benzene (Table 2.4). The N_2 purged solutions of CHD (0.30 M) with varying

Table 2.4 Effect of $DBMBF_2$ concentrations on the quantum
yield of adduct in different solvents[a]

[DBMBF₂] M	Adduct Quantum Yield ($10^3\Phi_A$)				
	1,3-COD			CHD	
	benzene	CH₂Cl₂	dioxane	benzene	dioxane
0.01	29.7	0.50	2.74	13.6	2.45
0.03	32.1	0.68	3.58	15.0	3.73
0.05	33.7	0.76	4.01	14.6	4.90
0.07	32.6	0.73	4.17	14.9	5.63

Notes: [a] A 3 mL solution of CHD (0.3 M) or 1,3-COD (0.3 M) with varying concentrations of $DBMBF_2$ was purged with N_2 for 4 min and irradiated at 350 nm for 2 hrs for the sample in non-aromatic solvent, but 20~30 min for the sample in aromatic solvent. The conversion of $DBMBF_2$ was controlled to less than 15%.

concentrations of DBMBF$_2$ (0.01 M ~ 0.07 M) were irradiated in a Rayonet Photoreactor with a 350 nm light source. The incident light intensity was measured using the benzophenone-benzhydrol actinometer. The measured light intensity, at DBMBF$_2$ conversion <15%, was used for calculating the moles of photons absorbed by DBMBF$_2$. The adduct formation was determined by GC analysis using an internal standard. Then the adduct quantum yield could be obtained as a mole ratio of the formed product to the absorbed photons.

The data are plotted as a relative adduct quantum yield $(\Phi/\Phi_o)_A$ versus the concentration of DBMBF$_2$ (Figure 2.4), where Φ_o is the quantum yield of adduct at [DBMBF$_2$] = 0.01 M and Φ refers to that at [DBMBF$_2$] = 0.03, 0.05 and 0.07 M. As can be seen, in dioxane the quantum yield of adduct formation between DBMBF$_2$ and CHD increases with the concentration of DBMBF$_2$.

Under similar conditions, the quantum yield of DBMBF$_2$ addition to 1,3-cycloocta-diene (9) was determined in dioxane and in methylene chloride. The obtained results showed a similar trend as the photoaddition reaction of 1,3-cyclohexadiene (1) (Figure 2.4).

However, in benzene, the photoaddition of DBMBF$_2$ to either 1 or 9 does not depend on the DBMBF$_2$ concentration (Figure 2.4). This result, combined with those of DBMBF$_2$ fluorescence quenching in benzene (Table 2.2), leads to the same conclusion: the singlet excited DBMBF$_2$ forms an exciplex with a ground state benzene molecule, and this acts as the principal reactive species even at the high concentration of DBMBF$_2$.

Finally it should be noted that, despite the variation of DBMBF$_2$ concentrations, the dimer formation of 1,3-cyclohexadiene showed the constant dimer quantum yield (Φ_D = 0.012 in benzene and 0.004 in dioxane) as well as the constant dimer distribution.
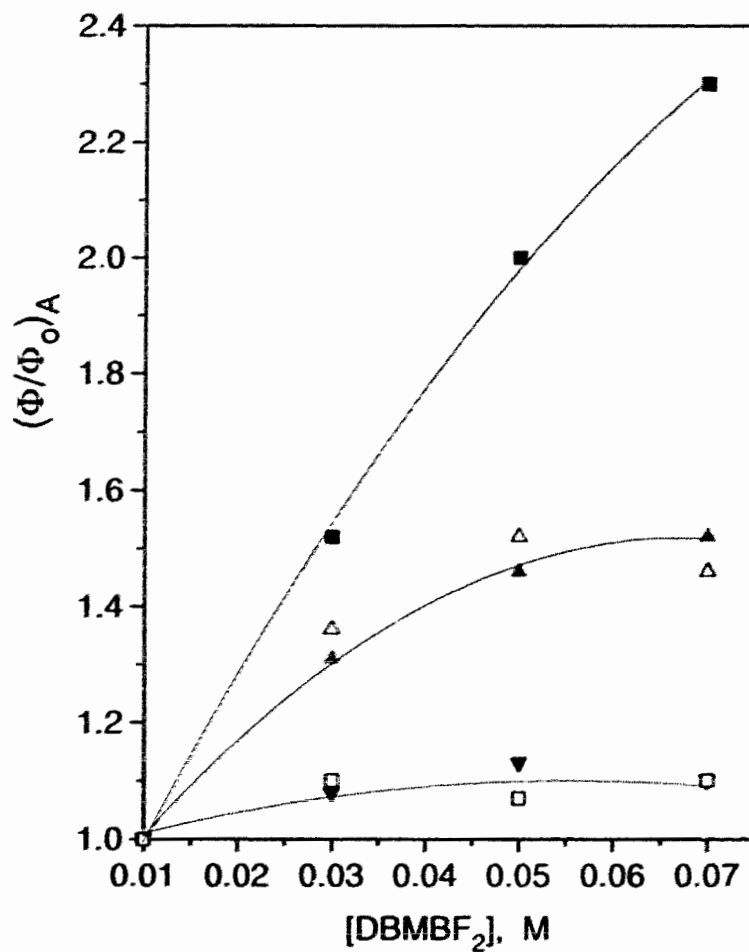
Fig. 2.4 Effect of DBMBF$_2$ concentration on the cycloaddition quantum yields (Φ_A) with cyclic dienes: with CHD in dioxane (■) and in benzene (□); with 1,3-COD in dioxane (▲), in CH$_2$Cl$_2$ (△) and in benzene (▼). Φ_0 refers to the adduct quantum yield at [DBMBF$_2$] = 0.01 M.

(c) Effect of 1,3-COD Concentration

Several Stern-Volmer constants (K_{SV}) of 1,3-COD have been obtained from fluorescence quenching studies. In dioxane, the quenching of singlet excited $DBMBF_2$ monomer produced the quenching constant $K_{SV}^m = 3.7 \ M^{-1}$ (Figure 2.1B). In benzene, the quenching of the $DBMBF_2$-benzene exciplex gave $K_{SV}^{ex} = 10.2 \ M^{-1}$ (Figure 2.3). These Stern-Volmer quenching constants can be also obtained from measurements of the adduct quantum yield as a function of the diene concentration, [1,3-COD].

Quantum yields for the photocycloaddition of $DBMBF_2$ to 1,3-COD were determined in dioxane and in benzene. The dioxane solution of $DBMBF_2$ (0.03 M), with the varying concentrations of 1,3-COD (0.063 – 1.0 M), was irradiated in a Rayonet Photoreactor for two hours with a 350 nm light source. The variation of adduct quantum yield with diene concentrations is shown in Table 2.5, and a double reciprocal plot of $1/\Phi_A$ vs. $1/[1,3\text{-COD}]$ is linear (Figure 2.5). From this plot, the Stern-Volmer quenching constant (K_{SV}^y) can be calculated according to equation 2.15 (in Section 2.2.5) as the ratio of the intercept to the slope. This leads to a value of $K_{SV}^y = 3.1 \ M^{-1}$ as the Stern-Volmer quenching constant of the photoreaction of $DBMBF_2$ with 1,3-COD in dioxane.

Benzene solutions of $DBMBF_2$ (0.03 M) and 1,3-COD (9, 0.063 – 1.5 M) were irradiated under similar conditions for 40 minutes. The plot of $1/\Phi_A$ versus $1/[1,3\text{-COD}]$, based on equation 2.16 (in Section 2.2.5), yields the value $K_{SV}^y = 10.3 \ M^{-1}$ for the $DBMBF_2$ - 1,3-COD photoreaction in benzene (Table 2.6 and Figure 2.5).

Table 2.5 Quantum yields of the photoaddition of $DBMBF_2$ to 1,3-COD in dioxane.[a]

[1,3-COD] M	$10^3\Phi_A$ of 12	1/[1,3-COD] M^{-1}	$(10\Phi_A)^{-1}$
0.063	1.28	15.9	78.1
0.077	1.63	13.0	61.3
0.10	1.98	10.0	50.5
0.14	2.61	7.14	38.3
0.30	3.22	3.33	31.1
1.0	5.98	1.0	16.7
2.0	8.74	0.50	11.4
K_{SV}^y			$3.1 \pm 0.6 \ M^{-1}$

Note: [a] A 3 mL dioxane solution of $DBMBF_2$ (0.03 M) and 1,3-COD (0.06 – 2 M) was purged with N_2 for 3.5 min and irradiated at 350 nm for 2 hrs. The $DBMBF_2$ conversion was less than 15%.
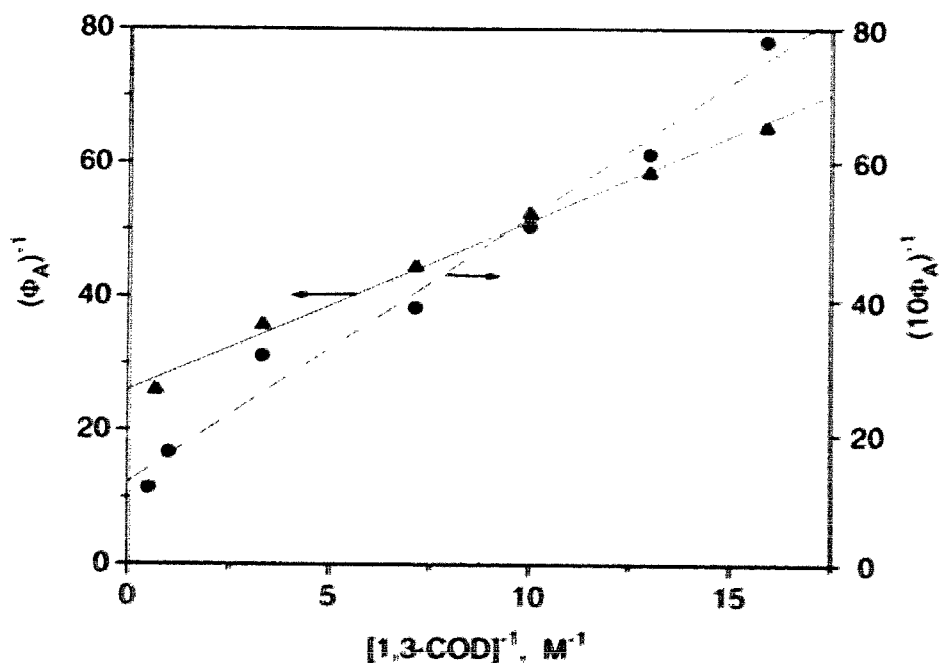
Fig. 2.5 Effect of 1,3-COD concentrations on the quantum yield (Φ_A) of adduct in dioxane (•) and in benzene (▲).

Table 2.6 Quantum yields of the photoaddition of DBMBF$_2$ to 1,3-COD in benzene solvent.[a]

[1,3-COD] M	$10^3 \Phi_A$ of 12	1/[1,3-COD] M^{-1}	$1 / \Phi_A$
0.063	15.3	15.9	65.3
0.077	17.1	13.0	58.5
0.10	19.1	10.0	52.4
0.14	22.5	7.14	44.4
0.30	28.0	3.33	35.7
1.5	38.6	0.67	25.9
K_{SV}^y		10.3 ± 0.6 M^{-1}	

Note: [a] A 2 mL benzene solution of DBMBF$_2$ (0.03 M) and 1,3-COD (0.06 ~ 1.5 M) was degassed with N$_2$ for 4 min and irradiated at 350 nm for 40 min. The DBMBF$_2$ conversion was less than 15%.

The Stern-Volmer constants for 1,3-COD, from the quenching of DBMBF$_2$ fluorescence (K_{SV}^f, in Table 2.1 and 2.2) and from measurements of the adduct quantum yield (K_{SV}^y, in Table 2.5 and 2.6), are listed in Table 2.7 for comparison. If the same intermediate is involved in fluorescence quenching and in adduct formation, then the values of K_{SV}^f and K_{SV}^y should be the same[39] (Section 2.2.5). The data in Table 2.7 show that the K$_{SV}$-values obtained by the two methods agree. This correlates the process of fluorescence quenching with that of adduct formation. In benzene, the quenching of DBMBF$_2$-benzene exciplex by 1,3-COD leads to the addition of DBMBF$_2$ to the diene, but in dioxane, the reaction of 1,3-COD with the singlet excited DBMBF$_2$ monomer is responsible for the adduct formation.

Table 2.7 Comparison of the Stern-Volmer quenching constants for the photoreaction of DBMBF$_2$ with 1,3-COD: K_{SV}^f refers to the fluorescence quenching and K_{SV}^y to the quantum yield measurements of adduct.

Solvent	K_{SV}^f (M^{-1})	K_{SV}^y (M^{-1})
benzene	10.2 ± 0.5^a 10.0 ± 0.3^f	10.3 ± 0.6^b 9.9 ± 1.0^f
dioxane	3.8 ± 0.2^c 3.7 ± 0.2^d	3.1 ± 0.6^e 4.4 ± 0.3^f

Notes: [a] At [DBMBF$_2$] = 5 x 10^{-6} M (Fig. 2.3); [b] At [DBMBF$_2$] = 0.03 M (Table 2.6); [c] At [DBMBF$_2$] = 0.03 M (Fig 2.2A); [d] At [DBMBF$_2$] = 5 x 10^{-6} M (Fig. 2.1B); [e] At [DBMBF$_2$] = 0.03 M (Table 2.5); [f] The results of repeated experiments.

(d) Effect of CHD Concentration

Quantum yields for the photoreactions of DBMBF$_2$ with CHD were determined as a function of the CHD concentration in deaerated benzene, p-xylene, THF and dioxane (Table 2.8), using the same procedure as that for the DBMBF$_2$-1,3-COD photoreactions. When a double reciprocal relationship of $1/\Phi_A$ vs. $1/[CHD]$ was examined by plotting the quantum yield data, linear and flat lines are obtained for the photoreactions in benzene, xylene and dioxane but a curve in THF (Fig. 2.6).

Examination of the data in Table 2.8 allows us to suggest the following:

(1) The quantum yield (Φ_A) of DBMBF$_2$ photoaddition to CHD appears to depend very little on the CHD concentration in the solvents benzene, xylene and dioxane; in THF, an increase in the CHD concentration causes the decrease of adduct quantum yield. The overall effect of increasing CHD concentrations is the quenching of adduct formation.

(2) The total dimer quantum yield (Φ_D) of CHD increases with the CHD concentration, and this increase of Φ_D is mainly due to the endo-[4+2] dimer 2.

Table 2.8 Quantum yields of the photoreaction of DBMBF$_2$ with CHD in different solvents: CHD concentration effect

in benzene

[CHD] M	$10^3\Phi_A$ of 6[a]	$10^3\Phi_D$ of CHD dimer			$10^3\Phi_A$ of 6[b]	$10^3\Phi_D$ of CHD dimer		
		(2 + 3)	(4 + 5)	2 : 3		(2 + 3)	(4 + 5)	2 : 3
0.5	18.4	18.8	6.1	2.6	26.5	13.1	4.4	2.6
0.3	18.0	14.4	4.5	2.6	25.9	11.1	6.0	1.8
0.1	18.5	6.9	6.1	1.6	25.9	6.3	6.0	1.2
0.05	19.2	4.5	6.4	1.2	28.2	6.5	7.1	1.1
0.02	18.9	2.1	4.9	0.5	22.1	3.2	6.6	0.5
0.009	17.6	1.3	4.7	~0	18.1	1.1	3.3	~0

The rightmost four columns are labelled **in p-xylene**.

Table 2.8 (continued)

in THF / **in dioxane**

[CHD] M	$10^3\Phi_A$ of 6[c]	$10^3\Phi_D$ of CHD dimer			[CHD] M	$10^3\Phi_A$ of 6[d]	$10^3\Phi_D$ of CHD dimer		
		(2+3)	(4+5)	2 : 3			(2+3)	(4+5)	2 : 3
1.0	2.8	11.3	11.9	1.3	1.0	6.3	9.4	5.6	2.0
0.3	3.6	2.7	4.3	0.7	0.3	5.0	2.1	3.7	0.75
0.1	5.5	1.1	1.9	0.4	0.14	5.5	1.4	2.9	0.36
0.05	7.0	0.4	1.0	0.2	0.10	5.5	2.1	5.8	0.23
0.02	9.2	0.3	0.7	~0.2	0.077	4.9	1.3	4.0	0.21
0.01	9.5	0.2	0.5	0	0.063	6.0	1.7	5.4	0.16

Notes: [a] A 3 mL benzene solution of DBMBF$_2$ (0.03 M) and CHD was irradiated at 350 nm for 30 min; [b] A 3 mL xylene solution of DBMBF$_2$ (0.03 M) and CHD was irradiated at 350 nm for 30 min. [c] A 2 mL THF solution of DBMBF$_2$ (0.20 M) and CHD was irradiated at 350 nm for 60 min; [d] A 3 mL dioxane solution of DBMBF$_2$ (0.05 M) and CHD was irradiated at 350 nm for 90 min.
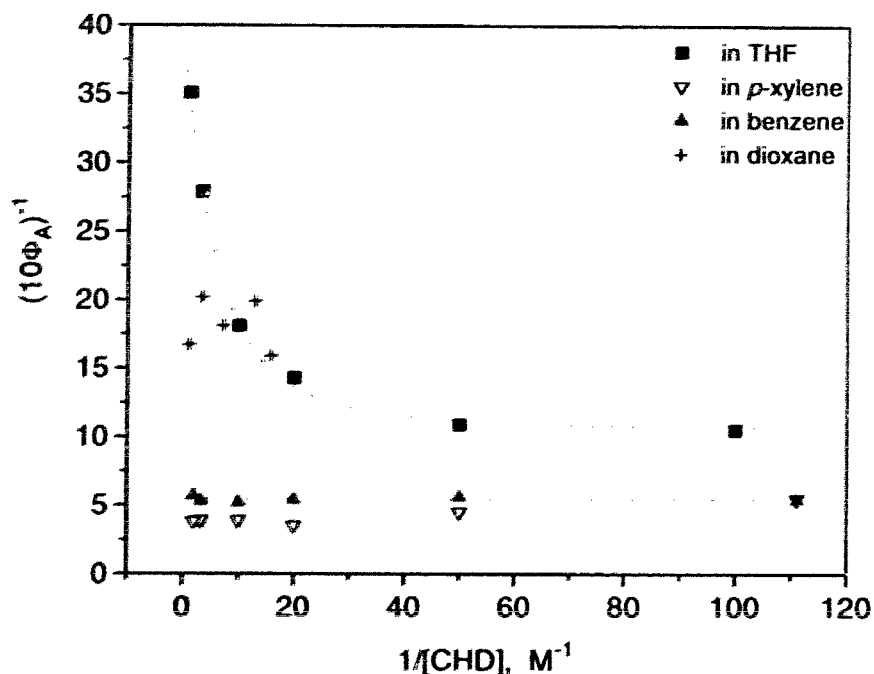
Fig. 2.6 Effect of the CHD concentration on the quantum yield of adduct in different solvents.

2.1.2 Photoreactions of DBMBF₂ with Vinyl Ethers[†]

2.1.2.1 The Photoreaction Profile

In acetonitrile, the photolysis of $DBMBF_2$ and phenyl vinyl ether (13, PVE) leads mainly to the sensitised dimerization of the vinyl ether. Only trace amounts of adduct are found. The dimerization proceeds via a head-to-head orientation to yield a mixture of cis- and trans-1,2-diphenoxycyclobutane (14 : 15 ≈ 6 : 4, in Eq. 2.5). Both dimers show a molecular ion at m/z = 240 as the base peak. The major dimer has the same ^{1}H NMR spectrum as the known cis-dimer (14).[64][65]

[†] This part of the work was carried out in co-operation with Mr. Matteo Vanossi, Pavia University, Italy. The results may also be reported in his thesis.

57

Eq. 2.5:

PhO

0.2 M
(13)

hv, 350 nm
→
CH₃CN

0.03 M DBMBF₂

□—OPh
|
□—OPh

(14)

+

□—OPh
|
□—''OPh

(15)

61 : 39
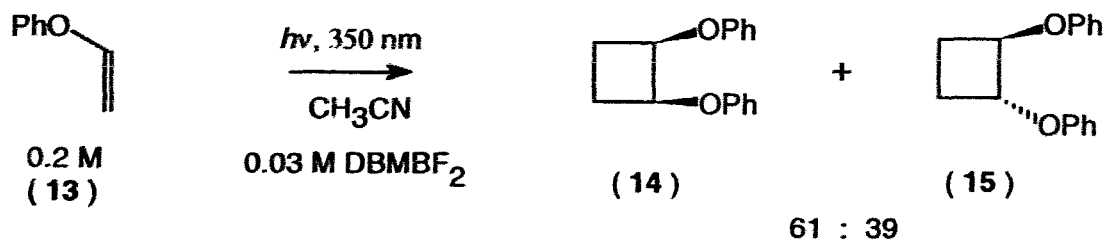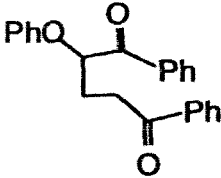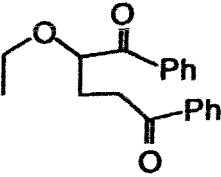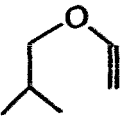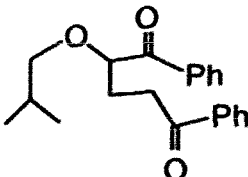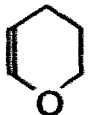
The photolysis of an ether solution of DBMBF₂ and a vinyl ether leads mainly to the adduct formation, shown in Eq. 2.6. The irradiation time, the conversion of DBMBF₂ and the isolated product yield are summarized in Table 2.9. The dimer of phenyl vinyl ether, under this condition, accounts for less than 2% of the products.

Eq. 2.6:

F   F
 \   /
  B
 / \
O   O
| |
Ph   Ph

0.018 M

+

RO

0.2 ~ 0.5 M

hv, 350 nm
→
ether

RO a   O
      \ ||
b   c—Ph
      /
     c—Ph
        ||
        O
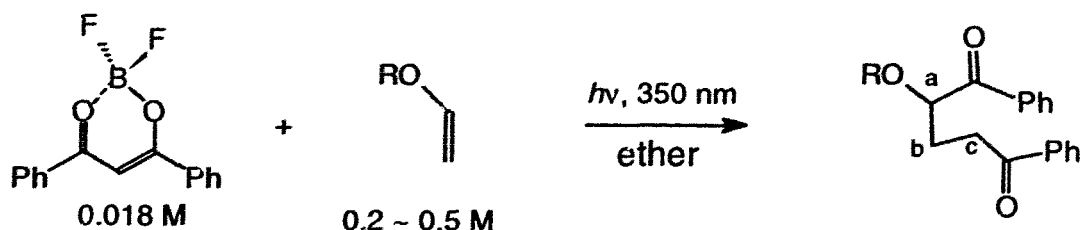
The adducts from alkyl vinyl ethers have similar EI-MS fragmentation patterns. In general, the parent ions were not detected and underwent cleavage to a benzoyl ion and a moiety of $m/z = 191$ (Scheme 2.1). The benzoyl ion usually accounted for the base peak and further eliminated a CO to give a phenyl ion. The $m/z = 191$ fragment underwent loss of an ethylene or isobutene (from the product of isobutyl vinyl ether), to yield the 3-benzoyl-1-propanol ion ($m/z = 163$), and / or loss of ether, to produce the fragment ion of $m/z = 117$. In the CI-MS spectrum, the adducts of alkyl vinyl ethers showed the parent ion (M + 1) as base peak, which then eliminated ethanol or 2-methyl-propanol to yield 1,5-diketone fragment of $m/z = 251$ (Scheme 2.1).

Table 2.9 Photocycloaddition of DBMBF$_2$ with vinyl ethers in ether solvent

Vinyl ether	Irradiation time (hr.)	Conversion of DBMBF$_2$ (%)	Product	Isolated yield(%)[a]
phenyl vinyl ether (13)	3.0	63	(16)	50[b]
ethyl vinyl ether (17)	3.7	40	(18)	79
isobutyl vinyl ether (19)	3.0	38	(20)	64[b]
3,4-dihydro-2H-pyran (21)	4.0	0	no adduct detected	--

Notes: [a] Based on consumed DBMBF$_2$; [b] Prepared by M. Vanossi.

(18, M = 296)

m/z = 297 (100%)

m/z = 251 (16%)

EtOH

m/z = 191 (19%)

-e

M+

CH₂=CH₂

m/z = 191 (96%)

m/z = 163 (10%)

Ph—C≡O⁺
m/z = 105 (100%)

CO

Et₂O

C_8H_5O]⁺
m/z = 117 (60%)

C₆H₅⁺
m/z = 77 (87%)
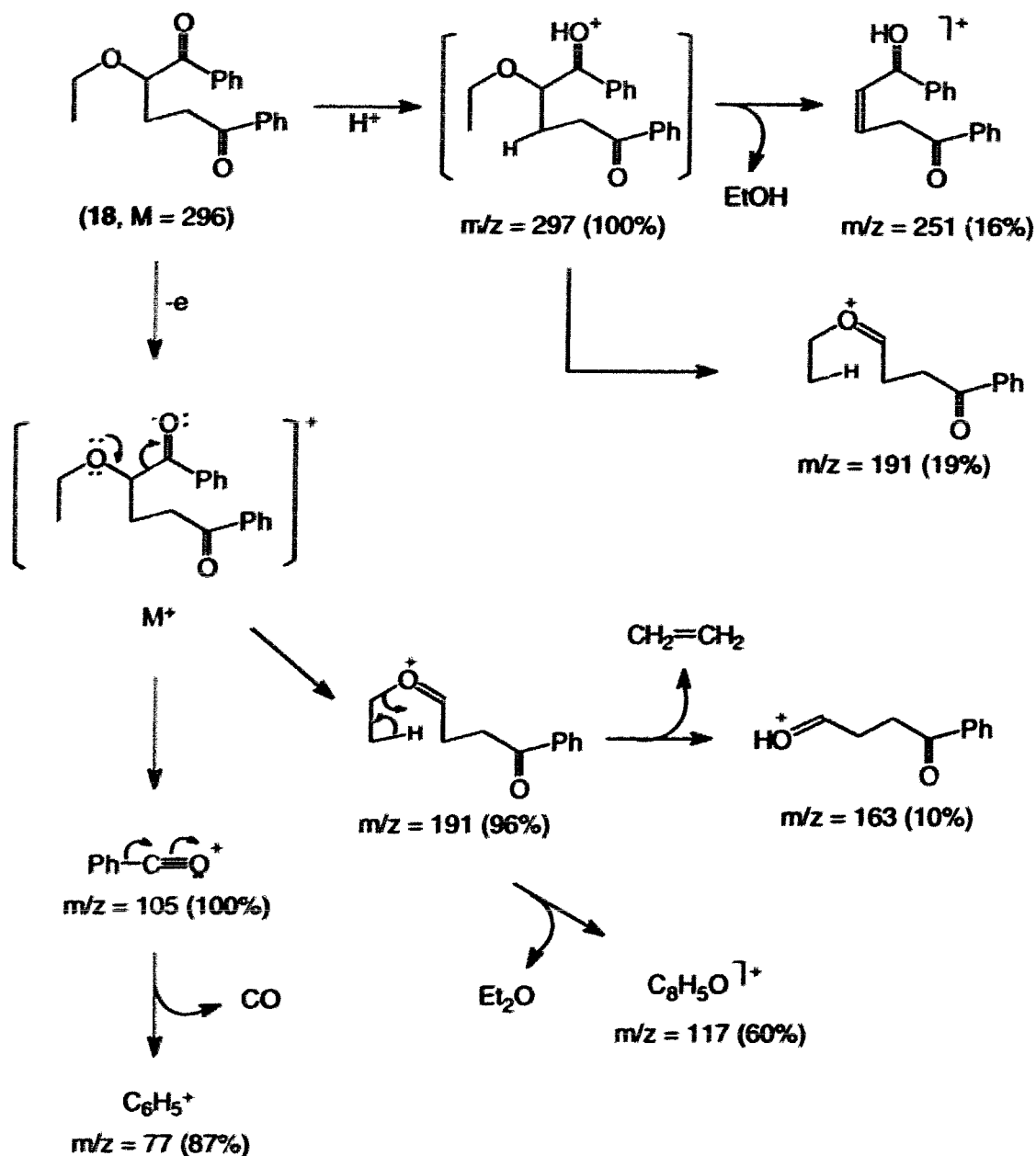
The adduct (16) from phenyl vinyl ether, in contrast to those from alkyl vinyl ethers, exhibited a parent ion peak in the EI-MS. Fragmentation of 16 proceeded by cleavage of a benzoyl fragment, followed by loss of carbon monoxide, ethyl phenyl ether and phenol (Scheme 2.2). The 3-benzoyl-1-propanol ion (m/z = 163) was not observed.

Scheme 2.2:
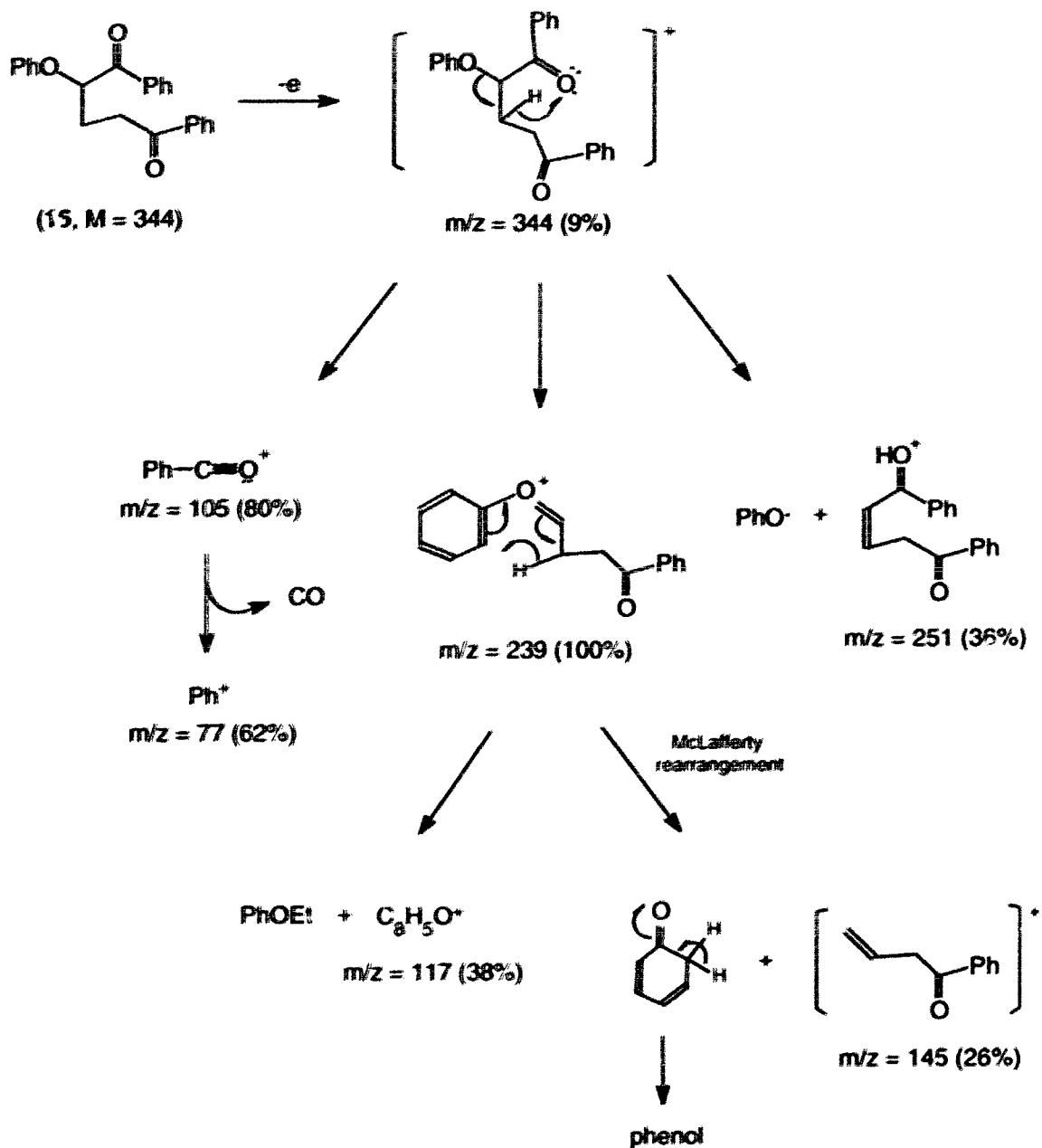
The addition products **18** and **20** from the two alkyl vinyl ethers have similar NMR spectra: (1) two singlet carbon peaks appeared at 200.4 and 199.6 ppm for the two carbonyl groups; (2) the methine carbons were around 81.7 ppm, deshielded by a neighbouring oxygen atom and a carbonyl group; and (3) this deshielding also shifted

the methine proton (H$_a$) to 4.7 ppm (Table 5.6). The connections of the benzoyl and phenacyl groups to the alkyl vinyl ethers were determined from the coupling of the methine proton (H$_a$) to its adjacent methylene protons: H$_b$ at 2.2 ppm with J$_{ab}$ = 9 Hz, and H$_{b'}$ at 2.4 ppm with J$_{ab'}$ ≈ 5 Hz (Table 5.6).

For the photoadduct **16** of DBMBF$_2$ to phenyl vinyl ether, the two carbonyl carbons were found at 199.27 and 198.13 ppm, and the methine carbon at 78.92 ppm. The methine proton (H$_a$) of adduct **16** appeared at 5.65 ppm with vicinal couplings to the methylene protons: H$_b$ at 2.34 ppm (J$_{ab}$ = 9.1 Hz) and H$_{b'}$ at 2.61 ppm (J$_{ab'}$ = 4.0 Hz).

The following discussion refers to byproducts of the reactions:

(1) Thermal reaction of 3,4-dihydro-2H-pyran (**21**)

The photolysis of DBMBF$_2$ with the dihydropyran **21** in several solvents did not lead to photoadducts, and the DBMBF$_2$ was recovered. GC analysis revealed that a product had formed, with a parent ion of m/z = 168 (M$^+$, 70) in EI-MS and 169 (M+1, 100) in CI-MS spectra. Further investigation showed that this was formed from a fast, dark reaction. This reaction could be accelerated by the addition of boron trifluoride etherate or retarded in THF or in the presence of 2,6-lutidine. The same product was also obtained by treatment of **21** (0.15 M) with boron trifluoride etherate (3 x 10^{-3} M) in acetonitrile. The product showed olefinic carbon absorptions at 141.42 and 114.15 ppm and a proton singlet at 6.68 ppm. The IR spectrum showed a strong C=C peak at 1667 cm^{-1} and was identical to that of the dimer **22**, prepared by treatment of the dihydropyran (**21**) with HBr.[82]
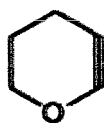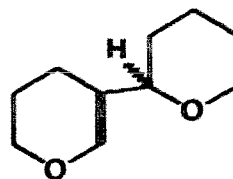
(21)   (22)

(2) Formation of 3,5-dioxa-2,6-diphenyltricyclo[2,2,1,0^{2,6}]heptane (23)

When DBMBF$_2$ (0.03 M) and ethyl vinyl ether (0.3 M) were irradiated in dioxane (30 mL), a crystalline product was isolated in 10% yield, in addition to the adduct **18** (24%). The crystalline compound had m/z = 250 (EI) and 251 (M+1, CI), and one set of phenyl peaks in the ^{1}H NMR and ^{13}C NMR spectra (Table 5.6). There was no carbonyl absorption in the IR and ^{13}C NMR spectra. The ^{13}C NMR (DEPT) spectra showed a quaternary carbon at 66.31 ppm, one CH$_2$ at 33.72 ppm and two CH groups at 19.24 and 96.56 ppm respectively. The CH at 96.56 ppm could be assigned to a carbon bonded to two oxygen atoms; the upfield shift of the second CH group suggested that it was part of a cyclopropane ring.[78a, 80] The ^{1}H-^{1}H connectivity of the four alkyl protons was determined by 2D-COSY NMR, and from the coupling patterns. The data are consistent with the cage structure **23**. The compound was also observed in the photolysis of DBMBF$_2$ and isobutyl vinyl ether in ether (4% yield) or in THF (4% yield). However, the compound was not formed in the absence of light, or when 2,6-lutidine was included in the photochemical reactions. It is believed that a zwitterionic intermediate, from the photoinduced electron transfer between the singlet excited DBMBF$_2$ and the vinyl ether, is probably involved in the formation of cage product **23**.

(23)
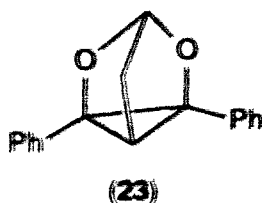
(3) Coupling reaction of DBMBF$_2$ / DBM with THF

The 5 hour irradiation of a 40 mL THF solution of DBMBF$_2$ (0.03 M) and isobutyl vinyl ether (**19**, 0.30 M) produced the major adduct **20** of DBMBF$_2$ to the vinyl ether (14%

yield), as well as two minor coupling products (11%). These were isolated and found to

be stereoisomers of **24**. The IR spectrum of each isomer showed a strong band at 3444

(24)
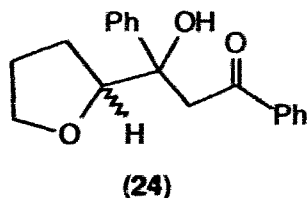
or 3470 cm^{-1} and a strong C=O stretch at 1668 cm^{-1}. The exchange with D$_2$O supported

the presence of OH group in **24**. ^{13}C NMR spectrum showed one carbonyl peak at ~202

ppm. The CI-MS spectrum showed a molecular ion at m/z = 297 (M+1). Under EI-MS

conditions, the molecular ion eliminated THF to yield dibenzoylmethane ion.

When only the THF solution of DBMBF$_2$ was irradiated, the formation of product

24 was found not to be affected by the presence of iodomethane or by oxygen.

However, a higher concentration of either DBMBF$_2$ or vinyl ether could depress the

coupling reaction. In addition, two facts should be also noted: (1) THF did not quench

the fluorescence of DBMBF$_2$ in acetonitrile. (2) The direct photolysis of dibenzoyl-

methane in THF also gave the product **24** although the yield was very low (3%, after 6

hours irradiation).

2.1.2.2 Steady State Fluorescence Quenching Studies

(a) Monomeric Fluorescence Quenching

The quenching of DBMBF$_2$ (5 x 10^{-6} M) fluorescence by vinyl ethers in THF

solvent was examined using the right-angle illumination technique (section 5.2).

Fluorescence quenching by ethyl vinyl ether and isobutyl vinyl ether is shown in Figure

2.7, together with the Stern-Volmer plots based on Eq. 1.16. The efficiencies (K_{sv}^{m}) of

quenching the excited DBMBF$_2$ monomer are summarised in Table 2.10.

(b) Excimer Fluorescence Quenching

The quenching of DBMBF$_2$ (0.20 M) fluorescence by vinyl ethers in THF was studied with the front-face illumination technique (section 5.2). The quenching of DBMBF$_2$ excimer by ethyl vinyl ether and isobutyl vinyl ether was analysed using the modified Stern-Volmer equation 1.18,[75b] in which the Stern-Volmer plot is obtained by plotting $(I^o/I)_{ex} \div (I^o/I)_{mon}$ versus the vinyl ether concentration. A linear relationship was observed with slope K_{SV}^{ex}. These linear plots and the fluorescence spectra are shown in Figure 2.8. The efficiencies (K_{SV}^{ex}) for quenching the DBMBF$_2$ excimer fluorescence are summarised in Table 2.10.

Table 2.10 Quenching efficiency of DBMBF$_2$ monomer (K_{SV}^{m}) and excimer (K_{SV}^{ex}) fluorescence by vinyl ethers in THF

Quencher	ethyl vinyl ether (17)	isobutyl vinyl ether (19)	phenyl vinyl ether (13)
K_{SV}^{m} (M^{-1}) [a]	2.3 ± 0.2	2.2 ± 0.2	3.4 ± 0.3
K_{SV}^{m} (M^{-1}) [b]	2.1 ± 0.2	2.3 ± 0.1	7.4 ± 1.0
K_{SV}^{ex} (M^{-1}) [b]	22.7 ± 0.4 (21.2 ± 0.6)	19.6 ± 0.3	17.0 ± 0.3

Notes: [a] [DBMBF$_2$] = 5 x 10^{-6} M, excited at λ_{ex} = 365 nm and monitored at λ_{mon} = 417 nm; [b] [DBMBF$_2$] = 0.20 M, excited at λ_{ex} = 365 nm and monitored at λ_{mon} = 440 nm for measuring K_{SV}^{m} and at λ_{mon} = 524 nm for measuring K_{SV}^{ex}.
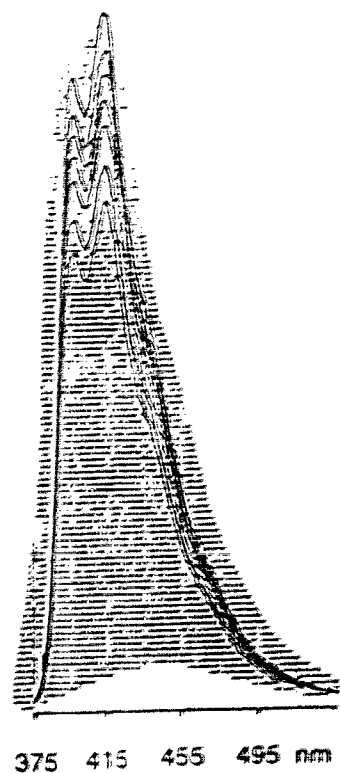
A: $K_{SV}^m = 2.3 \pm 0.2 \text{ M}^{-1}$
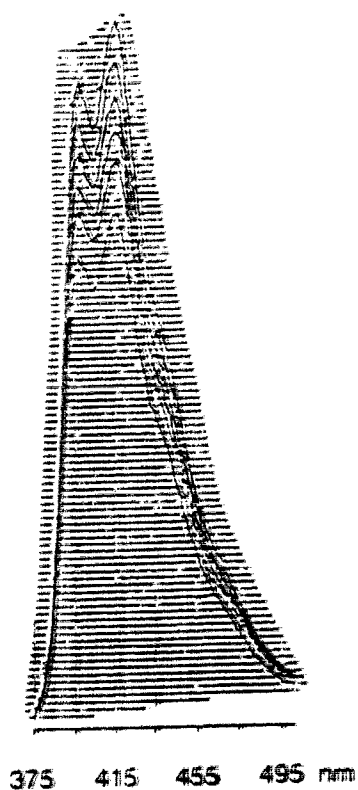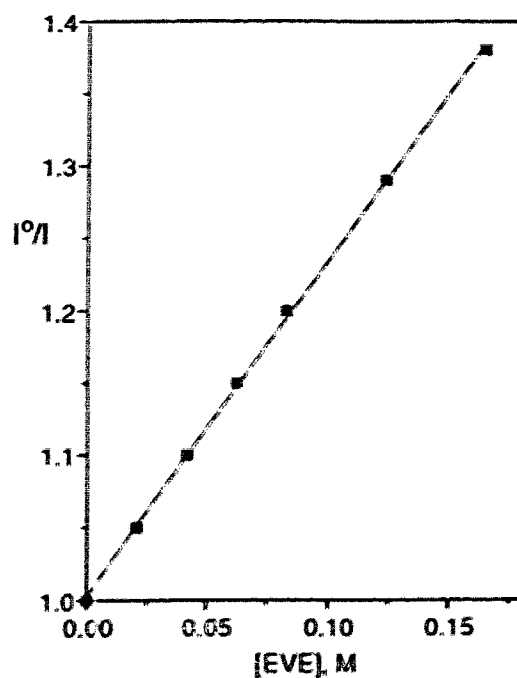
B: $K_{SV}^m = 2.2 \pm 0.2 \text{ M}^{-1}$
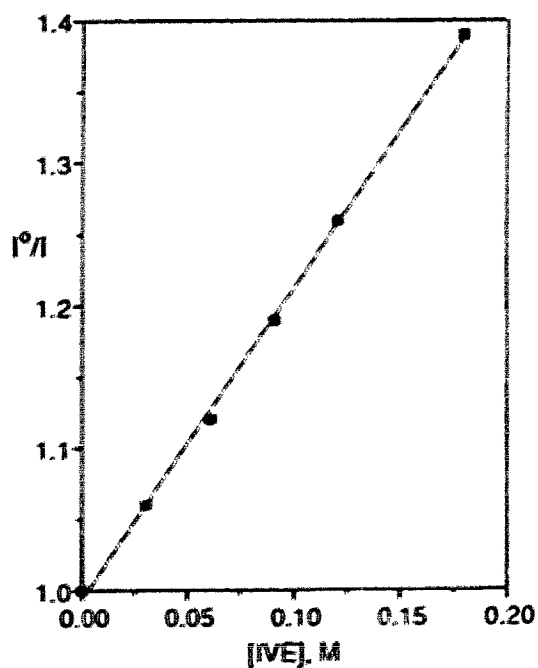
Fig. 2.7 The quenching of DBMBF$_2$ (5 x 10^{-6} M) fluorescence by vinyl ethers in THF, excited at λ_{ex} = 365 nm and monitored at λ_{moni} = 398 or 417 nm: (A) by EVE, $K_{SV}^m = 2.3 \pm 0.2 \text{ M}^{-1}$; (B) by IVE, $K_{SV}^m = 2.2 \pm 0.2 \text{ M}^{-1}$.

A: $K_{SV}^{ex} = 22.7 \pm 0.4$ M^{-1}
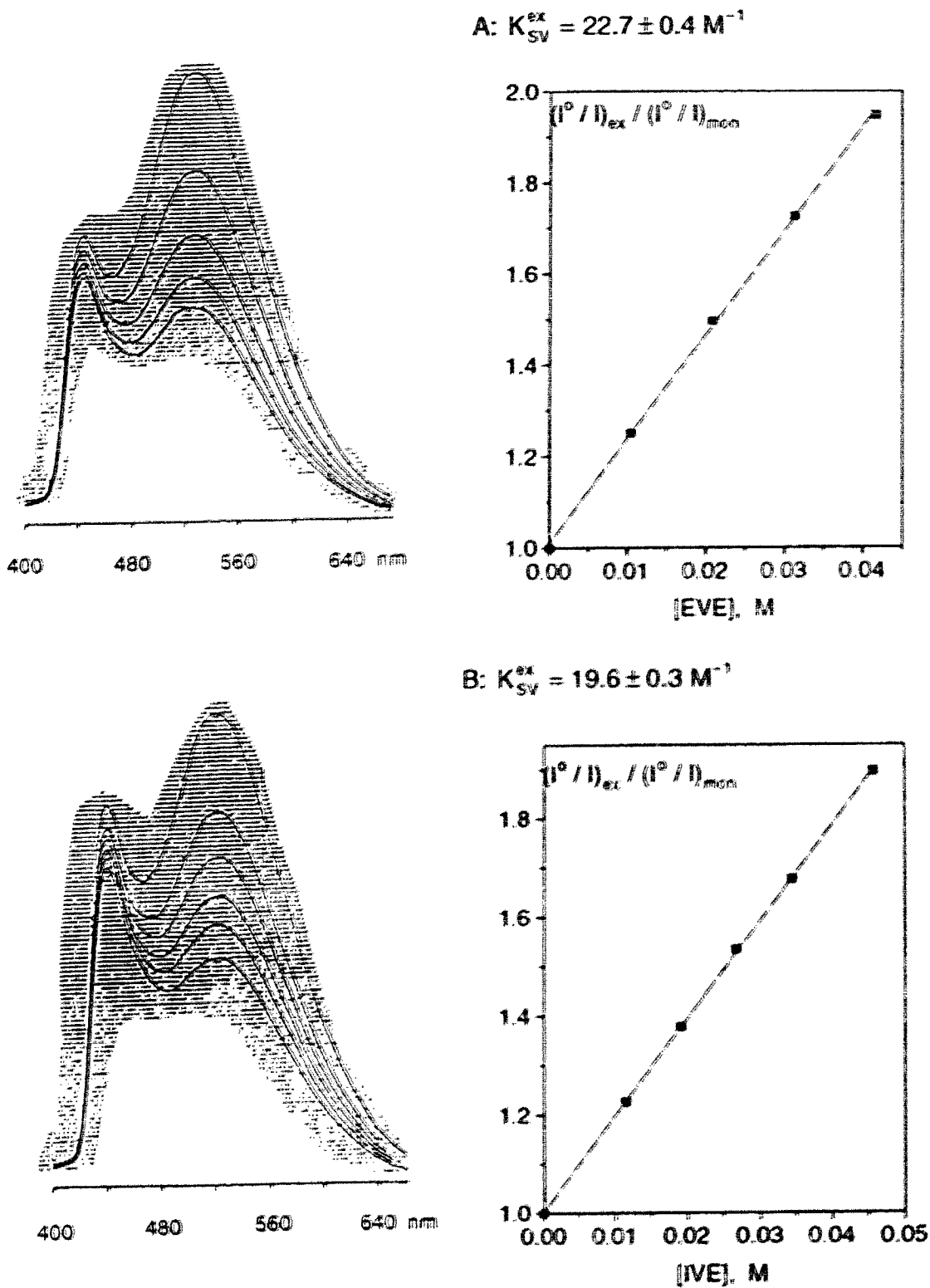
B: $K_{SV}^{ex} = 19.6 \pm 0.3$ M^{-1}

Fig. 2.8 The quenching of DBMBF$_2$ (0.20 M) fluorescence by vinyl ethers in THF, excited at λ_{ex} = 365 nm and monitored at λ_{moni} = 524 nm:

(A) by EVE, $K_{SV}^{ex} = 22.7 \pm 0.4$ M^{-1}; (B) by IVE, $K_{SV}^{ex} = 19.6 \pm 0.3$ M^{-1}.

2.1.2.3 Studies on the Photoreaction Quantum Yield

(a) Solvent Effect

A solvent effect, similar to that found in the DBMBF$_2$-cyclic diene system, was observed in the photoreaction of DBMBF$_2$ with vinyl ethers (Table 2.11). Quantum yields for the photoreaction of DBMBF$_2$ (0.03 M) with isobutyl vinyl ether (19, 0.30 M) or phenyl vinyl ether (13, 0.20 M) were determined in different solvents, using a Rayonet photoreactor equipped with a 350 nm light source. To avoid the thermal reaction of IVE,

Table 2.11 Quantum yields of the photoreaction of DBMBF$_2$ with isobutyl vinyl ether (IVE) and phenyl vinyl ether (PVE) in different solvents [a]

Solvent	ε	$10^2\Phi_A$ of Adducts		Dimers of PVE	
		from IVE	from PVE	$10^2\Phi_D$	14 : 15
CH$_3$CN	37.5	0.32	0.22	10.4	6 : 4
CH$_2$Cl$_2$	8.93	1.26	--	--	--
THF	7.58	0.96	1.69	0.29	--
dioxane	2.21	1.52	4.44	0.66	--
ether	4.34	2.52	8.83	1.40	5.3 : 1
benzene	2.27	4.37	10.7	1.11	22 : 3
toluene	2.40	4.90	13.0	--	--
p-xylene	2.27	4.15	16.2	1.87	9 : 1

Notes: [a] A 3 mL solution of DBMBF$_2$ (0.03 M) in the solvent was purged with N$_2$ for 4 min, and then the vinyl ether was added to an IVE concentration of 0.3 M or a PVE concentration of 0.2 M. Irradiation was usually conducted at 350 nm for 30 min, but the sample of PVE in an aromatic solvent was irradi ed for 15 min. The conversion of DBMBF$_2$ was less than 15%.

2,6-lutidine (1.1×10^{-3} M) was added before irradiation. The irradiation time was controlled to limit the percentage conversion of $DBMBF_2$ to less than 15%. The results in Table 2.11 showed that the dimerization of phenyl vinyl ether was dominant in the polar solvent acetonitrile, but in benzene solvents adduct formation predominated.

(b) $DBMBF_2$ Concentration Effect

The quantum yield for photoadditions of $DBMBF_2$ to vinyl ethers was determined in THF as a function of the $DBMBF_2$ concentration. Throughout the experiments, the concentration of vinyl ether was maintained at 0.30 M while that of $DBMBF_2$ was varied from 0.01 to 0.20 M. The results, summarized in Table 2.12, indicate that the quantum yield of adduct formation depends on the concentration of $DBMBF_2$.

Table 2.12 $DBMBF_2$ concentration effect on its photoaddition to
isobutyl vinyl ether (IVE) and ethyl vinyl ether (EVE) in THF

[$DBMBF_2$] M	$10^2\Phi_A$ of Adducts	
	from IVE	from EVE
0.01	0.89	1.59
0.03	1.03	2.02
0.05	1.18	2.42
0.07	1.36	2.71

Notes: [a] A 3 mL solution of IVE (0.3 M) with varying concentrations of $DBMBF_2$ was purged with N_2 for 4 min at $-6\,°C$ and irradiated at 350 nm for 30 min. In the photolysis of EVE (0.3 M), the vinyl ether was added by injection after the $DBMBF_2$ solution had been deaerated.

(c) Vinyl Ether Concentration Effect

The quenching of DBMBF$_2$ excimer fluorescence by cyclic dienes or vinyl ethers suggested the involvement of the excimer serving as a reactive species in the photoreactions of DBMBF$_2$. To correlate the quenching of excimer fluorescence with the photoreactions, the adduct quantum yield was studied as a function of substrate concentrations.

The THF solution of DBMBF$_2$ (0.20 M) and varying concentrations of ethyl vinyl ether (EVE, 0.063 – 0.57 M) was irradiated at 350 nm in a Rayonet photoreactor for 35 minutes. The incident light intensity was determined using the benzophenone-benzhydrol actinometer.[80] GC analysis showed that the major product arose from the photoaddition of DBMBF$_2$ to EVE, while only a trace of the by-product **24** was detected. The analysis also showed that the adduct quantum yield increased with an increase in the concentration of EVE (Table 2.13). The Stern-Volmer plot of $1/\Phi_A$ *versus* $1/[EVE]$ (Eq. 2.17A in section 2.2.5) was linear, giving an intercept-slope ratio as $K_{SV}^y = 18.4$ M^{-1} (Fig. 2.9).

The quantum yields for the photoaddition of DBMBF$_2$ (0.20 M) to isobutyl vinyl ether (IVE, 0.076 – 0.57 M) were determined in a 30 min irradiation time. The data are listed in Table 2.14, and the double reciprocal plot of $1/\Phi_A$ *versus* $1/[IVE]$ yielded $K_{SV}^y = 14.5$ M^{-1} calculated according to Eq. 2.17A (Fig. 2.10).

Table 2.13 Quantum yields of the photoaddition of DBMBF$_2$ (0.2 M) to EVE in THF: ethyl vinyl ether (EVE) concentration effect.

[EVE] M	$10^2\Phi_A$ of 18	1/[EVE] M^{-1}	$1/\Phi_A$
0.063	1.99	15.87	50.3
0.11	2.53	9.09	39.5
0.19	2.78	5.26	36.0
0.57	3.46	1.75	28.9
K_{SV}^y			18.4 ± 1.6
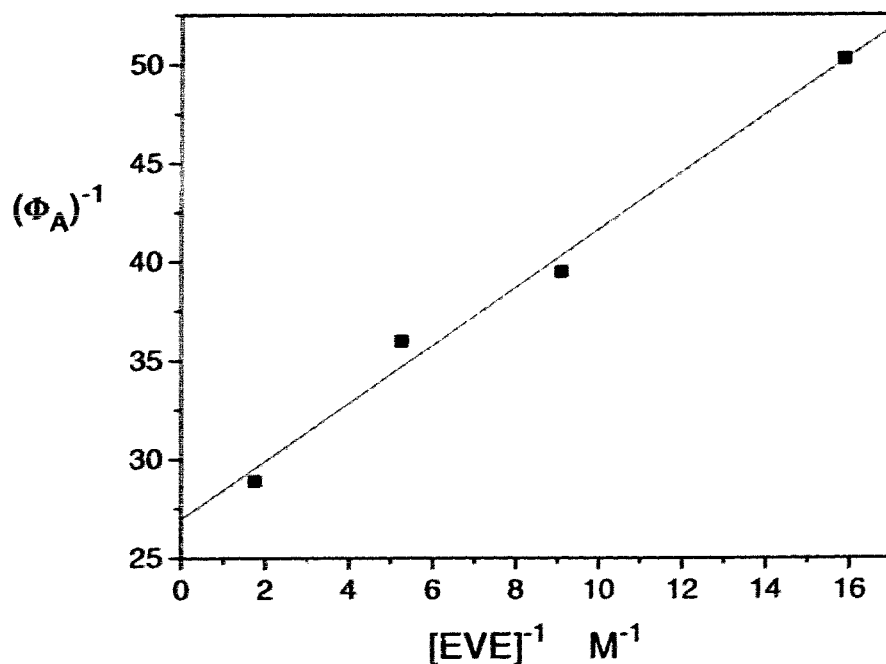
Fig. 2.9 Stern-Volmer plot of $1/\Phi_A$ vs. 1/[EVE] for the cycloadditon of DBMBF$_2$ to ethyl vinyl ether in THF.

Table 2.14 Quantum yields of the photoaddition of DBMBF$_2$ to IVE in THF: isobutyl vinyl ether (IVE) concentration effect.

[IVE] M	$10^2\Phi_A$ of **20**	1/[IVE] M^{-1}	$1/\Phi_A$
0.076	1.67	13.17	59.8
0.11	2.09	9.09	47.9
0.19	2.42	5.26	41.3
0.57	2.86	1.75	35.0
K_{SV}^y			14.5 ± 1.3
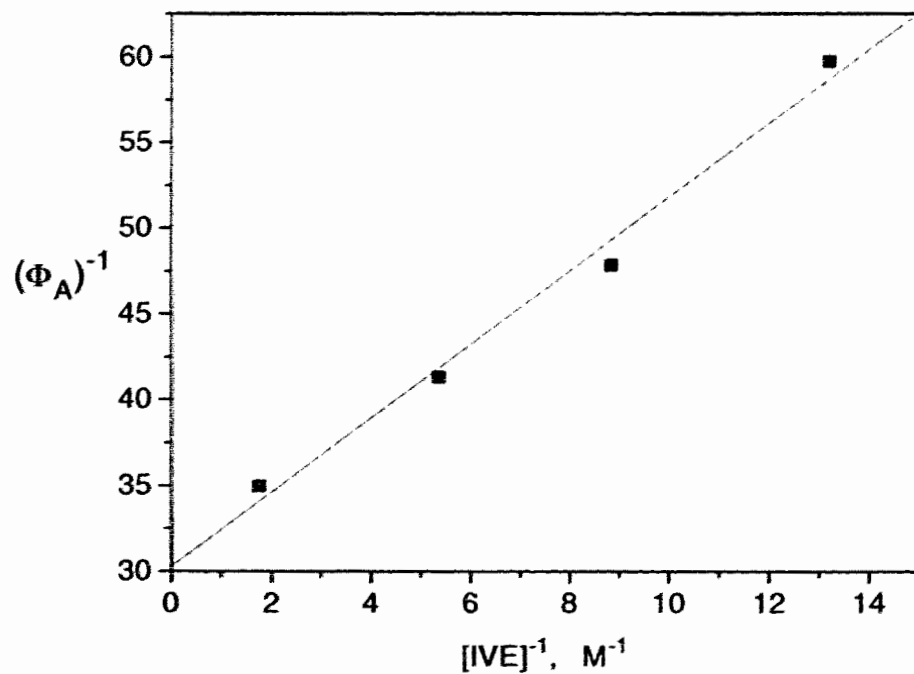
Fig. 2.10 Stem-Volmer plot of $1/\Phi_A$ vs. 1/[IVE] for the cycloadditon of DBMBF$_2$ to isobutyl vinyl ether in THF.

All of the Stern-Volmer quenching constants (K_{SV}) of the DBMBF$_2$-vinyl ether systems are summarized in Table 2.15. The constant K_{SV}^m was obtained from the fluorescence quenching of excited DBMBF$_2$ monomer (at [DBMBF$_2$] = 5 x 10^{-6} M) according to Eq. 1.16. K_{SV}^{ex} was derived from the fluorescence quenching of DBMBF$_2$ excimer (at [DBMBF$_2$] = 0.2 M) according to Eq. 1.18, and also at this concentration of DBMBF$_2$, K_{SV}^y was determined from the measurements of the adduct quantum yield according to Eq. 2.17A. In examination of Table 2.15, it is noticeable that the value of K_{SV}^y is comparable to K_{SV}^{ex} at the high concentration of DBMBF$_2$ (0.20 M). This indicates that the excimer fluorescence quenching is related to the adduct formation, namely at [DBMBF$_2$] = 0.20 M, the photocycloaddition of DBMBF$_2$ to vinyl ethers is dominated by an excimer mediated reaction.[63b]

Table 2.15   Comparison of Stern-Volmer quenching constants

Vinyl ethers	K_{SV}^m, M^{-1}	K_{SV}^{ex}, M^{-1}	K_{SV}^y, M^{-1}
EVE, 17	2.3 ± 0.2 [a]	22.7 ± 0.4 [a]	18.4 ± 1.8 [b]
		21.2 ± 0.6 [a]	17.5 ± 1.5 [d]
IVE 19	2.2 ± 0.2 [a]	19.6 ± 0.3 [a]	14.5 ± 1.3 [c]
			18.7 ± 3.0 [d]
PVE, 13	3.4 ± 0.3 [a]	17.0 ± 0.3 [a]	14.6 ± 2.6 [e]

Notes: [a] Data from Table 2.10; [b] From Table 2.13; [c] From Table 2.14; [d] The repeated experiment results; [e] From Table 5.11.

2.2 Discussion

2.2.1 An Overview

The photolysis of $DBMBF_2$ with 1,3-cyclohexadiene (CHD) or phenyl vinyl ether (PVE) resulted in the formation of products in two types: the sensitized dimerization of CHD or PVE and the cycloaddition of $DBMBF_2$ to the diene or vinyl ether. The products are dependent on the solvent (Tables 2.3 and 2.11). In acetonitrile, the excitation of $DBMBF_2$ in the presence of CHD leads mainly to a radical cation [4 + 2] dimerization of the diene, and a trace amount of triplet CHD [2 + 2] dimerization. The radical cation CHD^+ is thought to be formed by single electron transfer from the diene to the singlet excited state of $DBMBF_2$,[50a] as in the Diels-Alder dimerization of CHD under PET conditions (Table 1.1).[27a, 36, 40] This electron transfer is consistent with expectation from the Rehm-Weller equation:[5, 88]

$$\Delta G_{ET} = E_D^{ox} - (E_A^{red} + E_S) + C \qquad \text{(Eq. 2.7)}$$

where E_D^{ox} is the oxidation potential of CHD, E_A^{red} is the reduction potential of $DBMBF_2$, E_S is the singlet energy of excited $DBMBF_2$, and C is the interaction energy of the ion pair formed at an encounter distance a = 7 Å (-0.06 eV in CH_3CN).[4]

Table 2.16 Physical Constants of Cyclic Dienes and $DBMBF_2$

	E_{red}, (V)[a]	E_{ox}, (V)[a]	E_S, (eV)	E_T, (eV)
$DBMBF_2$	-0.91[b]	2.45[b]	3.19[b]	2.69[b]
CHD	--	1.58[c,d] 1.53[e]	3.25[f] 4.21[g]	2.29[h]
1,3-COD	--	1.89[d]	--	3.04 - 3.17[i]
PVE	--	1.62[j]	--	--

Notes: [a] vs. SCE in acetonitrile; [b] Ref. 58a; [c] Ref. 83a; [d] Ref. 14; [e] Ref. 38a; [f] Ref. 3; [g] Ref. 87; [h] Ref. 36b, 87 and 79; [i] Ref. 79; [j] Ref. 28b.

Phenyl vinyl ether (PVE) is also an electron-rich alkene whose radical cation mediated [2+2] dimerization has received much attention.[33, 32, 26, 35b] A chain reaction of PVE[+] is reported to occur upon sensitization of the singlet excited 9,10-dicyanoanthracene in acetonitrile (Scheme 1.2).[26c] Other photoinduced dimerizations of vinyl ethers, such as ethyl vinyl ether (EVE), has been accomplished using 1,4-dicyanonaphthalene or 1,4-dicyanobenzene as the acceptor sensitizer.[45] With the sensitization by DBMBF$_2$, PVE gave the [2+2] dimers **14** and **15** as the major products in acetonitrile. Since the dimer ratio followed a known product pattern of the reported chain reaction (Eq. 1.7),[26] it appears that the PVE radical cation is generated in the reaction of singlet excited DBMBF$_2$ with PVE in acetonitrile.

The yield of DBMBF$_2$ sensitized dimerization decreases with a decrease in the solvent polarity (Tables 2.3 and 2.11). Since the *endo*-[4+2] dimerization of CHD is the major route of radical ion reaction, its yield is reduced sharply on going from the polar solvent acetonitrile to the less polar solvent ether. In the less polar solvents, the main reaction becomes the photocycloaddition of DBMBF$_2$ to CHD.

Scheme 2.3:

75
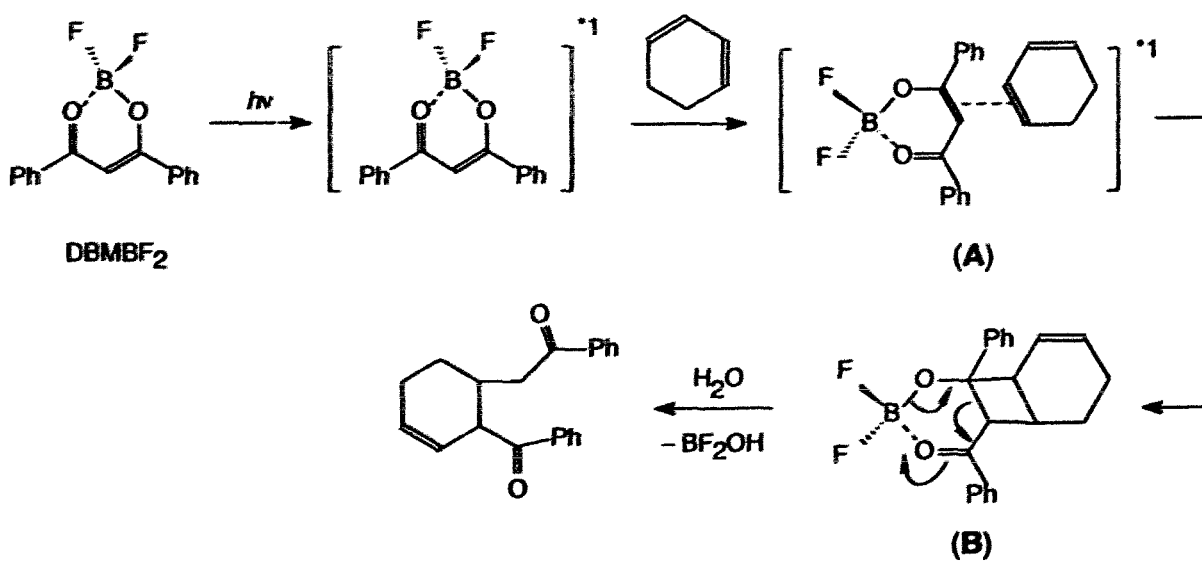
Scheme 2.3 is proposed to describe the photocycloaddition of DBMBF$_2$ to cyclic dienes (or vinyl ethers). The photocycloaddition proceeds via A, an exciplex between singlet excited DBMBF$_2$ and the ground state olefin, which then is converted to the cycloadduct B. Hydrolysis of B produces the 1,5-diketone product. Adducts containing a stable cyclobutane ring have been isolated in the photoaddition of enaminoketonato-boron difluoride, a DBMBF$_2$ analogue, to trans-stilbene.[89]
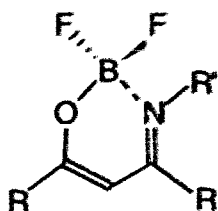
Enaminoketonatoboron Difluoride:

R = R = phenyl, a DBMBF$_2$ analogue

R' = alkyl and phenyl

The singlet excited state of DBMBF$_2$ can be quenched by cyclic dienes and vinyl ethers at the diffusion controlled rate.[49] The quenching process is related to the photocycloaddition to DBMBF$_2$. Thus, a similarity between the Stern-Volmer constants obtained from the quenching of DBMBF$_2$ fluorescence by 1,3-COD (K_{SV}^f) and from measurements of the adduct quantum yield (K_{SV}^y, in Table 2.7) has been observed. From these K_{SV} - values, the rate constant (k_q) of quenching the singlet excited DBMBF$_2$ by 1,3-COD can be calculated. For example, the $K_{SV}^f = 3.7$ M^{-1} of fluorescence quenching in dioxane (Table 2.7) leads to the rate constant $k_q = 1.1 \times 10^{10}$ M^{-1}s^{-1} by using Eq. 1.16 in Section 1.6.1; the $K_{SV}^y = 3.1$ M^{-1} from measuring the adduct quantum yields in dioxane (Table 2.7) leads to $k_q = 1.0 \times 10^{10}$ M^{-1}s^{-1}, according to Eq. 2.15A in Section 2.2.5. The two different measurements produce the comparable k_q - values (Table 2.17). This supports the contention of Scheme 2.3 that the photoaddition is initiated by collision of the singlet excited state of DBMBF$_2$ with 1,3-COD.

Table 2.17 Comparison of quenching rate constants

in the DBMBF$_2$-1,3-COD photoreaction [a]

Sovlent	Quenching rate constant (k_q, M^{-1}s^{-1})	
	from quenching fluorescence	from measuring adduct formation
Dioxane	$(1.1 \pm 0.1) \times 10^{10}$ [b]	$(1.0 \pm 0.2) \times 10^{10}$ [c]
THF	$(2.4 \pm 0.3) \times 10^{10}$ [d]	$(2.9 \pm 0.4) \times 10^{10}$ [e]

Notes: [a] k_q is calculated according to Eq. 1.16 or Eq. 2.15A from the corresponding K_{SV}-

data, where $\tau_a = 0.34$ ns and $k_m = 2 \times 10^{10}$ M^{-1}s^{-1}; [b] From $K_{SV} = 3.7$ M^{-1} with

[DBMBF$_2$] = 5×10^{-6} M (Table 2.7); [c] From $K_{SV} = 3.1$ M^{-1} with [DBMBF$_2$] = 0.03 M

(Table 2.7); [d] From the $K_{SV} = 8.1$ M^{-1} with [DBMBF$_2$] = 5×10^{-6} M (Fig. 2.1);

[e] From $K_{SV} = 4.2$ M^{-1} with [DBMBF$_2$] = 0.2 M (Table 5.10).

Upon the quenching of singlet excited DBMBF$_2$ by a cyclic diene or vinyl ether,

one of the possible consequences would be formation of an exciplex between the

excited DBMBF$_2$ and the donor olefin (Scheme 2.3). The existence of exciplexes and

excimers was demonstrated by Förster[11, 23b] and Weller long ago,[8] but the intervention

of these species in photocycloaddition reactions was not established until the 1970's.[16]

Since then, exciplexes have often been postulated as intermediates in donor-acceptor

photoreactions.[2, 9, 75b, 16] Since the photoadditions of DBMBF$_2$ to simple olefins have

been postulated to proceed via an exciplex mechanism,[50] it is logical to postulate the

participation of the DBMBF$_2$-diene or vinyl ether exciplexes in the photoreactions.

The exciplex mediated cycloaddition reactions are often concerted and give the

product with specific stereochemistry that is determined more by π-orbital overlap than

by steric effects.[9a,b] Our observations of DBMBF$_2$ photoadditions to electron donor olefins are consistent with the properties of an exciplex reaction. For example in the photoreaction of DBMBF$_2$ with 1,3-cyclohexadiene (CHD), the head-to-head addition product should result from a face-to-face configuration of the DBMBF$_2$ - CHD exciplex intermediate with the most π-orbital overlap.

head-to-tail
orientation

head-to-head
orientation
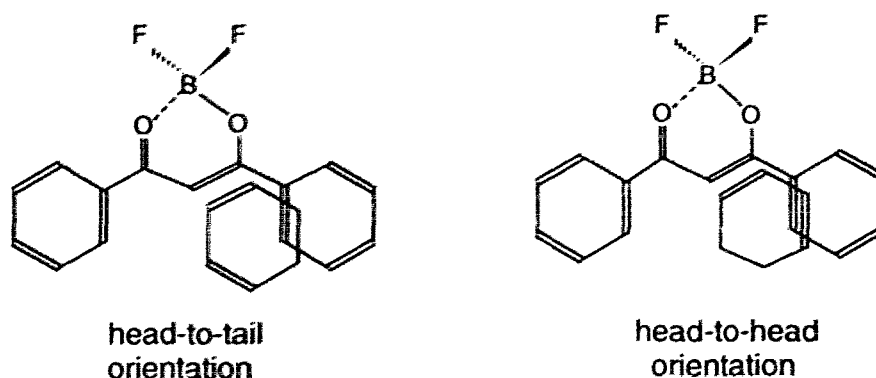
As a complication to the exciplex mechanism, the photoaddition of DBMBF$_2$ to CHD is found to be quenched by increasing the CHD concentration (Fig. 2.6). This concentration increase also promotes the endo-[4+2] dimerization of CHD even in the less polar solvents, such as xylene, benzene, dioxane and THF (Table 2.8). Schuster et al. have reported the similar observation in the 1,4-dicyanonaphthalene (DCN) sensitized dimerization of CHD, where the increase of CHD concentrations yielded more endo-[4+2] dimer in benzene.[37d] Because the radical cation CHD$^+$ is not formed by sensitization of DCN in this nonpolar solvent, the endo-[4+2] dimerization of CHD is suggested to proceed via a triplex intermediate, *DCN-CHD-CHD, and the formation of the triplex is through interception of the DCN-CHD exciplex by CHD.[37d, 42, 90] Similar triplex formation in CHD dimerization, sensitized by 9,10-dicyanoanthracene in CH$_2$Cl$_2$, was also suggested at high substrate concentrations.[27a, 36c] Our observations of the

CHD concentration effect on DBMBF$_2$ photoreactions (Table 2.8) are consistent with the DCN-CHD reaction patterns. In the solvent xylene, benzene, dioxane or THF, the enhanced *endo*-[4+2] dimerization of CHD may similarly result from a triplex intermediate, *DBMBF$_2$-CHD-CHD. To form this triplex, the DBMBF$_2$-CHD exciplex should be intercepted by CHD, and the interception quenches the formation of adduct.

2.2.2 Intermediacy of the DBMBF$_2$-Benzene Exciplex: (*AR)

Exciplexes of cyanoarene compounds as electron acceptors with alkylbenzenes as donors have been the subject of recent interest.[15, 19, 91, 92] It is noteworthy that quenching of singlet excited DBMBF$_2$ (5 x 10^{-6} M) by benzene, toluene and xylene in acetonitrile also leads to a strongly emissive exciplex (*AR).[58, 63, 64a] In neat benzene, toluene or xylene, the exciplex emission spectrum is observed as a red-shifted, strong and structureless fluorescence band. The DBMBF$_2$-arene exciplexes are characterized by a longer lifetime (2.1 ns in benzene and 15 ns in xylene) and higher fluorescence quantum yield (Φ_f = 0.44 in benzene and 0.59 in xylene).[58, 63] Consequently, in studies of the photoreaction of DBMBF$_2$ with cyclic dienes or vinyl ethers in aromatic solvents, the properties of *AR must be taken into account.

Excitation of DBMBF$_2$ in benzene leads first to the singlet excited DBMBF$_2$ (*A) which may react in several ways (Scheme 2.4). In the absence of cyclic dienes or vinyl ethers and at [DBMBF$_2$] = 5 x 10^{-6} M, the long lived exciplex *AR is the principal excited species. In the presence of the donor olefin, the mole ratio of benzene (11.3 M) : DBMBF$_2$ (0.03 M) : olefin (0.3 M) is estimated to be 100 : < 0.3 : < 3 for the typical photoreaction run in benzene solvent. Still we would expect that the exciplex *AR

$$A \xrightarrow{h\nu} {}^*A \longrightarrow
\begin{cases}
\xrightarrow{R,\, k_e} {}^*AR & \text{exciplex formation: } k_e[{}^*A][R] \\[6pt]
\xrightarrow{D,\, k_y} {}^*A\text{----}D & \text{encounter complex: } k_x[{}^*A][D] \\[6pt]
\xrightarrow{A,\, k_m} {}^*AA & \text{excimer formation: } k_m[{}^*A][A] \\[6pt]
\xrightarrow{k_d} A & \text{unimolecular decay: } k_d[{}^*A]
\end{cases}$$
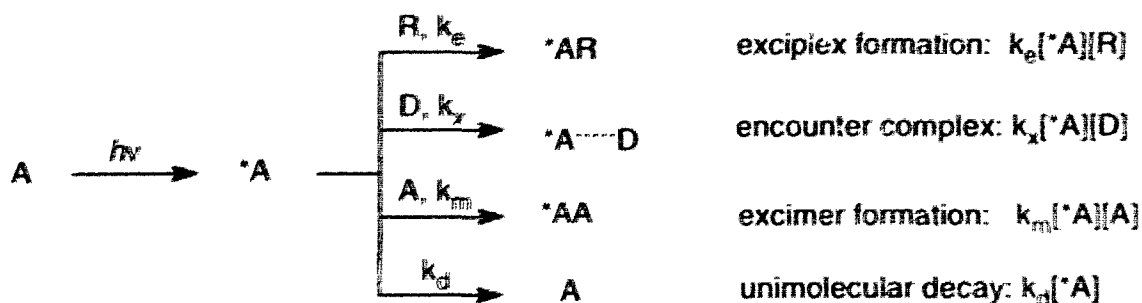
$A = DBMBF_2$; D = Diene, Vinyl ether; R = Arene compound.

should be the principal species for the photoreactions. The following results are obtained to support the intermediacy of the $DBMBF_2$-arene exciplex:

(1) The fluorescence quenching of $DBMBF_2$-benzene exciplex by cyclic dienes is not affected by the change of $DBMBF_2$ concentrations (Table 2.2), indicating that the $DBMBF_2$-benzene exciplex is the principal species in benzene.

(2) Also in benzene, $DBMBF_2$ photoadditions to the cyclic dienes did not show any dependency upon $DBMBF_2$ concentrations (Table 2.4). This finding, combined with the results in Table 2.2, suggests the dominant role of ${}^*AR$ to react with the olefins by suppressing the ${}^*AA$ formation (Scheme 2.4).

(3) The fluorescence quenching and the photoaddition of $DBMBF_2$ in benzene can be correlated by comparing the Stern-Volmer constants: the $K_{SV}^f = 10.2$ M^{-1} from quenching the ${}^*DBMBF_2$ - benzene exciplex fluorescence by 1,3-COD, and the $K_{SV}^y = 10.3$ M^{-1} from examining quantum yields for the $DBMBF_2$ photoaddition to 1,3-COD in benzene (Table 2.7). From these K_{SV}-values, the rate constant k_q of quenching the $DBMBF_2$-benzene exciplex by 1,3-COD can be calculated. Using the relationship of $K_{SV}^f = k_q \tau_{AR}$ where $\tau_{AR} = 2.1$ ns as the exciplex lifetime, thus the $K_{SV}^f = 10.2$ M^{-1} leads to

$k_q = 4.9 \times 10^9$ M^{-1}s^{-1} and the $K_{SV}^y = 10.3$ M^{-1} leads to $k_q = 5.0 \times 10^9$ M^{-1}s^{-1}. This consistency in k_q-values presents a clear demonstration that, in benzene, the photoaddition of DBMBF$_2$ to 1,3-COD occurs primarily from the DBMBF$_2$-arene exciplex *AR (Scheme 2.4).

Although the reaction of DBMBF$_2$-benzene exciplex with cyclic dienes results in adduct formation, it is not known whether a triplex is formed during this reaction process. A triplex can be formed through the reaction of excimers or exciplexes.[9a, 9e, 16, 93] For example, the triplex *(ST-ST-F) was proposed in the reaction of trans-stilbene excimer *(ST-ST) with dimethyl fumarate (F).[9c, d] In other examples, the quenching of an exciplex *(AD) by the same molecule D [97d, 90, 91c, 93, 94] or a different one[95] also resulted in the formation of triplex. However, the reaction of exciplex substitution was also reported in the quenching of an exciplex *(cyanoarene-anethole) by aniline. This quenching resulted in a new emission that was assigned to the exciplex of *(cyanoarene-aniline) from the substitution reaction.[75b, 96] In the photoreactions of DBMBF$_2$ with cyclic dienes in aromatic solvents, the quenching of exciplex *AR by the diene (D) may either form a nonemissive triplex *(ARD) or proceed via an exciplex substitution to form *AD. Either possibility should lead to the adduct formation.

2.2.3 The Role of DBMBF$_2$ Excimer: *(AA)

It is reported that the photoadditions of DBMBF$_2$ to simple olefins involve reaction of the DBMBF$_2$ excimer.[80c] This excimer reaction was proposed on the basis of fluorescence quenching measurements and dependence of the adduct formation on DMBBF$_2$ concentrations.

A concentration dependence has also been observed in the photocycloaddition of DBMBF$_2$ to cyclic dienes or vinyl ethers in non-aromatic solvents. The following findings suggest a dual pathway, initiated from the excited DBMBF$_2$ monomer and from excimer, for the DBMBF$_2$-diene photoreactions. However, the quenching of DBMBF$_2$ excimer can be the main route of DBMBF$_2$ addition to vinyl ethers.

(1) The fluorescence quenching experiments show that the DBMBF$_2$ excimer is more efficiently quenched than the singlet excited DBMBF$_2$ by either cyclic dienes or vinyl ethers (Fig. 2.2B and 2.8);

(2) The photocycloaddition is dependent on the DBMBF$_2$ concentration in non-aromatic solvents. The adduct quantum yield increases with higher concentrations of DBMBF$_2$ (Fig. 2.4 and Table 2.12);

(3) Under similar conditions, both the fluorescence quenching of the DBMBF$_2$ excimer by vinyl ethers and the measurements of adduct quantum yield produce the comparable Stern-Volmer quenching constants (K_{SV}, in Table 2.15). The results indicate that, at high [DBMBF$_2$], the cycloadduct formation is initiated mainly by the quenching of the DBMBF$_2$ excimer with vinyl ethers.

The observation detailed in point 3 also implies that, in the DBMBF$_2$-vinyl ether system, the excimer formation can dominate over the other bimolecular quenching processes in non-aromatic solvents (Scheme 2.4). For example, the relative rates of excimer (*AA) and monomer (*A) reactions can be estimated upon the concentrations of DBMBF$_2$ (0.20 M), vinyl ether (0.30 M) and the available rate constants defined in Scheme 2.4:

$$\frac{\text{Rate of *AA formation}}{\text{Rate of quenching *A by EVE}} = \frac{k_m[A][^*A]}{k_x[D][^*A]} = \frac{2.7 \times 10^{10} \times 0.2}{0.7 \times 10^{10} \times 0.3} \cong 2.6$$

$$\frac{\text{Rate of quenching}^* AA \text{ by EVE}}{\text{Rate of quenching }^*A \text{ by EVE}} = \frac{k_{11}\tau_{AA}[D]}{k_x\tau_a[D]} = \frac{0.63 \times 10^9 \times 36}{7 \times 10^9 \times 0.34} \cong 9$$

In the above equations, ethyl vinyl ether (EVE) is used as quencher. The rate constant for quenching the singlet excited $DBMBF_2$ by EVE is calculated to be $k_x = 7 \times 10^9$ $M^{-1}s^{-1}$ from $K_{SV}^m = (k_x \tau_a) = 2.3$ M^{-1} in THF (Fig. 2.7). The rate constant for excimer formation is $k_m = 2.7 \times 10^{10}$ $M^{-1}s^{-1}$ from Fig. 4.9 in acetonitrile. The rate constant for quenching the excimer by EVE is $k_{11} = 0.63 \times 10^9$ $M^{-1}s^{-1}$ from $K_{SV}^{ex} = (k_{11} \tau_{AA}) = 22.7$ M^{-1} in THF (Fig. 2.8). The lifetimes $\tau_a = 0.34$ ns and $\tau_{AA} = 36$ ns in aerated acetonitrile[62b] were used in the above calculations. Based on these estimations, both the formation of $DBMBF_2$ excimer and its quenching by EVE are predominant over the competing reaction of singlet excited $DBMBF_2$ (*A) with EVE.

In the reaction of $DBMBF_2$ with 1,3-COD, the rate constant $k_x = 2.5 \times 10^{10}$ $M^{-1}s^{-1}$ is from $K_{SV}^m = 8.1$ M^{-1} in THF (Fig. 2.1) and $k_{11} = 1.5 \times 10^9$ $M^{-1}s^{-1}$ is from $K_{SV}^{ex} = 56$ M^{-1} in THF (Fig. 5.5). Similar estimations suggest that even at 0.2 M $DBMBF_2$, the monomer (*A) reaction is still significant. This can be understood on basis of the following

$$\frac{\text{Rate of }^*AA \text{ formation}}{\text{Rate of quenching }^*A \text{ by COD}} = \frac{k_m[A][^*A]}{k_x[D][^*A]} = \frac{2.7 \times 10^{10} \times 0.2}{2.5 \times 10^{10} \times 0.3} \cong 0.72$$

$$\frac{\text{Rate of quenching }^*AA \text{ by COD}}{\text{Rate of quenching }^*A \text{ by COD}} = \frac{k_{11}\tau_{AA}[D]}{k_x\tau_a[D]} = \frac{1.5 \times 10^9 \times 36}{2.5 \times 10^{10} \times 0.34} \cong 6.4$$

considerations. In view of the relative quenching rate, while the singlet excited $DBMBF_2$ (*A) has a higher reactivity than the $DBMBF_2$ excimer (*AA) towards 1,3-COD, the long

lifetime of *AA is mostly responsible for the selective quenching of *AA by 1,3-COD.

However, in view of the excimer formation, the competition for capturing *A by $DBMBF_2$

itself $(k_m[*A][A])$ and by the donor 1,3-COD $(k_x[*A][D])$ should determine the pathway of

photoreactions. When the rate constants k_x and k_m are similar, higher concentrations of

1,3-COD than $DBMBF_2$ should promote the reaction through the monomer pathway.

2.2.4 The Intermediacy of the $DBMBF_2$-Olefin Exciplex (*AD)

2.2.4.1 Mataga and Weller's equations

It is generally known that the extent of charge transfer (CT) in an exciplex can

change with the solvent polarity and that the electronic structure of the exciplex will

determine the selectivity of its subsequent reactions.[20] Polar solvents increase the CT

extent of an exciplex, and the resultant changes in electronic structure of the exciplex

have been used to account for the variation of the emission quantum yield and lifetime of

the exciplex with the variation of solvent polarity.[10, 13a, 97, 92b, 91d] The CT content within

an exciplex can be so strongly promoted by the solvation that the exciplex dissociates

into a solvent-separated ion pair (SSIP), which may then initiate ionic reactions. An

empirical relationship of the exciplex ionic dissociation with the solvent polarity (ε) has

been established by Mataga and Weller (Scheme 2.5).[98, 99]

Scheme 2.5:

$$*AD \xrightarrow{k_i} A^{-\cdot} + D^{+\cdot} \quad \text{ionic dissociation}$$
$$*AD \xrightarrow{k_D} A + D$$

ionic dissociation

emission, intersystem crossing
and chemical reaction.
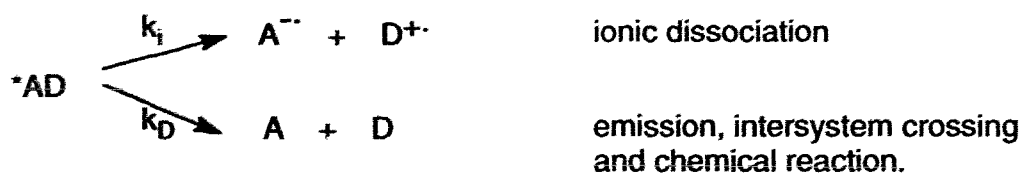
Mataga proposed an empirical equation (Eq. 2.9) that correlates $\log(1/\Phi_i)$ to $1/\varepsilon$,[99] where the quantum yield of the exciplex dissociation (Φ_i) was defined as:

$$\Phi_i = \frac{k_i}{k_i + k_D} \tag{Eq. 2.8}$$

$$\log\left(\frac{1}{\Phi_i} - 1\right) = \frac{p}{\varepsilon} + q \tag{Eq. 2.9}$$

which assumes unit efficiency for exciplex formation. The two constants p and q are independent of solvent. Weller also found that rate constant of the exciplex dissociation (k_i) is much more dependent on solvent than the rate constant (k_D) of other non-radiative and radiative decay.[98] The empirical equation (Eq. 2.10) suggests that a semi-logarithmic plot of $\ln k_i$ vs. $1/\varepsilon$ should be linear. According to Eq. 2.10, $\ln k_i$ is related to the differential solvation of *AD and SSIP.[4, 7]

$$k_i = \frac{2.3 \times 10^9}{\eta} \exp\left(-\frac{e_o^2}{\varepsilon kT}\left(\frac{1}{d} - \frac{1}{a}\right)\right) \tag{Eq. 2.10}$$

In this equation, η is the solvent viscosity (in cP), ε is the dielectric constant of the solvent, k is the Boltzmann constant, $a \approx 7$ Å is the centre-to-centre distance of SSIP, and $d \approx 3$ Å is the interplanar separation in the exciplex.

2.2.4.2 The relationship between Φ_A and k_i

The quantum yields for the photoreactions of $DBMBF_2$ (0.03 M) with cyclic dienes (0.30 M) or vinyl ethers (0.30 M) were determined in various solvents, ranging from acetonitrile to xylene (Table 2.3 and 2.11). The quantum yield (Φ_A) for the $DBMBF_2$

photoaddition to the cyclic diene or vinyl ether is defined in Eq. 2.11, based on Scheme 2.6. In Eq. 2.11, Φ_A is the product of the efficiency (n) to form the exciplex *AD and the efficiency to form the adduct from the exciplex (k_p), in competition with the unimolecular decay (k_D) and the ionic dissociation (k_i).

Scheme 2.6:

$$*AD \quad \overset{k_i}{\nearrow} \quad A^{-\cdot} + D^{+\cdot} \qquad \text{ionic dissociation}$$
$$\overset{k_p}{\longrightarrow} \quad \text{Adduct} \qquad \text{product formation}$$
$$\overset{k_D}{\searrow} \quad A + D \qquad \text{unimolecular decay}$$
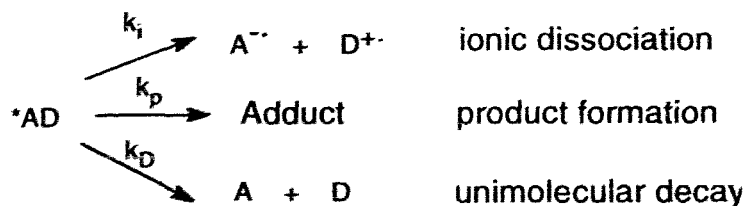
$$\Phi_A = n \, \frac{k_p}{k_D + k_i + k_p} \qquad\qquad \text{(Eq. 2.11)}$$

$$\text{or} \quad k_i = \left(\frac{n}{\Phi_A} - 1 - \frac{k_D}{k_p}\right) k_p \qquad\qquad \text{(Eq. 2.12)}$$

Based on Eq. 2.11, the variation of adduct quantum yields (Φ_A), with solvent polarity, should be caused mainly by exciplex ionic dissociation (k_i). In contrast, the processes of the exciplex decay (k_D) and product formation (k_p) depend very little on the solvent.[98, 99] Given these approximations, the change in rate constant k_i, as a function of solvent polarity (ϵ), should be proportional to (n/Φ_A) in Eq. 2.12. Therefore, it is possible to correlate the adduct quantum yield (Φ_A) with the solvent polarity (ϵ) in a similar way to that of $\ln k_i$ vs. $1/\epsilon$ in Eq. 2.10.[4, 7] Based on this idea, the correlation of $\ln(1/\Phi_A)$ vs. $1/\epsilon$ was examined using the adduct quantum yields of Table 2.3. The obtained plots are linear as shown in Fig. 2.11 for the substrates CHD and 1,3-COD in all solvents but dioxane and the aromatic solvents.
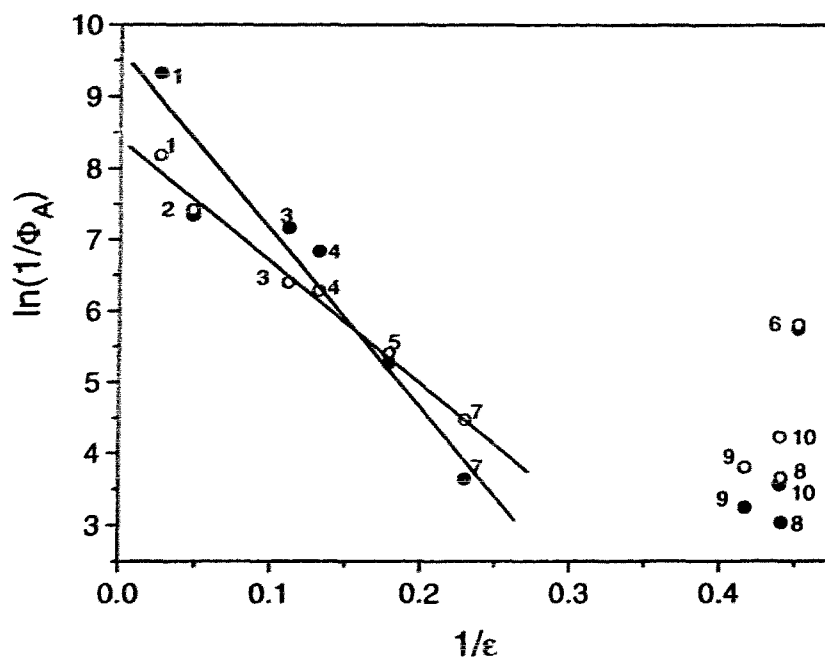
Fig. 2.11 Plots of *ln* (1/Φ_A) *vs.* 1/ε for the photoaddition of DBMBF$_2$ to

CHD (●) and 1,3-COD (o) in various solvents:

1, acetonitrile; 2, acetone; 3, CH$_2$Cl$_2$; 4, THF; 5, THP; 6, dioxane;

7, ether; 8, benzene; 9, toluene; 10, p-xylene.

2.2.4.3 The empirical solvent polarity scale: ε and E$_T$(30)

The deviations from the linear fit in Fig. 2.11 are probably caused by the solvent

polarity scale (ε) which is only an approximation of the real solvation of the exciplex

intermediate. A complete description of solvation would take into account all types of

intermolecular forces,[81a] including nonspecific electrostatic forces (Coulombic, dipole-

dipole and Van der Waals' forces) in a macroscopic scale and specific hydrogen

bonding, electron donor-acceptor interaction, *etc.* in a microscopic scale. Because the

intermolecular forces function not only within solvent-solute, but also in solvent-solvent

and solute-solute interactions, the structures of the solvent and solute must be also

considered. Since the ε -scale can only describe the solvent effect on a macroscopic

scale by disregarding specific intermolecular interactions, the structural effect of dioxane and the polarizability of aromatic solvents are not reflected.

The $E_T(30)$ scale, a well-known empirical solvent polarity parameter,[81a, 100] is one of the most comprehensive measures of solvation. Proposed by Dimroth and Reichardt,[100b] this solvent polarity scale $E_T(30)$ is defined as the molar transition energy of a pyridinium-N-phenolate betaine dye, (2,4,6-triphenyl-1-pyridinio)-phenolate,[100] measured from its intermolecular charge transfer (π - π^*) absorption band at the longest

$$E_T(30) = h\frac{c}{\lambda}N_A = \frac{28591}{\lambda\,(nm)} = 2.8591 \times 10^{-3}\bar{v}\ (cm^{-1}) \qquad (Eq.\ 2.13)$$

h = Planck's constant; c = the velocity of light; N_A = Avogadro's number; λ and $\bar{v}$ = the wavelength and the wavenumber of the excitation light corresponding to the charge transfer transition. $E_T(30)$ unit: kcal/mole

wavelength (λ_{max}) of its UV spectrum. Because of the negative solvatochromism of the betaine dye, a larger $E_T(30)$ value should correspond to a higher solvent polarity.

Table 2.18 Empirical solvent polarity parameters[a]

Solvent	CH_3CN	acetone	CH_2Cl_2	THF	THP
ε	37.5	20.7	8.93	7.58	5.60[b]
$E_T(30)$, kcal/mol	45.6	42.2	40.7	37.4	36.6
Solvent	dioxane	ether	benzene	toluene	p-xylene
ε	2.21	4.34	2.27	2.40	2.27
$E_T(30)$, kcal/mol	36.0	34.5	34.3	33.9	33.1

Notes: [a] From Ref. 81a and 81b; [b] From Ref. 81b and 81c.
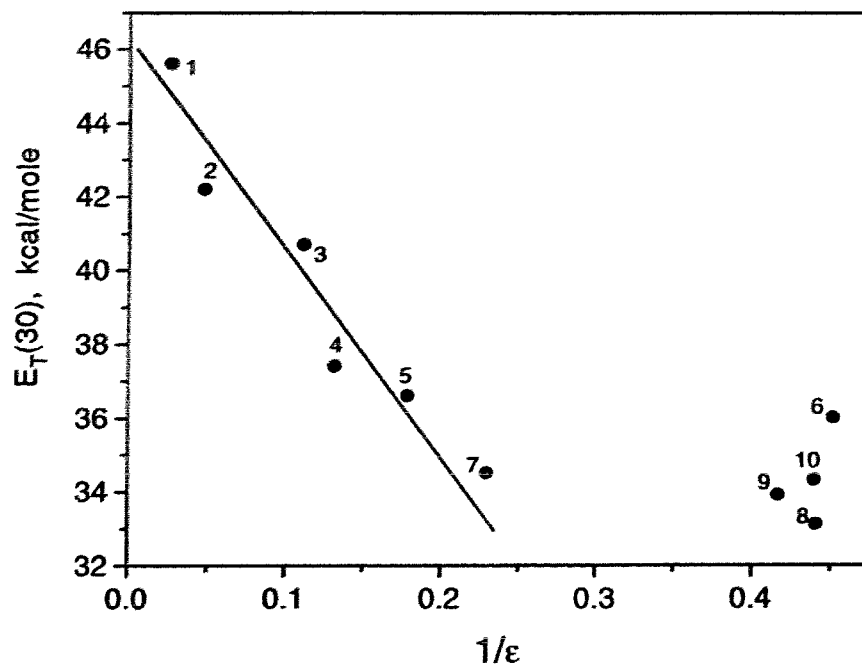
Fig. 2.12 Correlation between $E_T(30)$ and $1/\varepsilon$ of the following solvents:

1, acetonitrile; 2, acetone; 3, CH_2Cl_2; 4, THF; 5, THP; 6, dioxane;

7, ether; 8, benzene; 9, toluene; 10, p-xylene.

The $E_T(30)$ values of 10 solvents are shown in Table 2.18, together with the plot of $E_T(30)$ vs. $1/\varepsilon$ in Figure 2.12. It should be noted that deviations similar to those seen in Fig. 2.11, are again observed for the solvents dioxane, benzene, toluene, and p-xylene.

2.2.4.4 The relationship between $ln(1/\Phi_A)$ and $E_T(30)$

Previous studies have correlated the rate constants of photoreactions to the $E_T(30)$ scale.[26b, 45b, 101] In the work of Evans et al., a linear relationship corresponding to equation 2.12 was demonstrated for the 9,10-dicyanoanthracene sensitized dimerization of phenyl vinyl ether (PVE).[26b] A mechanism similar to Scheme 2.5 was proposed for the quenching of 9,10-dicyanoanthracene fluorescence by PVE, and the rate constant

(k_q) was linearly related to the rate of exciplex dissociation (k_i). The observed linear plot of $ln(k_q)$ vs. $E_T(30)$ therefore represents a linear correlation of $ln(k_i)$ to $E_T(30)$. This semi-logarithmic plot supports the mechanistic postulate, and corresponds to a linear free energy relationship.[100a, 101]

In section 2.2.4.3, the $E_T(30)$ scale was introduced as a measure of solvent polarity, and found to be linearly related to $1/\varepsilon$ for some non-aromatic solvents (Fig. 2.12). Encouraged by the work of Evans,[26b] Peters[101] and Pac[45b], we decided to replot the adduct quantum yields (in Fig. 2.11) as a function of the solvent polarity $E_T(30)$. Fig. 2.13 and 2.14 show the semi-logarithmic plots of $ln(1/\Phi_A)$ vs. $E_T(30)$ for the photocycloaddition of DBMBF$_2$ to cyclic dienes (Table 2.3) and vinyl ethers (Table 2.11). For comparisons, the double reciprocal plots of $ln(1/\Phi_A)$ vs. $1/E_T(30)$ are displayed in Appendix I.

The plots in Fig. 2.13 and Fig. 2.14 support our postulate of exciplex intermediacy in DBMBF$_2$ photoreactions with cyclic dienes and vinyl ethers (Scheme 2.6). Based on the foregoing discussions, a comprehensive picture of the DBMBF$_2$ photoreactions can now be given as follows:

(1) The exciplex of DBMBF$_2$-cyclic diene or DBMBF$_2$-vinyl ether responds to solvent polarity and partitions among ionic dissociation, formation of addition product, and decay to starting materials (Scheme 2.6).

(2) The exciplex of DBMBF$_2$ with conjugated cyclic dienes must have a high charge transfer character. This accounts for the poor yield of adduct and the strong tendency for solvent induced dissociation of the exciplex. However, the exciplex of DBMBF$_2$ with 1,5-COD consists mainly of its local excited state and leads to the high yield of adduct with little dependence on solvent polarity (Table 2.3).[9a, 102]
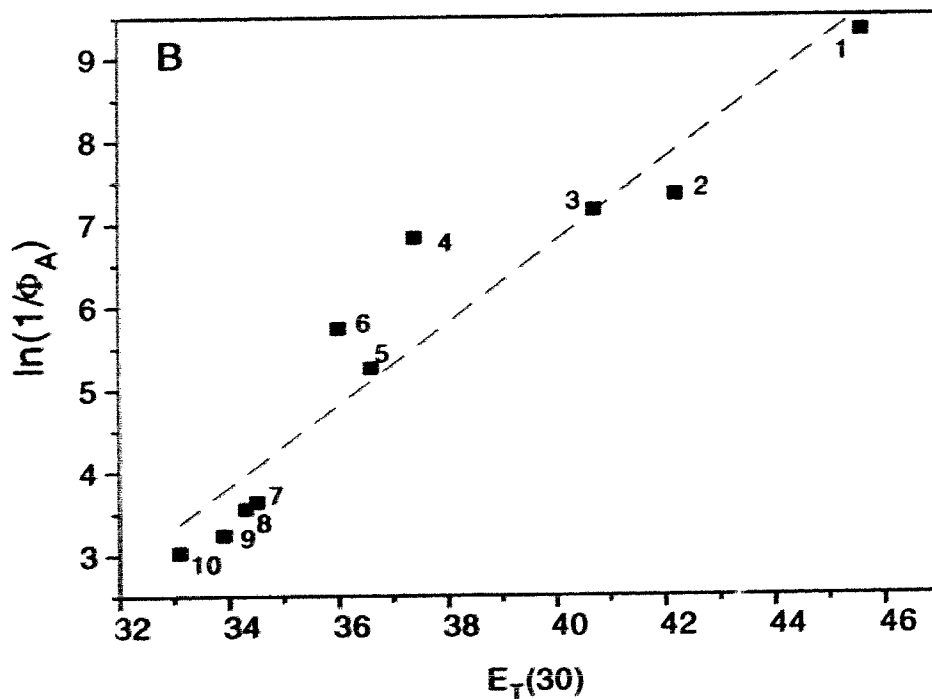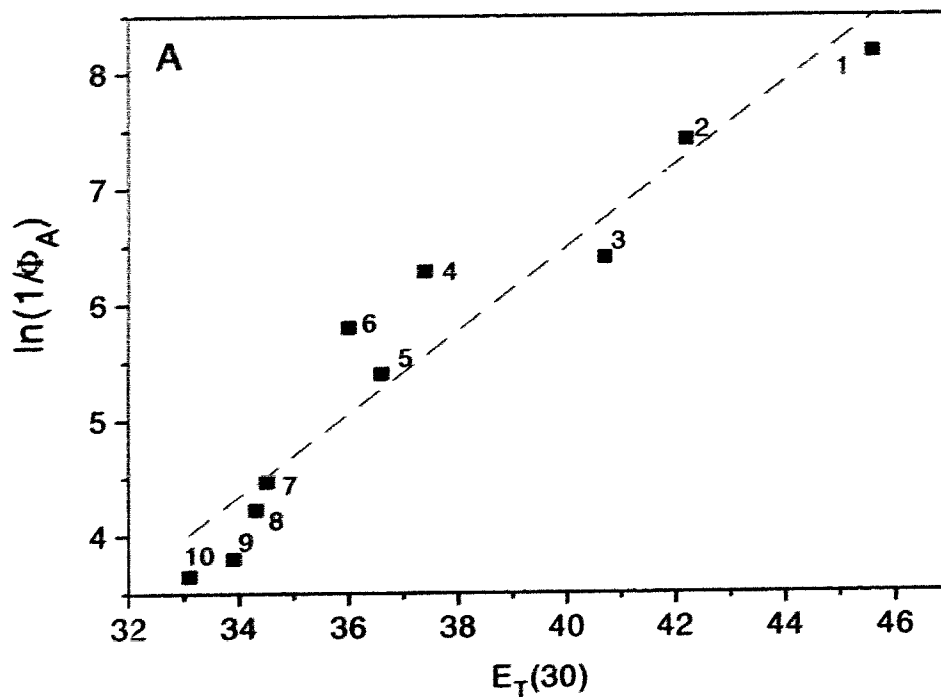
Fig. 2.13 The plots of $ln(1/\Phi_A)$ vs. $E_T(30)$ for the $DBMBF_2$ photoaddition to (A) CHD and (B) 1,3-COD in the solvents: 1, acetonitrile; 2, acetone; 3, CH_2Cl_2; 4, THF; 5, THP; 6, dioxane; 7, ether; 8, benzene; 9, toluene; 10, p-xylene.
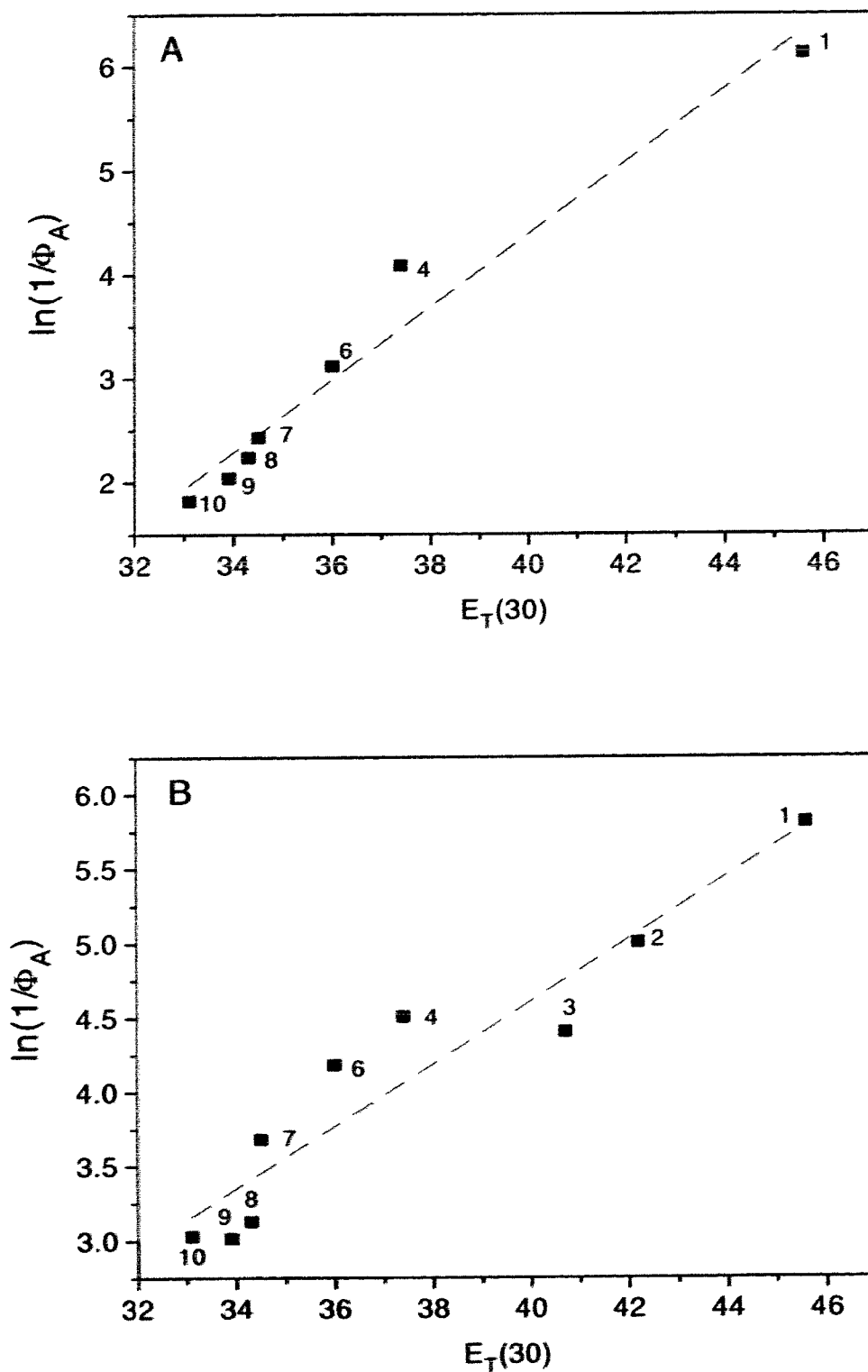
Fig. 2.14 The plots of $ln(1/\Phi_A)$ vs. $E_T(30)$ for the DBMBF$_2$ photoaddition to (A) PVE and (B) IVE in the solvents: 1, acetonitrile; 2, acetone; 3, CH$_2$Cl$_2$; 4, THF; 5, THP; 6, dioxane; 7, ether; 8, benzene; 9, toluene; 10, p-xylene.

(3) In non-aromatic solvents, the singlet excited DBMBF$_2$ monomer (*A) and its

excimer (*AA) act as the reactive species (Section 2.2.3). In aromatic solvents, the

DBMBF$_2$-arene exciplex (*AR) mainly initiates the reaction with cyclic dienes or vinyl

ethers (Section 2.2.2). Despite differences in the primary reaction step, the overall

results show a common pattern by linearly relating the adduct quantum yield $ln(1/\Phi_A)$ to

the solvent polarity E$_T$(30). One possible interpretation is that all of the species (*A, *AA

and *AR) convert to one common intermediate (*AD) upon interaction with an electron

rich olefin (D).

(4) The plots of ln (1/Φ_A) vs. E$_T$(30) reflect the relative rate of the exciplex

dissociation in different solvents. This may mean that the ionic dimerization of 1,3-

cyclohexadiene or phenyl vinyl ether, according to Scheme 2.6, should be initiated

mainly from the solvent induced exciplex dissociation.

The exciplex of DBMBF$_2$ with electron-rich olefins should be considered as an

intermediate in acetonitrile, even though there is large exothermicity for the electron

transfer from the electron-rich olefins to the singlet excited DBMBF$_2$. An example is the

DBMBF$_2$ sensitized isomerization of quadricyclane (QC) to norbornadiene (NBD), where

the radical ion QC$^+$ is thought to arise from exciplex dissociation of *(DBMBF$_2$-QC) in

acetonitrile.[50b, 74] Also according to Farid's work on the mechanism of exciplex

formation in cyanoarene-alkylbenzene systems, the formation of a polar exciplex can

occur in a solvent as polar as acetonitrile even with an electron transfer exothermicity as

large as $\Delta G_{ET} = -1$ eV.[10, 91d]

2.2.5 Mechanistic Considerations

On the basis of the above discussions, Scheme 2.7 is postulated for the overall

photoreaction of DBMBF$_2$ with electron-rich olefins. Under steady-state conditions, the

93

total quantum yield of the cycloaddition reaction (Φ_A) is expressed by Eq. 2.14 (the derivation is given in Appendix II), which includes the efficiency of adduct formation from an exciplex *AD and the sum of the efficiencies for exciplex formation from the different species *A, *AA and *AR.

Scheme 2.7:
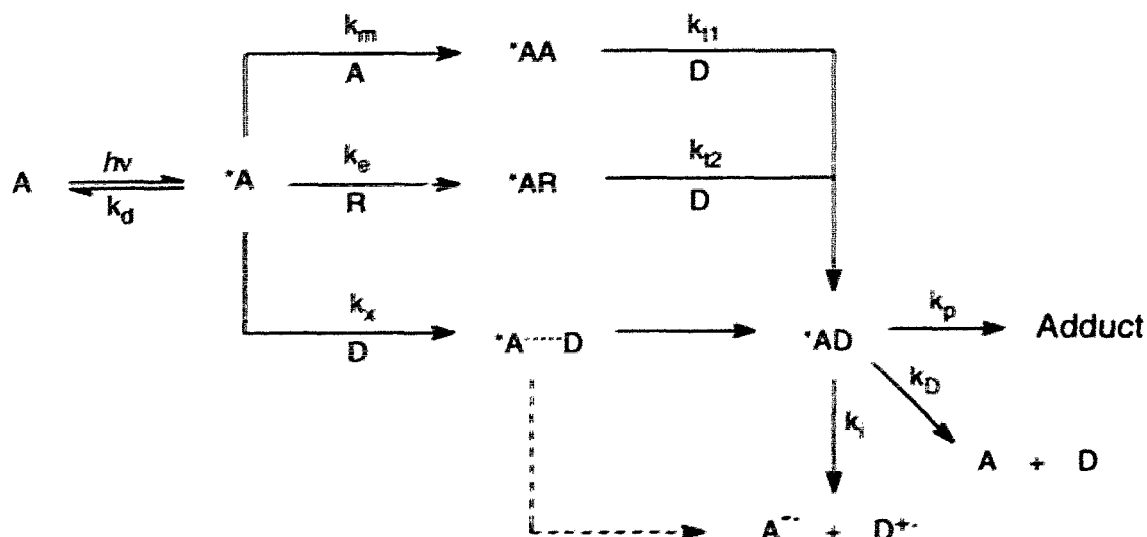
here A = DBMBF$_2$; R = Benzene, Toluene or Xylene; D = CHD, 1,3-COD or Vinyl ether.

$$\Phi_A = \frac{k_p}{k_p + k_D + k_i} \; \frac{1}{\tau_a^{-1} + k_m[A] + k_e[R] + k_x[D]} \left(\frac{k_m[A]\, k_{t1}}{\tau_{AA}^{-1} + k_{t1}[D]} + \frac{k_e[R]\, k_{t2}}{\tau_{AR}^{-1} + k_{t2}[D]} + k_x \right) [D]$$

(Eq. 2.14)

The interpretation of each term of Eq. 2.14 is as follows:

$\dfrac{k_p}{k_p + k_D + k_i}$ the efficiency for the exciplex *AD to form adduct;

$\dfrac{k_m[A]}{\tau_a^{-1} + k_m[A] + k_e[R] + k_x[D]} \; \dfrac{k_{t1}}{\tau_{AA}^{-1} + k_{t1}[D]}$ the efficiency of *AD formation via *AA;

94

$$\frac{k_e[R]}{\tau_a^{-1} + k_m[A] + k_e[R] + k_x[D]} \frac{k_{12}}{\tau_{AR}^{-1} + k_{12}[D]} \qquad \text{the efficiency of *AD formation via *AR;}$$

$$\frac{1}{\tau_a^{-1} + k_m[A] + k_e[R] + k_x[D]} k_x \qquad \text{the efficiency of *AD formation via *A}\cdots\text{D.}$$

Before Eq. 2.14 can be analyzed, it is necessary to discuss the reaction probabilities of singlet excited DBMBF$_2$ (*A) in different solvents. This is done in Table 2.19, for the concentrations [DBMBF$_2$] = 0.03 M, [1,3-COD] = 0.3 M, and the available quenching rate constants (Appendix III).

The solvents chosen here represent non-aromatic and aromatic solvents, respectively. Inspection of Table 2.19 leads to two conclusions: (1) In the non-aromatic solvent THF, the reaction of singlet excited DBMBF$_2$ (*A) with 1,3-COD is the predominant process. (2) In the aromatic solvent toluene, the principal process is the reaction of singlet excited DBMBF$_2$ with the arene to form the DBMBF$_2$-toluene exciplex (*AR).

Table 2.19 Reaction probabilities of singlet excited DBMBF$_2$ (*A) with
1,3-COD (D) or toluene (R) in THF and in toluene

Solvent	$*A \xrightarrow[k_m]{A} *AA$	$*A \xrightarrow{k_d} A$	$*A \xrightarrow[k_x]{D} *A\cdots D$	$*A \xrightarrow[k_e]{R} *AR$
THF	7.2%	26.1%	66.7%	--
Toluene	1.7%	6%	15.4%	76.9%

Note: [DBMBF$_2$] = 0.03 M; [1,3-COD] = 0.3 M; k_m = 2.7 x 10^{10} M^{-1}s^{-1} (from Fig. 4.9);

k_d = 1/τ_a = 2.94 x 10^9 s^{-1}[82] k_x = 2.5 x 10^{10} M^{-1}s^{-1} (from K_{SV}^m = 8.1 M^{-1} in Fig. 2.1);

k_e = 4 x 10^9 M^{-1}s^{-1}[83] and neat toluene is 9.35 M.

Based on the analyses of Table 2.19, three extreme cases can be considered:

(1) Singlet excited DBMBF$_2$ monomer as the principal reaction species.

In non-aromatic solvents, the k_a[R] term should be zero. At [DBMBF$_2$] = 0.03 M and [1,3-COD] = 0.3 M, the excimer formation is insignificant to affect adduct formation (Table 2.19), so that the equation 2.14 becomes:

$$\Phi_A = \frac{k_p}{k_p + k_D + k_i} \; \frac{k_x}{\tau_a^{-1} + k_m[A] + k_x[D]} [D]$$

or

$$\frac{1}{\Phi_A} = (1 + \frac{k_D + k_i}{k_p})(1 + \frac{\tau_a^{-1} + k_m[A]}{k_x} \; \frac{1}{[D]}) \qquad \text{(Eq. 2.15)}$$

According to equation 2.15, the double reciprocal plot of $1/\Phi_A$ vs. $1/[D]$ should be linear with an intercept-slope ratio corresponding to the Stern-Volmer quenching constant:

$$K_{SV}^x = k_x / (\tau_a^{-1} + k_m[A]). \qquad \text{(Eq. 2.15A)}$$

This expression is identical to that of K_{SV}^f from the fluorescence quenching experiments (in Eq. 1.16 where k_q corresponds to k_x). Thus, given the lifetime τ_a, the DBMBF$_2$ concentration and the rate constant k_m, the quenching rate constant can be calculated by two ways: from the measured K_{SV}^x to give k_x, and from K_{SV}^f to give k_q. Theoretically, both k_q and k_x in Scheme 2.7 are identical, i.e., as the rate constant for quenching of the singlet excited DBMBF$_2$ (*A) by 1,3-COD. Experimentally, the values of k_q and k_x were found to be consistent and are shown in Table 2.17.

(2) Exciplex DBMBF$_2$-arene (*AR) as the principal reaction species.

In aromatic solvents, the exciplex *AR formation should be dominant among all reactions: k_a[R] $\gg$ k_x[D], and the excimer formation is negligible (Table 2.19). Then the equation 2.14 is simplified to:

$$\Phi_A = \frac{k_p}{k_p + k_D + k_i} \frac{k_e[R]}{\tau_a^{-1} + k_m[A] + k_e[R]} \frac{k_{t2}}{\tau_{AR}^{-1} + k_{t2}[D]} [D]$$

or
$$\frac{1}{\Phi_A} = (1 + \frac{k_D + k_i}{k_p})(1 + \frac{\tau_a^{-1} + k_m[A]}{k_e[R]})(1 + \frac{1}{k_{t2}\tau_{AR}} \frac{1}{[D]}) \qquad \text{(Eq. 2.16)}$$

At constant concentrations of [A] and [R], the double reciprocal plot of $1/\Phi_A$ vs.

$1/[D]$ should be linear and the intercept-slope ratio should give: $\quad K_{SV}^y = k_{t2}\tau_{AR}$

The quenching rate constant k_{t2} of exciplex *AR by 1,3-COD can thus be obtained from

the experimental values of K_{SV}^y and K_{SV}^i in Table 2.7 (see Section 2.2.2).

(3) *Excimer (*AA) as the principal reaction species.*

In the photoreactions of $DBMBF_2$ with vinyl ethers, the $DBMBF_2$ excimer reaction

prevails at concentrations of $DBMBF_2$ higher than 0.20 M in THF. As the $k_e[R]$ term is

zero in non-aromatic solvents, equation 2.14 can be simplified to:

$$\Phi_A = \frac{k_p}{k_p + k_D + k_i} \frac{1}{\tau_a^{-1} + k_m[A] + k_x[D]} (\frac{k_m[A] k_{t1}}{\tau_{AA}^{-1} + k_{t1}[D]} + k_x) [D] \qquad \text{(Eq. 2.17)}$$

Based on our calculations concerning the relative rates of $DBMBF_2$ excimer (*AA) and

monomer (*A) reactions with ethyl vinyl ether (Section 2.2.3), the reaction of $DBMBF_2$

excimer with the vinyl ether dominates over the reaction of the $DBMBF_2$ monomer. If the

k_x-term is relatively unimportant, $(\tau_a^{-1} + k_m[A]) > k_x[D]$, then Eq. 2.17 can be simplified to

Eq. 2.17A:

$$\Phi_A \approx \frac{k_p}{k_p + k_D + k_i} \frac{k_m[A]}{\tau_a^{-1} + k_m[A]} \frac{k_{t1}}{\tau_{AA}^{-1} + k_{t1}[D]} [D]$$

or
$$\frac{1}{\Phi_A} = (1 + \frac{k_D + k_i}{k_p})(1 + \frac{1}{k_m \tau_a [A]})(1 + \frac{1}{k_{11} \tau_{AA}} \frac{1}{[D]})$$
(Eq. 2.17A)

Here a linear relationship can be established by plotting $1/\Phi_A$ against $1/[D]$. The intercept-slope ratio of this plot should be: $K_{SV}^y = k_{11} \tau_{AA}$, where k_{11} is the rate constant for quenching the DBMBF$_2$ excimer and τ_{AA} its lifetime. It is noticeable that this Stern-Volmer constant K_{SV}^y should be identical to K_{SV}^{ex} (= $k_q^{ex} \tau_{AA}$) from the excimer fluorescence quenching in Eq. 1.18 (Section 1.6), since both K_{SV}^y and K_{SV}^{ex} are reflecting the same quenching process. A good consistency in these experimental K_{SV}-values should be seen as a support for the intermediacy of DBMBF$_2$ excimer. Table 2.15 shows such agreement in the reactions of DBMBF$_2$ excimer with vinyl ethers and supports the reactive role of DBMBF$_2$ excimer in adduct formation.

2.3 Conclusions and Proposals

The following conclusions are reached as a result of the investigations in this chapter:

(1) Singlet excited DBMBF$_2$ is quenched at close to the diffusion controlled rate by electron-rich olefins, conjugated cyclic dienes and vinyl ethers. This quenching may lead to radical cation dimerization of olefins in more polar solvents and cycloaddition of DBMBF$_2$ to an olefin in less polar solvents (Tables 2.3 and 2.11). Both processes are proposed to proceed through a common intermediate, the DBMBF$_2$-olefin exciplex (Scheme 2.7).

(2) The presence of the polar $DBMBF_2$-olefin exciplex is inferred from solvent effects on photoreactions of $DBMBF_2$ with conjugated cyclic dienes and vinyl ethers. The ionic dissociation of $DBMBF_2$-olefin exciplexes competes with the cycloadduct formation and follows a linear correlation with the empirical solvent polarity $E_T(30)$ (Fig. 2.13 and Fig. 2.14).

(3) The efficient photocycloaddition of $DBMBF_2$ to the non-conjugated cyclic diene, 1,5-COD, depends very little on the solvent (Table 2.3). This reflects the less polar nature of the $DBMBF_2$-1,5-COD exciplex.

(4) The formation of an emissive $DBMBF_2$ excimer promotes the photocycloaddition of $DBMBF_2$ to electron-rich olefins. With the conjugated cyclic dienes, the cycloaddition follows a dual pathway involving both the singlet excited $DBMBF_2$ monomer and its excimer (Fig. 2.2B, Fig. 2.4 and Table 2.19), but with vinyl ethers the excimer reaction predominates (Table 2.15).

(5) In aromatic solvents, the singlet excited $DBMBF_2$ converts to its emissive exciplex with a solvent molecule. It is the $DBMBF_2$-arene exciplex that reacts with electron-rich olefins to form cycloadducts (Tables 2.2, 2.4, 2.7 and 2.19).

There are still unanswered questions in Scheme 2.7 regarding the formation of the $DBMBF_2$-olefin exciplex (*AD), as a precursor of the cycloaddition product. For example, it is not known how the $DBMBF_2$ excimer (*AA) and the $DBMBF_2$-arene exciplex (*AR) react with an electron-rich olefin (D) to give addition product via the exciplex precursor (*AD). It may occur through exciplex substitution, and / or triplex (*AAD) or (*ARD) may be involved.

The transient emission or absorption spectroscopy should be examined in the reactions of excimer (*AA) or exciplex (*AR) with a quencher olefin. In this way, one may observe and study the possible triplex intermediate. Alternatively an intramolecular

DBMBF$_2$ excimer may be derived from the irradiation of the BF$_2$-complex of 1,1,5,5-tetrabenzoylpentane. This compound is expected to allow a DBMBF$_2$ excimer analogue to be studied at relatively low concentration. A synthesis of 1,1,5,5-tetrabenzoylpentane was attempted by reaction of dibenzoylmethane enolate with 1,3-dibromopropane or 1,3-propanediol di-*p*-tosylate, but was unsuccessful.
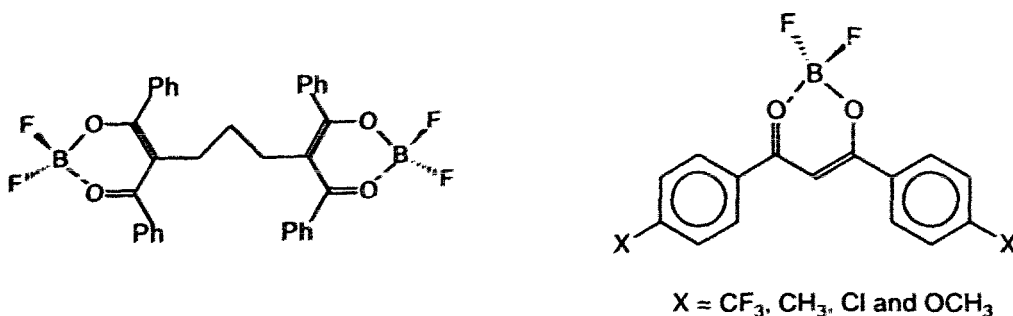
X = CF$_3$, CH$_3$, Cl and OCH$_3$

There are other derivatives of dibenzoylmethane (X = CF$_3$, CH$_3$, Cl and OCH$_3$)[103] whose BF$_2$-complexes, as analogues of DBMBF$_2$, are promising to be the electron acceptor sensitizer. Their different structures due to substituent effects may lead to new photophysical and photochemical properties. Studying these properties should provide insight into the mechanical details of PET reactions of 1,3-diketonatoboron difluorides.

CHAPTER THREE
PHOTOREACTION OF DBMBF₂ WITH CYCLIC DIENES
IN BINARY SOLVENT MIXTURES

In chapter two, the photoreactions of DBMBF₂ with cyclic dienes or vinyl ethers have been investigated in neat solvents. A linear correlation was observed between the logarithm of adduct quantum yield $ln(1/\Phi_A)$ and the empirical polarity scale $E_T(30)$ of the neat solvents. However, questions were raised concerning whether a similar linear relationship of $ln(1/\Phi_A)$ vs. $E_T(30)$ should be also observed if the photoreactions of DBMBF₂ with cyclic dienes were examined in binary solvent mixtures.

In this chapter, the effect of binary solvent mixtures on the photoreactions of DBMBF₂ is to be investigated using binary solvents with polarities ranging from acetonitrile to p-xylene.

3.1 Results

3.1.1 Quantum yield determinations in binary solvent mixtures

3.1.1.1 CH₃CN - Toluene and CH₃CN - Xylene mixtures

The quantum yields were determined in the solvent mixtures of acetonitrile and arene, to examine the effect of solvent polarity on the photoreactions. The experimental procedure was similar to that described earlier (Section 2.1.1.3). The $E_T(30)$ values of binary solvent mixtures were calculated according to equation 3.1, derived for a thermodynamically ideal solvent mixture.[104] The reason for using Eq. 3.1 is discussed

$$E_T(30) = x_A E_T(A) + x_B E_T(B) \qquad \text{(Eq. 3.1)}$$

$$x_A + x_B = 1$$

in Section 3.2.1.1. In Eq. 3.1, x_A and x_B are the mole fractions of the component

solvents, and $E_T(A)$ and $E_T(B)$ are the empirical solvent polarity parameters of pure

solvent A and pure solvent B.

The quantum yields of adduct formation (Φ_A) and dimer formation (Φ_D) are

measured as a function of the xylene or toluene mole fraction. The results are listed in

Tables 3.1 and 3.2 for the photoreactions of $DBMBF_2$ (0.03 M) with CHD (0.3 M) in the

CH_3CN - xylene and CH_3CN - toluene solvent systems.

In Table 3.3, the quantum yields of the $DBMBF_2$ photoreaction with 1,3-COD are

also given as a function of the p-xylene mole fraction in acetonitrile.

Table 3.1 Quantum yields of $DBMBF_2$ photoreactions with CHD
in acetonitrile-xylene solvent mixtures

p-Xylene mole % in CH_3CN	[Xylene] M	$E_T(30)$ (kcal/mole)	$10^3\Phi_A$ (of 6)	Φ_D	CHD dimer ratio	
					(2+3) : (4+5)	2 : 3
0	0.0	45.6	0.28^a	0.04^c	100 : 0	7.3
1.1	0.2	45.5	$-^{b, c}$	0.17^c	100 : 0	7.3
2.7	0.5	45.3	$-^{b, c}$	0.32^c	100 : 0	6.7
5.7	1.0	44.9	$-^{b, c}$	0.47^c	100 : 0	6.1
8.8	1.5	44.5	1.82^c	0.59^c	100 : 0	5.7
12.2	2.0	44.1	$1.82^{a, c}$	0.56^c	99.2 : 0.8	5.7
40.3	5.0	40.6	1.09^a	0.15	96.8 : 3.2	4.8
54.3	6.0	38.8	0.35^a	0.043	92.9 : 7.1	4.4
71.8	7.0	36.6	0.97^a	0.007	73.3 : 26.7	2.9
95.4	8.0	33.7	13.8^a	0.008	58.6 : 40.4	1.8
100	8.2	33.1	26.0^a	0.014	73.6 : 26.4	2.2

Notes: [a] Samples of $[DBMBF_2]$ = 0.03 M and [CHD] = 0.3 M were irradiated at 350 nm for 30
minutes; [b] No adduct was detected on GC; [c] Irradiation for 10 minutes.

Table 3.2 Quantum yields of DBMBF$_2$ photoreactions with CHD in acetonitrile-toluene solvent mixtures [a]

Toluene mole % in CH$_3$CN	[Toluene] M	E$_T$(30) (kcal/mole)	$10^3\Phi_A$ (of 6)	Φ_D	CHD dimer ratio (2+3) : (4+5)	2 : 3
0	0.0	45.6	0.56	0.050	99.9 : 0.1	8.1
11.7	2.0	44.2	0.99	0.250[b]	99.1 : 0.9	7.7
35.7	5.0	41.4	1.65	0.130[b]	97.2 : 2.8	6.5
46.3	6.0	40.2	0.99	0.046	95.2 : 4.8	5.8
58.7	7.0	38.7	0.90	0.009	89.2 : 10.8	4.8
81.6	8.5	36.1	3.40	0.001	71.9 : 28.1	2.2
100	9.4	33.9	22.3	0.006	84.9 : 15.1	2.7

Notes: [a] Samples of [DBMBF$_2$] = 0.03 M and [CHD] = 0.3 M were irradiated at 350 nm for 40 minutes; [b] Irradiation for 10 minutes.

Table 3.3 Quantum yields of DBMBF$_2$ photoreactions with 1,3-COD in acetonitrile-xylene solvent mixtures[a]

p-Xylene mole % in CH$_3$CN	[Xylene] M	E$_T$(30) (kcal/mole)	$10^3\Phi_A$ (of 12)	$10^3\Phi_D{}^c$
0	0	45.6	~0.09	1.3
2.7	0.5	45.3	0.11	3.9
12.1	2.0	44.1	0.12	6.1
29.1	4.0	42.0	0.12	6.5
54.3	6.0	38.8	0.20	1.8
71.8[b]	7.0	36.6	0.58	0.8
95.4[b]	8.0	33.7	16.1	1.8
100[b]	8.2	33.1	48.1	5.8

Notes: [a] Samples of [DBMBF$_2$] = 0.03 M and [1,3-COD] = 0.5 M were irradiated at 350 nm for 190 minutes; [b] Irradiation for 60 minutes; [c] As a complex mixture.

The above data are summarized in Fig. 3.1 and 3.2:
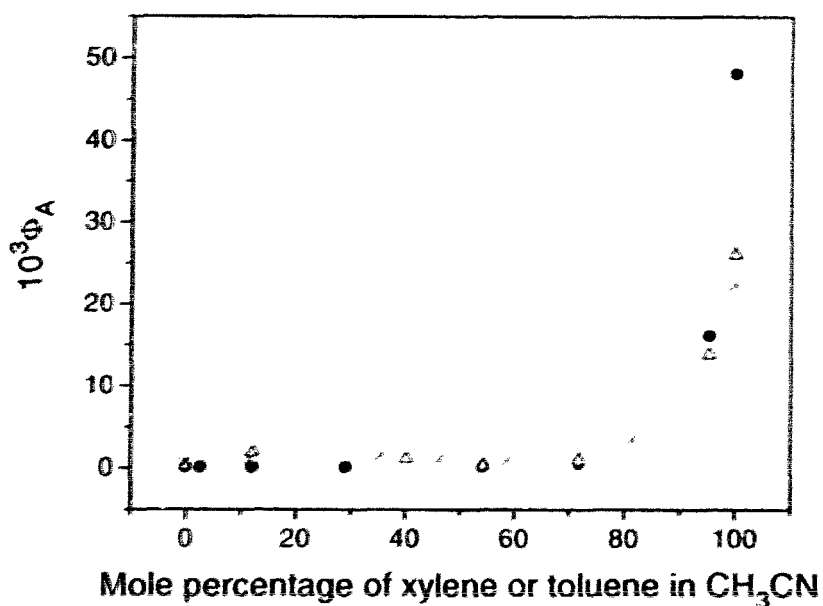
Fig. 3.1 Adduct quantum yields (Φ_A) as a function of the mole fraction of toluene or
xylene in acetonitrile: (1) Φ_A of **12** in CH_3CN-xylene (●); (2) Φ_A of **6** in CH_3CN-
xylene (Δ) and (3) in CH_3CN-toluene (×). (Data from Tables 3.1, 3.2 and 3.3)
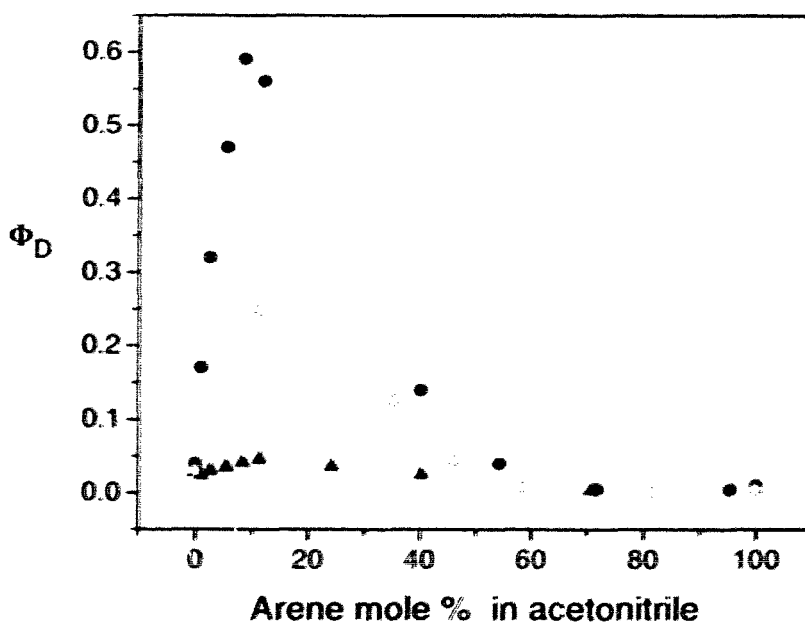
Fig. 3.2 Dependence of the [4+2] dimer quantum yield (Φ_D) of CHD upon the mole
fraction of arene in acetonitrile: (1) in CH_3CN-xylene (●), (2) in CH_3CN-toluene (○)
and (3) in CH_3CN-benzene (▲). (Data from Tables 3.1, 3.2 and 5.16)

Interestingly the quantum yields of **2** and **3**, from the [4+2] dimerization of CHD (0.3 M) sensitized by $DBMBF_2$ (0.03M), exhibited a maximum $\Phi_D \approx 0.6$ at xylene mole fraction of 10% in acetonitrile (Fig. 3.2). Under these optimized solvent conditions, the dimerization reaction was further examined as a function of the CHD concentration. The dimer quantum yield (Φ_D) of **2** and **3**, listed in Table 3.4 and Fig. 3.3, showed a large sensitivity to the CHD concentration. The dimer ratio remained constant throughout the CHD concentration range.

Table 3.4 The dimer quantum yield (Φ_D) of CHD sensitized by $DBMBF_2$ in acetonitrile containing 10% xylene.[a]

[CHD] M	Φ_D	[4+2] dimer ratio 2 : 3
0.010	0.076	85 : 15
0.0125	0.104	86 : 14
0.015	0.153	86: 14
0.02	0.165	86 : 14
0.0286	0.252	86 : 14
0.050	0.395	86 : 14
0.10	0.640	86 : 14
0.30	0.590	85 : 15
0.50	0.420	85 : 15
1.00	0.263	85 : 15

Note: [a] Samples of $DBMBF_2$ (0.03 M) and CHD were irradiated at 350 nm for 3 minutes. No [2+2] dimers **4** and **5** were detected in the photolysis.
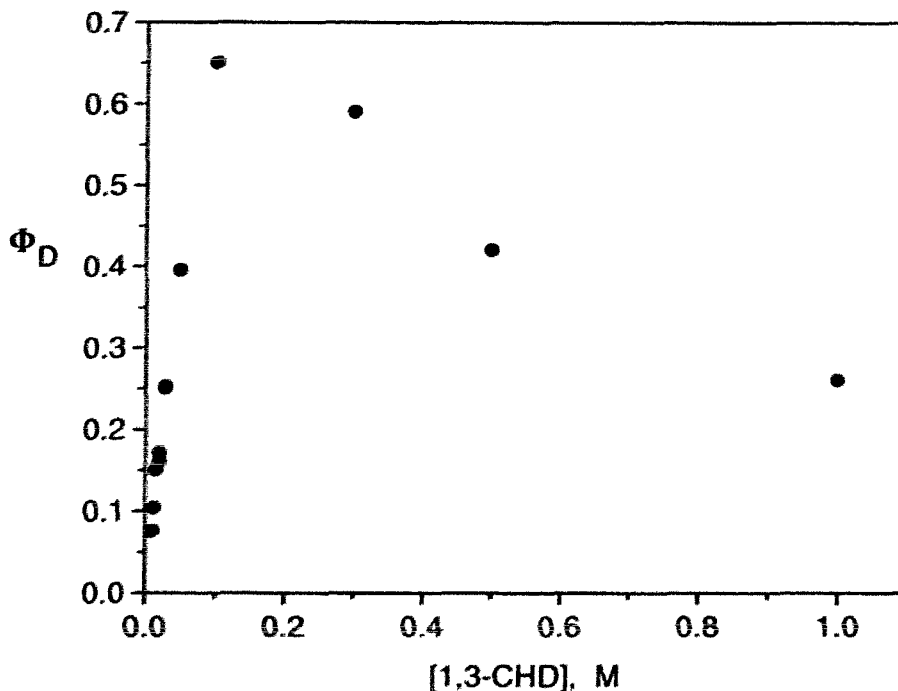
Fig. 3.3 The [4+2] dimer quantum yield (Φ_D) of CHD cosensitized by
DBMBF$_2$ in acetonitrile with 10% xylene: CHD concentration effect.

In summary, an efficient Diels-Alder dimerization of CHD was found with DBMBF$_2$

and xylene as the cosensitizers in acetonitrile solvent. Interpretation of the above

results allows the following conclusions to be made:

(1) Adduct quantum yields of the DBMBF$_2$ photoreaction with cyclic dienes are

nearly constant at $\Phi_A \approx 10^{-3}$ when the mole fraction of xylene or toluene (x_{BZ}) is less than

0.8, but the quantum yields increase sharply at $x_{BZ} > 0.8$ (Fig. 3.1);

(2) The [4+2] dimerization of CHD is sensitive to the mole fractions of xylene or

toluene (x_{BZ}). The dimer quantum yield (Φ_D) sharply increases at $x_{BZ} < 0.1$, but

decreases at $x_{BZ} > 0.1$. A maximum of $\Phi_D = 0.6$ is observed at $x_{BZ} = 0.1$ (Fig. 3.2);

(3) The CHD concentration effect reveals a self-quenching process which causes

a decrease in dimer formation at [CHD] larger than 0.1M (Fig. 3.3).

3.1.1.2 Binary solvent mixtures of benzene-ether types

In benzene-ether solvent systems, correlations of adduct quantum yield (Φ_A) with the benzene mole fraction (x_{BZ}) showed a similar pattern to that observed in the acetonitrile-xylene system (Fig. 3.1). The adduct quantum yield (Φ_A) increased with greater x_{BZ}-values, but the increase of Φ_A as the function of x_{BZ} became smaller in the following sequence: THF - benzene, dioxane - benzene and THP - benzene, to ether - benzene (Fig. 3.4). In diethyl ether-benzene solvent mixture, the adduct quantum yield Φ_A is almost constant despite large changes in the mole fraction of benzene (x_{BZ}). This may be attributed to the similar solvent polarities of ether and benzene, with the $E_T(30)$
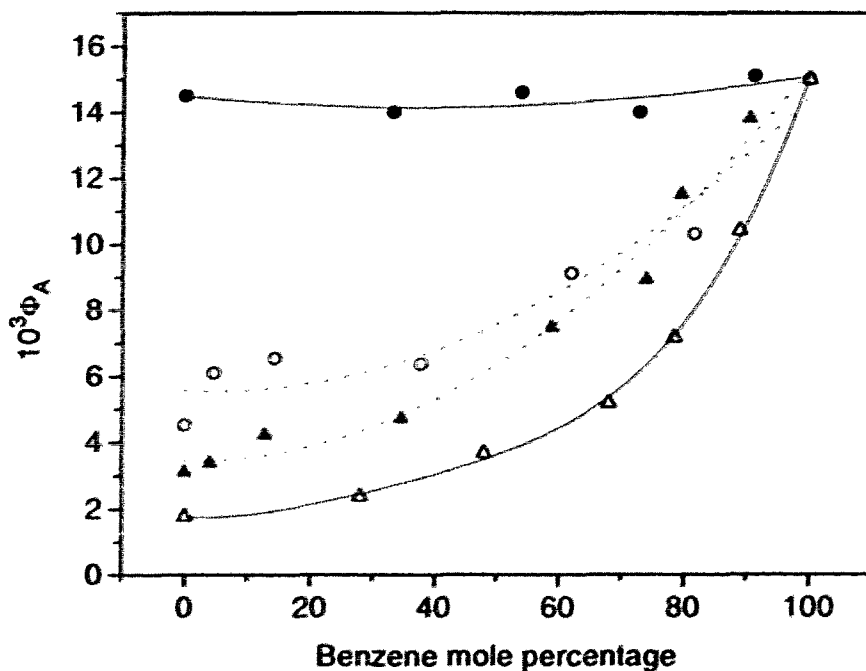
Fig. 3.4 Photoaddition quantum yield (Φ_A) of DBMBF$_2$ (0.03 M) to CHD (0.3 M) as a function of the benzene mole fraction (x_{BZ}): in ether-benzene (●); in THP-benzene (○); in dioxane-benzene (▲) and in THF-benzene (△); All the data are from Tables 5.9, 5.10, 5.11 and 5.12.

values of 34.5 and 34.3 kcal/mole respectively. The variation of adduct quantum yields is thus related to the change in solvent polarity.

3.1.1.3 CH$_3$CN - THF and CH$_3$CN - Dioxane Mixtures

In CH$_3$CN - THF and CH$_3$CN - dioxane solvent mixtures, there should be no involvement of the DBMBF$_2$-arene exciplex intermediate. Examination of the photoreactions of DBMBF$_2$ (0.03 M) with CHD (0.3 M) or 1,3-COD (0.3 M) in these solvents demonstrated a similar solvent effect pattern: the decreased solvent polarity enhanced the DBMBF$_2$ cycloaddition reaction but depressed CHD dimerization (Tables 3.5 and 3.6).

Table 3.5   Quantum yields of DBMBF$_2$ photoreactions with CHD
in CH$_3$CN - THF solvent mixtures[a]

THF mole % in CH$_3$CN	E$_T$(30) (kcal/mole)	$10^3 \Phi_A$ (of 6)	$10^3 \Phi_D$	CHD dimer ratio	
				(2 + 3) : (4 + 5)	2 : 3
0	45.6	0.30	32.0	96.2 : 3.8	7.8
21.6	43.8	0.49	9.4	83.8 : 16.2	5.5
49.0	41.6	0.68	6.1	57.8 : 42.2	2.3
72.0	39.7	0.68	5.1	43.8 : 56.2	1.2
85.2	38.6	0.93	5.3	36.7 : 63.3	0.71
100	37.4	1.80	6.5	32.0 : 68.0	0.42

Note: [a] Irradiation for 60 min.

Dioxane mole % in CH$_3$CN	E$_T$(30)		$10^3\Phi_A$ (of 12)
	Calculated [b] (kcal/mole)	Experimental [c]	
0	45.6	45.6	~0.09
23.5	43.3	45.2	0.18
47.9	41.0	43.7	0.27
77.6	38.2	41.3	0.76
92.1	36.8	38.3	1.36
100	36.0	36.0	3.22

Notes: [a] Irradiation for 170 min.; [b] Based on Eq. 3.1; [c] From Ref. 105.

3.1.2 The dehydrogenated coupling reaction of *p*-xylene sensitized by DBMBF$_2$

Two coupling products of *p*-xylene were found in $\leq 1\%$ GC yield based on
xylene, when an acetonitrile solution of *p*-xylene (2 M) and DBMBF$_2$ (0.01 M) was
irradiated at 350 nm for 4.5 hours. Both compounds had a molecular ion of m/z = 210
and showed fragmentation patterns in the MS identical to the standard compounds: 4-
tolyl-2,5-xylylmethane (**25**, major) and 1,2-bis-(4-tolyl)ethane (**26**, minor).[78, 106]
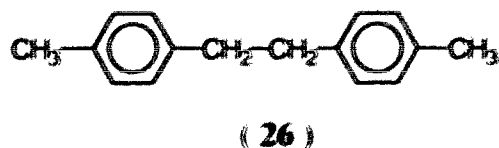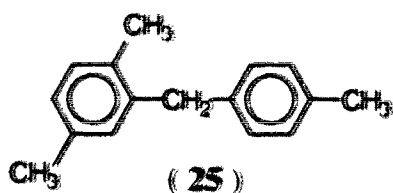
The structure of the major compound **25** was confirmed by GC coinjection with an authentic sample prepared by refluxing *p*-xylene with $CuCl_2$.[107] The Friedel-Crafts alkylation of 4-methylbenzyl chloride with *p*-xylene also produced the same diarylmethane product.[108] The minor compound **26**, which is possibly a radical coupling product, can be prepared from the photolysis of xylene with acetone or quinone as a sensitizer.[109, 110]

It was found that *p*-xylene could quench the singlet excited $DBMBF_2$ efficiently in acetonitrile ($k_q = 1.5 \times 10^{10}$ $M^{-1}s^{-1}$).[63] At [xylene] $\approx$ 1.3 M, the quenching resulted in a total disappearance of $DBMBF_2$ fluorescence. The emission of $DBMBF_2$-xylene exciplex began to appear at [xylene] > 5 M and became stronger at higher xylene concentrations. It was also found that this exciplex fluorescence could be quenched by conjugated cyclic dienes CHD ($k_q = 3.8 \times 10^9$ $M^{-1}s^{-1}$) and 1,3-COD ($k_q = 0.8 \times 10^9$ $M^{-1}s^{-1}$) in pure xylene solvent.[63] As a consequence of this quenching, the presence of conjugated cyclic dienes drastically reduced the coupling reactions of xylene.

In the absence of a conjugated cyclic diene, the formation of the coupling product, sensitized by $DBMBF_2$ (0.01 M) in acetonitrile, was investigated as a function of xylene concentration (Fig. 3.5). The highest yield of products **25** and **26** occurred at [xylene] = 4 to 5 M, or at a xylene mole fraction of 0.3 – 0.4. The product yield then decreased at the concentration of xylene greater than 5 M since the emission of $DBMBF_2$-xylene exciplex became its major decay route.[63]

In the presence of lithium perchlorate ($LiClO_4$), the sensitized coupling reaction of *p*-xylene was enhanced, consistent with a salt effect in acetonitrile (Table 3.7).

$E_T(30)$, kcal/mole
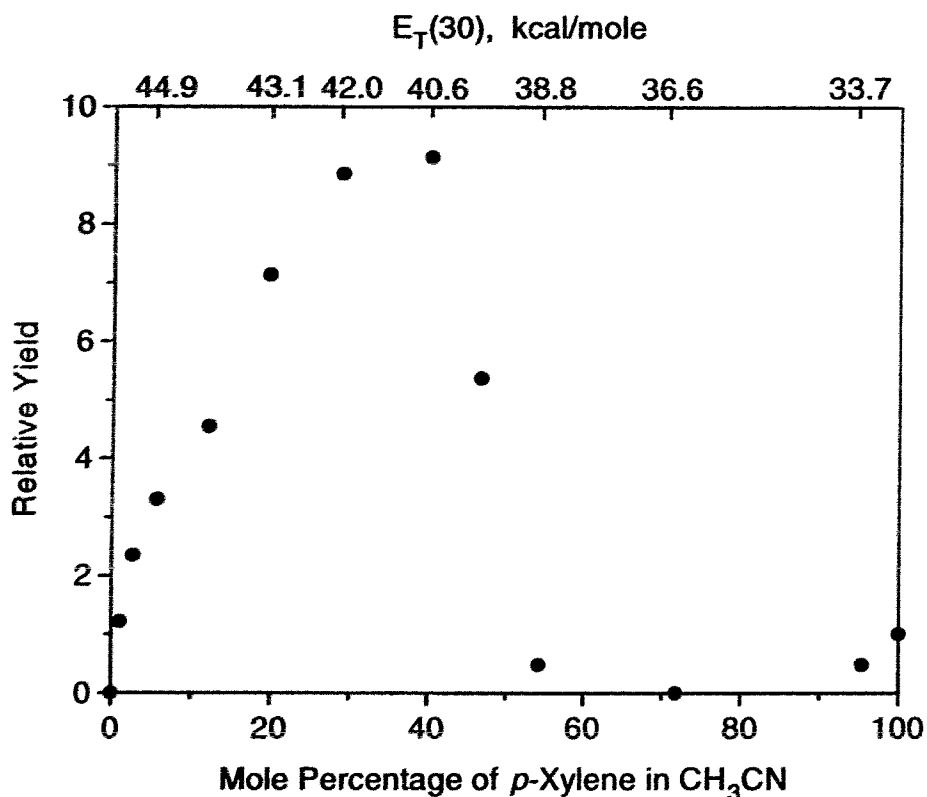
Fig. 3.5   Relative yields of (25 + 26) as a function of p-xylene concentration: [DBMBF$_2$] = 0.01 M and the product yield in neat xylene defined to be 1.00.

Table 3.7   Salt effect on the p-xylene coupling reaction in the presence of DBMBF$_2$ (0.01 M) [a]

p-xylene mole % in CH$_3$CN	[p-xylene] M	[LiClO$_4$] M	Relative yield of (25 + 26)
12.2	2	0.00	1.00
12.2	2	0.01	1.76
12.2	2	0.20	1.55

Note: [a] Irradiation at 350 nm for 3 hours.

3.2 Discussion

3.2.1 Solvent effect on DBMBF$_2$ photoreactions in binary solvent mixtures

3.2.1.1 The E$_T$(30)-values of binary solvent mixtures

E$_T$(30) values of pure solvents are widely used as comprehensive solvent polarity measures, but the E$_T$(30) values for binary solvent mixtures should be used with caution. This is due to the preferential or selective solvation of the pyridinium N-phenolate betaine dye by the polar solvent component. In most cases, the binary solvent mixtures behave as non-ideal solvents, and the experimental E$_T$(30) values of the mixtures are not linearly related to the solvent composition (Fig. 3.6).[105]

It may not be valid to apply the preferential solvation of the betaine dye to measuring the solvation of other solutes with different chemical structures,[105, 100a]
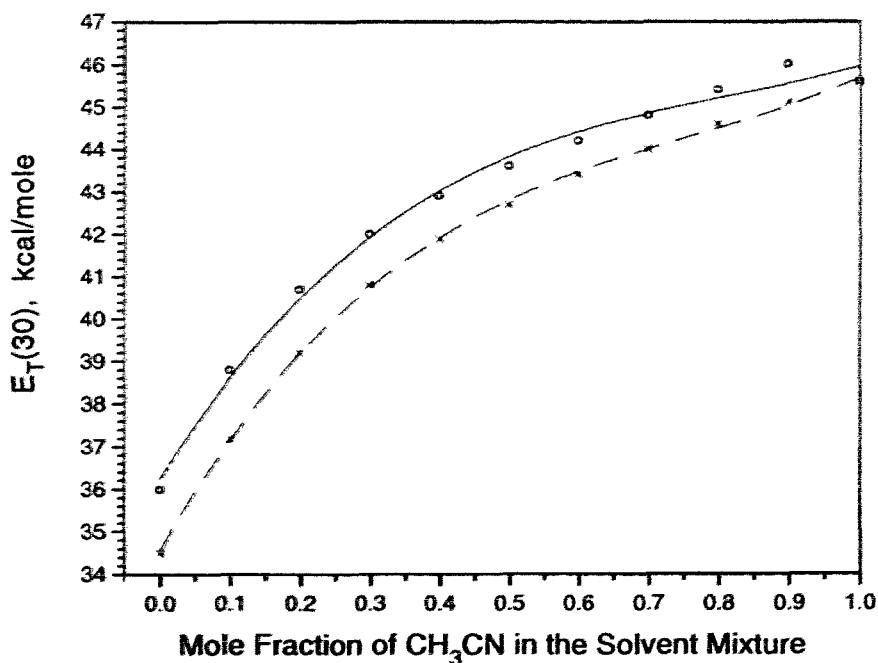
Fig. 3.6 Correlations of the experimental E$_T$(30)-values with mole fractions of acetonitrile in the binary dioxane - CH$_3$CN (o) and benzene - CH$_3$CN (x) systems.[105]

because preferential solvation is dependent on the solute nature or its chemical structure. The $E_T(30)$-values of solvent mixtures are actually a microscopic scale measure of solvent polarity, i.e., around the solvation shell of the betaine dye molecule. In applying the $E_T(30)$ scale, there is an assumption that the interactions between the solvent and the betaine solute should represent those interactions between the solvent and the particular substrate. However, in binary solvent mixtures, this assumption can break down, especially when there are strong interactions between solute and solvent molecules.

In choosing a solvent polarity scale for DBMBF$_2$ photoreactions in binary solvent mixtures, we faced two difficulties: (1) the experimental $E_T(30)$ values for solvent mixtures may not be suitable to describe our experiments, due to concerns about the observed preferential solvation, and (2) experimental $E_T(30)$ values for most of our solvent mixtures are not available in the literature. Therefore, we used equation 3.1 to calculate the composite $E_T(30)$ values for the binary solvent mixtures.

3.2.1.2 Preferential solvation in DBMBF$_2$ photoreactions

The DBMBF$_2$ photoreaction with conjugated cyclic dienes in binary solvent mixtures showed a marked similarity to the reactions in pure solvents. For example, the solvent polarity determines the adduct quantum yield (Φ_A) in binary solvent mixtures (Fig. 3.1 and 3.4). However, in contrast to the linear relationship of $ln(1/\Phi_A)$ to $E_T(30)$ in pure solvents (Fig. 2.13), the corresponding plots of $ln(1/\Phi_A)$ vs. $E_T(30)$ for DBMBF$_2$ photoreactions in binary solvent mixtures are curves (Fig. 3.7 for the data in Tables 3.1 ~ 3.3 and Fig. 3.8 for Tables 3.5, 5.12, 5.14 and 5.15).
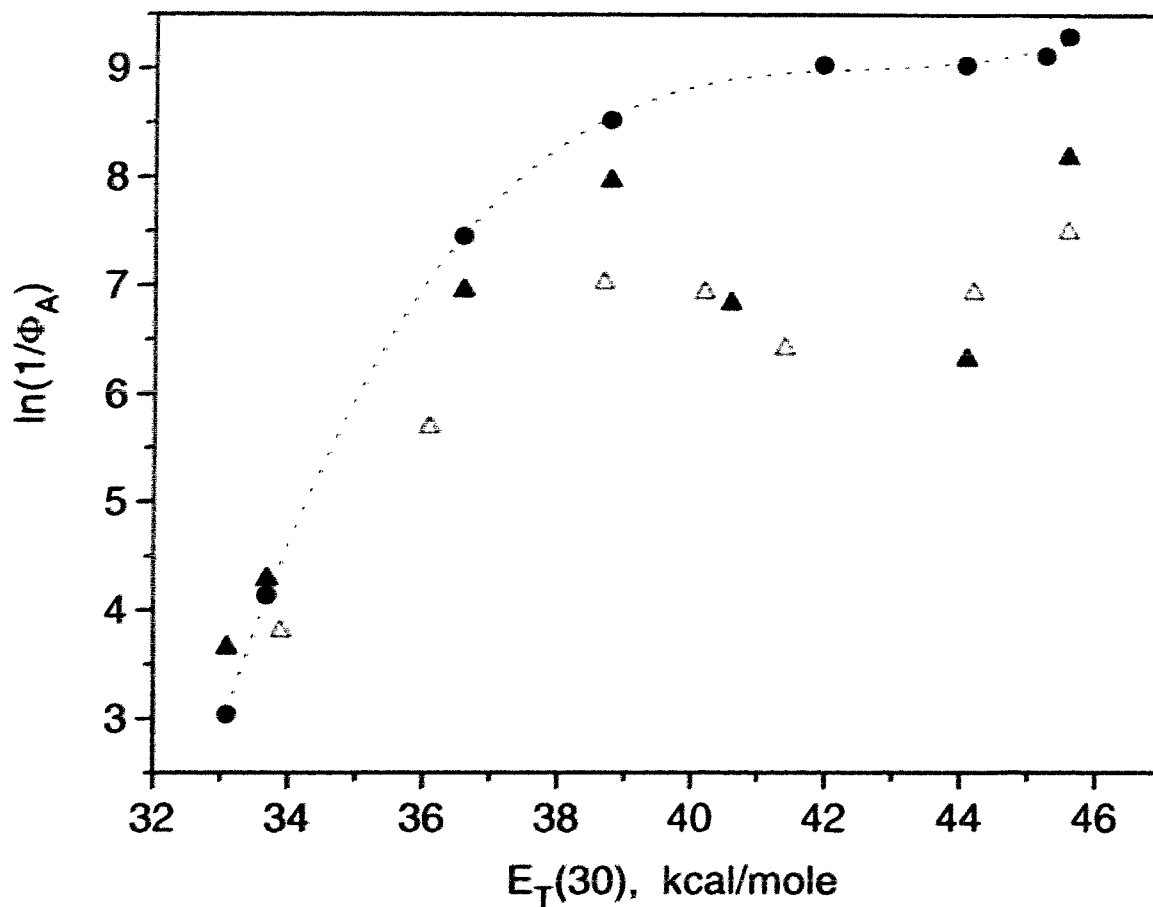
Fig. 3.7 Plots of $ln(1/\Phi_A)$ vs. $E_T(30)$ for DBMBF$_2$ photoreactions with cyclic dienes in binary solvent mixtures: 1,3-COD in xylene - CH_3CN (●), CHD in xylene - CH_3CN (▲) and in toluene - CH_3CN (△). (Data are from Tables 3.1, 3.2 and 3.3)
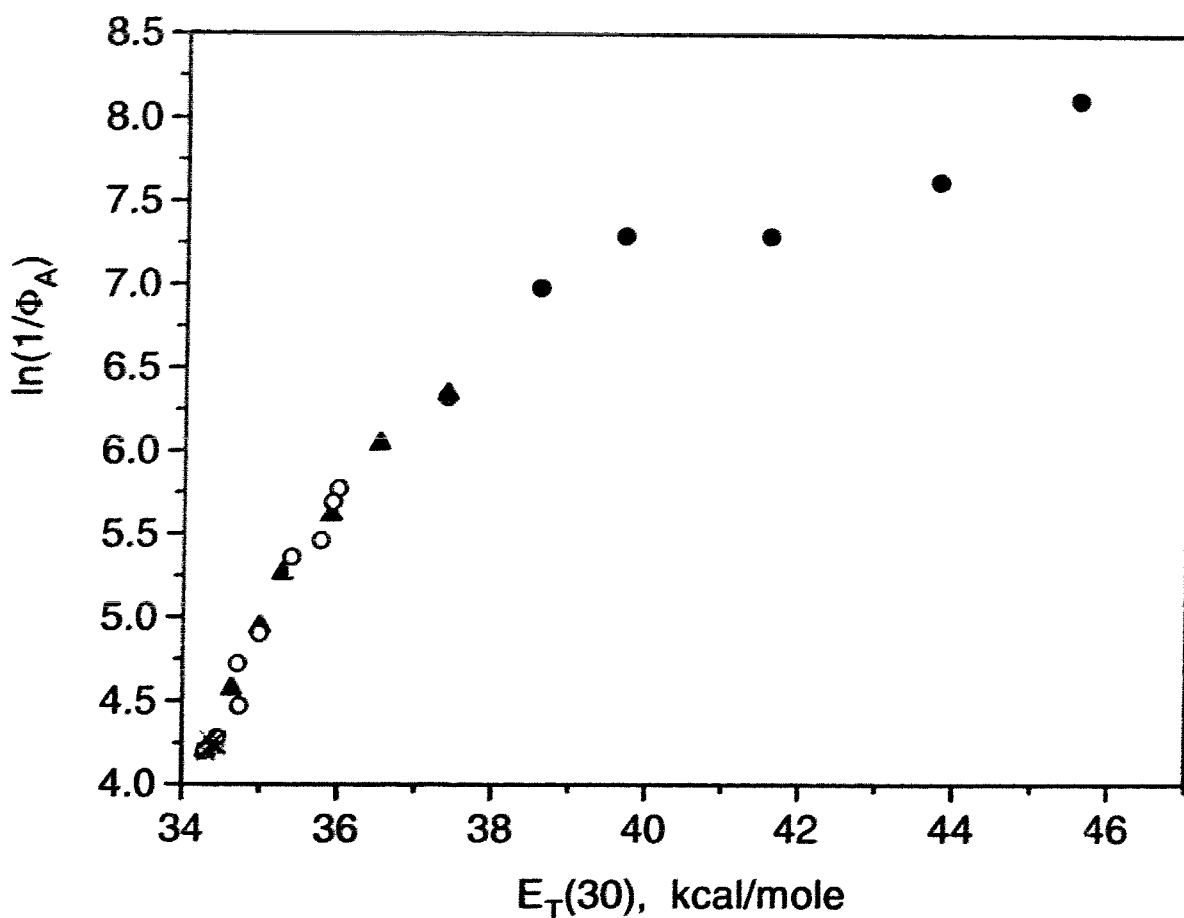
Fig. 3.8 Plots of $ln(1/\Phi_A)$ vs. $E_T(30)$ for DBMBF$_2$ photoreactions with CHD in binary solvent mixtures: benzene - ether (×), benzene - dioxane (O), benzene - THF (▲) and THF - CH$_3$CN (●). (Data are from Tables 3.5, 5.12, 5.14 and 5.15)

Both figures exhibit a trend where a decrease in adduct quantum yield (Φ_A) occurs when solvent polarity $E_T(30)$ is increased. But in Fig. 3.7, the addition of a small amount of acetonitrile to the DBMBF$_2$-diene solution in xylene or toluene caused a bigger drop in Φ_A. This suggests that the solvent polarity around the local solvation shell of the DBMBF$_2$ - olefin exciplex may actually be much higher than the bulk media as a result of preferential solvation. We believe that the exciplex intermediate is solvated

selectively by the more polar acetonitrile molecules, thus the exciplex ionic dissociation should be enhanced and the adduct formation depressed. This provides a rationale for the curvature of $ln(1/\Phi_A)$ - $E_T(30)$ plot.

It should be also noted in Fig. 3.7 that some triangle-points deviate from the $ln(1/\Phi_A)$ curve plot, within the range of $E_T(30)$-values from 39 to 46 kcal/mole (corresponding to the mole-percentage of xylene or toluene from ~54% to 0% in acetonitrile). This deviation in adduct quantum yields (Φ_A) coincides with the cosensitized CHD dimerization by $DBMBF_2$ and xylene (Tables 3.1 and 3.2, Fig. 3.2). At $E_T(30) \approx 44$ kcal/mole (p-xylene% $\approx$ 12), the dimer quantum yield $\Phi_D \approx 0.6$ was observed for CHD (Fig. 3.2), but the adduct quantum yield (Φ_A) was ≤ 0.002 for the photocycloaddition of $DBMBF_2$ to CHD (Table 3.1). Although the Φ_A- variation in this part is not understood yet, it is evident that the dimerization of CHD is the dominant process here and warrants further investigation.

3.2.2 Cosensitized Diels-Alder dimerization of 1,3-cyclohexadiene

Benzene, toluene and xylene can all enhance the $DBMBF_2$ sensitized [4+2] dimerization of CHD in acetonitrile. For example, the dimer quantum yield (Φ_D) shows a sharp increase on an addition of small amount of xylene to the acetonitrile solution (Fig. 3.2). A maximum dimer quantum yield appears at about 1.5 M xylene, and further addition of xylene reduces the dimer formation reaction because the overall solvent polarity should decrease with the increased xylene concentration.

Taking the above observations into consideration, Scheme 2.7 must be modified to reflect the enhanced CHD dimerization. We propose that the cosensitized CHD

dimerization is mediated by the radical cation $CHD^{+\cdot}$. With regard to the formation of this radical cation, there would be two possibilities (Scheme 3.1): (i) it is formed through a secondary electron transfer process from CHD to the radical cation $xylene^{+\cdot}$ that is the ionic dissociation product of the $DBMBF_2$-xylene exciplex $^*(AR)$ in acetonitrile; (ii) it is formed by a triplex $^*(ARD)$ mechanism in which an inner-sphere electron transfer occurs from CHD to excited $DBMBF_2$ mediated by xylene molecule, followed by the triplex dissociation to give $CHD^{+\cdot}$ (Scheme 3.1).

Scheme 3.1: The initiation of $CHD^{+\cdot}$
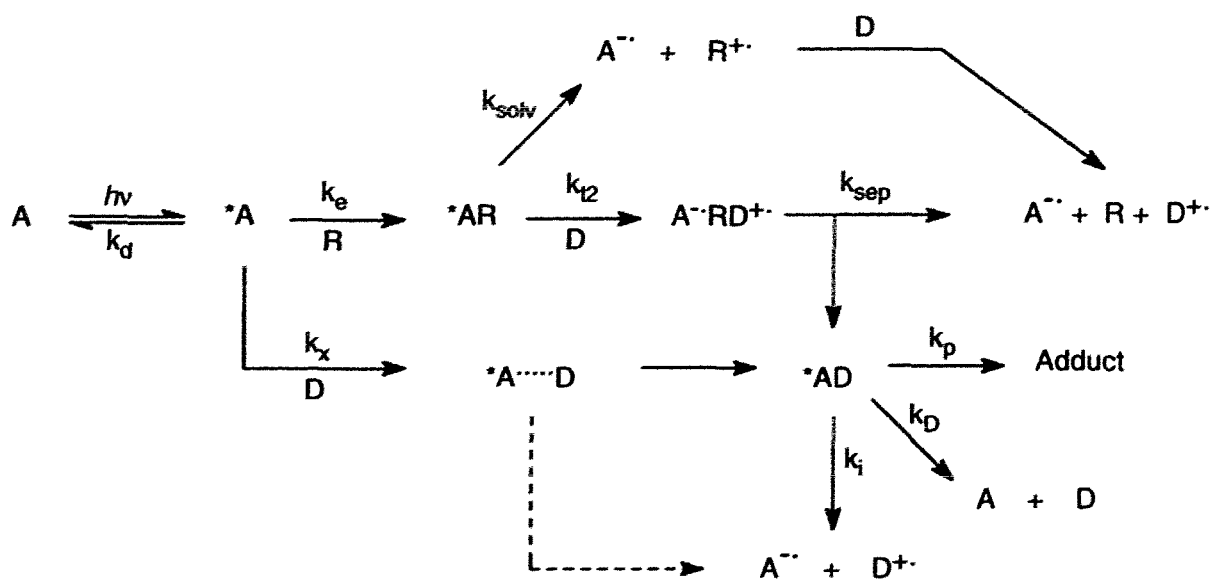
$A = DBMBF_2$, $R = $ Xylene, $D = $ CHD.

Here k_{solv} is the rate constant of ionic dissociation for the exciplex $^*AR$, and k_{sep} is for the triplex $^*ARD$ dissociation.

Based on this scheme, p-xylene could have two functions in the $DBMBF_2$ photoreaction: (1) to quench singlet excited $DBMBF_2$ forming the exciplex $^*AR$, which favours the cycloaddition pathway in a nonpolar solvent and dissociates in a polar solvent to give a xylene radical cation causing subsequent CHD dimerization, and (2) to

change the solvent polarity, which will affect the decay pathways of the $DBMBF_2$-xylene exciplex. In quenching the singlet excited $DBMBF_2$ fluorescence, there was a complete disappearance of the fluorescence emission when the quencher p-xylene reached 1.3 M in acetonitrile.[32] When [p-xylene] = 6 M, the overall solvent polarity was significantly reduced, and a very weak emission band of the exciplex began to emerge, and this emission continued to increase at higher xylene concentrations.[63] But at [p-xylene] < 6 M, the exciplex decayed mainly through nonradiative pathways. One possibility is the ionic dissociation of the $DBMBF_2$-xylene exciplex, leading to p-xylene coupling product formation in the absence of cyclic dienes (Fig. 3.5). In the presence of CHD and at [p-xylene] ≤ 2 M, the solvent polarity is still close to that of acetonitrile, thus it is possible for the exciplex *AR (or the triplex *ARD) to decay by an ionic dissociation which initiates the reaction of CHD dimerization (Scheme 3.1).

According to Scheme 3.1, the effect of CHD concentrations on the dimer quantum yield (Φ_D) should be primarily determined by two competing processes between k_e[*A][R] via the exciplex *AR and k_x[*A][D] via the encounter complex *A ⋯ D in acetonitrile. It should be noted that the latter pathway is not as efficient as the former one in the dimer production (Tables 3.1 and 3.2). The competition for capturing the singlet excited $DBMBF_2$ (*A) by xylene (R) or by CHD (D) can be analyzed by comparing the rates of k_e[*A][R] and k_x[*A][D]:

$$\frac{\text{Rate of *AR formation}}{\text{Rate of quenching *A by CHD}} = \frac{k_e[R][*A]}{k_x[D][*A]} = \frac{1.5 \times 10^{10} \times 1.5}{3.1 \times 10^{10} \times 0.1} \cong 7$$

here $k_e = 1.5 \times 10^{10}$ s⁻¹M⁻¹ is for quenching $DBMBF_2$ fluorescence by p-xylene in acetonitrile,[63] $k_x = 3.1 \times 10^{10}$ s⁻¹M⁻¹ is for quenching $DBMBF_2$ fluorescence by CHD in acetonitrile,[63] [R] = 1.5 M is the xylene concentration corresponding to the highest Φ_D in

Fig. 3.2, and [D] = 0.1 M is the CHD concentration corresponding to the highest Φ_D in

Fig. 3.3. It is estimated that at a fixed xylene concentration (1.5 M), an increase of

[CHD] from 0.1 to 0.3 M will reduce the relative rate of $k_e[{}^*A][R]$ to $k_x[{}^*A][D]$ from 7 to 2.

This can provisionally explain why high concentrations of CHD should depress the

formation of exciplex ${}^*AR$ and reduce the dimer production (Fig. 3.3).

The following findings are put forward to support the postulate of exciplex ${}^*AR$

dissociation followed by a secondary electron transfer between the xylene radical ion

and a CHD molecule:

(1) Under comparable conditions, the enhancement of dimer production by

arene molecules is in the order p-xylene > toluene > benzene. This is consistent with

the trend in exciplex polarity, i.e., ${}^*DBMBF_2$-xylene > ${}^*DBMBF_2$-toluene > ${}^*DBMBF_2$-

benzene. A more polar exciplex dissociates more readily in polar solvents.

(2) The quenching rate constant (k_q) of $DBMBF_2$ monomer fluorescence by the

arene in acetonitrile shows a similar order: p-xylene $(1.5 \times 10^{10}\ M^{-1}s^{-1})$ > toluene $(4 \times 10^9$

$M^{-1}s^{-1})$ > and benzene $(\sim 10^9\ M^{-1}s^{-1})$.[60, 74a] The strongest quenching of singlet excited

$DBMBF_2$ by p-xylene results in the most enhanced dimer production.

(3) The secondary electron transfer is a highly exothermic process. For each

reaction below, an electron transfer from CHD to the arene radical cation $(R^\bullet)$ has a free

energy change of $\Delta G_{ET} < -0.2$ V (Eq. 3.2), and it has been argued that values of this

magnitude are sufficiently exothermic for the electron transfer to proceed at the

diffusion-controlled rate.[24b]

$$R^\bullet + D \rightarrow R + D^\bullet \qquad \Delta G_{ET} = E_D^{ox} - E_R^{ox} \qquad \text{(Eq. 3.2)}$$

Compound:	Xylene	Toluene	Benzene	CHD
E^{ox} :	2.06	2.25	2.63	1.55 V (vs. SCE in CH_3CN)
ΔG_{ET}	-0.51	-0.70	-1.08 V	

(4) In the absence of 1,3-cyclohexadiene, the photolysis of the $DBMBF_2$ - xylene system in acetonitrile yields the xylene coupling products **25** and **26**, and the coupling reaction is promoted by salt effects (Table 3.7). This observation is consistent with ionic dissociation of the $DBMBF_2$-xylene exciplex.

However, there are some arguments against the above postulate of $DBMBF_2$-xylene exciplex dissociation in acetonitrile. CIDNP studies on the $DBMBF_2$-toluene exciplex in CD_3CN suggested that the exciplex did not form its solvent-separated ion pair.[74] When the $DBMBF_2$ - toluene exciplex reacted with norbornadiene (NBD), the formation of the triplex *($DBMBF_2$-Toluene-NBD) was proposed as a key step to initiate the isomerization of NBD to quadricyclane (QC).[74a] Similar to this NBD reaction, the $DBMBF_2$-toluene or xylene exciplex may also react with CHD to form a triplex intermediate in the sensitized CHD dimerization. CIDNP studies should lend support to the possibility of a triplex *ARD in Scheme 3.1.

Listed in Table 3.8 are the results of the exciplex fluorescence quenching by 1,3-cyclohexadiene (CHD). The quenching efficiency (K_{SV}^{ex}) reflects the lifetime of exciplex in following order: *$DBMBF_2$-xylene > *$DBMBF_2$-toluene > *$DBMBF_2$-benzene, but the

Table 3.8 Fluorescence quenching of $DBMBF_2$ exciplex (*AR) by CHD[63]

Exciplex *AR (solvent)	R = p-xylene (xylene)	R = toluene (toluene)	R = benzene (benzene)
K_{SV}^{ex} ($= k_q\tau_{ex}$),[a] M^{-1}	56.6	25.2	18.8
τ_{ex}, ns	15.0	4.1	2.1
$k_q \times 10^{-9}$, $M^{-1}s^{-1}$	3.8	6.2	9.0

Note: [a] K_{SV}^{ex} is Stern-Volmer quenching constant, k_q is the rate constant of quenching *AR and τ_{ex} is the lifetime of *AR.

quenching rate constant (k_q) follows a reverse sequence for: *DBMBF$_2$-xylene < *DBMBF$_2$-toluene < *DBMBF$_2$-benzene (Table 3.8). Although it is not clear yet whether these exciplex quenching results are related to the proposed intermediacy of a triplex (*ARD), an orbital energy diagram for *AR exciplex formation and quenching by CHD (Fig. 3.9) can be proposed, using the FMO model suggested by Caldwell to explain the quenching of exciplexes and excimers by various electron donor quenchers.[75b]

The data for the FMO diagram are listed in Table 3.9, in which the ionization potential (IP) is related to the HOMO and LUMO energies by:[3]

$$E_{HOMO} = -IP \qquad \text{and} \qquad E_{LUMO} = -IP + E_S$$

Since IP values refer to the gas phase, the data for the singlet excited state (E_S) were taken from measurements in the nonpolar solvent cyclohexane. In addition to the HOMO-LUMO energies for the acceptor DBMBF$_2$ and the donor components of the exciplex (Fig. 3.9), the energy gap between the exciplex orbitals Ψ_2 and Ψ_3 could be estimated as the transition energies of the exciplexes, measurable from their emissions (λ_{em}^{max}, Table 3.10).

For the exciplex of DBMBF$_2$ with p-xylene, each exciplex component has a different HOMO and LUMO, and orbital interaction between DBMBF$_2$ and xylene leads to four exciplex orbitals (Ψ_1, Ψ_2, Ψ_3 and Ψ_4, Fig. 3.9). The HOMO$_A$ - HOMO$_R$ interaction produces Ψ_1 and Ψ_2, and LUMO$_A$ - LUMO$_R$ produces Ψ_3 and Ψ_4. Since Ψ_2 and Ψ_4 contain more xylene character, and Ψ_1 and Ψ_3 have more contribution from DBMBF$_2$, the transfer of an electron from xylene (HOMO$_R$) to *DBMBF$_2$ (HOMO$_A$) can be nearly complete in the exciplex formation. This accounts for the high charge transfer (CT) character of the DBMBF$_2$ - xylene exciplex. However, this CT feature decreases in the exciplexes of DBMBF$_2$ with toluene and benzene. As shown in Fig. 3.9, there is

Table 3.9 HOMO-LUMO energies of DBMBF$_2$, CHD and the arenes

	IP (eV) [a]	EA (eV) [b]	E$_S$ (eV) [c]	E$_{LUMO}$ (eV) [d]
DBMBF$_2$	(9.06) [e]	--	3.19 [27]	-5.82
Benzene	9.23	-1.15	4.76	-4.47
Toluene	8.80	-0.40	4.61	-4.19
p-Xylene	8.44	-1.07	4.51	-3.93
CHD	8.25	-0.73	4.25	-4.0
1,3-COD	8.40	--	--	--

Notes: [a] Vertical ionization potential cited from Ref 111; [b] Electron affinity cited from Ref. 112b; [c] The energy of the singlet excited state measured in cyclohexane solvent, from Ref. 112b; [d] The energy of the LUMO: $E_{LUMO} = (-IP + E_S)$ as defined in Ref. 3; [e] Estimated from the corresponding value of $E_{ox} = 2.45$ V.[58]

Table 3.10 Transition energy of exciplex *AR in cyclohexane

Exciplex *AR	λ_{em}^{max}, nm [a]	Transition energy (eV) [b]
*DBMBF$_2$-benzene	413	3.00
*DBMBF$_2$-toluene	429	2.89
*DBMBF$_2$-xylene	448	2.77

Notes: [a] λ_{em}^{max} is the wavelength of exciplex emission, cited from Ref. 58;

[b] Calculated from λ_{em}^{max} according to Eq. 2.13.
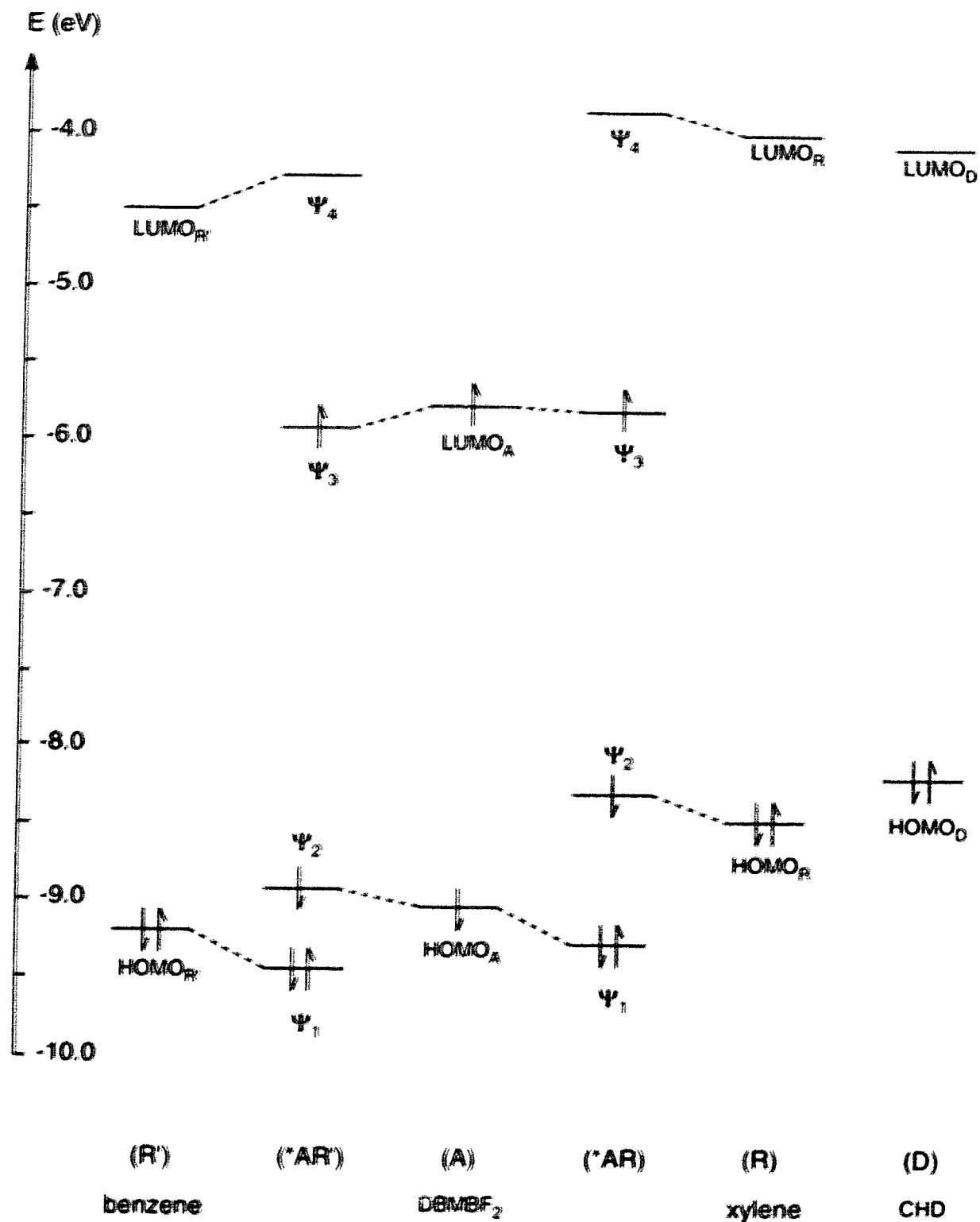
Fig. 3.9 Schematic orbital energy diagram of the DBMBF₂-arene exciplex formation and its interaction with CHD.

no electron transfer in the DBMBF$_2$-benzene exciplex, i.e., this exciplex has the least charge transfer character.

In quenching the exciplex *AR by CHD, an electron will be transferred from the HOMO$_D$ of CHD to the exciplex orbital Ψ_2 (Fig. 3.9). Since the exothermicity of this process is determined by the energy difference between HOMO$_D$ and Ψ_2,[75b] the rate constant (k_q) for quenching the exciplex emission by CHD is expected in the following order for: *DBMBF$_2$-benzene (9.0 x 10^9 s^{-1} M^{-1}) > *DBMBF$_2$-toluene (6.2 x 10^9 s^{-1} M^{-1}) > *DBMBF$_2$-xylene (3.8 x 10^9 s^{-1} M^{-1}, in Table 3.8).

A geometric requirement for quenching the exciplex *AR by CHD can be suggested based on Fig. 3.9, namely, *(A$^{\delta-}$···· R$^{\delta+}$···· D$^{\delta+}$). Because an electron is transferred from the HOMO$_D$ of CHD to the exciplex orbital Ψ_2 that is localized on the arene (R = p-xylene), the electron donor CHD should preferentially approach the exciplex from the arene side, where the partially positive charge is developed. For such a structure, a triplex *ARD can be expected to form upon further orbital interactions.

As a summary of this chapter, the photoreactions of DBMBF$_2$ with conjugated cyclic dienes were investigated in binary solvent mixtures. The plots of the adduct quantum yield, $ln(1/\Phi_A)$, versus the composite E$_T$(30) scale (or the solvent composition) show a nonlinear relationship. This is rationalized as a result of the preferential solvation of DBMBF$_2$-diene exciplex in binary solvent mixtures. A very efficient Diels-Alder dimerization of CHD is found to proceed by the cosensitization of DBMBF$_2$ and xylene in acetonitrile. The sensitized dimerization of CHD is ascribed to the reaction of a DBMBF$_2$-xylene exciplex which has a longer lifetime than singlet excited DBMBF$_2$ itself. The reaction of this exciplex may involve either its ionic dissociation or its interaction with CHD to form a triplex intermediate.

CHAPTER FOUR

PHOTOCYCLOADDITIONS OF DBMBF₂ TO ELECTRON - DEFICIENT OLEFINS
α,β-UNSATURATED CARBONYL COMPOUNDS

4.1 Results

4.1.1 The profiles of photocycloadditions

Photolysis of $DBMBF_2$ and an α,β-unsaturated ketone or ester in acetonitrile

leads to the efficient [2+2] cycloaddition, by way of a presumed cyclobutane intermediate

which undergoes ring opening to give triketone products.

Scheme 4.1:

head-to-head   head-to-tail

(28)   (29)
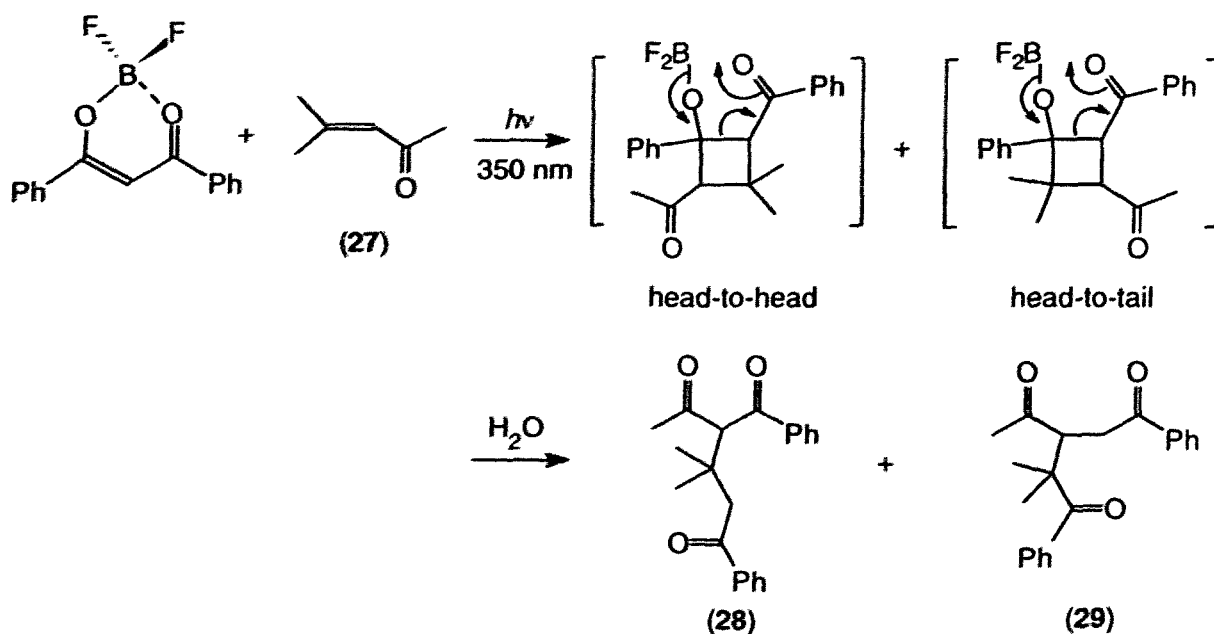
The photocycloadditions are regioselective and adopt a head-to-head orientation

for most of the substrates listed in Table 4.1. However, additional β-methyl substitution

(compounds 27, 33 and 46) leads to a head-to-tail orientation. It should be noted that

methyl methacrylate (31), which has α-methyl substitution, displays the best reactivity

among all of the substrates (Table 4.1). Photolysis of DBM with mesityl oxide (27) or methyl methacrylate (31) does not produce an adduct.

The results of photocycloaddition of DBMBF$_2$ to α,β-unsaturated ketones and esters are summarized in Table 4.1. The structures of the addition products were determined on the basis of spectral data (Table 5.8). In general, the mass spectra showed a molecular ion peak consistent with addition of DBM to the olefinic substrate, and IR and NMR confirmed the presence of benzoyl and phenacyl groups in the adducts. If the chiral carbon atom in an addition product is vicinal to two carbonyl groups, its methine proton has a larger chemical shift $\delta > 5.7$ (or 4.5) ppm. This indicates a head-to-head orientation. If the chiral carbon is adjacent to only one carbonyl group, the methine proton has a lower chemical shift $\delta < 4.3$ (or 3.9) ppm, indicative of head-to-tail orientation. The coupling patterns of these methine protons give the information about the relative position of the benzoyl and phenacyl groups.

The cycloaddition of DBMBF$_2$ to mesityl oxide

The photocycloaddition of DBMBF$_2$ to mesityl oxide (27) in acetonitrile yielded two products after 5 hours of irradiation. The type A and type B products have been proposed previously for the photocycloadditions of DBMBF$_2$ to acyclic enones (Scheme 4.2),[49] corresponding to a head-to-head orientation between DBMBF$_2$ and the enone.

Scheme 4.2:

head-to-head
addition

(28)
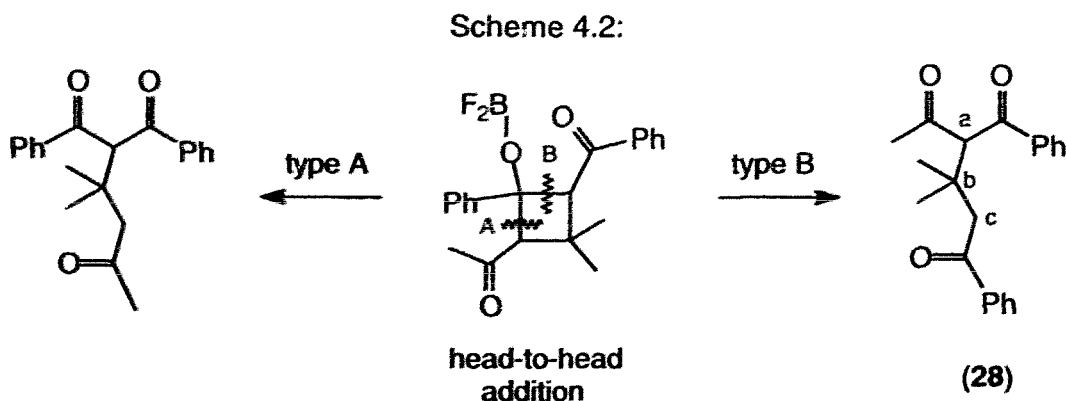
Table 4.1 Photocycloaddition of DBMBF$_2$ (0.05 M) to α,β-unsaturated carbonyl compounds (0.5 M) in acetonitrile
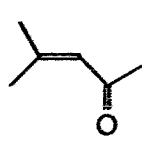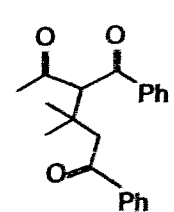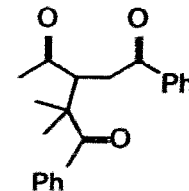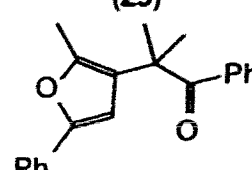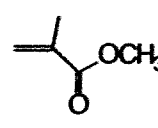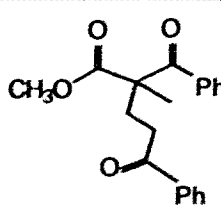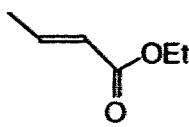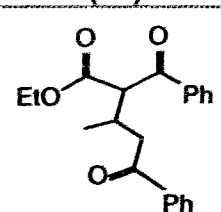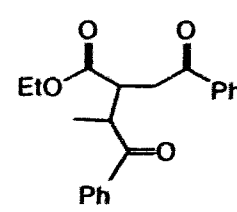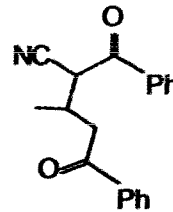
Substrate	t$_{irrad.}$ (hr)[a]	Addition Product (head-to-head)	(head-to-tail)	yield[b] %	Φ$_A$[c]
mesityl oxide (27)	2	(28)	(29)	48[d] 3	0.17
			(30)	34	
methyl methacrylate (31)	2	(32)		85	0.35
ethyl crotonate (33)	6	(34)	(35)	65[f] 16	0.027
crotononitrile[e] CH$_3$CH=CHCN (36)	26	(37)		41[e,f]	--

Table 4.1 (Continued)
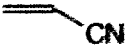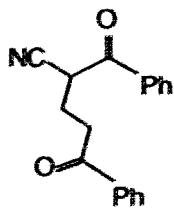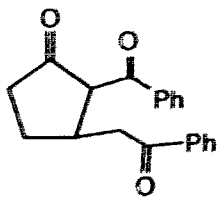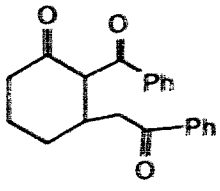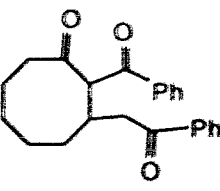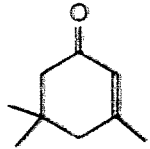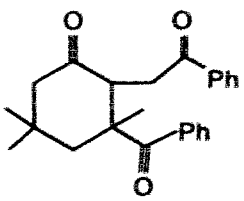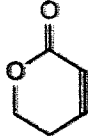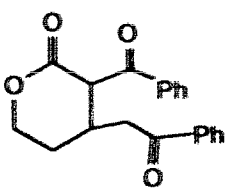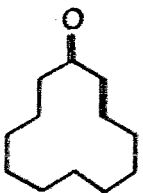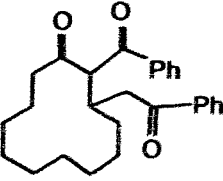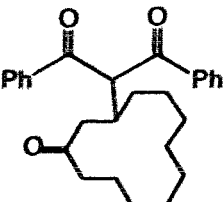
Substrate	t_{irrad} (hr)[a]	Addition Product (head-to-head)	(head-to-tail)	yield[b] %	Φ_A[c]
acrylonitrile (38)	26	(39)		59[g]	--
cyclopentenone (40)	25	(41)		61[i]	0.003
cyclohexenone (42)	15	(43)		47[i]	0.007
2-cyclooctenone (44, 0.08 M)	22	(45)		46[i]	0.052
isophorone (46)	37		(47)	44	0.006
5,6-dihydro-2H-pyran-2-one (48)	9 days	(49)		37[i,h]	--

Table 4.1 (Continued)

Substrate	t_{irrad} (hr)[a]	Addition Product (head-to-head)	(head-to-tail)	yield[b] %	Φ_A[c]
2-cyclodode-cenone (50, 0.2 M)	16	(51) (52)		42[f] 14	0.057

Notes: [a] The irradiation time (t_{irrad}); [b] The isolated chemical yield is based on consumed DBMBF$_2$; in most cases the conversion is greater than 95%. [c] Quantum yield of adduct formation. [d] A known compound identified by X.E. Cheng,[49] and the yields of products are based on GC analysis. [e] The substrate is a E- / Z-mixture (41 / 59), based on ^{1}H NMR analysis, with a DBMBF$_2$ conversion of 47%. [f] Two diastereomers were found with cis- and trans- orientations of the two hydrogen atoms on the chiral carbons. [g] DBMBF$_2$ conversion 25%. [h] DBMBF$_2$ conversion 70%.

These two types of addition product should be readily distinguishable by their NMR spectra. One of the products in the photoreaction of DBMBF$_2$ with mesityl oxide was easily recognized as the B type adduct 28. The presence of a chiral center at the methine carbon leads to nonequivalence of the methylene protons of 28: 2.96 ppm

(H_c, d, J = 17.8 Hz) and 3.63 ppm ($H_{c'}$, d, J = 17.8 Hz).[49] However, the second product

was not a type A product shown in Scheme 4.2. This new product has a parent ion peak

of m/z = 304, corresponding to the adduct of DBM to mesityl oxide minus H_2O. The

fragmentation pattern is not complex and is dominated by loss of a benzoyl fragment.

The ^{13}C NMR spectrum showed only one carbonyl carbon, with a chemical shift of 203

ppm, larger than that of benzoyl group (< 200 ppm). This suggests that the carbonyl

group is adjacent to a dimethyl substituent which could hinder C=O conjugation with a

phenyl ring. In addition to the eight carbon peaks of two phenyls, four olefinic carbons

appeared at 151.4, 147.1, 125.6 and 104.5 ppm. The first three are quaternary carbons,

showing the chemical shift pattern of a furan ring.[83] The ^{1}H NMR spectrum exhibited a

singlet for the olefinic proton at 6.66 ppm, together with two singlets in a 1 : 2 ratio for

the methyl substituents. The collective data strongly suggested the cyclized structure **30**.

When the photocycloaddition of $DBMBF_2$ with mesityl oxide was followed by GC,

the product profile revealed an additional product **29** (Fig. 4.1). This compound

appeared to be a major component in the early stages of photolysis, and then decreased

with prolonged irradiation and finally yielded the major cyclized product **30**.

The photoreaction was also carried out with similar regioselectivity and chemical

yields in dichloromethane, THF and benzene solvents (Table 4.2), except that in THF

solvent the new product **29** dominated throughout the photolysis.

the structure of **29** was assigned on the basis of the following analysis. In the [1]H

NMR spectrum a quartet at 4.25 ppm was assigned to the methine proton attached to

the chiral carbon atom. Compared to the singlet peak at 5.74 ppm from the methine

proton of the head-to-head adduct **28**, this chemical shift indicated the presence of one

adjacent carbonyl group. In the ^{13}C NMR, one carbonyl peak appeared at 206.8 ppm,
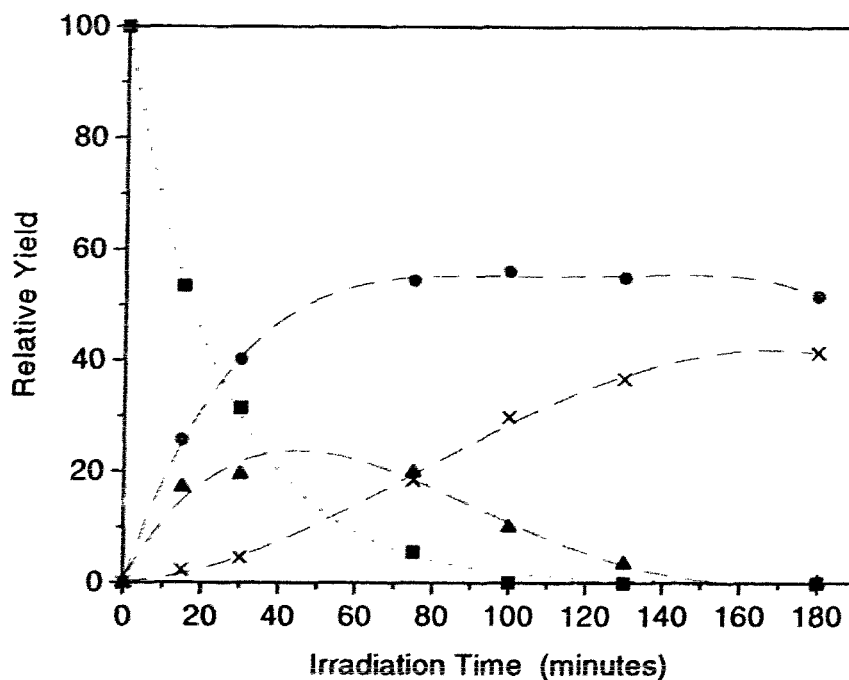
Fig. 4.1 The product profile of DBMBF₂ photocycloaddition reaction with mesityl oxide in CH₃CN: DBMBF₂ (■); product **28** from head-to-head addition (●); and from head-to-tail addition (**29**, ▲ and **30**, ×).

Table 4.2: DBMBF₂ photoaddition to mesityl oxide in different solvents^a

Solvent	Product Distribution		total chemical
	head-to-head	head-to-tail	yield %
CH₃CN	36	64^b	62
CH₂Cl₂	36	64^b	66
THF	36	64^c	58
Benzene	37	63^b	63

Notes: ^{a} Irradiation for 5 hours; ^{b} Cyclized product **30** only; ^{c} Product **30** and **29** in the ratio 25 : 75.

corresponding to a non-conjugated C=O. In the mass spectrum, cleavage at C–C

bonds β to the carbonyl groups produced benzoyl and dimethyl substituted phenacyl

fragments. This compound was sensitive to acid, and addition of one drop HCl solution

in acetonitrile (overall [H⁺] < 0.1 M) caused its rapid conversion to the cyclized product

30 (Scheme 4.3). The solvent THF, which is more basic than the other solvents in Table

4.2, can retard this acid catalyzed dark reaction.

Scheme 4.3: Acid catalysed cyclization
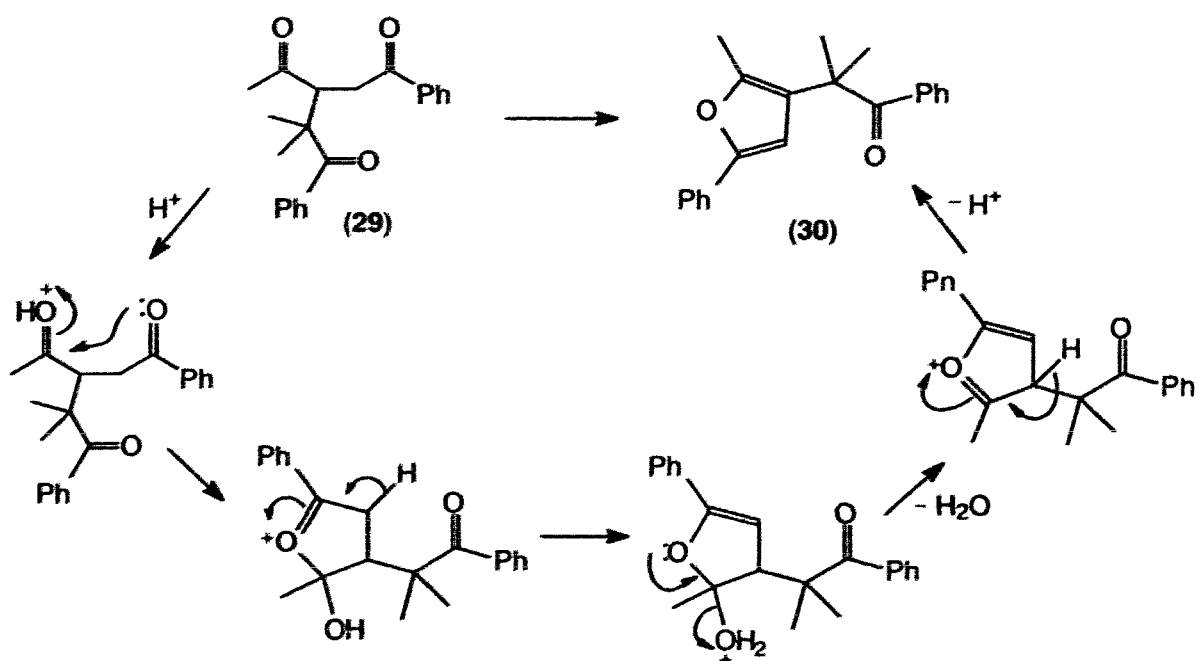
The cycloaddition of DBMBF₂ to ethyl crotonate and crotononitrile

The photocycloaddition of DBMBF₂ to *trans*-ethyl crotonate **33** yielded two

primary cycloaddition products in acetonitrile. The major one (**34**) displayed an R_f of

0.13 and the minor one (**35**) an R_f of 0.08 on TLC (SiO₂, hexane / ether = 6 / 1)

immediately after photolysis. Column chromatography gave the minor product (R_f = 0.08) in pure form. Its molecular ion (m/z 339 in CI-MS) corresponds to the sum of DBM and a protonated crotonate molecule. Loss of an ethanol gave the base peak at m/z 293. Two methine protons (H_a and H_b) attached to chiral carbon atoms exhibited multiplets at 3.82 and 3.87 ppm respectively, indicating one adjacent carbonyl group compared to the methine proton with δ = 4.6 ppm in **34** having two neighboring C=O. The vicinal coupling of H_a to a CH_2 (H_c 3.13 ppm with J = 17.5, 4.2 Hz and $H_{c'}$ 3.56 ppm with J = 17.5, 8.5 Hz) confirmed the connection of a phenacyl chain α to the acetate group. The above data are consistent with the structure of product **35** from a head-to-tail addition of $DBMBF_2$ to ethyl crotonate.

From the column chromatography, the major product **34** (R_f 0.13) was found to be a mixture with a new spot at R_f 0.11 on TLC (SiO_2, hexane / ether = 6 / 1). Immediate separation of the mixture using TLC produced two ether fractions, each containing one component and giving one spot on TLC. In the presence of silica gel, those in ether became equilibrated after a few days. The mixture of product **34** from column chromatography was used for structural analysis.

The MS (EI) spectrum of **34** exhibited a weak molecular ion at m/z 338, indicating the addition of DBM to ethyl crotonate. The major cleavages consisted of the loss of benzoyl and phenacyl fragments. With NMR analysis, the mixture was well resolved and showed two sets of spectra. In the ^{1}H NMR, two doublet peaks of methine H_a appeared at 4.52 and 4.56 ppm indicating head-to-head orientation of $DBMBF_2$ and ethyl crotonate. The ratio of two isomers was calculated to be 3 : 1 on these methine protons. In the ^{13}C NMR two sets of carbonyl peaks appeared at 198.5 ± 0.1, 194.8 (overlap) and 169.2 ± 0.1 ppm. Though the configurations of the products remain unknown at this

stage, the spectroscopic data suggest that the primary head-to-head addition of

DBMBF$_2$ to *trans*-ethyl crotonate yields the *erythro*-diastereomer at R$_f$ 0.13 which then

isomerizes to its *threo*-diastereomer at R$_f$ 0.11 by enolization of the 1,3-dicarbonyl

system (Scheme 4.4). This conjecture is supported by the observation that proton H$_a$

undergoes H / D exchange after several days in CDCl$_3$-D$_2$O solution containing pyridine.

Scheme 4.4: the enolization

erythro-34   threo-34
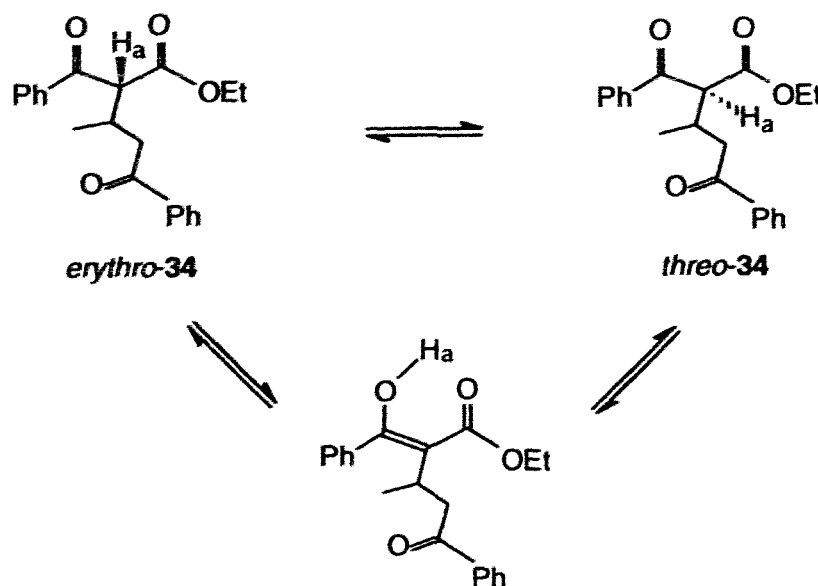
The photocycloaddition of DBMBF$_2$ to crotononitrile **36** follows a similar stereo-

chemistry to the reaction of ethyl crotonate **33** and yields the *erythro*-diastereomer **37** as

a primary adduct which then isomerizes to give the *threo*-**37** (Table 5.8).

The cycloaddition of DBMBF$_2$ to cyclic enones

Two types of products were usually observed for the photoreactions of DBMBF$_2$

with cyclic enones: dimerization of the cyclic enones and cycloaddition of DBMBF$_2$. The

former reaction can be initiated by direct photolysis and is well-known.[113] The latter

reaction afforded mainly one head-to-head addition product.

The photoaddition of DBMBF$_2$ to 2-cyclohexenone **42** showed mainly one product spot at R$_f$ 0.17 on TLC (SiO$_2$, hexane / CH$_2$Cl$_2$ / ether = 3 / 0.9 / 0.4) with a very faint spot at R$_f$ 0.13. Column chromatography afforded only the product of R$_f$ 0.13 (**43**), presumably a result of isomerization of the product of R$_f$ 0.17.

The product **43** had a parent ion at m/z 320, equal to the sum of DBM and cyclohexenone. A doublet peak in the ^{1}H NMR appeared at 4.51 ppm and is assigned to the methine proton H$_a$ on the carbon atom vicinal to two C=O groups. The vicinal coupling constant is $^3J_{ab}$ = 9.2 Hz, which corresponds to *axial - axial* coupling of the H$_a$ and H$_b$ protons of cyclohexane ring.[78a, 83] The two side chains of the adduct therefore have a *trans*-configuration and adopt an *equatorial - equatorial* conformation:
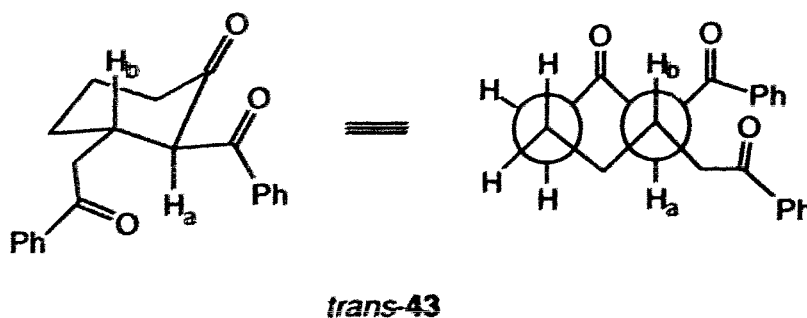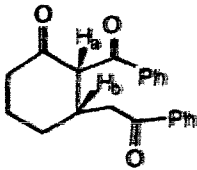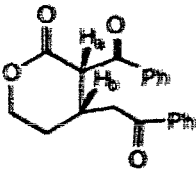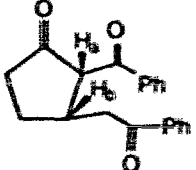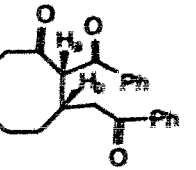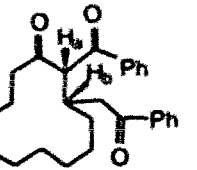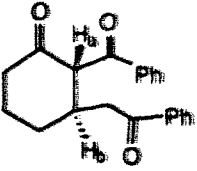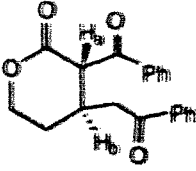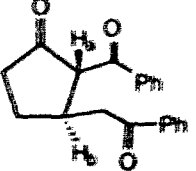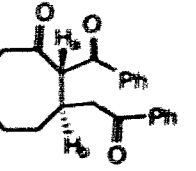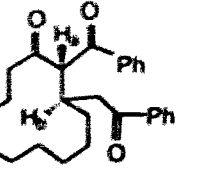
trans-**43**

The analytical sample of this *trans*-addition product (*trans*-**43**) contains 9 – 10% of its *cis*-isomer (*cis*-**43**), which has a methine proton at 4.86 ppm with $^3J_{ab}$ = 4.9 Hz (*axial - equatorial*).

The photoreaction of DBMBF$_2$ with 5,6-dihydro-2H-pyran-2-one **48** is very slow. After several days of photolysis, one product spot was observed at R$_f$ 0.11 (SiO$_2$, hexane / ethyl acetate = 4 / 1). Chromatography gave the product which appeared at R$_f$ 0.09 (SiO$_2$, hexane / dichloromethane / acetone = 2 / 0.9 / 0.1). The compound had a doublet methine proton H$_a$ at 4.59 ppm (J$_{ab}$ = 8.2 Hz), which follows the coupling pattern of the analogue *trans*-**43**. Therefore, the product was assigned to structure **49** (Table

4.3). The *cis*-49 (9%) was also seen in the ^{1}H NMR spectrum of the adduct, with a doublet at 5.07 ppm and a vicinal coupling constant J_{ab} = 4.6 Hz (Table 4.3).

Two adducts were isolated from the photocycloaddition of DBMBF$_2$ to 2-cyclododecenone 50. The structure of the major product 51, white powder, was determined mainly from the following spectral data: (1) its Cl-MS spectrum showed a parent ion at m/z 405 (M+1), equal to the sum of DBM and cyclododecenone; (2) the ^{13}C NMR spectrum had three carbonyl absorptions at 196.13, 199.28 and 206.09 ppm, among which the C=O peak at 206.09 ppm corresponds to a cyclic ketone moiety; (3) ^{1}H NMR showed a doublet at 4.92 ppm for the methine proton H$_a$ with a vicinal coupling of J_{ab} = 11.1 Hz, similar to the NMR-absorption pattern of the *trans*-adducts of Table 4.3.

Table 4.3 Chemical shift and coupling constant of the methine proton (H$_a$) in *cis*-and *trans*- addition products, (in CDCl$_3$)

	(*cis*-43)	(*cis*-49)	(*cis*-41)	(*cis*-45)	(*cis*-51)
δ (ppm)	4.86	5.07	4.76	4.93	5.21
$^3J_{ab}$ (Hz)	4.9	4.6	7.8	3.6	3.5

	(*trans*-43)	(*trans*-49)	(*trans*-41)	(*trans*-45)	(*trans*-51)
δ (ppm)	4.51	4.59	4.21	4.88	4.92
$^3J_{ab}$ (Hz)	9.2	8.2	10.1	11.0	11.1

The structure of *trans*-51 was tentatively assigned. The minor product 52 was obtained as sticky oil showing carbonyl peaks at 212.58, 195.99 and 195.80 ppm. The CI-MS spectrum had a parent ion at m/z 405 (M+1), which cleaved to give the DBM (base peak) and the cyclic enone. This compound also showed a methine H_a at 6.14 ppm (J_{ab} = 9.1 Hz), deshielded by two adjacent benzoyl substituents.

The photocycloaddition of DBMBF$_2$ to 2-cyclooctenone 44 showed initially one major spot at R_f 0.25 and a minor product at R_f 0.31 on TLC (SiO$_2$, hexane / EtOAc = 5 / 1). After column chromatography, the originally minor spot of R_f 0.31 increased at the expense of the major spot. Preparative TLC eventually produced two mixtures used as analytical samples: one contained 75% of the product R_f 0.25 (*cis*-45) and the other 89% of its isomer R_f 0.31 (*trans*-45). The parent ions were found at m/z = 348 on GC-EI-MS. The ^{1}H NMR and ^{13}C NMR spectra showed two sets of peaks arising from the mixture of *cis*- and *trans*-45. For *cis*-45, the methine protons appeared as a doublet at 4.93 ppm (H_a, J_{ab} = 3.6 Hz) and a multiplet at 3.45 ppm (H_b), which is consistent with the observations made on the *cis*-adducts, such as *cis*-8 of addition of DBMBF$_2$ to 1,5-cyclooctene.[50c] Therefore the *cis*-configuration was assigned to the benzoyl and phenacyl substituents. In *trans*-45, the methine protons appeared at 4.88 ppm (H_a, d, J_{ab} = 11.0 Hz) and 3.44 ppm (H_b, m), following the coupling pattern of *trans*-8.[50c]
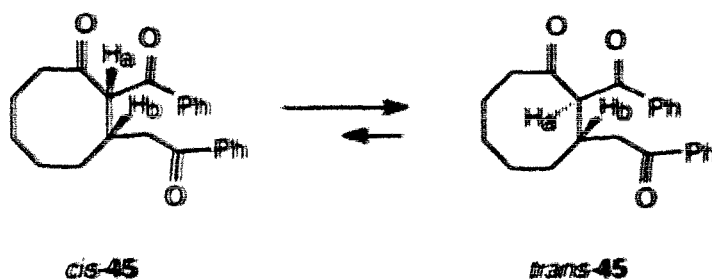
cis-45   trans-45

Table 4.4 ^{1}H NMR analysis of the transformation
between *cis*- and *trans*-45

Sample	Time (days)	Percentage % [a]	
		cis-45	*trans*-45
1	0	75	25
	29	70.6	29.4
	260	50.8	49.2
2	0	11	89
	29	~5	~95
	260	5	95

Note: [a] The percentage of each diastereomer was calculated by integration of the methine
proton peak (H$_a$ at 4.88 ppm for *trans*-45 and at 4.93 ppm for *cis*-45). The two
analytical samples, one containing 75% of *cis*-45 and the other 89% of *trans*-45, were
dissolved respectively in chloroform-d solvent and submitted to ^{1}H NMR measurements.

A time-dependent ^{1}H NMR analysis, to examine the thermal stability of these two
diastereomers, showed an equilibrium between *cis*-45 and *trans*-45 (Table 4.4).

As summarized in Table 4.3, the chemical shifts and vicinal coupling constants of
the methine proton H$_a$ exhibited some regularities related to the structures of the addition
products of excited DBMBF$_2$ to cyclic enones: (1) the chemical shift of H$_a$ in the *cis*-
adduct is larger than that of its *trans*-isomer; (2) the vicinal coupling of H$_a$ to H$_b$ in the
cis-adduct is smaller than that of the *trans*-isomer.

The cycloaddition of DBMBF$_2$ to isophorone

The photoaddition of DBMBF$_2$ to isophorone 46 is rather slow, but it is
regioselective and stereoselective giving only one head-to-tail addition product 47, as
described below. The parent ion of m/z 362 lost its side chains to give fragments of m/z
= 257 (57%) and 105 (benzoyl, 100%). Three carbonyls were seen in the ^{13}C NMR at

199.43, 205.45 and 206.93 ppm, but the methine proton (H_a) appeared at 3.20 ppm, indicating only one adjacent carbonyl group. The H_a proton is coupled to methylene protons H_b at 2.65 ppm (J = 18.4, 2.7 Hz) and $H_{b'}$ at 4.34 ppm (J = 18.4, 7.6 Hz). As the methylene protons (H_b and $H_{b'}$) belong to a phenacyl substituent, their coupling to H_a suggested that the phenacyl was attached α to the isophorone carbonyl. Such a product arises from a head-to-tail orientation between $DBMBF_2$ and the isophorone.

4.1.2 The photodimerization of cyclic enones in the presence of $DBMBF_2$

The photodimerization of cyclic enones has been studied extensively.[113] Detailed investigations have been made on 2-cyclohexenone (42, CH), 2-cyclopentenone (40, CP) and isophorone (46). The photodimerization of CH and CP are highly efficient yielding *cis-anti*-fused head-to-head and head-to-tail cyclodimers from a triplet excited enone (Eq. 4.1).[114] The dimer formation could be initiated either by direct photolysis of CH or CP in acetonitrile or in other solvents using a variety of light sources (313 nm,[115] 360 nm[116] or medium pressure mercury lamp with Pyrex filter[117]), or by

Eq. 4.1:

(42)   (54)   (55)
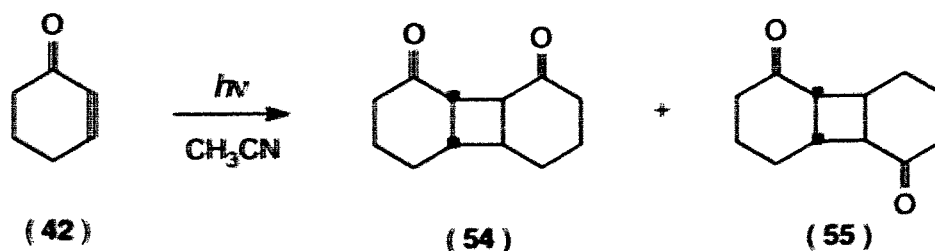
sensitizations of benzophenone (E_T 69 kcal/mole) and acetophenone (E_T 73 kcal/mole).[116]

Table 4.5 lists the singlet (E_S) and triplet (E_T) state energies of CH and CP, together with those of $DBMBF_2$. The data of this table suggest that a triplet sensitization

from the triplet excited $DBMBF_2$ to the cyclic enone should be possible but not very favorable, because of the endothermic energy transfer process. Table 4.6 lists the data of enone UV absorption which extends to more than 300 nm, as shown by the UV spectra of 2-cyclohexenone in acetonitrile (Fig. 4.2). This UV absorption should allow the cyclic enone to dimerize directly under our photolysis conditions in the presence of $DBMBF_2$ (λ_{ex} = 350 nm).

Table 4.5 Singlet and triplet energies of cyclic enones

Compound	E_S (kcal/mole)	E_T (kcal/mole)
$DBMBF_2$	73	62
2-cyclohexenone	80[a]	61,[b] 62.6,[c] 63[d]
2-cyclopentenone	83[a]	74,[a] 73[c]

Notes: [a] From Ref. 3; [b] From Ref. 115; [c] From Ref. 118; [d] From Ref. 119.

It has been found that photolysis of $DBMBF_2$ with the cyclic enone (CH or CP) resulted in a dimerization, and this was assumed to be a $DBMBF_2$ sensitized reaction.[49] Aiming at examining the efficiencies of dimer formation by a sensitization and by a direct photolysis, the following photodimerization of cyclic enones was performed with and without the presence of $DBMBF_2$.

Photolysis of an acetonitrile solution of CH (0.3 M) or CP (0.3 M) at 350 nm yielded dimers in high quantum yield (Φ_D), but under the same conditions, the presence of $DBMBF_2$ reduced Φ_D by 50-fold (Table 4.7). The decrease in dimer production could be attributed to competing light absorption by $DBMBF_2$ (Table 4.7). Clearly, direct photolysis is mainly responsible for the formation of enone dimers. The sensitized dimerization of cyclic enone by $DBMBF_2$, showing a different dimer distribution, must be inefficient.
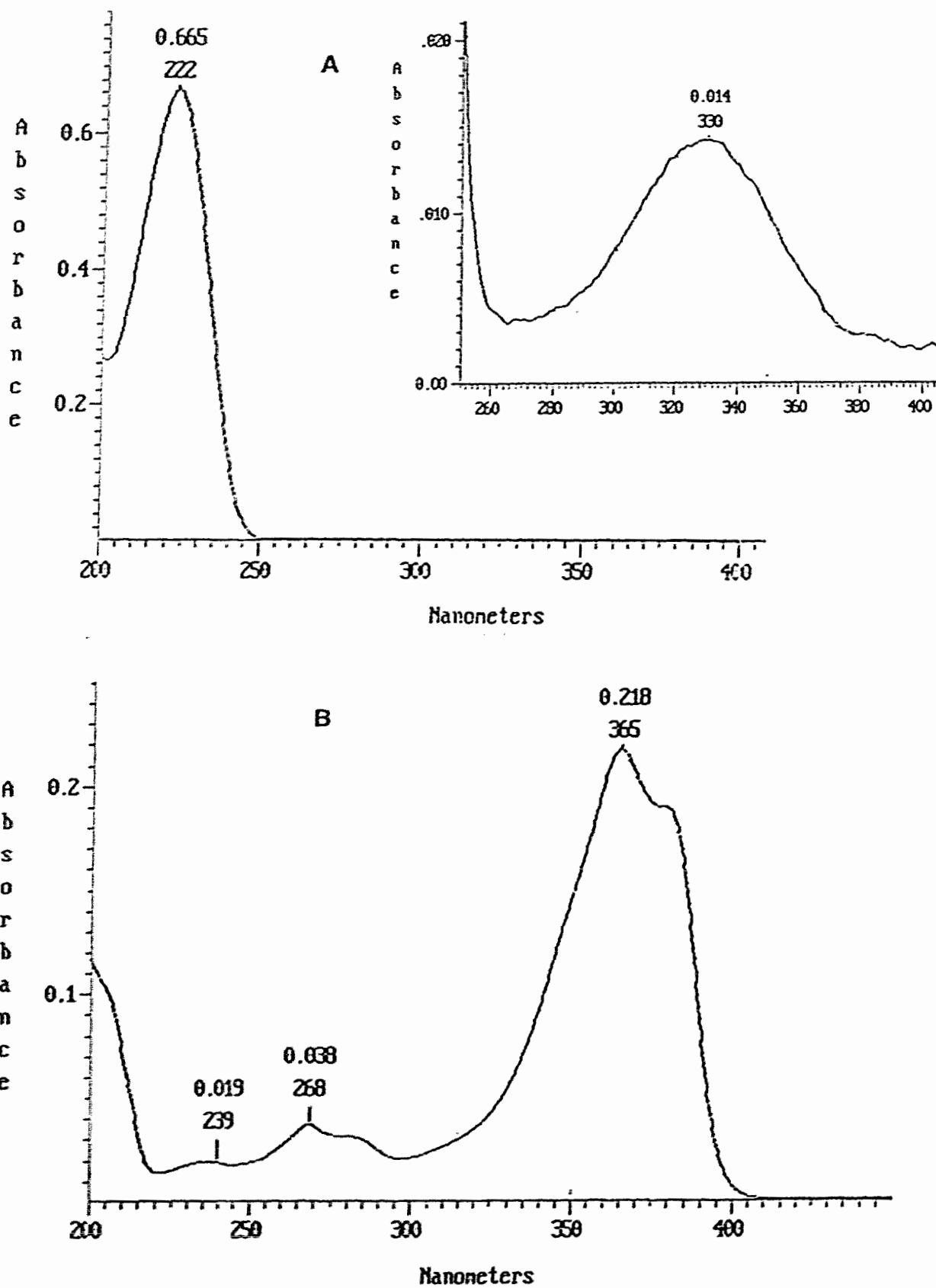
Fig. 4.2 UV spectra of A: 2-cyclohexenone (6.1 x 10^{-5} M, inset: 4.3 x 10^{-4} M) and B: DBMBF$_2$ (5 x 10^{-6} M) in acetonitrile.

Table 4.6 Absorption data for conjugated cyclic enones

Compound	Solvent	λ_{max}, nm	ε	Ref.
Cyclohexenone	CH_3CN	223 330	9310 32.9	this work
Cyclopentenone	CH_3CN	217 316	7640 30.7	this work
Cyclooctenone	CH_3CN (in cyclohexane)	228 (223) 317 (321)	6790 (7600) 73.4 (70)	this work [120]
Isophorone	MeOH	235 311	13700 50	[113b]
DBMBF$_2$	CH_3CN	270 365 378	4900 41700 37200	this work

Table 4.7 Photodimerization of cyclic enones (0.3 M) in acetonitrile in the presence and absence of DBMBF$_2$, λ_{ex} = 350 nm.

Enone	DBMBF$_2$ M	Absorption %[a] (DBMBF$_2$: Enone)	Φ_D[b]	Dimer Ratio (head-to-head : head-to-tail)
CH (42)	0.03 0	99.5 : 0.5 0 : 100	0.003 0.12	2.0 : 1 2.3 : 1
CP (40)	0.03 0	99.6 : 0.4 0 : 100	0.006 0.37	2.2 : 1 0.9 : 1

Notes: [a] Estimated from Fig. 4.7; [b] Φ_D is the total quantum yield of dimer formation which was analysed by GC. The absorbed photons by both DBMBF$_2$ and an enone are $I_a t = 980 \times 10^{-6}$ Einstein, where the irradiation time (t) is 120 min.

For *cis*-2-cyclooctenone **44**, it is known that isomerization to give *trans*-**44** occurs upon excitation and that this dimerizes in the dark, yielding cyclobutane dimers with unknown stereochemistry (Scheme 4.5).[120a] An authentic sample of the dimers was prepared according to the literature.[120] The photolysis of *cis*-**44** (0.2 M) in heptane, using a Hanovia medium pressure mercury arc lamp (200 W) with a Pyrex filter, produced a mixture of dimers (GC yield 30%). Noticeably, if the same sample of *cis*-**44** in heptane was irradiated at 350 nm in a Rayonet photoreactor, no product was detected. However under this condition, photolysis of an acetonitrile solution of *cis*-**44** (1 M) and DBMBF$_2$ (0.03 M) for 3 hours produced not only the expected addition product **45** (yield 77%) but also two new products **53** in the ratio of 81 : 19 on GC (yield 2.4%). The new products showed parent ions at m/z 248, corresponding to the dimer of 2-cyclooctenone, but was not the same as the authentic dimer samples analyzed by coinjection on GC. ^{13}C NMR (DEPT method) sorted the carbon atoms of the major component of **53**, showing the absence of a cyclobutane ring and only one bond connection between a cyclooctanone and a cyclooctenone. At the terminus of this linkage were two tertiary carbons in different chemical environments (δ 56.1 and 40.0 ppm in Table 5.8), indicating that one may be a carbon α to a carbonyl group and the other a carbon at the β-position. The connection sequence for the protons was traced by 2D-COSY, which revealed the structure of **53** to arise from a coupling reaction of cyclooctenone (Scheme 4.5). Following the identification of this product, we realized that it must be formed in a thermal reaction. Indeed, the addition of boron trifluoride etherate to an acetonitrile solution of 2-cyclooctenone (0.4 M) led to a rapid dark reaction which gave the product **53** (Scheme 4.5).

(cis-44)   (trans-44)   dimers of 44

(53)
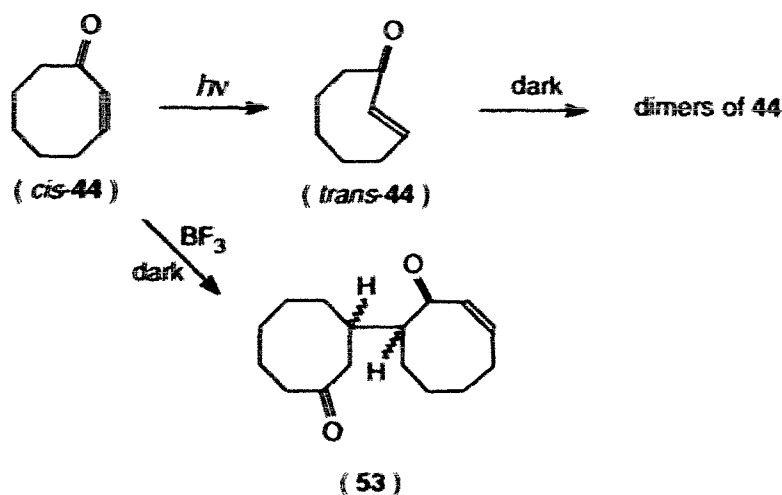
4.1.3 Steady state fluorescence quenching

The fluorescence quenching of DBMBF$_2$ (5 x 10^{-6} M) showed surprisingly high quenching constants (K$_{SV}$) for some enones[49] at the excitation wavelength of λ_{ex} = 365 nm. It was found later that the anomaly of K$_{SV}$-values for those enones was caused by the quencher absorption of excitation light at 365 nm.[58b] This competing absorption was a problem in the fluorescence quenching of DBMBF$_2$ at 5 x 10^{-6} M but could be avoided by shifting the excitation wavelength (λ_{ex}) from 365 to 390 nm, where the enone showed no absorption. At the high concentration of [DBMBF$_2$] = 0.1 M, no difference was found for the fluorescence quenching at λ_{ex} = 365 nm or at λ_{ex} = 390 nm.

When the quenching was done by directly injecting the neat quencher into DBMBF$_2$ solution, the concentration of DBMBF$_2$ would slightly change. This dilution effect was observed on the DBMBF$_2$ excimer emission due to its DBMBF$_2$ concentration dependence. In addition to this, there is also a spectrum overlap between the excited DBMBF$_2$ monomer and excimer fluorescence peaks at [DBMBF$_2$] $\geq$ 0.10 M (Fig. 4.4). In both cases, corrections are made and described in the experimental section.

The typical quenching of DBMBF$_2$ fluorescence by methyl methacrylate is shown in Fig. 4.3, at a DBMBF$_2$ concentration of 5×10^{-6} M, and in Fig. 4.4A where a 0.1 M DBMBF$_2$ solution was used. Both figures suggest that excited DBMBF$_2$ monomer is mainly quenched ($K_{SV}^m = 1.1$ M^{-1}) while excimer quenching in the 0.1 M DBMBF$_2$ is insignificant ($K_{SV}^{ex} \approx 0.09$ M^{-1}). Similar quenching experiments using mesityl oxide led to the same conclusion, where the Stern-Volmer constant is $K_{SV}^m = 2.3$ M^{-1} for quenching DBMBF$_2$ monomer and $K_{SV}^{ex} \approx 0.14$ M^{-1} for quenching DBMBF$_2$ excimer (Fig. 5.7 and 5.3).

The fluorescence quenching of DBMBF$_2$ excimer by 2-cyclooctenone is seen in Fig. 4.4B, where the decrease in the excimer fluorescence intensity at 520 nm is in contrast to the unchanged monomer emission at 437 nm.

$$K_{SV}^m = 1.1 \pm 0.1 \text{ M}^{-1}$$
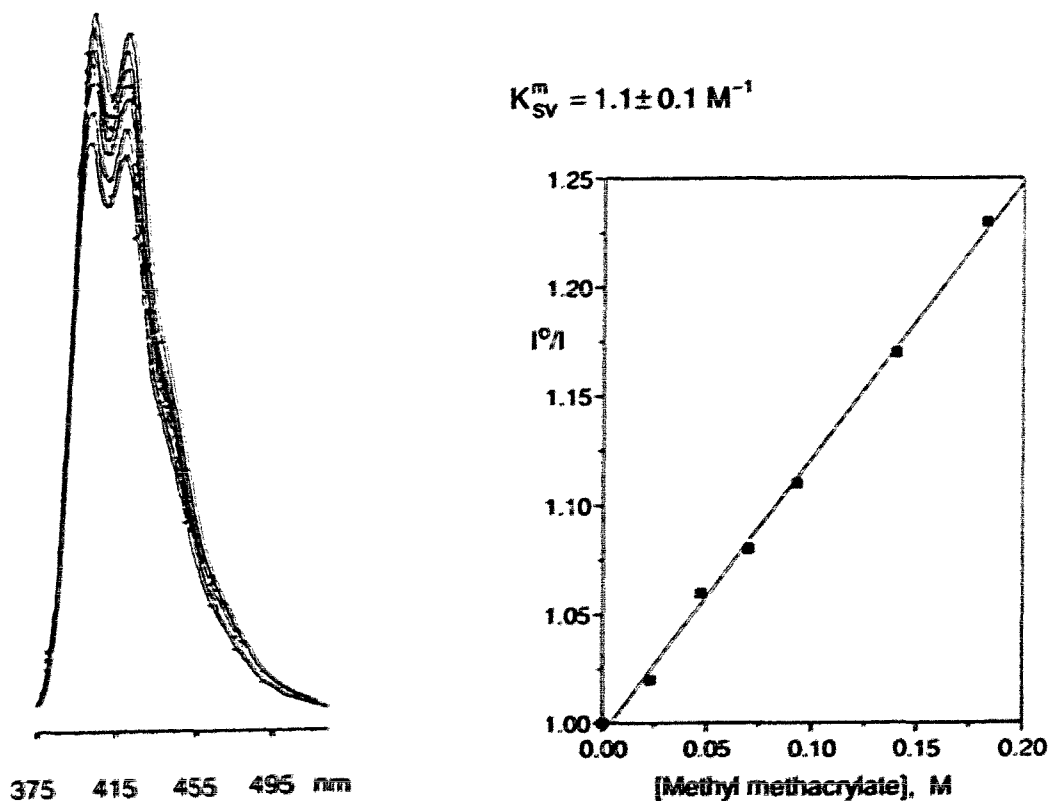
Fig. 4.3 The quenching of DBMBF$_2$ (5×10^{-6} M) fluorescence by methyl methacrylate in acetonitrile: excited at $\lambda_{ex} = 390$ nm, monitored at $\lambda_{moni} = 416$ nm and $K_{SV}^m = 1.1$ M^{-1}.
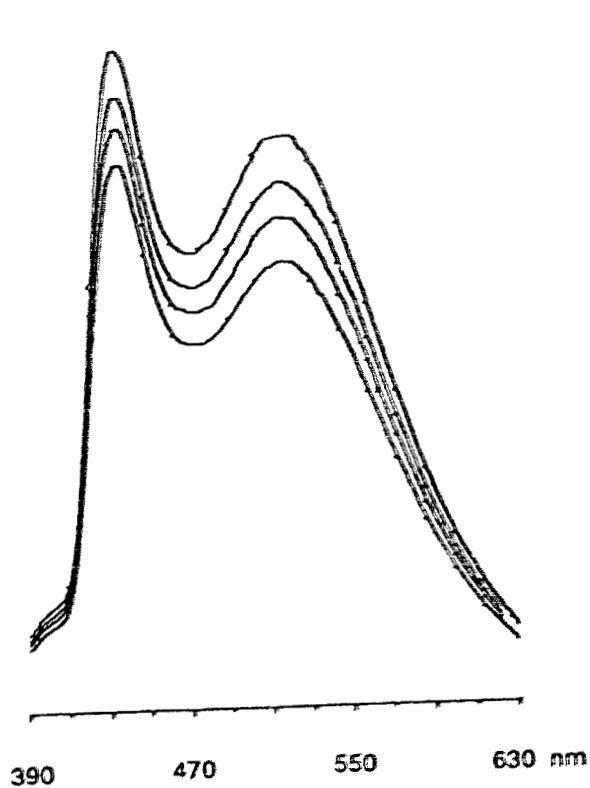
A: $K_{SV}^{ex} = 0.09 \pm 0.02 \text{ M}^{-1}$
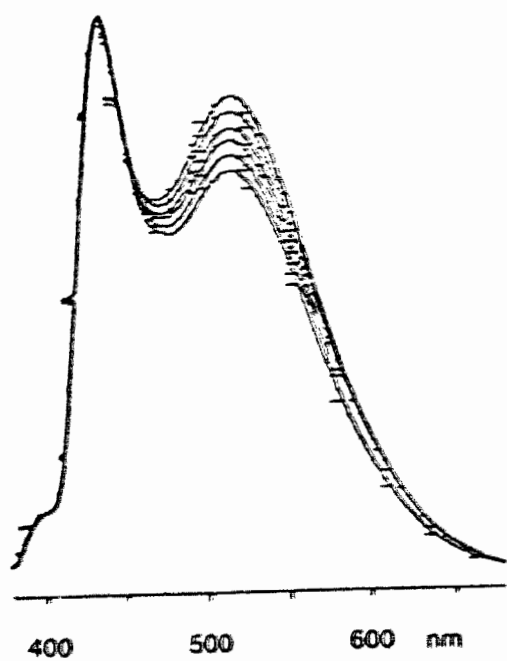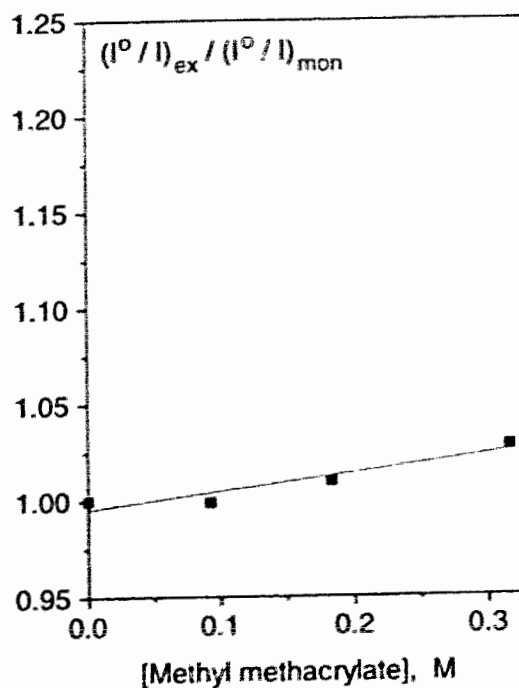
B: $K_{SV}^{ex} = 0.27 \pm 0.02 \text{ M}^{-1}$
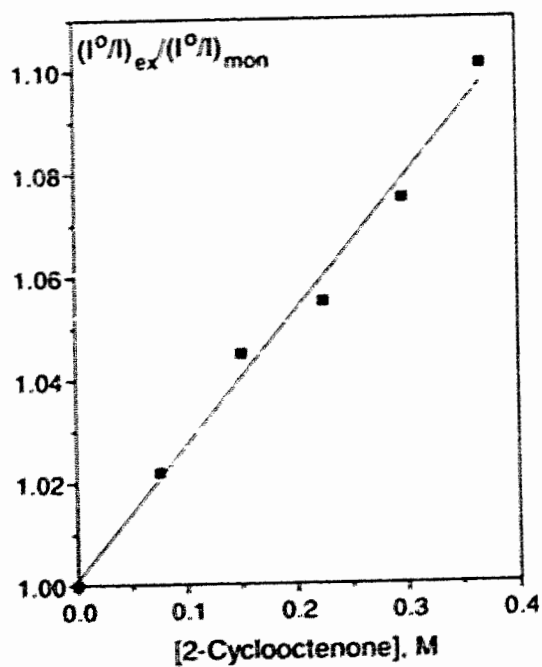
Fig. 4.4 The quenching of DBMBF$_2$ (0.1 M) fluorescence in acetonitrile: (A) by methyl methacrylate, $K_{SV}^{ex} = 0.09 \text{ M}^{-1}$; (B) by 2-cyclooctenone, $K_{SV}^{ex} = 0.27 \text{ M}^{-1}$.

(excited at $\lambda_{ex} = 365$ nm and monitored at $\lambda_{moni} = 520$ nm)

All the data for the quenching of $DBMBF_2$ fluorescence by acyclic and cyclic α,β-unsaturated ketones and esters are summarized in Table 4.8.

Table 4.8 Stern-Volmer constants (K_{SV}) for quenching $DBMBF_2$ fluorescence by α,β-unsaturated ketones and esters in acetonitrile

At $[DBMBF_2] = 5 \times 10^{-6}$ M:

Quencher [a]	[Quencher] (M)	IP (eV)	K_{SV}^{m} (M^{-1})[b] (non-corrected)	(corrected)	$10^{-9} k_q^{m}$ (M^{-1}s^{-1})[c]
MMA (31)	0.023 ~ 0.18	10.28 [g]	1.26, 1.1;	1.1, 1.0;	3.2, 3.0;
MO (27)	0.022 ~ 0.23	9.11 [g]	---	2.3 [h]	6.9
CH (42)	0.026 ~ 0.47	9.27 [g]	---	0.26, 0.24;	0.76, 0.71;
CO (44)	0.075 ~ 0.30	9.18 [g]	---	1.3 [h]	3.8
CD (50)	0.023 ~ 0.11	---	1.50	1.4	4.1

At $[DBMBF_2] = 0.10$ M:

Quencher [a]	[Quencher] (M)	K_{SV}^{m} (M^{-1})[d]	K_{SV}^{ex} (M^{-1})[e] (non-corrected)	(corrected)	$10^{-7} k_q^{ex}$ (M^{-1}s^{-1})[f]
MMA (31)	0.093 – 0.49	0.61, 0.66;	0.06, 0.05;	0.09, 0.05;	0.25, 0.14;
MO (27)	0.044 – 0.21	0.81	0.08	0.14	0.39
CH (42)	0.10 – 0.54	~0	---	0.16, 0.18;	0.44, 0.50;
CO (44)	0.076 – 0.37	~0	---	0.27, 0.23;	0.75, 0.64;
CD (50)	0.023 – 0.11	~0.05	1.17	1.4	3.9

Notes: [a] MMA refers to methyl methacrylate, MO to mesityl oxide, CH to 2-cyclohexenone, CO to 2-cyclooctenone and CD to 2-cyclododecenone. [b] The quenching constant for excited $DBMBF_2$ monomer fluorescence at $\lambda_{ex} = 390$ and $\lambda_{moni} = 416$ nm. [c] The rate constant of quenching excited $DBMBF_2$ monomer calculated from $K_{SV}^{m} = k_q^{m} \tau_a$ where $\tau_a = 0.34$ ns.

[d] The corrected quenching constant for $DMBBF_2$ monomer at $\lambda_{ex} = 365$ and $\lambda_{moni} = 437$ nm. [e] The quenching constant for $DBMBF_2$ excimer fluorescence monitored at 520 nm. [f] The rate constant of quenching $DBMBF_2$ excimer calculated from $K_{SV}^{ex} = k_q^{ex} \tau_{AA}$ where $\tau_{AA} = 36$ ns in aerated acetonitrile.[62b] [g] Ref. 111. [h] Ref. 58b.

In summary, Table 4.8 shows two patterns of the $DBMBF_2$ fluorescence quenching at different $DBMBF_2$ concentrations: (1) At $[DBMBF_2] = 5 \times 10^{-6}$ M, only the quenching of the excited $DBMBF_2$ monomer was observed, but (2) at $[DBMBF_2] = 0.10$ M, the quenching of the long lived $DBMBF_2$ excimer became significant, especially when cyclic enones were used as the quencher.

As a result of excimer formation, the K_{SV}^m - values decrease with an increase in the $DBMBF_2$ concentration (Table 4.8). The concentration effect of $DBMBF_2$ on Stern-Volmer quenching constant was further investigated, using methyl methacrylate as a quencher (Table 4.9).

Table 4.9 Stern-Volmer quenching constant (K_{SV}^m) at various $DBMBF_2$ concentrations in acetonitrile, methyl methacrylate as quencher (0.023 ~ 0.12 M) [a]

$[DBMBF_2]$ M	λ_{mon} nm	K_{SV}^m M^{-1}	$1/K_{SV}^m$ M
5×10^{-3}	422	1.45	0.69
2.5×10^{-2}	426	1.25	0.80
5×10^{-2}	431	1.05	0.95
7.5×10^{-2}	437	0.95	1.05
0.10	437	0.78	1.28

Note: [a] $\lambda_{ex} = 365$ nm

4.1.4 $DBMBF_2$ Fluorescence Quenching by 2-Cyclopentenone

It was found that $DBMBF_2$ fluorescence was quenched differently by 2-cyclopentenone (CP) in acetonitrile with $[DBMBF_2] = 5 \times 10^{-6}$ M and 0.10 M. At the lower
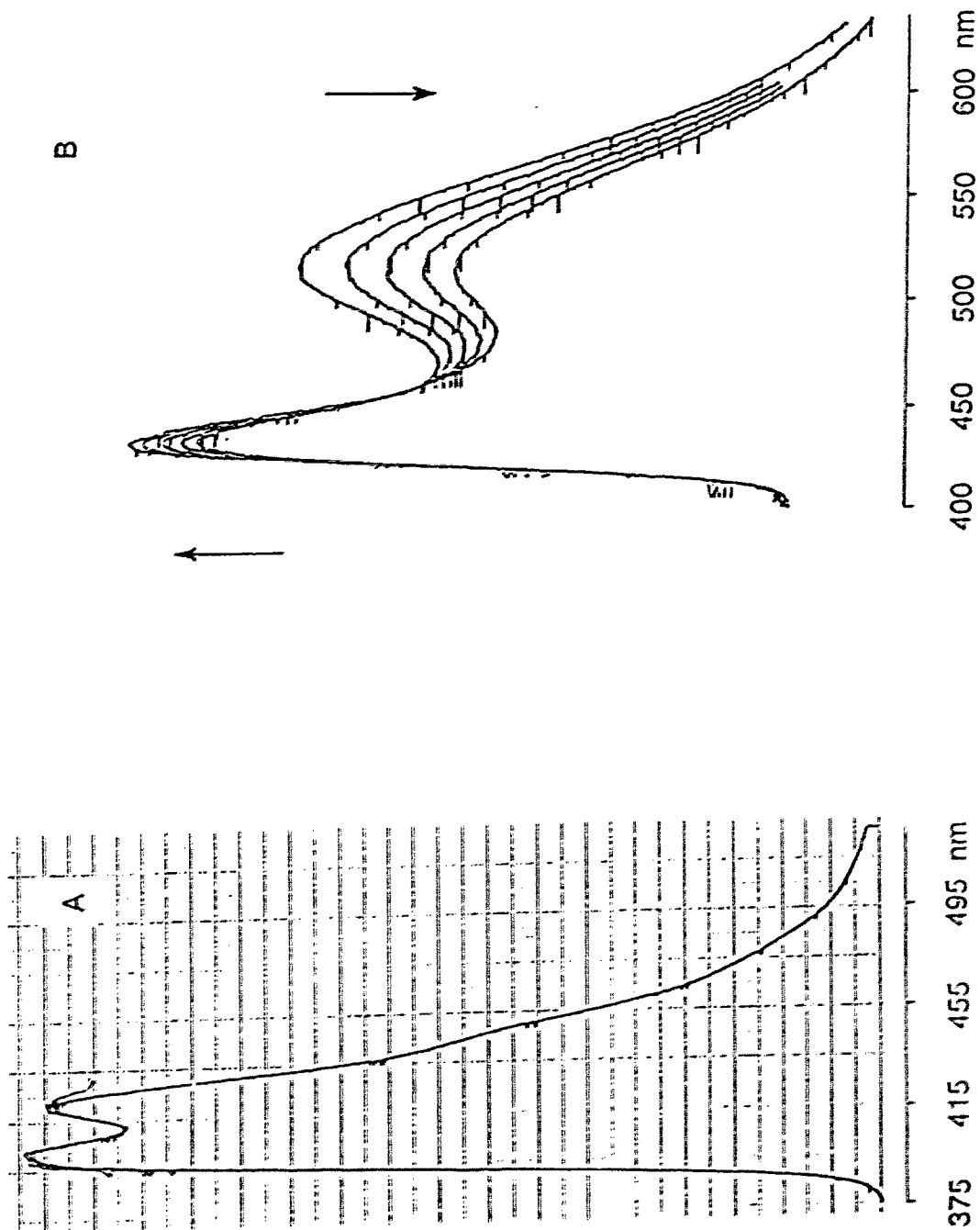
Fig. 4.5 The fluorescence quenching of DBMBF₂ by 2-cyclopentenone (CP) in acetonitrile:

A: at [DBMBF₂] = 5 x 10⁻⁶ M, [CP] = 0.00, 0.11, 0.23 and 0.56 M, λ_{ex} = 390 nm,[58b]

B: at [DBMBF₂] = 0.10 M, [CP] = 0.00, 0.18, 0.35, 0.51 and 0.68 M, λ_{ex} = 365 nm.

concentration, DBMBF$_2$ fluorescence emission arose mainly from the excited monomer species, and no fluorescence quenching was observed with the quencher CP, even up to [CP] = 0.56 M (Fig. 4.5A). At the higher concentration of DBMBF$_2$, the fluorescence quenching of DBMBF$_2$ excimer by CP at 520 nm was accompanied by the enhanced fluorescence intensity of the singlet excited DBMBF$_2$ monomer at 437 nm (Fig. 4.5B). This measurement was conducted with the front-face illumination method (Fig. 5.1) in a MPF 44B fluorometer, and reproduced in another fluorometer PTI LS-100.

This increase in the intensity of DBMBF$_2$ fluorescence at 437 nm might be a delayed fluorescence phenomenon, arising from the quenching of DBMBF$_2$ excimer by 2-cyclopentenone. As the lifetimes of excited DBMBF$_2$ monomer (0.34 ns) and excimer (~50 ns) were already known in deaerated acetonitrile,[62a] it was expected that the delayed fluorescence could be demonstrated by monitoring the decay profile of DBMBF$_2$ fluorescence at 437 nm, using a single photon counting technique. If the enhancement of fluorescence intensity at 437 nm was related to the quenching of DBMBF$_2$ fluorescence at 520 nm, then the decay profile, monitored at ≤ 437 nm, would produce a lifetime value corresponding to that of the DBMBF$_2$ excimer. This was not the case. The fluorescence decay was monitored at 420 nm, and the lifetime was found to be < 2 ns (overlapped with the flash lamp profile). Therefore, the results of Fig. 4.5 remain unexplained.

4.1.5 Quantum yield determination

The quantum yields for the photocycloaddition of DBMBF$_2$ to methyl methacrylate (31, MMA) and mesityl oxide (27, MO) were determined in acetonitrile as a function of DBMBF$_2$ concentration (0.01 – 0.07 M), at a substrate concentration of 1 M. The

results indicate a decrease in adduct production with an increase in the DBMBF$_2$ concentration (Table 4.10).

Table 4.10 Adduct quantum yield (Φ) of DBMBF$_2$ photoreactions with methyl methacrylate (MMA) and mesityl oxide (MO): DBMBF$_2$ concentration effect [a]

[DBMBF$_2$] M	Adduct of MMA Φ	Adducts of MO	
		Φ_{HH}	Φ_{HT}
0.01	0.42	0.14	0.13
0.03	0.39	0.15	0.14
0.05	0.35	0.13	0.11
0.07	0.24	0.08	0.09

Note: [a] All measurements were carried out in a Rayonet photoreactor with 350 nm light sources. Irradiation was for 5 minutes. The subscript HH refers head-to-head and HT refers to head-to-tail orientations.

The effect of methyl methacrylate (MMA) concentration upon the adduct production was also determined (Table 4.11), and the data for adduct quantum yield as a function of MMA concentrations were analysed according to Eq. 4.2 (Section 4.2). The plot of 1/Φ versus 1/[MMA] was linear, and gave the Stern-Volmer quenching constant (K_{SV}^{V}) for MMA as the ratio of intercept to slope (Fig. 4.6).

Table 4.11 Dependence of adduct quantum yield (Φ) on methyl methacrylate (MMA) concentration,[a] [DBMBF$_2$] = 0.01 M.

[MMA] M	Φ	Φ^{-1}	[MMA]$^{-1}$
0.062	0.051	19.61	16.13
0.077	0.063	15.88	12.99
0.099	0.071	14.09	10.13
0.138	0.106	9.47	7.25
0.243	0.153	6.54	4.12
0.904	0.440	2.26	1.11
K_{SV}^{y}		1.28 $\pm$ 0.47 M^{-1}	

Note: [a] The solution of DBMBF$_2$ and MMA was irradiated with a 350 nm light source for 5 minutes.
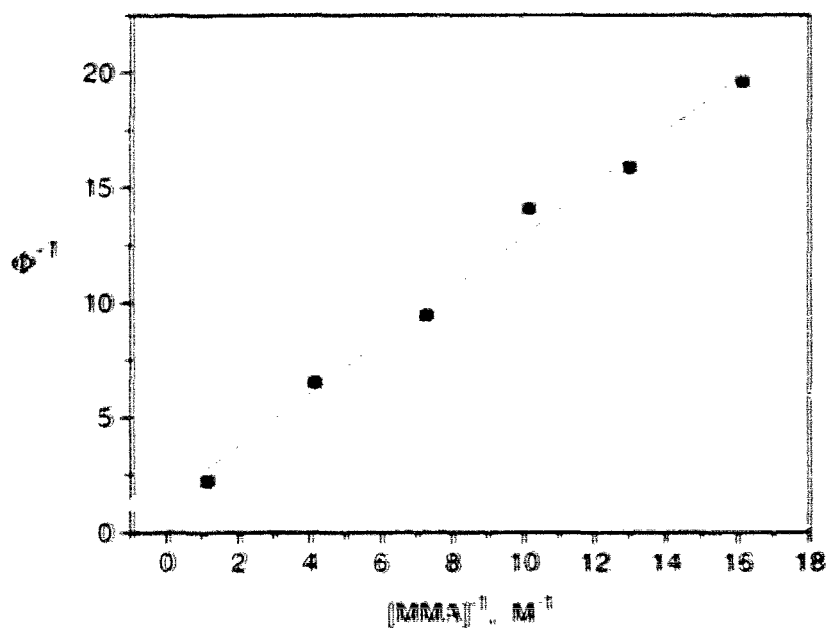
Fig. 4.6 Stern-Volmer plot of 1/Φ vs. 1/[MMA] for photocycloaddition of DBMBF$_2$ to methyl methacrylate (MMA) in acetonitrile: K_{SV}^{y} = 1.28 M^{-1}

In the photoreactions of DBMBF$_2$ with cyclic enones, the studies of adduct quantum yields were complicated by: (1) a competing light absorption by the cyclic enones, which led to dimerization ($\Phi_D = 0.19$ for cyclohexenone (0.9 M) in acetonitrile at 313 nm[115] and at 350 nm); (2) the fact that adduct formation was slow (Table 4.1), and higher concentrations of cyclic enones were needed for the quantum yield studies; (3) the finding that the addition product decomposed during GC analysis so that adduct yield had to be estimated from the sum of the product fragments.

Despite these difficulties, the quantum yields of the photoreactions of DBMBF$_2$ with 2-cyclohexenone and 2-cyclopentenone were examined as a function of the DBMBF$_2$ concentration. To estimate the percentages of light absorption by DBMBF$_2$ and by the cyclic enone in acetonitrile, a working plot was established (Fig. 4.7). In doing the plot, the light absorption of DBMBF$_2$ or the cyclic enone in varying concentrations was measured separately by area integration of the molar absorption coefficient (ϵ_A). The integration range is within 350 ± 40 nm that corresponds to the RPR 350 nm lamp profile (Fig. 4.8) and covers the absorptions of DBMBF$_2$ and the enones at 350 ± 40 nm (Fig. 4.2). Then the percentages of light absorption by DBMBF$_2$ were calculated and plotted against the concentration ratio of the enone to DBMBF$_2$ (Fig. 4.7).

In a typical run, a 3 mL deaerated acetonitrile solution of 2-cyclohexenone (0.85 M) and DBMBF$_2$ (0.01 ~ 0.07 M) was photolysed with a RPR 350 nm light source. The absorbed light intensity was measured with the benzophenone - benzhydrol actinometer, and adduct formation was analysed by GC and HPLC. The results are listed in Table 4.12, showing that the quantum yield of adduct decreases with a increase in the DBMBF$_2$ concentration. Although for the DBMBF$_2$- cyclopentenone system, the adduct
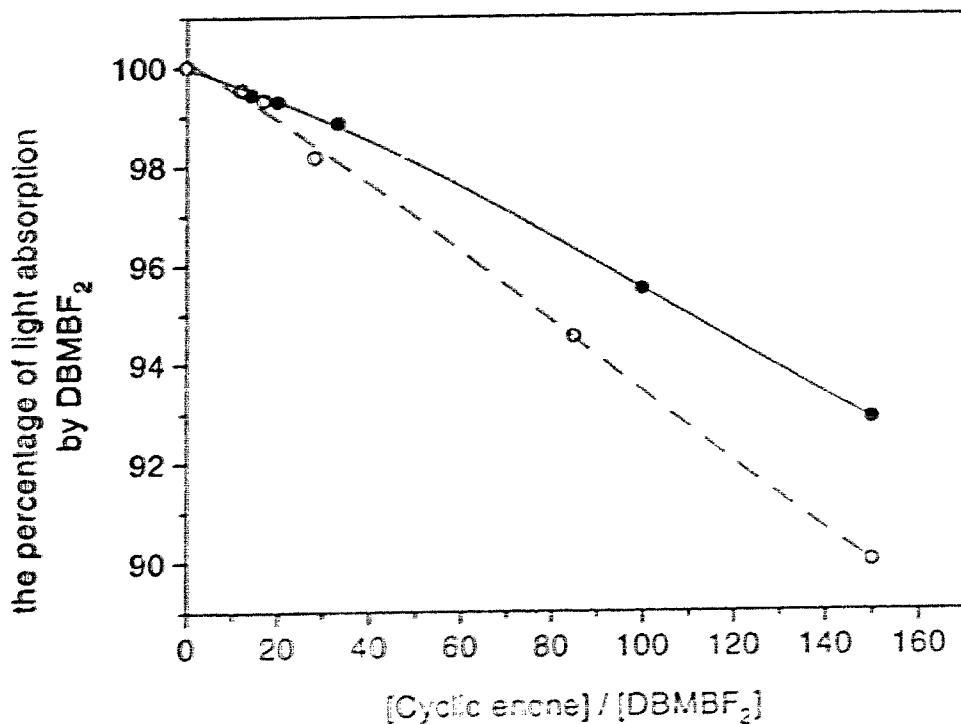
Fig. 4.7 The absorption percentage of $DBMBF_2$ and cyclic enone as a function of the concentration ratio of cyclic enone to $DBMBF_2$, 2-cyclopentenone (solid line) and 2-cyclohexenone (dash line).
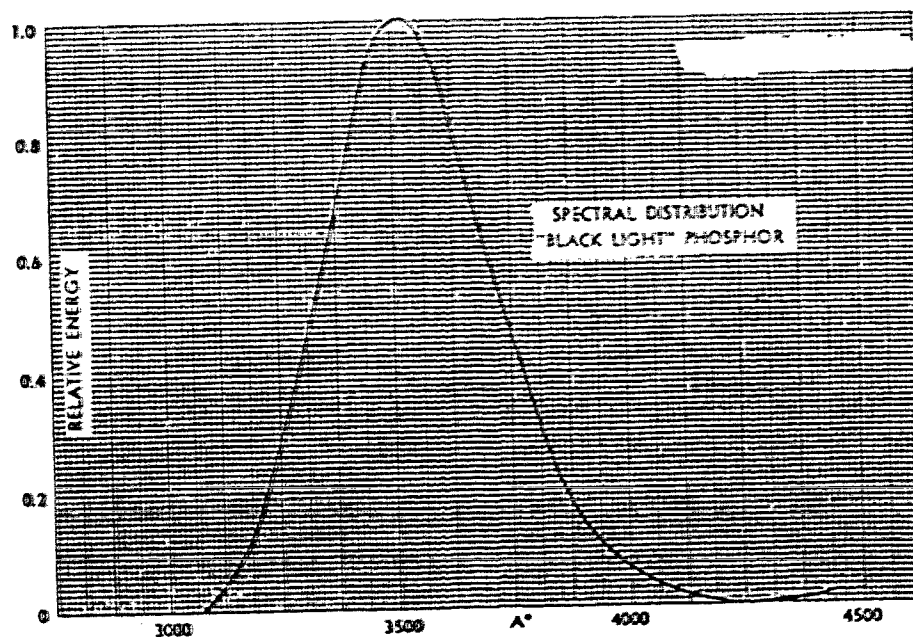
Fig. 4.8 The spectral distribution of the RPR 3500 Å lamp in the Rayonet photoreactor

Table 4.12 Effect of $DBMBF_2$ concentration on the adduct quantum yield (Φ_A) of the $DBMBF_2$ photoreaction with 2-cyclohexenone (CH, 0.85 M) [a]

[DBMBF₂] M	Adducts by GC HPLC (10⁻⁶ mole)		Dimers (10⁻⁶ mole)	Absorption% [b] DBMBF₂ : CH	Photons taken by DBMBF₂ : CH (10⁻⁶ Einstein) [c]	(Φ / Φ₀)_A by GC by HPLC	
0.01	5.3	3.2 [d]	10.3	94.5 : 5.5	386 : 22	1.0	1.0
0.03	4.4	3.1 [d]	5.6	98.2 : 1.8	401 : 7	0.8	1.0
0.05	3.8	2.6 [d]	3.0	99.3 : 0.7	405 : 3	0.7	0.8
0.07	3.8	2.6 [d]	2.7	99.5 : 0.5	406 : 2	0.7	0.8

Notes: [a] A 3 mL acetonitrile solution of CH (0.85 M) and $DBMBF_2$ (0.01 ~ 0.07 M) was purged with N_2 for 4 min. and then irradiated at 350 nm for one hour (t). The absorbed light intensity (I_a) was measured to be 6.8×10^{-6} Einstein / min so that $I_a t = 408 \times 10^{-6}$ Einstein. After photolysis, $DBMBF_2$ was precipitated by evaporating the solvent and mixing the residue with hexane / ether (1 / 1). Upon GC analysis, the solution showed the peaks of the internal standard (eicosane) at RT 2.16 min, unreacted $DBMBF_2$ at 5.07 min, one minor peak at 9.54 min and three major peaks at RT 10.39, 10.88 and 12.53 min from the decomposed adducts (on an OV-1 15 m x 0.2 mm capillary column at 245 °C). Φ_0 is the adduct quantum yield at [DBMBF₂] = 0.01 M and Φ are the quantum yields at [DBMBF₂] = 0.03, 0.05 or 0.07 M.

[b] From the plot in Fig. 4.7

[c] Calculated from $408 \times 10^{-6} \times$ absorption%

[d] Relative to benzophenone (internal standard) monitored at 250 nm

155

Table 4.13 Effect of DBMBF$_2$ concentration on the adduct quantum yield (Φ_A) of the DBMBF$_2$ photoreaction with 2-cyclopentenone (CP, 0.85 M) [a]

[DBMBF$_2$] M	Adducts (10^{-6} mole)	Dimers (10^{-6} mole)	Absorption%[b] DBMBF$_2$: CP	Photons taken by DBMBF$_2$: CP (10^{-6} Einstein) [c]	$10^2\Phi_A$	$(\dfrac{\Phi}{\Phi_0})_A$
0.01	3.6	10.2	96.2 : 3.8	398 : 16	0.9	1.0
0.03	3.7	7.1	98.9 : 1.1	409 : 5	0.9	1.0
0.05	3.2	4.2	99.4 : 0.6	412 : 2	0.8	0.9
0.07	3.7	4.1	99.6 : 0.4	412 : 2	0.9	1.0

Notes: [a] A 3 mL acetonitrile solution of CP (0.85 M) and DBMBF$_2$ (0.01 – 0.07 M) was photolysed as described in Table 4.12. The total photons absorbed by DBMBF$_2$ and CP were $I_a t = 414 \times 10^{-6}$ Einstein. Upon GC, the decomposed adduct peaks emerged after the internal standard (eicosane) at RT 2.47 min and unreacted DBMBF$_2$ at 5.77 min, and appeared from RT 7.67, 8.03, 8.29, 8.42 to 9.41 min (on an OV-1 15 m x 0.2 mm capillary column at 240 °C).

[b] From the plot in Fig. 4.7

[c] Calculated from 414×10^{-6} x absorption%

yield seems invariant to the DBMBF$_2$ concentration (Table 4.13), the decomposition of the product on GC makes these results unreliable.

For the quantum yield of dimer formation from the cyclic enone, CH or CP, the approximation was made that the DBMBF$_2$ sensitized cyclic enone dimerization could be neglected, because the high enone concentration was used (0.85 M) and the high efficiency of dimer formation was observed from direct photolysis ($\Phi_D = 0.18$ for CH and 0.34 for CP at 0.85 M[115]). The dimerization of the cyclic enones shown in Tables 4.12 and 4.13 was not investigated further.

4.2 Discussion

DBMBF$_2$ undergoes an efficient [2+2] photocycloaddition reaction with α,β-unsaturated ketones and esters to give 1,5-diketones. Photolysis of DBM itself with mesityl oxide or methyl methacrylate, under our experimental conditions (about 3 hours of irradiation), does not lead to addition.

Two orientations are found in the photoreactions of DBMBF$_2$: a head-to-head approach is most common (Table 4.1), but a head-to-tail is found when the substrate contains additional β-methyl substituents. In addition to regioselectivity, the DBMBF$_2$ photoaddition to the α,β-unsaturated carbonyl compounds shows a stereoselectivity in the cis-configuration of the benzoyl and phenacyl side chains. This primary adduct converts by enolization to the more stable trans-isomer (Table 4.4).

Scheme 4.6 is proposed for the photoreaction of DBMBF$_2$ with the acyclic substrates, methyl methacrylate and mesityl oxide. Several experimental findings support this mechanistic postulation:

(1) In the quenching of DBMBF$_2$ fluorescence, the substrates react with the singlet excited DBMBF$_2$ monomer with high efficiency, and the reaction with the excimer is insignificant (Table 4.8);

(2) The adduct production tends to be reduced by an increase in the formation of DBMBF$_2$ excimer or by an increase in the DBMBF$_2$ concentration (Table 4.10), so that acyclic substrates react with the singlet excited DBMBF$_2$ monomer;

(3) There is good agreement between the rate constant $k_q^m = 3.2 \times 10^9 \ M^{-1}s^{-1}$ (Table 4.8) from the fluorescence quenching and $k_x = 4.1 \times 10^9 \ M^{-1}s^{-1}$ from measuring the adduct quantum yields (Table 4.11). This indicates that the same singlet excited DBMBF$_2$ monomer reacts with methyl methacrylate in fluorescence quenching and forms

adduct. The rate constants k_q from fluorescence quenching and k_x from quantum yield studies refer to the same process of quenching the singlet excited DBMBF$_2$ (*A) by a quencher (D) in Scheme 4.6.

Scheme 4.6:

$$A \underset{k_d}{\overset{h\nu}{\rightleftharpoons}} {}^*A \xrightarrow[D]{k_x} {}^*AD \xrightarrow{k_{px}} \text{Adduct}$$

with $A \downarrow k_m$ leading to $^*AA$, and $k_{dx} \downarrow$ leading to $A + D$
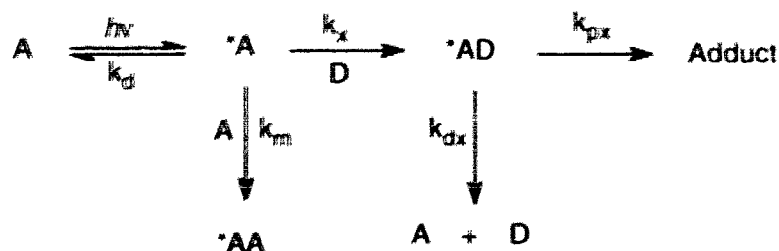
This Scheme gives the quantum yield of adduct formation (Φ_A) as equation 4.2:

$$\Phi_A = \frac{k_{px}}{k_{px} + k_{dx}} \frac{k_x}{\tau_a^{-1} + k_m[A] + k_x[D]} [D] \qquad \text{(Eq. 4.2)}$$

or

$$\frac{1}{\Phi_A} = \left(1 + \frac{k_{dx}}{k_{px}}\right)\left(1 + \frac{\tau_a^{-1} + k_m[A]}{k_x} \frac{1}{[D]}\right)$$

Here τ_a is the intrinsic lifetime of singlet excited DBMBF$_2$ in acetonitrile (0.34 ns).[62]

The double reciprocal plot of $1/\Phi_A$ vs. $1/[D]$ of the substrate should be linear with a ratio of the intercept to slope giving the Stern-Volmer quenching constant (K_{SV}^y, in equation 4.3):

$$\text{the intercept} = \left(1 + \frac{k_{dx}}{k_{px}}\right) \text{ and the slope} = \left(1 + \frac{k_{dx}}{k_{px}}\right)\left(\frac{\tau_a^{-1} + k_m[A]}{k_x}\right),$$

$$\text{thus} \quad K_{SV}^y = \frac{\text{the intercept}}{\text{the slope}} = \frac{k_x}{\tau_a^{-1} + k_m[A]} \qquad \text{(Eq. 4.3)}$$

From fluorescence measurements, the Stern-Volmer analysis of quenching the singlet excited DBMBF$_2$ should lead to the Eq. 4.4 according to Scheme 4.6:

$$\frac{\Phi_f^0}{\Phi_f} = 1 + \frac{k_x}{\tau_a^{-1} + k_m[A]}[D] = 1 + k_q\tau_A[D] \qquad \text{(Eq. 4.4)}$$

where Φ_f^0 and Φ_f is the quantum yield of fluorescence emission in the absence and the

presence of quencher (D), and the Stern-Volmer quenching constant (K_{SV}^m) is shown

as:
$$K_{SV}^m = k_q\tau_A = \frac{k_x}{\tau_a^{-1} + k_m[A]} = K_{SV}^y \qquad \text{(Eq. 4.5)}$$

That is:
$$k_q = k_x \qquad \text{and} \qquad \tau_A = \frac{1}{\tau_a^{-1} + k_m[A]}$$

here τ_A is the actual lifetime of singlet excited $DBMBF_2$, including its bimolecular decay

$k_m[^*A][A]$. The rate constant k_q is derived from the fluorescence quenching and k_x is

derived from the quantum yield measurements, but both k_q and k_x refer to the same

quenching process in Scheme 4.6 as correlated by Eq. 4.5.

With the known lifetime τ_a, the rate constant of excimer formation k_m, the

concentration of $DBMBF_2$ and the Stern-Volmer quenching constant K_{SV}^y, we can either

calculate the quenching rate constant k_x from Eq. 4.3, or determine k_x from fluorescence

quenching experiments (K_{SV}^m) by Eq. 4.5.

The Stern-Volmer constant K_{SV}^m of quenching excited $DBMBF_2$ monomer

fluorescence is concentration-dependent because of the $DBMBF_2$ excimer formation, as

has been described in Eq. 4.5:

or
$$\frac{1}{K_{SV}^m} = \frac{1}{k_q\tau_a} + \frac{k_m}{k_q}[A] \qquad \text{(Eq. 4.5A)}$$

According to this equation, we correlate the Stern-Volmer quenching constants in Table

4.9 as $1/K_{SV}^m$ to [A], the concentration of $DBMBF_2$. A linear plot was observed in
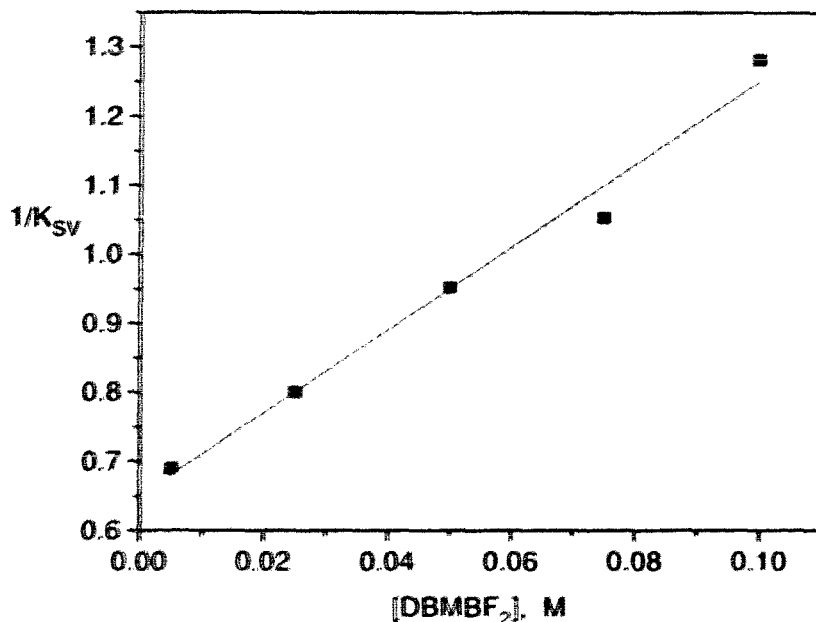
Fig. 4.9 Dependence of Stern-Volmer quenching constants (K_{SV}^{m}) on DBMBF$_2$

concentration in acetonitrile, methyl methacrylate as quencher.

Fig. 4.9. From the intercept ($1/k_q\tau_a = 0.65$ M) and slope ($k_m/k_q = 6.0$), the rate constant

k_q of quenching singlet excited DBMBF$_2$ by methyl methacrylate and the rate constant k_m

of excimer formation can be calculated respectively. Using $\tau_a = 0.34$ ns as the intrinsic

lifetime of the singlet excited DBMBF$_2$ in acetonitrile, we obtain the following rate

constants, $k_q = 4.5 \times 10^{9}$ M^{-1}s^{-1} and $k_m = 2.7 \times 10^{10}$ M^{-1}s^{-1}.

In Scheme 4.6, we assume that an exciplex intermediate is the precursor of the

addition product. An energy transfer from the singlet excited DBMBF$_2$ monomer to

methyl methacrylate or mesityl oxide is unlikely due to their large difference in singlet

energy. However, it is unexpected that these electron-deficient donors conform to the

photoreaction pattern of simple olefins.[50a, 50c]

In contrast to acyclic substrates, cyclic enones quench $DBMBF_2$ excimer selectively at high $DBMBF_2$ concentrations (Table 4.8). However, this excimer quenching has not been related to the photocycloaddition process. The adduct quantum yield studies are complicated by the low efficiency, the dimerization of cyclic enones from direct photolysis and the failure to achieve product analysis by GC. Qualitatively, although the increase of $DBMBF_2$ concentration should produce more $DBMBF_2$ excimer, the quenching of $DBMBF_2$ excimer by cyclic enones does not lead to the higher quantum yield of adduct formation.

In summary, $DBMBF_2$ reacts with α,β-unsaturated ketones and esters from its singlet excited state to give 1,5-diketones via a [2+2] cycloaddition. The regioselective and stereoselective photocycloaddition is proposed to proceed by way of an exciplex intermediate. The formation of the $DBMBF_2$ excimer is an energy-wasting step at least in the photoreactions of $DBMBF_2$ with acyclic substrates. The lack of excimer reactivity towards electron-deficient α,β-unsaturated carbonyl compounds is in striking contrast to the highly efficient reaction of $DBMBF_2$ excimer with electron-rich cyclic dienes and vinyl ethers. Compared to the triplet dimerization of cyclic enones by the direct irradiations, the sensitized cyclic enone dimerization by $DBMBF_2$ is inefficient.

CHAPTER FIVE

EXPERIMENTAL

5.1 General conditions

5.1.1 Chemicals

Reagent grade solvents were used for preparative photolysis, and spectrograde solvents were used for spectroscopic studies and quantum yield measurements. Spectrograde acetonitrile (BDH) was used as supplied for fluorescence quenching experiments. Reagent grade tetrahydrofuran (BDH) was freshly distilled from sodium benzophenone-ketyl. Reagent grade diethyl ether (BDH) was dried and distilled from sodium prior to use. Reagent grade acetone (BDH) was dried and distilled with phosphorus pentoxide. Reagent grade acetonitrile (Fisher) was used as supplied for photoreactions. Spectrograde dichloromethane (Mallinckrodt), spectrograde p-dioxane (Anachemia), certified or spectrograde benzene (Caledon), spectrograde toluene (Caledon) and reagent grade p-xylene (Fisher) were used as supplied for solvent effect studies.

For chromatography, reagent grade hexanes (BDH), acetone (BDH), dichloromethane (Anachemia), diethyl ether (BDH or Anachemia) and ethyl acetate (BDH) were used as supplied.

The deuterated solvents chloroform-d (CIL), benzene-d$_6$ (Aldrich), acetone-d$_6$ (ICN) and tetrahydrofuran-d$_8$ (Aldrich) were used as supplied for NMR studies.

Dodecane (Matheson), hexadecane (Sigma, 99%), eicosane (Aldrich, 99%) and octadecane (Eastman) were used as internal standard compounds for GC analysis.

Acetophenone (Aldrich or Matheson), acetylacetone (Aldrich, 99%) and benzonitrile (BDH) were distilled before use. Benzophenone (Fisher or Aldrich) and benzhydrol (Matheson) were used as supplied. Dibenzoylmethane (Aldrich) was used without further purification. $LiClO_4$ (Aldrich, 95+%) was used as supplied. Nitrogen gas was purified by scrubbing through concentrated sulfuric acid and then through potassium hydroxide pellets.

Olefins and α,β-unsaturated compounds used for photoreactions and fluorescence quenching were freshly distilled before use. They were: 1,3-cyclohexadiene (Aldrich, 98%), 1,3-cyclooctadien (Columbia Carbon 97%, with 2 ~ 3% of 1,5-cyclooctadiene), 1,5-cyclooctadiene (Aldrich 99+%), ethyl vinyl ether (Aldrich 99% or Eastman), isobutyl vinyl ether (Aldrich 99%), 3,4-dihydro-2H-pyran (Aldrich 97%), methyl methacrylate (Anachemia), ethyl crotonate (Matheson), methyl vinyl ketone (Aldrich 99%), mesityl oxide (Matheson), acrylonitrile (Matheson), crotononitrile (Aldrich 99%), 2-cyclohexenone (Aldrich 97%), 2-cyclopentenone (Aldrich 98%), isophorone (Aldrich, 97%), cyclooctanone (Aldrich 98%) and cyclododecanone (Aldrich 99%).

2-Cyclooctenone was prepared from cyclooctanone.[121] 5,6-Dihydro-2H-pyran-2-one was prepared by refluxing vinylacetic acid with paraformaldehyde in acetic acid.[122] 2-Cyclododecenone was synthesized starting from cyclododecanone.[123] Phenyl vinyl ether was prepared from 2-bromoethyl phenyl ether.[32, 124]

5.1.2 Analytical equipment

Melting points (mp) were determined on a Fisher-Johns apparatus and are uncorrected. Infrared (IR) Spectra were recorded with a Perkin-Elmer Model FT 1605 spectrophotometer using a neat liquid film, nujol mull or KBr pellet. Ultraviolet and visible spectra (UV / VIS) were taken with Milton Roy Spectronic 3000 Array or Varian

Cary - 210 Spectrophotometers. Mass spectra (MS) and Gas-chromatography-mass spectra (GC - MS) were obtained on a Hewlett-Packard 5985B GC-MS system either by electron ionization (EI, at 70 eV) or by chemical ionization (CI). Proton nuclear magnetic resonance (^{1}H NMR) spectra were recorded with Bruker AMX 600, Bruker AMX-400 or Bruker SY-100 spectrometers. The splitting patterns of ^{1}H signal are presented as s (singlet), d (doublet), t (triplet), q (quartet), or m (multiplet). Chemical shifts are reported in δ values in ppm, and coupling constants (J) in Hz. The chemical shifts of ^{13}C NMR spectra are also reported as δ values in ppm relative to TMS. Elemental analyses were carried out by Mr. M.K. Yang using a Carlo Erba Model-1106 Elemental Analyzer. Gas chromatography (GC) analyses were performed on a Hewlett - Packard 5790 and 5890 Series II chromatographer (FID), equipped with an 15 m x 0.2 mm DB -1 or OV-1 15 m x 0.2 mm capillary column and a Hewlett - Packard 3390A integrator. Retention times (RT) are reported in minutes (min). Preparative high performance liquid chromato-graphy (HPLC) was performed on a Waters Model 510 HPLC system, equipped with a Phenomenex Maxsil 10C18 (500 x 9.4 mm) column and a Lambda-Max, Model 481 UV detector at 250 nm). For HPLC analysis, a Phenomenex Spherisorb 10 ODS(1) column 250 x 4.6 mm was used. Elution was done with a mobile phase of acetonitrile and water. Steady state fluorescence spectra were recorded on a Perkin-Elmer MPF 44B spectrophotometer (PT1 LS-100 spectrofluorimeter). Emission spectra are uncorrected. Column chromatography was carried out with Merck Silica gel 60, mesh 230 - 400. Thin layer chromatography (TLC) was performed on aluminum plates precoated with Merck silica gel 60 F254, layer thickness 0.2 mm, and spots were visualized with iodine vapor or by spraying with a solution of $Ce(SO_4)_2$ (1%) and molybdic acid (1.5%) followed by heating on a hot plate.

5.1.3 Photolysis apparatus [112, 125]

External irradiation method

Apparatus I is a Rayonet Photochemical Chamber Reactor, equipped with RPR 300 nm (16 x 21 W) or RPR 350 nm (16 x 24 W) lamps. Pyrex test tubes (1.2 x 10 cm) containing samples were put in a "Merry-go-round" in the center of the photoreactor. A fan inside the reactor circulated the air to maintain a constant temperature of 30 – 35 $^{\circ}$C.

Immersion - Well method

Apparatus II employed a Hanovia mercury lamp as the light source and is suitable for large scale photoreactions. It had a cylindrical type of photocell, into which a water cooled lamp housing was inserted. The lamp was contained in a double walled immersion-well structure made of quartz or Pyrex glass. At the top of the photocell, a side arm was fitted for connection to a condenser and at the bottom, a gas inlet was attached to introduce nitrogen or other gas. The photolysis solution could also be stirred magnetically during irradiation. The volume capacity of the photocell was about 150 mL and the light source was a Hanovia medium pressure mercury lamp (200 W 654A36 and 100 W 608A36).

Apparatus III is similar to Apparatus II. The difference is that the photocell and the lamp housing are fused together, thus it is suitable for relatively small scale photoreactions. The capacity of the photocell was reduced to 50 mL.

5.2 Fluorescence Studies

5.2.1 General procedures

All fluorescence spectra were recorded at room temperature on a Perkin-Elmer MPF 44B fluorometer (uncorrected). Typically duplicate experiments were performed to obtain a reproducible quenching constant (K_{SV}), and both values were given in relevant tables where the quenching results needed to be correlated to kinetic analysis of photoreactions. The reported errors from plots were given as the standard deviation from least square analysis using MicroCal Origin Scientific and Technical Graphics in Window (version 3.0).

The geometry of sample illumination, as right-angle or front-face illumination,[75a] was adopted depending on the concentration of $DBMBF_2$ used (Fig. 5.1). The right-angle configuration was used when the $DBMBF_2$ concentration was lower than 10^{-4} M.

right-angle illumination

(square cuvette)   (triangular cuvette)

front-face illumination
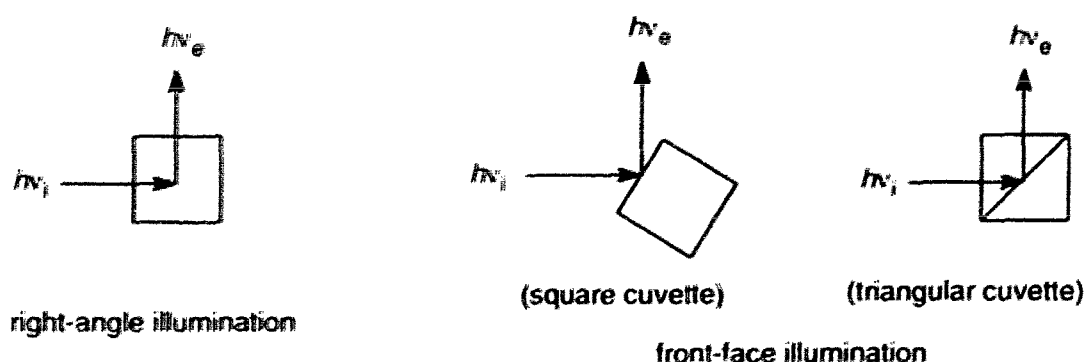
Figure 5.1 Geometric arrangements of the fluorometer cell, here hv_i for incident light and hv_e for emission.

For the fluorescence quenching of $DBMBF_2$ at 5×10^{-6} M, the slit was typically set at 3 or 4 nm for both excitation and emission light beam, and the signal gain was set at 3.0. For $[DBMBF_2] \geq 10^{-4}$ M, the front-face illumination was used to reduce the filtering effect

caused by the high absorbance of DBMBF$_2$ solution. Fig. 5.1 displayed two configurations for front-face illumination using square or triangular cuvette on MPF-44B fluorometer. The square cuvette is positioned about 60 - 65° from its illuminated surface to the incident light beam, while the triangular cuvette has an orientation of 40 - 45° towards the incident beam. For the fluorescence quenching of DBMBF$_2$ at 0.10 or 0.20 M, the slits were set at 10 to 15 nm and the signal gain was at 1.0. All the fluorescence quenching spectra from the front-face illumination were obtained using the square cuvette configuration, except for the spectra in Fig. 5.3.

Two quenching methods were applied in the fluorescence measurements.

Method One[75b] Solutions of DBMBF$_2$ (5 x 10^{-6} ~ 5 x10^{-5} M for the monomer fluorescence and 0.10 or 0.20 M for the excimer fluorescence spectra) in various solvents were freshly prepared before measurements. A 2 mL aliquot of the solution was placed in a quartz square cuvette (1 x 1 cm). To this solution, a known amount of neat quencher was directly added with a syringe. The fluorescence spectrum was then recorded under air. No effects due to the presence of oxygen were observed on the fluorescence intensity of DBMBF$_2$ (5 x 10^{-6} M) or its exciplex with benzene.[58a] When a large amount of quencher ($\geq$ 25 μL) was added, a dilution effect on the initial intensity (I°) must be corrected.

Method Two: Sample solutions were freshly prepared in a 5 mL volumetric flask either from a concentrated stock solution of DBMBF$_2$ or by weighing DBMBF$_2$ directly into the flask. After adding a known amount of quencher, the solution in flask was diluted with solvent to the mark. A 2 mL aliquot of the solution was transferred into a quartz square cuvette with a volumetric pipette, sealed with a septum and purged with dry N$_2$ for 6 min. The fluorescence spectrum was then recorded.

5.2.2 The appearance of DBMBF$_2$ fluorescence spectrum

The appearance of a fluorescence spectrum can be affected by the absorbance of a sample and by the geometry of the sample illumination.[75a] A high absorbance of the sample can distort its emission spectra due to self-absorption of the emission, even when front-face illumination is used.[75a] This is called an inner filter effect caused by the overlap between the absorption and the fluorescence spectra of the sample. Such a case also occurs in DBMBF$_2$ fluorescence spectra. Upon right-angle illumination with λ_{ex} = 365 nm light, the acetonitrile solution of DBMBF$_2$ (5 x 10^{-6} M) gave a fluorescence spectrum with maxima at 398, 417 and 440 nm (shoulder peak).[49, 64a] The intensity of 398 nm peak decreased with an increase in DBMBF$_2$ concentrations. Relevant to this, the UV spectrum of DBMBF$_2$ (5 x 10^{-6} M) showed its absorption close to 400 nm which increased with [DBMBF$_2$]. At [DBMBF$_2$] = 10^{-3} M, only the 416 nm peak was visible when the sample was excited through front-face illumination (Fig. 5.1).[49] Upto [DBMBF$_2$] $\geq$ 0.10 M in acetonitrile, where the absorbance at $\lambda \leq$ 423 nm for the DBMBF$_2$ sample was greater than one, the spectrum of DBMBF$_2$ fluorescence showed a peak at 440 nm as the remaining monomer emission, together with a peak at 522 nm assigned to the excimer.[49, 50c] However, it was found that a variation in the orientation of a sample cuvette towards incident light beam allowed us to observe the entire DBMBF$_2$ fluore- scence spectrum even at [DBMBF$_2$] $\geq$ 0.10 M (using the front-face illumination on a PT1 LS-100 spectrofluorimeter).[58b]

On MPF-44B fluorometer, the front-face illumination was found to involve two orientations for the illuminated surface of the fluorometer cell towards incident light (Fig. 5.1). When the fluorescence of DBMBF$_2$ (0.10 or 0.20 M) was measured using square cuvette configuration, the obtained spectra showed only two peaks of 440 and 522 nm

(Fig. 2.8 and 4.4). But when the fluorescence was recorded through trianglar cuvette configuration, all the peaks of 398, 417 and 440 nm were observed together with the excimer emission at 522 nm (Fig. 5.3).

5.2.3 Corrections in DBMBF$_2$ fluorescence quenching

5.2.3.1 DBMBF$_2$ monomer fluorescence quenching

For the quenching of DBMBF$_2$ monomer fluorescence, the working concentration of DBMBF$_2$ was usually at 5×10^{-6} M. A plot of relative fluorescence intensity as a function of DBMBF$_2$ concentrations (10^{-6} to 1.4×10^{-5} M) is shown in Fig. 5.2. The emission intensity showed a linear relationship to the DBMBF$_2$ concentration below 4×10^{-6} M. This can be described by the first term in eq. 5.1 for a weakly absorbing solution:[112c]

$$I_f = I_i \Phi_f (1 - 10^{\varepsilon l c})$$

$$I_f = I_i \Phi_f (2.3\varepsilon l c - (2.3\varepsilon l c)^2 / 2! + \cdots) \qquad \text{(Eq. 5.1)}$$

Here: I_f is fluorescence intensity, I_i is the intensity of excitation light,

Φ_f is the quantum yield of DBMBF$_2$ emission,

ε is the molar absorption coefficient,

l is the optical path length and c is the DBMBF$_2$ concentration.

Above 4×10^{-6} M, the plot of emission intensity starts to curve down as a result of inner filter effect which is represented by the later terms in eq. 5.1.

When fluorescence quenching was carried out using the direct addition method, each addition of neat quencher into the DBMBF$_2$ solution would exert a dilution effect on the DBMBF$_2$ concentration. Therefore, the initial fluorescence intensity (I^0), in the absence of quencher, should decrease corresponding to each quencher addition. This

dilution effect on I^o can be described by the relationship of the relative emission intensity (I_R) to DBMBF$_2$ concentration from Fig. 5.2:

$$I_R = 0.1155 + 0.9110 [DBMBF_2] - 0.04389 [DBMBF_2]^2 \qquad (Eq. 5.2)$$
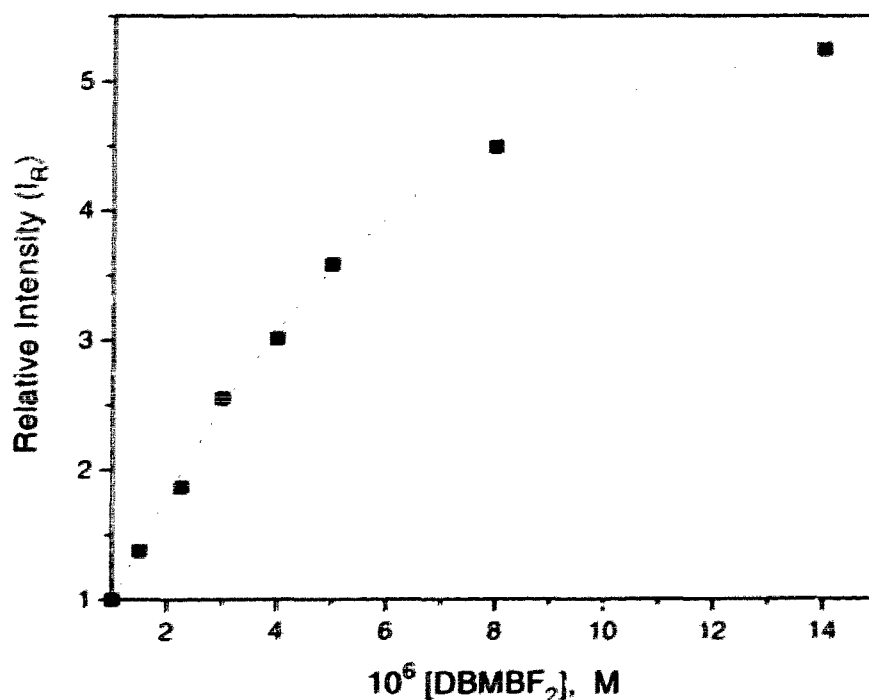
Fig. 5.2 The plot of relative fluorescence intensity of DBMBF$_2$ to its concentration in acetonitrile (λ_{ex} = 365 nm and λ_{mon} = 417 nm).

The correction of dilution effect was illustrated in Table 5.1, using an example of the fluorescence quenching of DBMBF$_2$ by methyl methacrylate (MMA) in acetonitrile (Fig. 4.3). In this quenching, the neat MMA was directly added by syringe to a 2 mL solution of DBMBF$_2$ (5×10^{-6} M). The fluorescence intensity (I) at 417 nm was measured and listed in Table 5.1. In the absence of quencher, the initial intensity was I^o = 174.2, but it would decrease with the addition of MMA. The decrease of I^o due to dilution effect follows Eq. 5.2 in which the relative intensity (I_R) is related to the change of [DBMBF$_2$].

The calculated I_R-values represent the fraction of I^0-decrease corresponding to each MMA addition, thus the initial intensity (I^0) can be corrected upon: $I^0_{corr} = 174.2\ I_R$. The obtained Stern-Volmer plot was shown in Fig. 4.3.

Table 5.1 Correction of the dilution effect on the quenching of DBMBF$_2$ monomer fluorescence by MMA in acetonitrile

MMA added (μL)	(M)	10^6[DBMBF$_2$] M ^{a}	I_R ^{b}	$I^0_{corr} = 174.2\ I_R$ ^{c} (at 417 nm)	I ^{d}	$(I^0 / I)_{417}$
0	0.000	5.000	1.0000	174.2	174.2	1.000
5	0.023	4.9875	0.9983	173.9	169.3	1.027
5	0.047	4.9751	0.9967	173.6	164.9	1.053
5	0.070	4.9628	0.9950	173.3	160.5	1.080
5	0.093	4.9505	0.9934	173.1	157.2	1.101
10	0.140	4.9261	0.9901	172.5	149.6	1.153
10	0.187	4.9020	0.9869	171.9	143.1	1.201
K^m_{SV}						1.1 ± 0.1 M^{-1}

Notes: ^{a} The corrected concentration of DBMBF$_2$ included the dilution effect.

^{b} The relative fluorescence intensity (I_R) is firstly calculated by Eq. 5.2 and then normalized by defining $I_R = 1.000$ at [MMA] = 0 M or in the absence of quencher.

^{c} I^0_{corr} is the corrected fluorescence intensity of DBMBF$_2$ in the absence of quencher.

^{d} The observed fluorescence intensity, in arbitrary unit.

5.2.3.2 DBMBF$_2$ excimer fluorescence quenching

The quenching of DBMBF$_2$ excimer fluorescence was carried out employing the front-face illumination method, and a square cuvette was used for the sample solution (Fig. 5.1). Since the observed fluorescence intensity was found sensitive to the

fluorometer cell movement, a direct addition method was chosen so that the cell arrangement was not disturbed. According to this method, the neat quencher was added directly to a 2 mL solution of DBMBF$_2$ (0.10 or 0.20 M) and then the fluorescence was recorded.

Two corrections were needed in the quenching of DBMBF$_2$ excimer fluorescence. The first one was due to the dilution effect caused by direct addition of neat quencher. This correction should produce an actual quenching constant (K_{sv}^m) smaller than its observed value. The second correction was due to the spectrum overlap between DBMBF$_2$ monomer and excimer fluorescence. Where the quenching of DBMBF$_2$ excimer fluorescence was much more efficient than the quenching of DBMBF$_2$ monomer, this spectrum overlap gave rise to an increased quenching constant (K_{sv}^m) for excited DBMBF$_2$ monomer but a reduced quenching constant (K_{sv}^{ex}) for DBMBF$_2$ excimer. Thus the correction of spectrum overlap should produce an actual K_{sv}^{ex}-constant bigger than its observed value.

Spectrum overlap correction

The correction of spectrum overlap was made through the spectral subtractions that produced the fluorescence profile of DBMBF$_2$ excimer. In doing the subtraction, a profile of DBMBF$_2$ monomer fluorescence should be superimposed with a spectrum of DBMBF$_2$ (0.10 or 0.20 M). The overlaid spectra were shown in Fig. 5.3, where the spectrum A was from the sample of [DBMBF$_2$] = 0.2 M in THF solvent and the spectrum C was of [DBMBF$_2$] = 0.1 M in acetonitrile. Both fluorescence spectra were recorded by front-face illumination using a triangular cuvette for the sample solution. The slit for excitation light is set at 15 nm and the slit for emission light is at 4 nm with the signal gain of 1.0 on MPF 44B fluorometer. Under these conditions, the spectra B and D were
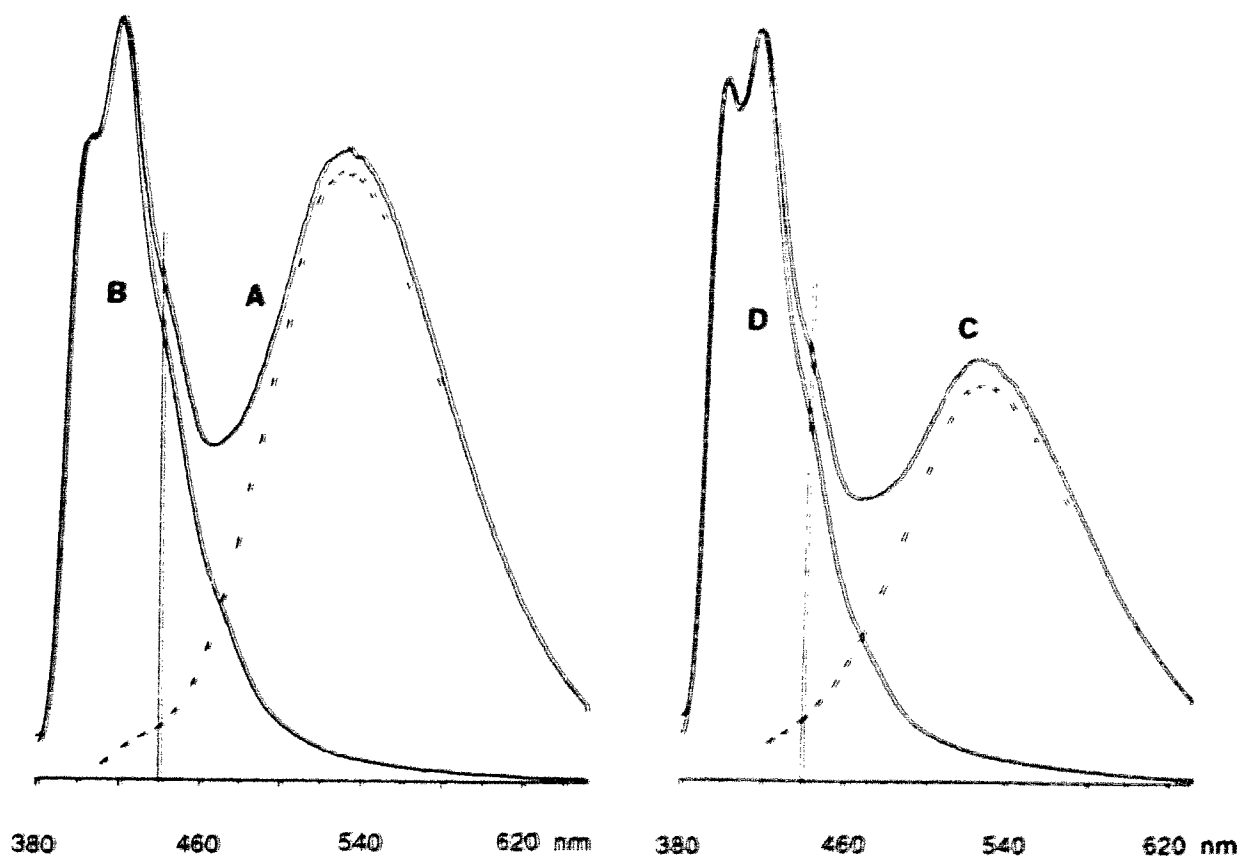
Fig. 5.3 The spectral subtractions of DBMBF₂ fluorescence: λ_{ex} = 365 nm

A: [DBMBF₂] = 0.20 M in THF; B: [DBMBF₂] = 0.01 M in THF;

C: [DBMBF₂] = 0.10 M in CH₃CN; D: [DBMBF₂] = 0.01 M in CH₃CN.

also recorded using the samples of [DBMBF$_2$] = 0.01 M in THF and acetonitrile solvent respectively (Fig. 5.3). The latter two spectra were then subtracted from the former two spectra, in the ways of (A - B) and (C - D). This gives the fluorescence profile of the DBMBF$_2$ excimer, shown as dash-line peaks in Fig. 5.3.

In Fig. 5.3, the fluorescence profile of DBMBF$_2$ excimer showed an overlap with the peak of DBMBF$_2$ monomer fluorescence. When the excimer profile (dash-line) was superimposed with the original excimer peak (solid-line) and normalized at 524 nm, the fraction of spectrum overlap could be estimated. For example in the spectra A and B (Fig. 5.3), a line drawn at 440 nm gave intensity readings of both excimer (I_{ex} = 19) and monomer (I_{mon} = 122) fluorescence, and the ratio of the excimer intensity to the monomer intensity at 440 nm was I_{ex} / I_{mon} = 16% which represented a fraction of the spectrum overlap at this wavelength. Similarly estimated from the spectra C and D, the fraction is about 18% at 440 nm. These results will be used in the spectrum overlap corrections of DBMBF$_2$ (0.10 or 0.20 M) fluorescence, which is described below.

In the quenching of DBMBF$_2$ excimer fluorescence by isobutyl vinyl ether (IVE, Fig. 2.8), a total of 12 µL neat IVE was added to the 2 mL THF solution of DBMBF$_2$ (0.20 M), and the dilution effect was considered to be insignificant ($\leq$ 1%). The initial fluorescence intensity of DBMBF$_2$ at 440 nm is measured to be I_{440} = 141.8 (Table 5.2). A 16% of this intensity, as estimated from spectral subtractions in Fig. 5.3, should come from the overlapped DBMBF$_2$ excimer fluorescence: i_{ex} = 141.8 x 16% = 22.7 at the wavelength of 440 nm. Subtraction of this value from the observed fluorescence intensity at 440 nm (I_{440}) produces the corrected intensity (I') for DBMBF$_2$ monomer fluorescence: I' = (I_{440} - i_{ex}) = 141.8 - 22.7 = 119.1. Table 5.2 lists all the corrected intensity of I_{440} at different [IVE], upon which the quenching constants K_{SV}^m =

2.3 and $K_{SV}^{ex} = 19.6 \, M^{-1}$ were obtained (Table 5.2). The fluorescence spectrum and corresponding Stern-Volmer plot were shown in Fig. 2.8

Table 5.2 Spectrum overlap correction in the quenching of DBMBF₂ (0.20 M) fluorescence by IVE

[IVE] (M)	I_{440}	I_{524}	$\dfrac{I_{524}}{175.2}$	i_{ex} [a]	I' [b]	$(I°/I')_{440}$ = a	$(I°/I')_{524}$ = b	b / a
0.000	141.8	175.2	1.000	22.7	119.1	1.000	1.000	1.000
0.012	133.0	138.0	0.788	17.9	115.1	1.035	1.270	1.227
0.019	129.0	121.0	0.691	15.7	113.1	1.051	1.448	1.378
0.027	125.0	1.6.6	0.608	13.8	111.2	1.071	1.644	1.535
0.034	122.0	96.1	0.549	12.5	109.5	1.088	1.823	1.676
0.046	118.5	83.5	0.477	10.8	107.7	1.106	2.098	1.897

$$K_{SV}^{m} = 2.3 \, M^{-1} \qquad K_{SV}^{ex} = 19.6 \, M^{-1}$$

Notes: [a] The fluorescence intensity of DBMBF₂ excimer at 440 nm: $i_{ex} = 22.7 \times (\dfrac{I_{524}}{175.2})$;

[b] The corrected fluorescence intensity of DBMBF₂ monomer at 440 nm: $I' = (I_{440} - i_{ex})$.

Dilution effect correction

In the quenching of DBMBF₂ excimer fluorescence by methyl methacrylate (Fig. 4.4A), a total of 110 μL neat methyl methacrylate (MMA) was added to a 2 mL CH₃CN solution of DBMBF₂ (0.10 M). Two corrections are described below for the spectrum overlap and the dilution effect. The former correction is shown in Table 5.3 with the corrected intensity ratio $(I°/I')_{440}$ of DBMBF₂ monomer emission at 440 nm, and the latter is shown in Table 5.5 giving the corrected intensity ratio $(I°/I)_{520}$ of DBMBF₂ excimer fluorescence at 520 nm. The combined corrections from Tables 5.3 and 5.5 result in the quenching constant K_{SV}^{ex} (Table 5.5).

The spectrum overlap correction follows the procedure just described. Thus from Fig. 4.4A, the fluorescence intensity at 440 nm (I_{440}) and 520 nm (I_{520}) were measured and listed in Table 5.3. In the absence of MMA, the intensity of $DBMBF_2$ fluorescence at

Table 5.3 Spectrum overlap correction in the quenching of
$DBMBF_2$ (0.10 M) fluorescence by MMA in acetonitrile

[MMA] M	I_{440}	I_{520}	$\dfrac{I_{520}}{141.6}$	i_{ex} $= 29.5 \times (I_{520}/141.6)$	I' $= (I_{440} - i_{ex})$	$(I^0/I')_{440}$
0.00	163.9	141.6	1.00	29.5	134.4	1.000
0.093	152.1	130.2	0.919	27.1	125.0	1.075
0.183	144.5	121.4	0.857	25.3	119.2	1.127
0.316	135.4	110.5	0.780	23.0	112.4	1.196
K_{SV}^{m}						0.61 M^{-1}

440 nm is measured to be 163.9, and its 18% is contributed by the overlapped part of $DBMBF_2$ excimer emission: i_{ex} = 163.9 x 18% = 29.5 at 440 nm. Subtraction of this value from I_{440} gives the corrected intensity (I') for $DBMBF_2$ monomer fluorescence at 440 nm: I' = 163.9 – 29.5 = 134.4. From the values of I', the intensity ratio $(I^0/I')_{440}$ for $DBMBF_2$ monomer fluorescence at 440 nm was calculated, and the corresponding Stern-Volmer quenching constant (K_{SV}^{m} = 0.61 M^{-1}) was obtained (Table 5.3).

The dilution effect was corrected by a control experiment (Fig. 5.4) which was carried out together with the quenching experiment under the identical conditions. In the control experiment, the pure solvent instead of the quencher was added directly to the 2 mL $DBMBF_2$ (0.10 M) solution in the same way as the addition of MMA. Each solvent addition decreased the fluorescence intensity (I^0) of the $DBMBF_2$ excimer at 520 nm (Table 5.4). The intensity decrease could be described by a dilution factor (f), defined

CH₃CN added (μL)	[DBMBF₂] M	Intensity (I) at 520 nm	$f = 1/141$
0	0.100	141.0	1.00
20	0.0990	139.2	0.987
20	0.0980	137.8	0.977
30	0.0966	135.4	0.960
30	0.0952	133.0	0.943

390   470   550   630 nm
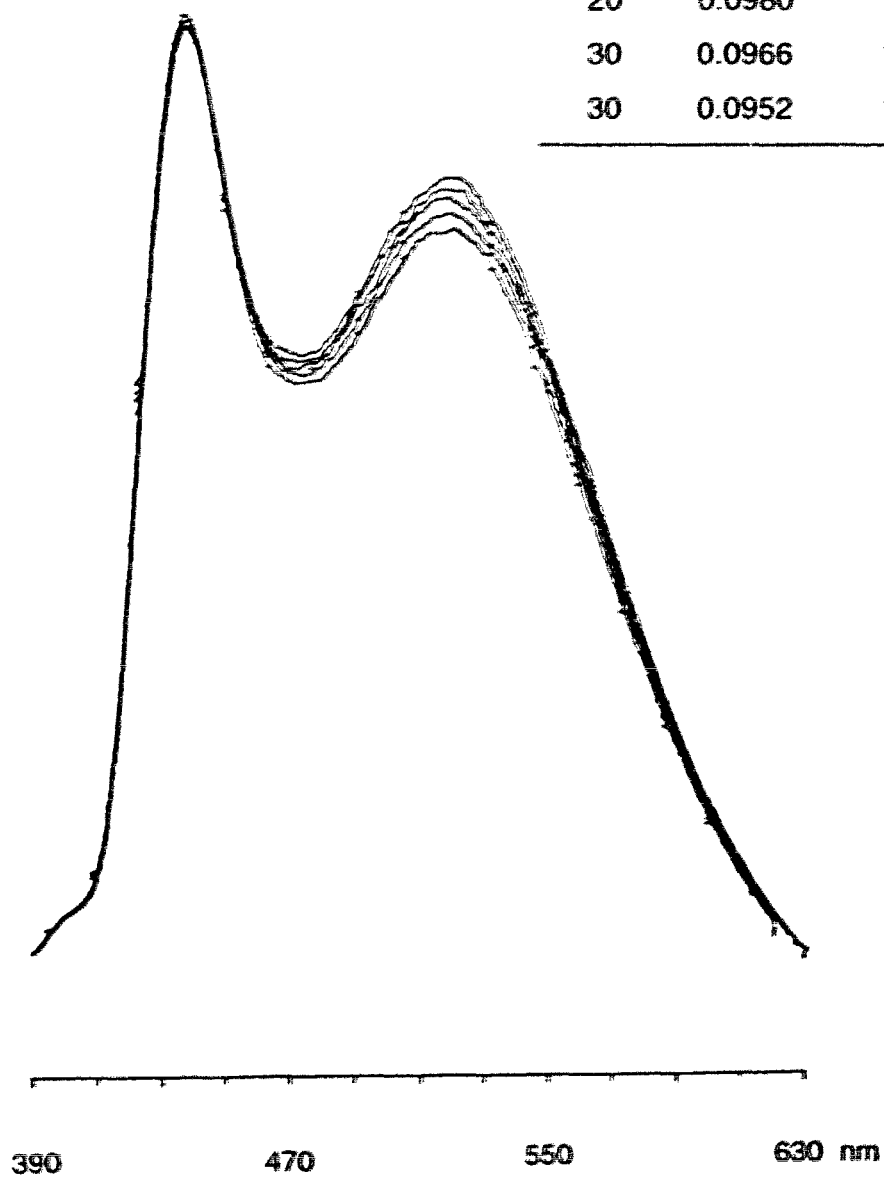
Fig. 5.4 Solvent dilution effect on DBMBF₂ (0.10 M) fluorescence intensity
in acetonitrile (λ_{ex} = 365 nm)

to be the ratio of the fluorescence intensity with and without the solvent dilution (Table 5.4).

The dilution factor (f) from the control experiment was then applied to the quenching experiment. Thus the initial fluorescence intensity (I^o) of DBMBF$_2$ excimer was corrected for each addition of MMA, upon which the intensity ratio (I^o / I)$_{520}$ of DBMBF$_2$ excimer fluorescence at 520 nm was calculated (Table 5.5). The linear plot of (I^o / I)$_{520}$ / (I^o / I')$_{440}$ versus the concentration of MMA was displayed in Fig. 4.4A with $K_{SV}^{ex} = 0.09$ M^{-1} as a slope.

Table 5.5 Correction of the dilution effect on the quenching of DBMBF$_2$ excimer fluorescence (at 520 nm) by methyl methacrylate (MMA) in acetonitrile

MMA added		[DBMBF$_2$]	Intensity at 520 nm		(I^o / I)$_{520}$	(I^o / I)$_{440}$	
(µL)	(M)	M	observed (I)	corrected [a] ($I^o = 141.6f$)	= b	= a [b]	b / a
0	0	0.100	141.6	141.6	1	1	1
20	0.093	0.0990	130.2	139.8	1.074	1.075	1
20	0.183	0.0980	121.4	138.3	1.139	1.127	1.010
30	0.316	0.0966	110.5	135.9	1.230	1.196	1.028
K_{SV}^{ex}							0.09 M^{-1}

Notes: [a] The corresponding f-values are from Table 5.4;

[b] Data from Table 5.3.

5.2.4 Stern-Volmer plots for DBMBF$_2$ fluorescence quenching

The following figures display the Stern-Volmer plots of DBMBF$_2$ fluorescence quenchings. The quenching experiments followed the described procedures in earlier sections. The plots of $(I^o/ I)_{ex}/(I^o/ I)_{mon}$ vs. [D] were obtained by using Eq. 1.18 for the quenching of DBMBF$_2$ excimer. The plots of (I^o/ I) vs. [D] were according to Eq. 1.12 for DBMBF$_2$-benzene exciplex quenching and Eq. 1.16 for DBMBF$_2$ monomer fluorescence quenching (Section 1.6). Here K_{SV}^{ex} refers to the Stern-Volmer constant for quenching DBMBF$_2$ excimer or exciplex, and K_{SV}^{m} refers to the constant for quenching DBMBF$_2$ monomer fluorescence.

Cyclic dienes and phenyl vinyl ether as quencher
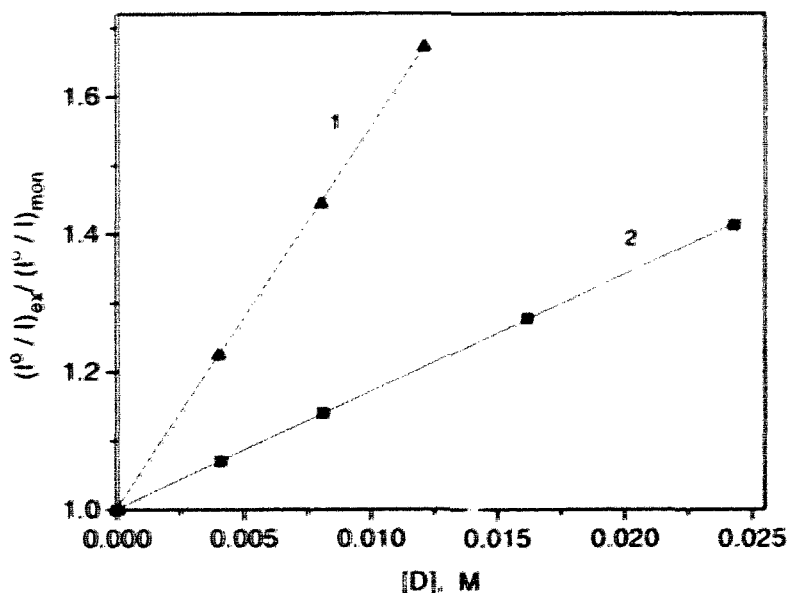
Fig. 5.5 Stern-Volmer plots of DBMBF$_2$ (0.20 M) fluorescence quenching in THF: excited at λ_{ex} = 365 nm and monitored at λ_{mon} = 524 nm (1) by 1,3-COD (▲), K_{SV}^{ex} = 56 ± 1 M^{-1}; (2) by PVE (■), K_{SV}^{ex} = 17 ± 1 M^{-1}
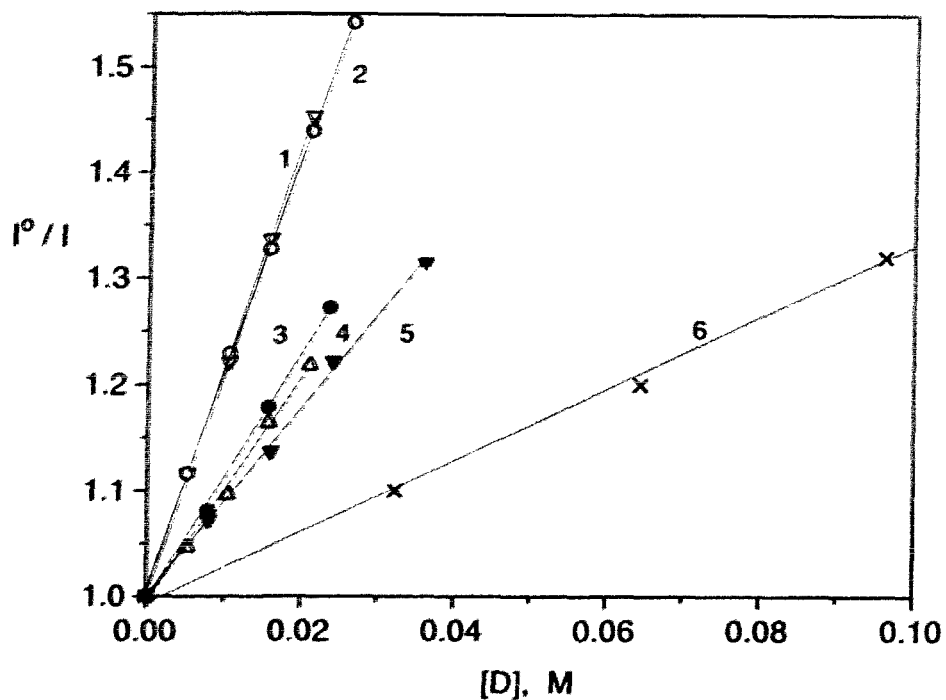
Fig. 5.6 Stern-Volmer plots of DBMBF$_2$ fluorescence quenching by cyclic dienes and PVE in different solvents, λ_{ex} = 365 nm:

(1) CHD, [ᴊMBF$_2$] = 0.03 M in benzene, λ_{moni} = 441 nm, K_{SV}^{ex} = 21.4 ± 1.1 M^{-1};

(2) CHD, [DBMBF$_2$] = 5 x 10^{-6} M in benzene, λ_{moni} = 424 nm, K_{SV}^{ex} = 20.6 ± 1.0 M^{-1};

(3) CHD, [DBMBF$_2$] = 5 x 10^{-6} M in THF, λ_{moni} = 417 nm, K_{SV}^{m} = 11.6 ± 0.3 M^{-1};

(4) CHD, [DBMBF$_2$] = 0.03 M in dioxane, λ_{moni} = 432 nm, K_{SV}^{m} = 10.6 ± 0.4 M^{-1};

(5) 1,3-COD, [DBMBF$_2$] = 0.03 M in benzene, λ_{moni} = 441 nm, K_{SV}^{ex} = 8.8 ± 0.4 M^{-1}.

(6) PVE, [DBMBF$_2$] = 5 x 10^{-6} M in THF, λ_{moni} = 417 nm, K_{SV}^{m} = 3.4 ± 0.3 M^{-1}.
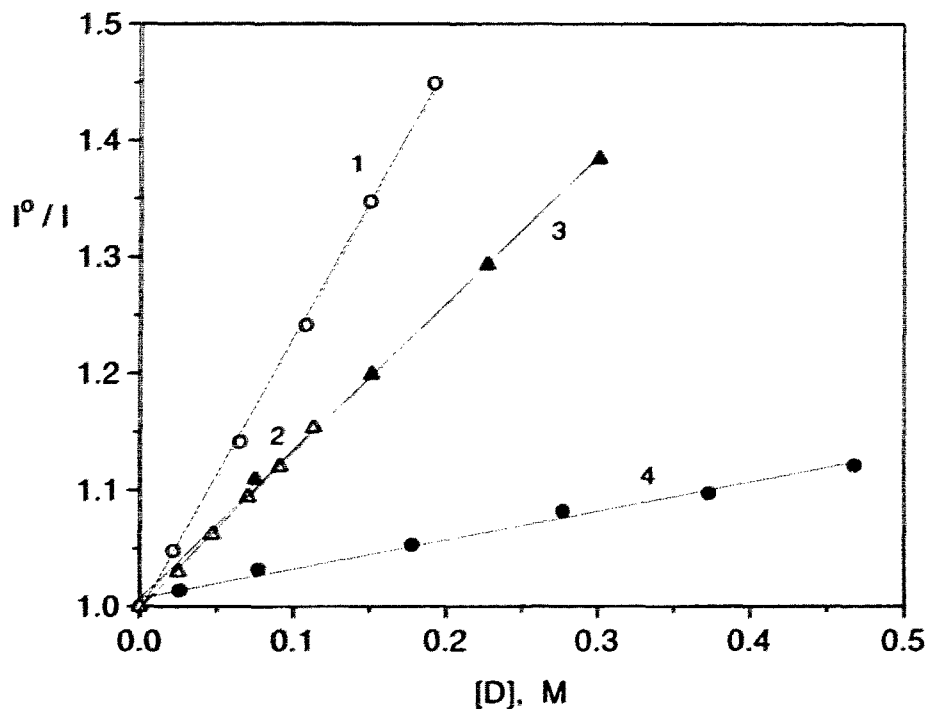
Fig. 5.7 Stern-Volmer plots of $DBMBF_2$ (5×10^{-6} M) fluorescence quenching by α,β-unsaturated carbonyl compounds in acetonitrile:

(1) mesityl oxide, $K_{SV}^m = 2.3 \pm 0.1$ M^{-1};

(2) 2-cyclododecenone, $K_{SV}^m = 1.4 \pm 0.1$ M^{-1};

(3) 2-cyclooctenone, $K_{SV}^m = 1.3 \pm 0.1$ M^{-1};

(4) 2-cyclohexenone, $K_{SV}^m = 0.27 \pm 0.03$ M^{-1}.

(excited at λ_{ex} = 390 nm and monitored at λ_{moni} = 417 nm)
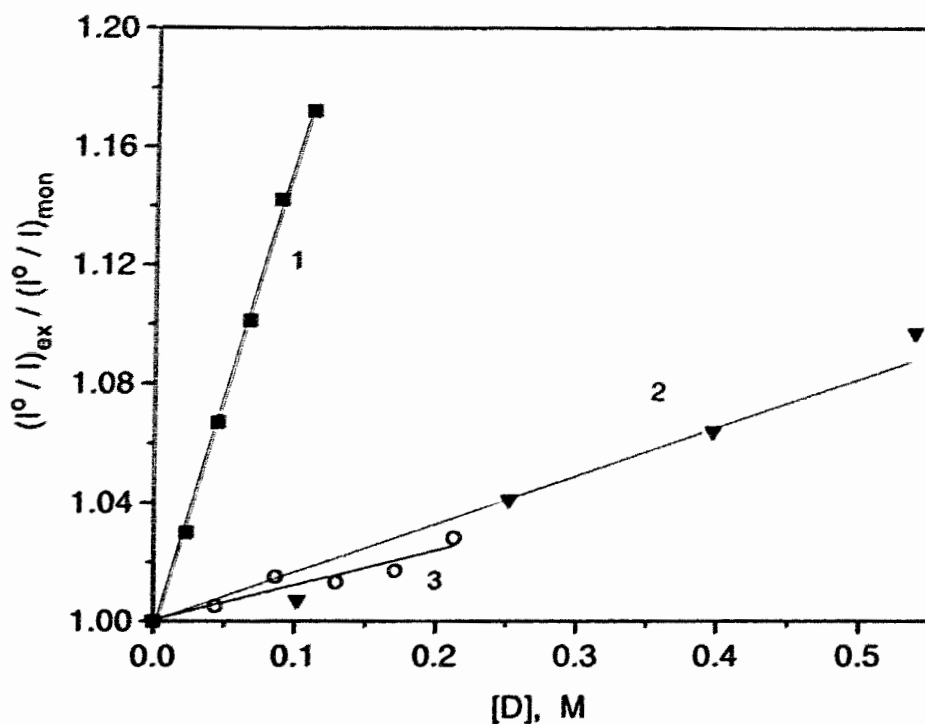
Fig. 5.8 Stern-Volmer plots of DBMBF$_2$ (0.10 M) fluorescence quenching

by α,β-unsaturated carbonyl compounds in acetonitrile:

(1) 2-cyclododecenone, $K_{SV}^{ex} = 1.4 \pm 0.1$ M^{-1};

(2) 2-cyclohexenone, $K_{SV}^{ex} = 0.16 \pm 0.03$ M^{-1};

(3) mesityl oxide, $K_{SV}^{ex} = 0.14 \pm 0.02$ M^{-1}.

(excited at $\lambda_{ex} = 365$ nm and monitored at $\lambda_{moni} = 520$ nm)
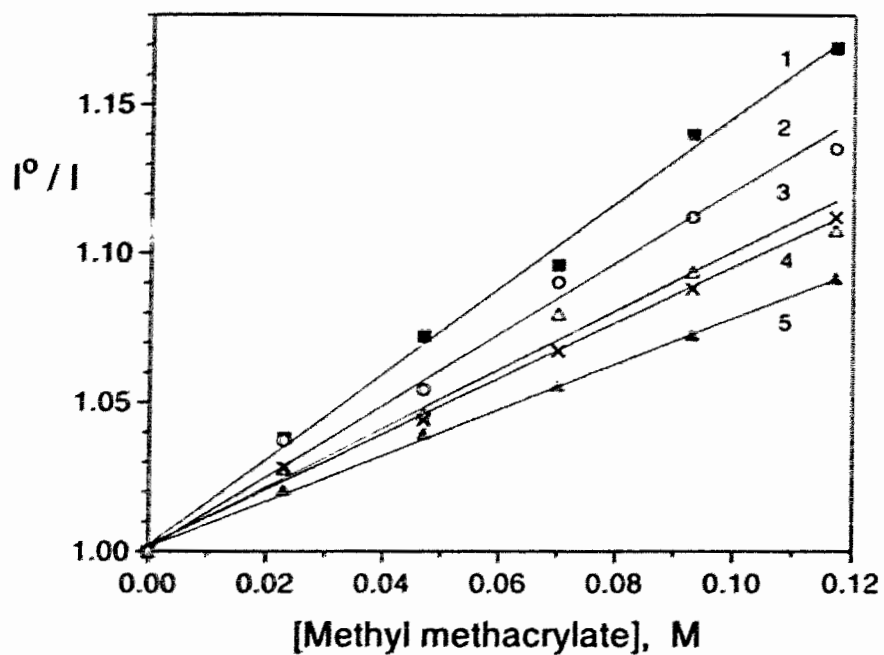
Fig. 5.9 Stern-Volmer plots of DBMBF$_2$ fluorescence quenching by methyl methacrylate at different DBMBF$_2$ concentrations in acetonitrile: excited at $\lambda_{ex} = 365$ nm

(1) 5×10^{-3} M, $\lambda_{moni} = 422$ nm, $K_{SV}^m = 1.45$ M^{-1};

(2) 2.5×10^{-2} M, $\lambda_{moni} = 426$ nm, $K_{SV}^m = 1.25$ M^{-1};

(3) 5×10^{-2} M, $\lambda_{moni} = 431$ nm, $K_{SV}^m = 1.05$ M^{-1};

(4) 7.5×10^{-2} M, $\lambda_{moni} = 434$ nm, $K_{SV}^m = 0.95$ M^{-1};

(5) 10^{-1} M, $\lambda_{moni} = 437$ nm, $K_{SV}^m = 0.78$ M^{-1}.

5.3 Photocycloaddition of DBMBF₂ to electron-rich olefins, cyclic dienes and vinyl ethers

General Procedure

Unless otherwise specified, the following procedures were followed. A solution of $DBMBF_2$ and a diene or vinyl ether was distributed equally among several Pyrex test tubes which were evenly placed in a "merry-go-round" mounted in the centre of a Rayonet photoreactor. This photoreactor was equipped with lamps of RPR-350 nm (16 x 24 W) or RPR-300 nm (16 x 21 W). The temperature during photolysis within the photoreactor was maintained at 30-35 °C by ventilation. The photoreaction was followed by GC / TLC analysis to monitor product formation and $DBMBF_2$ conversion.

After photolysis, the photolysates were usually yellow or brown. A standard work-up procedure included the flash evaporation of the solvent followed by mixing of the residue with hexane : ether (2 : 1 by volume) to precipitate unreacted $DBMBF_2$. Final isolation included filtration, adsorption of the filtrate onto a few grams of silica gel and chromatography on a silica gel column. When the product was sensitive to acidic condition, it was necessary to wash the photolysate with aqueous sodium bicarbonate before the evaporation of solvent.

Photoaddition to 1,3-Cyclooctadiene (9)

A 30 mL benzene solution of $DBMBF_2$ (1.5 mmol, 0.41 g) and 9 (15 mmol, 1.6 g) was distributed and sealed under nitrogen into six Pyrex test tubes (11 x 100 mm), which were irradiated with a RPR 350 nm light source for 22 hours. A thin film of polymer was observed on the test tubes. The photolysate was concentrated and then mixed with

hexane : ether (3 : 1). Unreacted DBMBF$_2$ precipitated as 0.19 g of yellow powder, corresponding to a 55% conversion. The solution showed two adduct peaks: the minor peak had a retention time (RT) of 10.01 min from the reaction of 1,5-COD (7)[†] and the major peak of 10.54 min from 1,3-COD (9) based on GC analysis at 245°C.

Chromatography of the crude product, on a 3 x 30 cm silica gel column eluted with hexane:ethyl acetate (10 : 1), yielded fractions having the peak of RT 10.54 and then the peak of RT 10.01 min as the major component. The former fraction was further purified on preparative TLC plates to give 0.13 g (43% yield) of a sticky oil which corresponded to the cis-addition product of 12 from 1,3-COD: GC purity > 93%, R$_f$ = 0.17 (Merck silica gel 60F254, hexane : CH$_2$Cl$_2$: Et$_2$O = 5 : 0.8 : 0.2), Calcd. for C$_{23}$H$_{24}$O$_2$: C, 83.13; H, 7.23; found: C, 82.91; H, 7.37.

The second fraction was similarly treated by preparative TLC to afford 12 mg of oil which contained the major component with RT 10.01 and a GC purity of 69%. Further separation of this mixture was done by HPLC (Waters Model 510, Phenomenex Maxsil 10C18 Column 500 x 9.4 mm, CH$_3$CN-H$_2$O), to yield two fractions: the product with RT 10.01 min (R$_f$ = 0.14) and a GC purity of 77% corresponding to the known cis-addition product 8 from 1,5-COD; the other, RT 9.91 min (R$_f$ = 0.12) and a GC purity of 87% corresponding to the trans-addition product 12 from 1,3-COD (Table 5.6).

Photocycloaddition to 1,3-cyclohexadiene (1)

Photolysis of a 30 mL ether solution of DBMBF$_2$ (1.5 mmol, 0.41 g) and 1 (15 mmol, 1.2 g) was conducted for 19 hours. After irradiation, the solution was concentrated and then mixed with hexane, to precipitate the remaining DBMBF$_2$ as 66

[†] 1,5-COD is an impurity (2–3%) in the 1,3-COD reagent.

mg of a yellow powder (84 % conversion). The solution showed only one product on TLC but two peaks in the GC in the ratio 91 : 9. Chromatography, on 3 x 30 cm silica gel column with hexane : ethyl acetate of 10 : 1 as eluent, yielded 0.14 g of an oil (35 % yield) which contained two isomers in the ratio 87 : 13 on GC. Using a hexane : dichloromethane : ether (5 : 0.8 : 0.2) eluent, TLC showed a major component at R_f 0.16 and a minor component at R_f 0.14. Preparative TLC failed to purify the product further. Spectroscopic data revealed the major product to be the cis-addition product 6 from 1,3-CHD (Table 5.6).

Photocycloaddition to ethyl vinyl ether (17)

A 30 mL ether solution of DBMBF$_2$ (0.54 mmol, 0.15 g) and 17 (15 mmol, 1.1 g) was distributed and sealed under nitrogen in 6 Pyrex test tubes. Irradiation with 350 nm light was carried out for 220 minutes and the originally colorless solution became pale yellow. Standard work-up recovered DBMBF$_2$ as 90 mg of yellow powder (40% conversion). Chromatography on a 8 x 2.8 cm silica gel column (hexane : ethyl acetate = 15 : 1) gave 50.4 mg of pale yellow oil as the addition product 18 (79% yield): R_f 0.24 (SiO$_2$, hexane : ethyl acetate = 9 : 1).

The cage compound (23)

A 30 mL dioxane solution of DBMBF$_2$ (0.9 mmol, 0.24 g) and 17 (9 mmol, 0.65 g) was irradiated for 4.5 hours. Standard work-up gave DBMBF$_2$ 135 mg (45% conversion). Chromatography with hexane : ethyl acetate (15 : 1) firstly produced 23 mg of white crystals 23: mp 128 – 129 °C (recrystallized from hexane), C$_{17}$H$_{14}$O$_2$ calcd: C,

81.58; H, 5.64; found: C, 81.32; H, 5.70, and then 30 mg of oil as the addition product 18 (24% yield).

Photocycloaddition to phenyl vinyl ether (13)

Phenyl vinyl ether (13) was prepared from 2-bromoethyl phenyl ether according to a literature procedure.[32, 124] ^{1}H NMR (100 MHz, CDCl$_3$) δ (ppm): 4.45 (1H, dd, J = 6.1, 1.5 Hz), 4.78 (1H, dd, J = 13.9, 1.5 Hz), 6.67 (1H, dd, J = 13.9, 6.1 Hz), 6.90 - 7.50 (5H, m).

A 30 mL ether solution of DBMBF$_2$ (0.54 mmol, 0.15 g) and 13 (6 mmol, 0.72 g) was irradiated with 350 nm light for 3 hours. The chromatography, on a silica gel column (17 x 3 cm) eluted with hexane : ethyl acetate (15 : 1 to 10 : 1), afforded three fractions: the first gave 28 mg of yellow oil as the dimers 14 and 15 (84 : 16). The second gave 94 mg (50% yield) of the addition product 16 as white powder: mp 101 ~ 102 °C (recrystallized from hexane), C$_{23}$H$_{20}$O$_3$ calcd: C, 80.21; H, 5.85; found: C, 80.11; H, 5.94. The third fraction, 55 mg of yellow powder, was unreacted DBMBF$_2$ (63% conversion).

Further chromatography of the dimers (hexane : ethyl acetate = 20 : 1) yielded 12 mg of the cis-[2+2] dimer 14 as yellowish liquid, showing GC peak of RT 21.25 min (at 150°C) and R$_f$ 0.42 on TLC (SiO$_2$, hexane : ethyl acetate = 10 : 1), and 4 mg of the trans-[2+2] dimer 15 with RT 21.61 min and R$_f$ 0.30 under the same conditions. The EI-MS of 14, showed m/z: 240 (100, M$^+$), 212 (17), 120 (90), 91 (30) and 77 (15). The ^{1}H NMR spectrum was identical to that of the known compound.[32] Both dimers were also identified by GC coinjection with the authentic material prepared from benzonitrile sensitized PVE dimerization in acetonitrile solvent.[32]

Photocycloaddition to isobutyl vinyl ether (19)

A 40 mL ether solution of DBMBF$_2$ (0.72 mmol, 0.2 g) and **19** (12 mmol, 1.2 g) was irradiated for 3 hours. The clear pale yellow solution was worked up to recover 0.12 g DBMBF$_2$ (38% conversion). GC analysis at 230 °C showed two product peaks at RT 8.35 min (**20**) and at RT 2.72 min (**23**, the cage product). Column chromatography, with hexane : ethyl acetate at 18 / 1 (v/v) and then at 15 / 1 (v/v), afforded the major product **20** (RT 8.35 min) as 56.8 mg of oil (64% yield) with a GC purity of >95%.

The coupling product of DBM with THF

In THF, the 5 hour irradiation of a 40 mL solution of DBMBF$_2$ (1.2 mmol, 0.33 g) and **19** (12 mmol, 1.2 g) yielded, after the standard work-up, 0.16 g DBMBF$_2$ (51% conversion). Chromatography with hexane : ethyl acetate (15 : 1) yielded three fractions: the first fraction gave 28 mg of the addition product **20** (14% yield); the second fraction gave 13 mg of white powder, mp 82 ~ 84 °C; the third fraction gave 18 mg of white powder, mp 60 ~ 63 °C. Both solid products were recrystallized from hexane and identified to be diastereomers of the coupling reaction product **24** from DBM and a THF (Table 5.6).

  cis-12	^{1}H NMR (CDCl$_3$) δ 1.33 - 1.98 (6H, m), 2.08 - 2.41 (2H, m), 2.70 (H$_e$, dd, J = 16.4, 10.0 Hz), 2.89 (H$_d$, m), 3.11 (H$_{e'}$, dd, J = 16.4, 3.4 Hz), 4.73 (H$_a$, dd, J = 9.3, 3.9 Hz), 5.97 (H$_c$, ddd, J = 10.4, 7.8, 7.8 Hz), 6.05 (H$_b$, dd, J = 10.4, 9.3 Hz), 7.30 - 8.10 (10H, m, phenyl). ^{13}C NMR (CDCl$_3$) δ 24.38, 27.18, 29.85, 31.72, 38.48, 39.01, 46.64, 125.83, 132.25, 128.10, 128.44 (2C), 128.72, 132.78, 133.03, 136.72, 137.17, 199.56, 201.36 ppm. MS (EI) m/z 332 (M$^+$, 4), 314 (M-18, 3), 213 (20), 105 (100), 77 (35); (CI) m/z 333 (M+1, 100), 213 (15). IR (NaCl plate) v: 3060, 3028, 2925, 2854, 1681(br), 1597, 1979, 1447, 1405, 1356, 1337, 1290, 1220, 1180, 1003, 971, 909, 849, 776, 692 cm^{-1}.
  trans-12	^{1}H NMR (CDCl$_3$) δ 1.29 - 2.48 (8H, m), 2.70 (H$_e$, dd, J = 14.1, 10.7 Hz), 2.93 (H$_d$, m), 3.02 (H$_{e'}$, dd, J = 14.1, 3.3 Hz), 4.43 (H$_a$, dd, J = 10.5, 10.5 Hz), 5.38 (H$_b$, dd, J = 10.5, 10.4 Hz), 5.92 (H$_c$, ddd, J = 10.4, 8.5, 8.5 Hz), 7.42 - 8.06 (10H, m, phenyl). ^{13}C NMR (CDCl$_3$) δ 23.42, 28.00, 28.06, 29.38, 37.63, 42.03, 49.94, 128.96, 132.88, 128.41, 128.51 (2C), 128.67, 133.21, 133.52, 136.94, 137.63, 199.96, 202.04 ppm. MS (EI) m/z 332 (M$^+$, 4), 314 (M-18, 3), 264 (2), 213 (25), 105 (100), 77 (28); (CI) m/z 333 (M+1, 100), 213 (15).

Table 5.6 (continued)
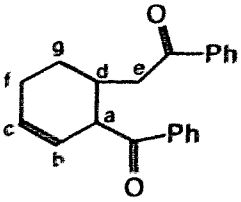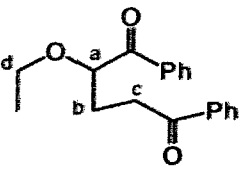
  cis-6	^{1}H NMR (CDCl$_3$) δ 1.75 (H$_g$, m), 2.10 (H$_{g'}$, m), 2.14 (H$_f$ and H$_{f'}$, m), 2.81 (H$_d$, m), 2.95 (H$_e$, dd, J = 17.1, 6.2 Hz), 3.06 (H$_{e'}$, dd, J = 17.1, 8.1 Hz), 4.43 (H$_a$, m)*, 5.77 (H$_b$, ddt, J = 9.7, 4.0, 2.2, 2.2 Hz), 5.93 (H$_c$, ddd, J = 9.7, 6.1, 3.9 Hz), 7.20 - 8.10 (10H, m, phenyl). *Note: J$_{ad}$ = 5.1 and J$_{ab}$ = 4.0 Hz were obtained from the decoupling experiments. ^{13}C NMR (CDCl$_3$) δ 23.68, 25.17, 32.00, 39.65, 45.84, 124.13, 129.91, 127.98, 128.44, 128.56, 128.72, 132.87, 132.99, 137.16, 137.27, 199.64, 201.26 ppm. MS (EI) m/z 304 (M$^+$, 6), 185 (13), 105 (100), 77 (42). (CI) m/z 305 (M+1, 100), 185 (10). IR (NaCl plate) v: 3059, 3027, 2926, 2874, 1682 (br), 1650, 1596, 1580, 1448, 1372, 1320, 1283, 1213, 1180, 1075, 1002, 846, 753, 690 cm^{-1}.
  18	^{1}H NMR (C$_6$D$_6$) δ 1.04 (CH$_3$, dd, J = 7.1, 7.0 Hz), 2.21 (H$_b$, dddd, J = 14.5, 8.6, 6.8, 5.9 Hz), 2.43 (H$_{b'}$, dddd, J = 14.5, 7.9, 6.4, 4.8 Hz), 2.73 (H$_c$, ddd, J = 18.0, 6.4, 5.9 Hz), 3.09 (H$_{c'}$, ddd, J = 18.0, 7.9, 6.8 Hz), 3.13 (H$_d$, dq, J = 9.0, 7.1 Hz), 3.48 (H$_{d'}$, dq, J = 9.0, 7.0 Hz), 4.73 (H$_a$, dd, J = 8.6, 4.8 Hz), 7.00 - 8.40 (10H, m, phenyl). ^{13}C NMR (CDCl$_3$) δ 15.24, 27.50, 33.93, 65.70, 81.35, 128.04, 128.60, 128.67, 128.80, 133.10, 133.43, 135.11, 136.98, 199.64, 200.42 ppm. MS (EI) m/z 191 (96), 163 (10), 145 (22), 132 (12), 117 (60), 105 (100), 77 (87). (CI) m/z 297 (M+1, 100), 251 (16), 191 (19). IR (NaCl plate) v: 3062, 3028, 2973, 2929, 2873, 1687, 1597, 1580, 1448, 1374, 1223, 1120, 1062, 972, 758, 692 cm^{-1}.

Table 5.6 (continued)
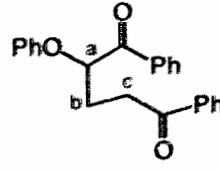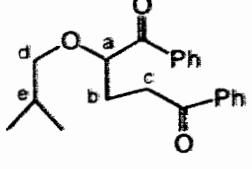
16	^{1}H NMR (CDCl$_3$) δ 2.34 (H$_b$, dddd, J = 14.5, 9.1, 6.4, 5.5 Hz), 2.61 (H$_{b'}$, dddd, J = 14.5, 8.2, 6.4, 4.0 Hz), 3.25 (H$_c$, ddd, J = 18.4, 6.4, 5.5 Hz), 3.45 (H$_{c'}$, ddd, J = 18.4, 8.2, 6.4 Hz), 5.65 (H$_a$, dd, J = 9.1, 4.0 Hz), 6.80 - 7.22 (5H, m, oph), 7.42 - 8.30 (10H, m, phenyl). ^{13}C NMR (CDCl$_3$) δ 27.40, 33.90, 78.92, 115.28, 121.54, 128.05, 128.65, 128.90 (2C), 129.58, 133.24, 133.82, 134.46, 136.84, 157.70, 198.13, 199.27 ppm. MS (EI) *m/z*. 344 (M$^+$, 9), 251 (36), 239 (100), 145 (26), 129 (12), 117 (38), 105 (80), 95 (18), 77 (62). IR (NaCl plate) ν: 3062, 3040, 2935, 1692, 1682, 1598, 1587, 1494, 1449, 1233, 1225, 1179, 1086, 1001, 975, 910, 754, 732, 690 cm^{-1}.
20	^{1}H NMR (C$_6$D$_6$) δ 0.82, 0.84 (2CH$_3$, d, J = 6.5, 6.5 Hz), 1.82 (H$_e$, ddqq, J = 6.5, 6.5, 6.5, 6.5 Hz), 2.23 (H$_b$, dddd, J = 14.3, 8.9, 6.8, 5.8 Hz), 2.45 (H$_{b'}$, dddd, J = 14.3, 8.0, 6.8, 4.8 Hz), 2.76 (H$_c$, ddd, J = 18.0, 6.8, 5.8 Hz), 2.91 (H$_d$, dd, J = 8.8, 6.5 Hz), 3.12 (H$_{c'}$, ddd, J = 18.0, 8.0, 6.8 Hz), 3.32 (H$_{d'}$, dd, J = 8.8, 6.5 Hz), 4.74 (H$_a$, dd, J = 8.9, 4.8 Hz), 7.00 - 8.50 (10H, m, phenyl). ^{13}C NMR (CDCl$_3$) δ 19.25, 19.32, 27.47, 28.69, 34.00, 77.08, 81.98, 128.01, 128.60, 128.62, 128.86, 133.07, 133.37, 135.14, 136.99, 199.54, 200.38 ppm. MS (EI) *m/z*. 219 (89), 163 (100), 145 (17), 117 (49), 105 (57), 85 (10), 77 (52), 57 (47). (CI) *m/z*. 325 (M+1, 100), 251 (93), 219 (85), 163 (61), 145 (16), 133 (41). IR (NaCl plate) ν: 3063, 2957, 2872, 1719, 1690, 1598, 1582, 1472, 1450, 1380, 1249, 1118, 1083, 1047, 759, 713, 690 cm^{-1}.

Table 5.6 (continued)
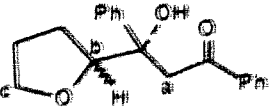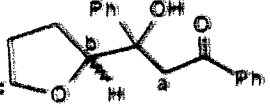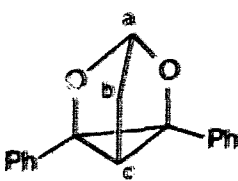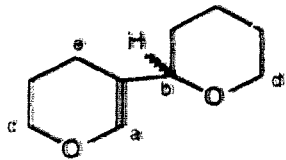
  mp: 82 - 84 °C D$_2$O exchange was done on ^{1}HNMR. **24a**	^{1}H NMR (CDCl$_3$) δ 1.10 - 1.90 (2CH$_2$, m), 3.47 (H$_a$, d, J = 17.4 Hz), 3.62 (H$_c$, ddd, J = 7.9, 7.0, 6.0 Hz), 3.68 (H$_{c'}$, ddd, 7.9, 7.0, 7.0 Hz), 4.10 (H$_{a'}$, d, 17.4 Hz), 4.22 (H$_b$, dd, J = 6.8, 6.8 Hz), 4.95 (OH, s), 7.15 - 7.95 (10H, m, phenyl). ^{13}C NMR (CDCl$_3$) δ 25.60, 26.42, 45.25, 69.03, 76.87, 84.79, 126.31, 126.93, 127.78, 128.22, 128.62, 133.62, 137.22, 142.83, 201.86 ppm. MS (EI) m/z 225 (50), 105 (100), 91 (6), 77 (42), 71 (25). (CI) m/z 297 (M+1, 17), 279 (M-18, 80), 225 (17), 177 (67), 121 (100). IR (NaCl plate) ν: 3470, 3087, 3058, 3027, 2975, 2952, 2927, 2871, 1669, 1597, 1580, 1494, 1448, 1407, 1355, 1216, 1182, 1063, 1003, 911, 753, 733, 704, 689 cm^{-1}.
  mp: 60 - 63 °C ^{1}HNMR in CDCl$_3$ was also done. **24b**	^{1}H NMR (C$_6$D$_6$) δ 1.30 - 2.15 (2CH$_2$, m), 3.45 (H$_a$, d, J = 16.4 Hz), 3.69 (H$_c$, ddd, J = 7.4, 7.4, 5.2 Hz), 3.79 (H$_{a'}$, d, J = 16.4 Hz), 3.95 (H$_{c'}$, ddd, J = 7.4, 7.4, 7.4 Hz), 4.15 (H$_b$, dd, J = 7.0, 7.0 Hz), 5.44 (OH, s), 6.90 - 7.80 (10H, m, phenyl). ^{13}C NMR (CDCl$_3$) δ 25.37, 26.27, 45.28, 69.39, 77.61, 85.57, 125.24, 126.86, 128.10, 128.18, 128.53, 133.31, 137.52, 144.24, 201.77 ppm. MS (EI) m/z 225 (43), 153 (41), 120 (10), 105 (100), 77 (42), 71 (60). IR (NaCl plate) ν: 3444, 3086, 3060, 2977, 2872, 1667, 1597, 1580, 1495, 1448, 1405, 1363, 1217, 1182, 1075, 1003, 927, 889, 749, 703 cm^{-1}.

Table 5.6 (continued)

^{1}H NMR (CDCl$_3$)* δ 1.93 (H$_b$, dd, J = 1.5, 0.7 Hz), 2.46 (H$_c$, dt, J = 1.5, 0.4 Hz), 5.90 (H$_a$, dt, J = 0.7, 0.4 Hz), 7.15 - 7.25 (10H, m, phenyl). *Note: 2D-COSY was done.

^{13}C NMR (CDCl$_3$) δ 19.24 (CH$_c$), 33.72 (CH$_2$), 66.31 (quaternary), 96.56 (CH$_a$), 127.29, 127.64, 128.19, 131.83 (phenyl) ppm.

MS (EI) m/z 250 (M$^+$, 25), 233 (M-17, 10), 221 (19), 205 (36), 145 (65), 144 (28), 127 (37), 117 (58), 115 (57), 105 (100), 91 (30), 77 (90), 51 (23).

MS (CI) m/z 251 (M+1, 100)

IR (Nujol, NaCl plate) v: 3068, 3028, 2997, 2923, 1604, 1503, 1448, 1179, 1142, 1079, 1074, 1052, 1033, 1005, 991, 891, 861, 833, 787, 767, 756, 716, 695, 598 cm^{-1}.

23

^{1}H NMR (C$_6$D$_6$) δ 1.15 - 1.70 (8H, m), 2.00 (H$_e$, ddd, J = 16.5, 6.6, 6.6 Hz), 2.11 (H$_{e'}$, ddd, J = 16.5, 6.0, 6.0 Hz), 3.30 (H$_d$, m), 3.51 (H$_b$, dd, J = 10.9, 1.7 Hz), 3.68 (H$_c$, ddd, J = 10.8, 8.0, 3.3 Hz), 3.77 (H$_{c'}$, ddd, J = 10.8, 6.5, 3.5 Hz), 3.95 (H$_{d'}$, m), 6.68 (H$_a$, s).

^{13}C NMR (CDCl$_3$) δ 19.76, 22.29, 23.80, 25.98, 30.19, 65.74, 68.66, 79.31, 114.15, 141.42 ppm.

MS (EI) m/z 168 (M$^+$, 70), 167 (51), 139 (11), 125 (24), 111 (100), 98 (64), 83 (52), 66 (56), 55 (50).

MS (CI) m/z 169 (M+1, 100)

22

IR (NaCl plate) v: 2935, 2848, 1667, 1440, 1266, 1237, 1151, 1112, 1085, 1052, 1031, 1011, 985, 941, 927, 857, 814 cm^{-1}.

5.4 Radical cation reactions sensitized by DBMBF₂

5.4.1 Diels-Alder dimerization of 1,3-cyclohexadiene (CHD) in xylene-acetonitrile solvent

(a) Authentic sample

Authentic samples of CHD [4+2]-dimers were prepared by the sensitized dimerization of the diene (1 M) with $DBMBF_2$ (0.01 M) in acetonitrile, irradiated at 350 nm.[49] GC analysis at 110 °C (15 m OV–1 capillary column) showed the *endo*-[4+2] dimer 2 at RT 4.96 min and the *exo*-[4+2] dimer 3 at RT 5.26 min in a 9 : 1 ratio. Trace amounts of the two [2+2] dimers were also seen at RT 5.41 and 6.74 min, and were identified as the *cis-anti-cis* (4) and *cis-syn-cis* dimers (5) by coinjection with authentic samples prepared by photolysis of an acetonitrile solution of benzophenone (5×10^{-3} M) and CHD (0.5 M) at 350 nm for 1.5 hour. This gave 2 : 3 : 4 : 5 = 0.4 : 22.3 : 57.0 : 20.3.[37a]

Direct photolysis of 1,3-cyclohexadiene (0.1 M) in benzene solvent with a 350 nm light source yielded no *endo*-[4+2] dimer 2 but only a 1 : 3 : 1 mixture of 3, 4 and 5.[36c, 126]

(b) Preparation of 1,3-cyclohexadiene dimers

An acetonitrile solution (25 mL) of $DBMBF_2$ (0.06 M), CHD (0.5 M) and xylene (1.5 M) was distributed into 5 Pyrex test tubes, purged with dry nitrogen gas for 2 min and irradiated for 6 hours at 350 nm. During photolysis, a reference sample containing dodecane (4×10^{-3} M) as an internal standard was followed by GC analysis.

After photolysis, the clear, pale yellow solution was concentrated under reduced pressure and hexane was added to precipitate the unreacted $DBMBF_2$. The recovery was 0.6 g (100%). The filtrate was concentrated and the p-xylene was removed by distillation. Vacuum distillation, at ~140 °C / ~90 mmHg, gave 0.48 g (50% yield) of a colorless liquid, the mixture 2 : 3 (87 : 13).

GC-MS (EI) for endo-[4+2] dimer 2, m/z: 160 (M+, 12), 115 (4), 91 (13), 82 (24), 81 (15), 80 (100), 79 (70), 78 (6), 77 (18), 65 (4), 51 (4); for exo-[4+2] dimer 3, m/z: 160 (M+, 6), 115 (3), 91 (9), 82 (14), 81 (9), 80 (100), 79 (41), 78 (4), 77 (10), 65 (2).

5.4.2 The coupling reaction of p-xylene

Several Pyrex test tubes were loaded with a 3 mL acetonitrile solution of $DBMBF_2$ (0.01 M) and p-xylene in concentrations ranging from 0.2 to 8.16 M (neat). The tubes were placed in a Rayonet Photoreactor and irradiated with a 350 nm light source for 175 minutes. The $DBMBF_2$ was not consumed on the basis of GC analysis. One mL dichloromethane solution of hexadecane (7.5 x 10^{-3} M) was added to each tube, and product formation was monitored by GC at 180 °C on a 15 meter OV-1 capillary column. Two peaks were observed at RT 3.49 min and at RT 3.54 min. In the GC-MS (EI) spectra, the major product 25 (RT 3.49 min) showed: 210 (M+, 65), 195 (100), 180 (30), 165 (33), 132 (20), 118 (99), 105 (24), 91 (20), 77 (31), and the minor product 26 (RT 3.54 min) displayed: 210 (M+, 25), 105 (100), 77 (9). The mass spectra correspond to the known compound 4-tolyl-2,5-xylylmethane and 1,2-bis-(4-tolyl)ethane respectively.[78, 106] The results of coupling product formation as a function of xylene concentration are shown in Table 5.7 and Fig. 3.5 (section 3.1.2).

Table 5.7 Relative yields of coupling products as the function
of p-xylene concentration,[a] [DBMBF$_2$] = 0.01 M

p-Xylene mole% in acetonitrile	[p-xylene] M	E$_T$(30) (kcal/mole)	Relative yield[b]	Product Ratio (25)	:	(26)
1.1	0.20	45.5	1.21	35		65
2.7	0.50	45.3	2.34	55		45
5.7	1.0	44.9	3.30	73		27
12.2	2.0	44.1	4.55	--		--
19.8	3.0	43.1	7.13	81		19
29.0	4.0	42.0	8.84	78		22
40.3	5.0	40.6	9.13	67		33
46.8	5.5	39.8	5.36	75		25
54.4	6.0	38.8	0.48	--		--
71.8	7.0	36.6	--[c]	--		--
95.4	8.0	33.7	0.48	50		50
100	8.2	33.1	1.00	36		64

Notes: [a] Irradiation for 3 hours; [b] The yield of coupling reaction in neat p-xylene is defined to 1.00; [c] No product was detected on GC.

5.4.3 The coupling reaction of 3,4-dihydro-2H-pyran (21)

Boron trifluoride etherate (21.2 mg, 0.15 mmol) was added under N$_2$ to a 50 mL of 1 : 1 acetonitrile - hexane mixture of 21 (7.5 mmol, 0.65 g). The dark reaction mixture was stirred at room temperature. The bottom acetonitrile layer became red-yellowish, and the top hexane layer remained colorless. Product formation was

analysed periodically by GC (140°C). After two hours, the hexane layer was separated, and found to contain mainly a product of RT 2.68 min on GC. More hexane (20 mL) was added and the extraction procedure was repeated in 5 times. The hexane extractions were combined and concentrated to give 0.75 g of a pale yellow oil. This was chromatographed on silica gel column (7 x 3 cm), and elution with hexane : ethyl acetate (25 : 1) yielded 31 mg of colorless oil (22, 5% yield) showing a GC-purity of 94%.

The structural data of 22 are listed in Table 5.6.

5.5 Photocycloaddition of DBMBF$_2$ to electron-deficient olefins α,β-unsaturated carbonyl compounds

General procedure

A 30 mL acetonitrile solution of DBMBF$_2$ (0.05 M) and freshly distilled α,β-unsaturated ketone or ester (0.5 M) was distributed into six Pyrex test tubes (100 x 13 mm). The solution was purged with dry nitrogen and then placed in the Rayonet photoreactor for irradiation with a 350 nm light source. The photoreaction was monitored by GC or TLC to follow the disappearance of DBMBF$_2$, and was stopped when the DBMBF$_2$ conversion reached more than 90%. The yellowish or brownish solution was then evaporated in vacuo, and the residue was chromatographed on silica gel. Some typical runs were described below.

Photoaddition to methyl methacrylate (31)

DBMBF$_2$ (0.37 g, 1.36 mmol) and **31** (1.5 g, 15 mmol) were dissolved in 30 mL of acetonitrile. After a 2 hour irradiation, GC analysis showed one product peak. Chromatography using hexane : ethyl acetate (5 : 1) yielded 0.38 g (85% yield) of white powder which was crystallized from ethyl acetate-hexane to give the product **32**. mp: 113.5 - 114 °C, Calcd for C$_{20}$H$_{20}$O$_4$: C, 74.07; H, 6.17; found: C, 74.07; H, 6.18.

Photoaddition to trans-ethyl crotonate (33)

DBMBF$_2$ (0.41 g, 1.5 mmol) and **33** (1.71 g, 15 mmol) were dissolved in 30 mL of acetonitrile. After a 6 hour irradiation, the yellow solution was mixed with 20 mL ether, washed twice with the saturated aqueous sodium bicarbonate and dried over anhydrous sodium sulfate. Two products were seen on TLC, at R$_f$ 0.13 (**34**) and R$_f$ 0.08 (SiO$_2$, hexane : ether = 6 : 1). Column chromatography and elution with hexane : ether (8 : 1) gave 0.33 g of oil (65% yield) which contained, in addition to the major adduct of R$_f$ 0.13, a second product at R$_f$ 0.11. From the following collected fractions, 0.09 g oil (16% yield) was obtained in GC purity 95% as the addition product of R$_f$ 0.08 (**35**).

The mixture of R$_f$ 0.13 and 0.11 was found to be *erythro-* and *threo-***34** in a 3 : 1 ratio, based on ^{1}H NMR analysis. Further separation of the mixture on TLC plate (hexane : ether = 7 :1) failed to produce the pure compound, because of the equilibrium between the two isomers. The mixture sample was used for elemental analysis, calcd for C$_{21}$H$_{22}$O$_4$: C, 74.56; H, 6.51; found: C, 74.42; H, 6.57.

Photoaddition to mesityl oxide (27)

DBMBF$_2$ (0.82 g, 3 mmol) and **27** (2.9 g, 30 mmol) were dissolved in 60 mL of THF. After a 9 hour irradiation, the yellowish solution was mixed with 40 mL of ether, washed twice with the saturated aqueous solution of sodium bicarbonate, dried over sodium sulfate and evaporated. TLC analysis showed three products at R$_f$ 0.47, 0.13 and 0.06 (SiO$_2$, hexane : dichloromethane : ether = 5 : 0.7 : 0.3) in a ratio of 1 : 2 : 4 on GC analysis. Chromatography on silica gel (30 x 3 cm) with hexane : dichloromethane : ether (6 : 0.9 ~ 0.7 : 0.1 ~ 0.3) yielded 76 mg of **30** as an oil R$_f$ 0.47 (8%), 110 mg of **28** R$_f$ 0.13 (11%) and 208 mg of **29** R$_f$ 0.06 (22%).

Samples for elemental analysis were further purified by chromatography:

30: R$_f$ 0.47   calcd for C$_{21}$H$_{20}$O$_2$: C, 82.89; H, 6.58;   found: C, 82.74; H, 6.46.

28: R$_f$ 0.13   calcd for C$_{21}$H$_{22}$O$_3$: C, 78.26; H, 6.83;   found: C, 78.58; H, 6.93.

29: R$_f$ 0.06   calcd for C$_{21}$H$_{22}$O$_3$: C, 78.26; H, 6.83;   found: C, 77.99; H, 6.86.

To a 2.5 mL acetonitrile solution of **29** (8.5 mg, 0.026 mmol) was added one drop of 6.2 M hydrogen chloride in acetonitrile (total [HCl] < 0.1 M). The colorless solution immediately became pale yellow and a quantitative conversion of the product **29** into **30** was observed by GC and TLC.

Photoaddition to acrylonitrile (38) and crotonitrile (36)

DBMBF$_2$ (340 mg, 1.25 mmol) and **38** (663 mg, 12.5 mmol) were dissolved in 25 mL of p-dioxane. After irradiation for 26.2 hours, some polymer had precipitated in the test tubes. This was collected (0.1 g, insoluble in acetone and water). The filtrate

contained one major product by GC and TLC analysis. Evaporation and addition of ether : hexane (1 : 2) gave DBMBF$_2$ as a yellow precipitate, 0.29 g (25% conversion). The filtrate was chromatographed on silica gel using hexane : dichloromethane : ether (5 : 0.8 : 0.2 ~ 3.5 : 0.8 : 0.2). The pale yellow oil **39** was isolated (66 mg, 59% yield based on consumed DBMBF$_2$): R$_f$ 0.074 (SiO$_2$, hexane : dichloromethane : ether = 3.5 : 0.8 : 0.2), calcd for C$_{18}$H$_{15}$O$_2$N: C, 77.98; H, 5.42; N, 5.05;   found: C, 78.01; H, 5.53; N, 5.17.

Similar photolysis of a 25 mL *p*-dioxane solution of DBMBF$_2$ (340 mg, 1.25 mmol) and **36** (839 mg, 12.5 mmol) for 26 hrs yielded no polymer. The DBMBF$_2$ was recovered as yellow powder 0.16 g (47% conversion). Chromatography (hexane : ethyl acetate = 8 : 1) produced 100 mg of **37** (41% yield, based on consumed DBMBF$_2$). mp 98 - 99°C, R$_f$ 0.21 (SiO$_2$, hexane : dichloromethane : ether = 5 : 0.8 : 0.2), calcd for C$_{19}$H$_{17}$O$_2$N: C, 78.35; H, 5.84; N, 4.81; found: C, 78.30; H, 5.89; N, 4.69.

Photoaddition to 2-cyclooctenone (44)

2-Cyclooctenone was prepared from cyclooctanone according to a literature procedure.[121] DBMBF$_2$ (408 mg, 1.5 mmol) and **44** (285 mg, 2.3 mmol) were dissolved in 30 mL acetonitrile. After 22 hour irradiation, the DBMBF$_2$ had almost disappeared, and one major product was found at R$_f$ 0.25 and also a faint spot at R$_f$ 0.31 (SiO$_2$, hexane : ethyl acetate = 5 : 1). The photolysate was mixed with 20 mL ether, washed with saturated aqueous solution of sodium bicarbonate and dried over magnesium sulfate. The crude product was chromatographed using hexane : ethyl acetate (9 : 1) to

give 0.24 g of **45**, as pale yellow oil (46% yield). This was found as a mixture of two components with R$_f$ 0.31 and 0.25.

Further purification was performed by preparative TLC (hexane : ethyl acetate = 13 : 1), to give two mixtures: one contained the products R$_f$ 0.31 and 0.25 in the ratio of 89 : 11 and the other contained the products in ratio 25 : 75 based on ^{1}H NMR analysis. In CDCl$_3$ solution, the ratio changed towards the formation of *trans*-**45** product, R$_f$ 0.31, on standing in CDCl$_3$ solution.

In another experiment, DBMBF$_2$ (24.5 mg, 0.09 mmol) and **44** (372 mg, 3 mmol) were dissolved in 3 mL of acetonitrile. The solution was irradiated for 3 hours by which time DBMBF$_2$ conversion reached > 90% by GC analysis. TLC showed two adduct spots at R$_f$ 0.17 and 0.13 (SiO$_2$, hexane : dichloromethane : ether = 3 : 0.8 : 0.2), and also a spot at R$_f$ 0.09 which could be visualized only by spraying with Ce(SO$_4$)$_2$ (1%) and molybdic acid (1.5%), and heating. The reaction product was chromatographed on a 8 x 3 cm silica gel column with hexane : dichloromethane : ether (6 ~ 3 : 0.8 : 0.2), to yield 24 mg of pale yellow solid (77% yield) as a nearly 1 : 1 mixture of *trans*-**45** (R$_f$ 0.17) and *cis*-**45** (R$_f$ 0.13). The following fractions gave 17.5 mg of **53** (R$_f$ 0.09), a colorless oil containing two components in the ratio 81 : 19 on GC.

The structural data of compounds **53**, *cis*-**45** and *trans*-**45** are listed in Table 5.8.

Photoaddition to 2-cyclohexenone (42)

DBMBF$_2$ (340 mg, 1.25 mmol) and **42** (240 mg, 2.5 mmol) were dissolved in 25 mL of acetonitrile. After 84 hour irradiation, the DBMBF$_2$ conversion reached 95% (GC). TLC showed a major product at R$_f$ 0.17 and a minor product at 0.13 (SiO$_2$, hexane :

dichloromethane : ether = 3 : 0.9 : 0.4). Column chromatography (hexane :

dichloromethane : ether = 3 : 0.8 : 0.2) gave 0.19 g of an oil (47 %), consisting of 90%

trans-43 (R_f 0.13) and only 10% *cis-43* (R_f 0.17). Elemental analysis for $C_{21}H_{20}O_3$: calcd

C, 78.75; H, 6.25; found C, 78.08; H, 6.17.

Photoaddition to 2-cyclopentenone (40)

DBMBF$_2$ (408 mg, 1.5 mmol) and **40** (1.23 g, 15 mmol) were dissolved in 30 mL

of acetonitrile. After 25 hour irradiation, GC analysis showed the conversion of DBMBF$_2$

to be 95%. Column chromatography with hexane : dichloromethane : ether (2 : 2 : 0.3)

gave 0.28 g of a sticky oil (61%) which contained 91% *trans-41* and 9% *cis-41* based on

^{1}H NMR spectrum. Elemental analysis for $C_{20}H_{18}O_3$: calcd C, 78.43; H, 5.88; found C,

78.30; H, 6.02.

Photoaddition to isophorone (46)

DBMBF$_2$ (204 mg, 0.75 mmol) and **46** (1.04 g, 7.5 mmol) were dissolved in 15

mL of acetonitrile. After 37 hours of irradiation, GC analysis showed that DBMBF$_2$ had

almost disappeared. One product spot was observed by TLC at R_f 0.18 (SiO$_2$, hexane :

ethyl acetate = 6 : 1). The photolysate was mixed with 50 mL ether and washed twice

with saturated sodium bicarbonate solution. The resulting solution was adsorbed onto 4

g of silica gel and chromatographed on a 27 x 3 cm silica gel column with hexane : ethyl

acetate (9 : 1) to yield 0.12 g (44%) of a pale yellow powder **47**. mp 37 - 40 °C, calcd

for $C_{24}H_{26}O_3$: C, 79.56; H, 7.18; found: C, 79.19; H, 7.50.

Photoaddition to 5,6-dihydro-2H-pyran-2-one (48)

5,6-Dihydro-2H-pyran-2-one was prepared[122] by refluxing of vinylacetic acid
(31.6 g, 1 mol) with paraformaldehyde (43 g, 0.5 mol) in 125 mL of acetic acid containing
3 mL concentrated sulfuric acid. Distilled at ~115 °C /18 mmHg gave 5.6 g of **48** (11%).
The GC purity was 98% with RT 3.32 min at 80 °C (on a 15 m OV−1 capillary column).
$C_5H_6O_2$ calcd: C, 61.16; H, 6.12; found: C, 60.03; H, 6.26. ^{1}H NMR (100 MHz, CDCl$_3$) δ
2.33 - 2.54 (2H, m), 4.40 (2H, t), 5.98 (H, dt), 6.93 (H, m) ppm. MS (EI) m/z: 98 (M$^+$,
23), 68 (M-18, 100).

DBMBF$_2$ (272 mg, 1 mmol) and **48** (981 mg, 10 mmol) were dissolved in 20 mL
of acetonitrile. After a 9 day irradiation, GC analysis showed that DBMBF$_2$ conversion
had reached 70 %, and on TLC one product spot was found at R$_f$ 0.11 (SiO$_2$, hexane :
ethyl acetate = 4 : 1). The clear brown photolysate was mixed with 60 mL ether and
washed with saturated aqueous sodium bicarbonate. The solution was then adsorbed
onto 3 g of silica gel and chromatographed on a 20 x 3 cm column with hexane : ethyl
acetate (6 ~ 4 : 1) to give 0.11 g of a yellow oil. Further purification was performed by
preparative TLC with hexane : dichloromethane : acetone (2 : 0.9 : 0.1) to yield 84 mg of
a oil (37%) identified as the *trans*-**49** (R$_f$ 0.09). *Cis*-**49** was also observed in the ^{1}H NMR
spectrum as ~5% impurity in the isolated product.

Photoaddition to E-2-cyclododecenone (50)

(a) Preparation of E-2-cyclododecenone[123]

2-Phenylthiocyclododecanone: To a 38 mL THF solution of diisopropylamine
(8.7 g, 86 mmol) at −78 °C under N$_2$, was added 35 mL of 2.5 M hexane solution of butyl
lithium (86 mmol). After stirring for 15 minutes, a solution of cyclododecanone (7.3 g, 40

mmol) in 9 mL THF was added and the clear enolate was continued stirring at –78 °C for one hour. The cooling bath was then removed and the solution was warmed to room temperature, at which point diphenyl disulfide (10.4 g, 48 mmol) was added. After 1.5 hours, the clear solution was poured into a mixture of 30 mL of 10% aqueous hydrochloric acid and 160 mL of ether. The top ether layer was washed successively with the 10% acid and then saturated aqueous sodium bicarbonate, dried and evaporated. TLC showed the presence of diphenyl disulfide at R_f 0.71 and the sulfide product at 0.42 (SiO_2, hexane : dichloromethane : ether = 5 : 0.8 : 0.2). Chromatography on a 32 x 3 cm silica gel column with hexane : dichloromethane : ether (6 : 0.8 : 0.2) yielded a 11 g mixture of 2-phenylthiocyclododecanone and the unreacted diphenyl disulfide in the ratio 1 : 2 (GC).

A portion of the crude product was purified on a 20 x 20 cm TLC plate eluted with hexane : dichloromethane : ether (5 : 0.8 : 0.2) to give an analytical sample of 2-phenylthiocyclododecanone. ^{1}H NMR (400 MHz, CDCl$_3$) δ 1.16 - 1.52 (15H, m), 1.69 - 2.06 (3H, m), 2.50 (1H, m), 2.76 (1H, m), 3.87 (1H, dd, J = 12.4, 3.6 Hz), 7.20 - 7.36 (5H, m, phenyl).

2-(Phenylsulfinyl)cyclododecanone. To a solution of the crude sulfide (~11 g) in methanol (200 mL) was added dropwise at 0 °C a solution of sodium periodate (2.9 g, 13.6 mmol) in 20 mL water. The unreacted diphenyl disulfide precipitated from the solution. After 24 hour of stirring at room temperature, TLC analysis showed nearly complete conversion of 2-phenylthiocyclododecanone at R_f 0.42 to its sulfoxide at R_f < 0.01 (hexane : dichloromethane : ether = 5 : 0.8 : 0.2).

The mixture was filtered and the precipitate was washed with 50 mL methanol. The combined methanolic solution was evaporated, and the residue was dissolved in 150 mL ether, dried over magnesium sulfate and adsorbed onto 4 g silica gel and

chromatographed on a 6 x 5.5 cm silica gel column. Elution with hexane : ether (19-10 : 1), then with ether and then with dichloromethane gave 2.82 g of a pale yellow powder as a 1 : 1 mixture of two diastereomers of 2-(phenylsulfinyl)- cyclododecanone. ^{1}H NMR (400 MHz, CDCl$_3$) δ 1.12 - 1.42 (12H, m), 1.53 - 1.94 (4H, m), 2.00 - 2.18 (2H, m), 2.40 - 2.63 (2H, m), 3.98 and 3.81 (1H, dd, J = 10.9, 3.2 Hz and 11.8, 3.3 Hz), 7.40 - 7.60 (5H, m).

E-2-Cyclododecenone (**50**): 2-Phenylsulfinylcyclododecanone (2.8 g, 9.1 mmol) was dissolved in 50 mL tetrachloromethane. The solution was stirred and heated in an oil bath at 58 °C under N$_2$. After 39 hour, TLC showed a complete conversion of the sulfoxide R$_f$ 0.05 into 2-cyclododecenone R$_f$ 0.34 (hexane : acetone = 15 : 1). The solution was evaporated and chromatographed on a 27 x 3 cm silica gel column with hexane : acetone (50 : 1), to yield 2.03 g of crude 2-cyclododecenone in 85% purity. Distillation *in vacuo* afforded 1.2 g of **50** with a GC purity of 96%: C$_{12}$H$_{20}$O calcd: C, 80.00; H, 11.11; found: C, 79.81; H, 10.99. ^{1}H NMR[127] (400 MHz, CDCl$_3$): 1.18 - 1.23 (10H, m), 1.57 - 1.66 (4H, m), 2.20 - 2.28 (2H, m), 2.44 - 2.53 (2H, m), 6.25 (1H, d, J = 16.0 Hz), 6.78 (1H, dt, J = 16.0, 7.0 Hz).

(b) Photocycloaddition of DBMBF$_2$ to 2-cyclododecenone (**50**)

DBMBF$_2$ (204 mg, 0.75 mmol) and **50** (540 mg, 3 mmol) were dissolved in 15 mL of acetonitrile. After a 16 hour irradiation, GC analysis showed nearly complete disappearance of DBMBF$_2$. TLC showed products at R$_f$ 0.18 and at 0.13 (hexane : acetone = 15 : 1).

The dark red solution was mixed with ether, and washed with saturated aqueous sodium bicarbonate, adsorbed onto silica gel and chromatographed on a 30 x 3 cm silica gel column. Elution with hexanes gave 0.1 g of an oil containing more than 10

components. Most of these showed similar dimer fragmentation on GC-MS (EI): m/z 360 (M⁺, 18), 342 (4), 275 (3), 233 (5), 222 (8), 207 (10), 193 (9), 181 (23), 180 (14), 162 (29), 152 (10), 135 (15), 121 (24), 109 (29), 95 (47), 81 (80), 79 (46), 69 (50), 67 (81), 55 (100).

Further elution with hexane : acetone (20 : 1) produced 0.17 g of a yellow solid (56%), as two components at R_f 0.18 and 0.13 in the ratio ~74 : 26. Recrystallization from hexanes yielded 109 mg of the major adduct **51** (R_f 0.18), mp: 155 - 157 °C, $C_{27}H_{32}O_3$ calcd: C, 80.20; H, 7.92; found: C, 79.94; H, 8.01. The mother liquor was chromatographed on a 20 x 20 cm TLC plate with hexanes : acetone (15 : 1) to yield 14 mg of the minor adduct **52** (R_f 0.13).

The structures of all the products were identified, on the basis of the spectroscopic data summarized in Table 5.8.

Table 5.8 Spectroscopic data of the addition products of DBMBF₂ photoreactions with α,β-unsaturated carbonyl compounds.

30
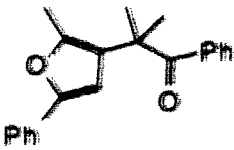
¹H NMR (C_6D_6) δ 1.60 (2CH₃, s), 1.98 (CH₃, s), 6.66 (1H, s), 7.0 - 8.1 (10H, m, phenyl).

¹³C NMR (CDCl₃) δ 12.70, 27.32, 45.21, 104.48, 123.28, 125.6, 127.02, 128.04, 128.65, 129.41, 131.93, 130.70, 136.0, 147.10, 151.40, 203.10 ppm.

MS (EI) m/z 304 (M⁺, 6), 199 (100), 105 (20), 77 (25).
   (CI) m/z 306 (M+2,), 305 (M+1, 100).

IR (NaCl plate) ν: 3076, 2977, 2932, 1673, 1595, 1576, 1550, 1480, 1460, 1440, 1382, 1359, 1252, 1220, 1178, 1155, 1090, 974, 934, 804, 766, 727, 700, 670 cm⁻¹.

Table 5.8 (continued)

29

^{1}H NMR (C$_6$D$_6$) δ 1.30 (CH$_3$, s), 1.32 (CH$_3$, s), 2.30 (CH$_3$, s), 2.98 (H$_b$ dd, J = 17.7, 10.0 Hz), 3.61(H$_{b'}$, dd, J = 17.7, 2.86 Hz), 4.25 (H$_a$, dd, J = 10.0, 2.86 Hz), 7.0 - 8.0 (10H, m, phenyl).

^{13}C NMR (C$_6$D$_6$) δ 22.85, 24.40, 32.48, 38.40, 48.95, 52.23, 127.73, 127.98, 128.11, 128.40, 130.60, 132.75, 136.62, 138.51, 197.71, 206.80, 209.01 ppm.

MS (EI) m/z 322 (M$^+$, 2), 304 (M-18, 2), 217 (8), 175 (11), 105 (100), 77 (40). (CI) m/z 323 (M+1, 10), 305 (95), 177 (63), 175 (55), 149 (100), 147 (40).

IR (NaCl plate) v: 3058, 2972, 2932, 1704, 1677, 1594, 1577, 1540, 1463, 1443, 1355, 1245, 1220, 1168, 971, 753, 700 cm^{-1}.

28

^{1}H NMR (C$_6$D$_6$) δ 1.25 (CH$_3$, s), 1.49 (CH$_3$, s), 1.84 (CH , s), 2.96 (Hb, d, J = 17.8 Hz), 3.63 (Hb', d, J = 17.8 Hz), 5.74 (Ha, s), 7.0 - 8.3 (10H, m, phenyl).

^{13}C NMR (C$_6$D$_6$) δ 26.46, 27.45, 30.86, 37.19, 47.59, 64.82, 128.58, 128.82, 128.97 (2C), 132.75, 133.24, 138.52, 139.05, 198.08, 199.90, 202.65 ppm.

MS (EI) m/z 304 (M-18, 4), 203 (22), 161 (25), 105 (100), 77 (62). (CI) m/z 323 (M+1, 20), 161 (100).

IR (NaCl plate) v: 3074, 2980, 2946, 1715, 1700, 1674, 1602, 1574, 1454, 1360, 1270, 1208, 1188, 1009, 950, 768, 717, 703, 672 cm^{-1}.

Table 5.8 (continued)
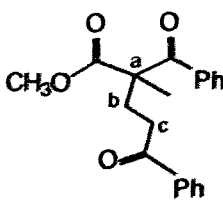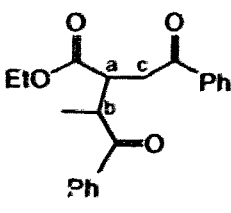
Structure	Data
CH₃O—C(=O)—C(a)(CH₃)(b)—...(c)—C(=O)Ph **32**	^{1}H NMR (100 MHz, CDCl₃) δ 1.60 (CH₃, s), 2.47 (H$_b$ and H$_{b'}$, m), 2.98 (H$_c$ and H$_{c'}$, m), 3.63 (CH₃, s), 7.3 - 8.0 (10H, m). ^{13}C NMR (CDCl₃) δ 21.57, 30.82, 33.57, 52.49, 56.24, 128.02, 128.48, 128.55, 128.60, 132.84, 133.04, 135.31, 136.68, 174.46, 197.08, 198.95 ppm. MS (EI) *m/z*: 324 (M⁺, 1), 293 (1), 264 (45), 224 (51), 219 (24), 160 (10), 105 (100), 77 (35). (CI) *m/z*: 326 (M+2, 20), 325 (M+1, 100), 193 (70), 133 (57), 105 (53). IR (NaCl plate) v: 2990, 2940, 1730, 1683, 1596, 1579, 1450, 1369, 1296, 1269, 1240, 1267, 1198, 1175, 1102, 1005, 970, 753, 715, 700 cm⁻¹.
EtO—C(=O)—C(a)(c)...(b)—C(=O)Ph **35**	^{1}H NMR (C₆D₆) δ 1.00 (CH₃, t), 1.20 (CH₃, d, J = 6.8 Hz), 3.13 (H$_c$, dd, J = 17.5, 4.2 Hz), 3.56 (H$_{c'}$, dd, J = 17.5, 8.5 Hz), 3.82 (H$_b$, m), 3.87 (H$_a$, m), 4.0 (OCH₂, m), 7.0 - 8.0 (10H, m, phenyl). ^{13}C NMR (C₆D₆) δ 13.77, 15.04, 38.56, 42.00, 43.47, 60.35, 128.04, 128.29, 128.40, 128.54, 132.51, 132.65, 136.68, 136.90, 173.42, 197.28, 201.11 ppm. MS (CI) *m/z*: 339 (M+1, 15), 321 (M-18, 25), 293 (100), 161 (14), 159 (15), 135 (54), 121 (25), 107 (25), 105 (63). IR (NaCl plate) v: 3060, 2980, 2940, 1722, 1682, 1597, 1580, 1451, 1365, 1305, 1268, 1265, 1185, 1035, 1004, 974, 764, 699 cm⁻¹.

Table 5.8 (continued)

erythro-**34**

^{1}H NMR (CDCl$_3$) δ 1.12 (CH$_3$, d, J = 7.0 Hz), 1.15 (CH$_3$, t), 2.85 (H$_c$, dd, J = 16.6, 7.7 Hz), 3.13 (H$_b$, m), 3.35 (H$_{c'}$, dd, J = 16.6, 5.5 Hz), 4.13 (OCH$_2$, m), 4.56 (H$_a$, d, J = 7.2 Hz), 7.3 - 8.1 (10H, m, phenyl).

^{13}C NMR (CDCl$_3$) δ 13.84, 17.30, 30.04, 43.26, 58.27, 60.95, 128.40, 128.62, 128.84, 128.96, 132.81, 133.29, 137.17, 137.53, 169.10, 194.82, 198.61 ppm.
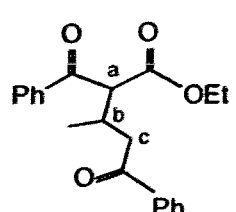
34

a mixture of two diastereomer: *erythro-* / *threo-* = 3 / 1

threo-**34**

^{1}H NMR (CDCl$_3$) δ 1.07 (CH$_3$, d, J = 6.8 Hz), 1.17 (CH$_3$, t), 2.96 (H$_c$, dd, J = 16.3, 9.0 Hz), 3.13 (H$_b$, m), 3.31 (H$_{c'}$, dd, J = 16.3, 3.9 Hz), 4.13 (OCH$_2$, m), 4.52, (H$_a$, d, J = 7.6 Hz), 7.3 - 8.1 (10H, m, phenyl).

^{13}C NMR (CDCl$_3$) δ 13.84, 18.39, 30.48, 42.70, 58.42, 61.07, 128.40, 128.62, 128.77, 128.84, 132.73, 133.20, 137.25, 137.63, 169.28, 194.82, 198.34 ppm.

erythro- and *threo*-diastereomer mixture

MS (EI) m/z: 338 (M$^+$, 2), 320 (5), 305 (3), 293 (55), 277 (14), 264 (31), 247 (26), 233 (59), 219 (67), 192 (21), 173 (10), 147 (6), 105 (100), 77 (33).

IR (NaCl plate) v: 3060, 2980, 2940, 1725, 1682, 1597, 1582, 1466, 1450, 1363, 1320, 1220, 1186, 1103, 1036, 1006, 976, 760, 698 cm^{-1}.

Table 5.8 (continued)
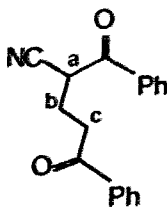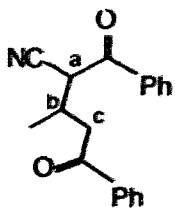
 O NC ⟍ a ⟍ Ph b ⟍ c O Ph **39**	¹H NMR (CDCl₃) δ 2.28 (H_b, dddd, J = 14.1, 9.7, 5.4, 5.4 Hz), 2.58 (H_b', dddd, J = 14.1, 9.0, 5.3, 5.3 Hz), 3.29 (H_c, ddd, J = 18.4, 5.4, 5.3 Hz), 3.42 (H_c', ddd, J = 18.4, 9.0, 5.4 Hz), 4.81 (H_a, dd, J = 9.7, 5.3 Hz), 7.45 - 8.30 (10H, m, phenyl). ¹³C NMR (CDCl₃) δ 24.44, 34.91, 39.31, 117.21, 128.14, 128.89, 129.10, 129.26, 133.76, 134.68, 134.02, 136.43, 190.90, 198.52 ppm. MS (EI) m/z 277 (M⁺, 7), 171 (2), 161 (3), 149 (7), 105 (100), 77 (45). IR (NaCl plate) ν: 3064, 2935, 2251, 1693, 1682, 1597, 1581, 1449, 1412, 1368, 1283, 1261, 1219, 1182, 1160, 1002, 973, 912, 690 cm⁻¹.
O NC ⟍ a Ph b ⟍ c O Ph *erythro-37*	¹H NMR (CDCl₃) δ 1.13 (CH₃, d, J = 6.9 Hz), 3.02 (H_b, m), 3.15 (H_c, dd, J = 18.6, 3.4 Hz), 3.44 (H_c', dd, J = 18.6, 10.2 Hz), 5.12 (H_a, d, J = 3.6 Hz), 7.40 - 8.25 (10H, m, phenyl). Note: containing 9.6% of *threo*-37 showed at 4.64 ppm (H_a, d, J = 4.8 Hz). ¹³C NMR (CDCl₃) δ 16.32, 30.29, 43.46, 46.43, 115.93, 128.17, 128.94, 129.24 (2C), 133.90, 134.48, 134.06, 136.52, 191.42, 198.77 ppm. MS (EI) m/z 291 (M⁺, 6), 223 (2), 184 (2), 175 (1), 149 (4), 147 (5), 120 (10), 105 (100), 77 (51). IR (NaCl plate) ν: 3064, 2970, 2935, 2248, 1688, 1682, 1597, 1581, 1448, 1409, 1367, 1312, 1274, 1220, 1183, 1001, 956, 912, 766, 692 cm⁻¹.

Table 5.8 (continued)
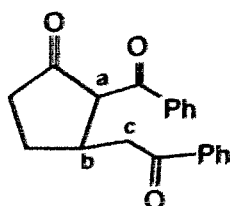
trans-40
with ~9% *cis*-40.

¹H NMR (CDCl₃) δ 2.36 - 2.69 (2CH₂, m), 3.07 (H_c, dd, J = 16.3, 7.9 Hz), 3.24 (H_{c'}, dd, J = 16.3, 5.7 Hz), 3.48 (H_b, m), 4.21 (H_a, d, J = 10.0 Hz), 7.30 - 8.00 (10H, m, phenyl).

¹³C NMR (CDCl₃) δ 26.94, 36.48, 38.90, 42.61, 63.26, 128.08, 128.54, 128.66, 129.44, 133.28, 133.42, 136.66, 136.95, 195.04, 198.44, 211.72 ppm.

MS (EI) *m/z* 306 (M⁺, 20), 288 (23), 260 (10), 201 (16), 186 (31), 185 (15), 105 (100), 77 (52).

IR (NaCl plate) ν: 3061, 2961, 2905, 1742, 1680, 1596, 1580, 1448, 1405, 1374, 1340, 1273, 1228, 1206, 1182, 1135, 1074, 1001, 915, 883, 843, 782, 754, 690 cm⁻¹.
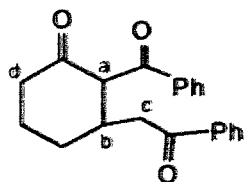
trans-43
with ~10% *cis*-43.

¹H NMR (CDCl₃) δ 1.60 - 2.20 (2CH₂, m), 2.50 (H_d, m), 2.60 (H_{d'}, m), 2.80 (H_c, dd, J = 17.3, 8.1 Hz), 3.10 (H_b, m), 3.15 (H_{c'}, dd, J = 17.3, 4.5 Hz), 4.51 (H_a, d, J = 9.2 Hz), 7.0 - 8.0 (10H, m, phenyl).

¹³C NMR (CDCl₃) δ 24.48, 28.94, 37.35, 41.75, 42.67, 63.31, 128.17, 128.49, 128.66, 128.68, 133.26, 133.32, 136.81, 137.31, 197.71, 198.60, 207.81 ppm.

MS (EI) *m/z* 320 (M⁺, 4), 302 (50), 215 (32), 201 (35), 105 (100), 77 (40). (CI) *m/z* 321 (M+1, 100), 201 (70).

IR (NaCl plate) ν: 3061, 2941, 2868, 1711, 1681, 1597, 1581, 1507, 1480, 1448, 1408, 1352, 1289, 1241, 1181, 1160, 1110, 1076, 1048, 1001, 753, 690 cm⁻¹.

Table 5.8 (continued)
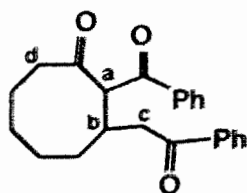
cis-45

^{1}H NMR (CDCl$_3$) δ 1.40 - 2.23 (4CH2, m), 2.40 (Hd, m), 2.90 (Hd', m), 2.95 (Hc, dd, J = 17.8, 6.2 Hz), 3.25 (Hc', dd, J = 17.8, 7.2 Hz), 3.45 (Hb, m), 4.93 (Ha, d, J = 3.6 Hz), 7.0 - 8.0 (10H, m, phenyl).

^{13}C NMR (CDCl$_3$) δ 23.82, 27.23, 27.83, 32.45, 33.62, 41.53, 41.91, 60.30, 127.87, 127.97, 128.53, 128.66, 133.03, 135.15, 136.91, 138.30, 198.11, 199.54, 212.20 ppm.

MS (EI) m/z 348 (M$^+$.10), 330(48), 320 (23), 302 (17), 243 (54), 229 (46), 201 (90), 120 (30), 105 (100), 77 (50).

45

trans-45

^{1}H NMR (CDCl$_3$) δ 1.30 - 2.00 (4CH$_2$, m), 2.37 (H$_d$, m), 2.75 (H$_c$, dd, J = 15.8, 9.1 Hz), 2.85 (H$_{d'}$, m), 3.06 (H$_{c'}$, dd, J = 15.8, 3.3 Hz), 3.44 (H$_b$, m), 4.88 (H$_a$, d, J = 11.0), 7.0 - 8.0 (10H, m, phenyl).

^{13}C NMR (CDCl$_3$) δ 24.04, 26.48, 26.78, 32.08, 35.38, 40.26, 43.11, 66.87, 128.16, 128.59, 128.80, 128.87, 133.08, 133.69, 136.87, 136.95, 195.51, 199.10, 210.45 ppm.

MS (EI) m/z 348 (M$^+$, 10), 330 (50), 320 (25), 302 (20), 243 (35), 229 (61), 201 (95), 120 (33), 105 (100), 77 (60).

IR (NaCl plate) v: 3062, 2931, 2859, 1704, 1680, 1596, 1580, 1447, 1410, 1322, 1269, 1242, 1209, 1181, 1125, 1078, 1002, 971, 760, 690 cm^{-1}.

Table 5.8 (continued)
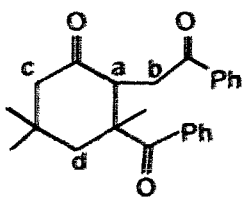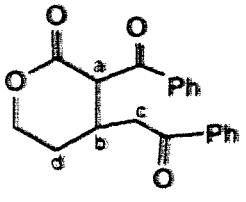
![structure 47] **47**	^{1}H NMR (CDCl$_3$) δ 0.74 (CH$_3$, s), 1.10 (CH$_3$, s), 1.55 (CH$_3$, s), 2.20 (H$_c$, d, J = 14.7 Hz), 2.30 (H$_d$, d, J = 14.8 Hz), 2.38 (H$_{d'}$, d, J = 14.8 Hz), 2.65 (H$_b$, dd, J = 18.4, 2.7 Hz), 2.71 (H$_{c'}$, d, J = 14.7 Hz), 3.20 (H$_a$, dd, J = 7.6, 2.7 Hz), 4.34 (H$_{b'}$, dd, J = 18.4, 7.6 Hz), 7.30 - 8.10 (10H, m, phenyl). ^{13}C NMR (CDCl$_3$) δ 27.19, 27.39, 34.09, 34.16, 34.87, 51.06, 53.40, 54.82, 55.72, 128.27, 128.40, 128.45, 128.83, 132.10, 132.92, 137.12, 137.35, 199.43, 205.45, 206.93 ppm. MS (EI) m/z: 362 (M$^+$. 25), 344 (M-18, 27), 329 (16), 257 (57), 243 (13), 224 (10), 137 (10), 105 (100), 77 (55). IR (NaCl plate) v: 3060, 2958, 2908, 2873, 1714, 1683, 1597, 1579, 1461, 1448, 1392, 1368, 1324, 1286, 1254, 1212, 1178, 1103, 1003, 968, 955, 910, 751, 730, 691 cm^{-1}.
![structure trans-49] *trans*-**49** with ~9% *cis*-**49**.	^{1}H NMR (CDCl$_3$) δ 1.82, 2.27 (H$_d$ and H$_{d'}$, m), 3.00 (H$_c$, dd, J = 17.2, 7.4 Hz), 3.13 (H$_{c'}$, dd, J = 17.2, 5.3 Hz), 3.29 (H$_b$, m), 4.53 (OCH$_2$, m), 4.59 (H$_a$, d, J = 8.2 Hz), 7.25 - 8.00 (10H, m, phenyl). ^{13}C NMR (CDCl$_3$) δ 27.54, 30.85, 42.55, 54.32, 68.19, 127.95, 128.69, 128.71, 129.15, 133.49, 133.73, 136.36, 136.45, 167.79, 195.48, 197.66 ppm. MS (CI) m/z: 323 (M+1, 46), 203 (100), 159 (50). IR (NaCl plate) v: 3062, 2967, 2913, 1731, 1682, 1597, 1581, 1478, 1448, 1407, 1359, 1364, 1201, 1078, 1001, 955, 912, 754, 690, 648 cm^{-1}.

Table 5.8 (continued)
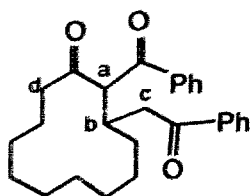
  trans-51 with ~8% *cis*-51.	^{1}H NMR (CDCl$_3$) δ 1.20 - 1.50 (8CH$_2$, m), 1.89 (H$_d$, m), 2.10 (H$_{d'}$, m), 2.86 (H$_c$, dd, J = 16.2, 7.3 Hz), 3.03 (H$_{c'}$, dd, J = 16.2, 3.7 Hz), 3.31 (H$_b$, m), 4.92 (H$_a$, d, J = 11.1 Hz), 7.30 - 8.00 (10H, m, phenyl). ^{13}C NMR (CDCl$_3$) δ 21.48, 22.66, 23.85 (3C), 24.72, 25.88, 28.65, 34.76, 37.60, 40.39, 68.04, 128.09, 128.53, 128.83 (2C), 132.91, 133.72, 136.99, 137.19, 196.13, 199.28, 206.09 ppm. MS (CI) m/z 405 (M+1, 100), 387 (12), 285 (8), 225 (12), 181 (10). IR (NaCl plate) v: 3064, 2994, 2862, 1711, 1682, 1670, 1596, 1579, 1467, 1448, 1413, 1359, 1271, 1200, 1181, 1120, 981, 960 cm^{-1}.
  52	^{1}H NMR (CDCl$_3$) δ 1.20 - 1.80 (8CH$_2$, m), 2.21 (H$_d$, ddd, J = 13.9, 9.1, 3.7 Hz), 2.48 (H$_c$, dd, J = 17.3, 6.0 Hz), 2.58 (H$_{d'}$, ddd, J = 13.9, 8.9, 3.5 Hz), 2.90 (H$_{c'}$, dd, J = 17.3, 4.0 Hz), 3.09 (H$_b$, m), 6.14 (H$_a$, d, J = 9.1 Hz), 7.30 - 8.10 (10H, m, phenyl). ^{13}C NMR (CDCl$_3$) δ 22.76, 22.82, 23.44, 24.19, 24.38, 25.71, 26.07, 28.38, 36.05, 41.40, 42.71, 59.78, 128.50, 128.65, 128.77, 128.86, 133.39, 133.45, 137.16(2C), 195.80, 195.99, 212.58 ppm. MS (CI) m/z 405 (M+1, 24), 387 (5), 299 (5), 225 (100), 197 (20), 181 (10). IR (NaCl plate) v: 3604, 2933, 2864, 1698, 1667, 1596, 1580, 1469, 1448, 1352, 1321, 1279, 1266, 1207, 1180 cm^{-1}.
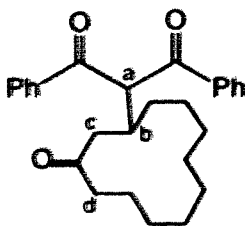
Table 5.8 (continued)
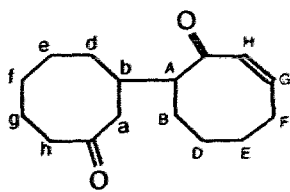
53

^{1}H NMR (600 MHz, C$_6$D$_6$) δ 1.03 (H$_d$, m), 1.19 (H$_E$, m), 1.21 - 1.42 (CH$_2$, m), 1.43 - 1.50 (H$_{d'}$, H$_g$, m), 1.60 (H$_{g'}$, m), 1.71 (H$_F$, dddd, J = 16.6, 7.5, 5.0, 5.0 Hz), 2.03 (H$_h$, ddd, J = 13.7, 6.8, 3.4 Hz), 2.15 (H$_a$, dd, J = 13.2, 11.1 Hz), 2.24 (H$_{a'}$, dd, J = 13.2, 3.4 Hz), 2.26 (H$_{h'}$, ddd, J = 13.7, 9.9, 3.5 Hz), 2.30 (H$_{F'}$, m), 2.45 (H$_b$, ddddd, J = 11.1, 10.9, 7.3, 3.4, 3.4 Hz), 2.56 (H$_A$, ddd, J = 10.9, 7.2, 5.7 Hz), 5.76 (H$_G$, ddd, J = 12.5, 7.5, 6.6 Hz), 5.95 (H$_H$, dd, J = 12.5, 2.0). Note: 2D-COSY experiment was performed.

^{13}C NMR (CDCl$_3$) δ 23.43, 23.93, 25.09, 25.35, 27.23, 27.94 and 28.61 (CH$_2$), 31.96 (CH$_2$C=C), 40.01 (CH), 42.54 (CH$_2$C=O), 44.81 (CH$_2$C=O), 56.12 (CHC=O), 132.82 and 140.15 (C=C), 208.71 and 216.68 (C=O) ppm. Note: The assignment was also based on DEPT spectrum.

MS (EI) m/z: 248 (M$^+$, 7), 230 (3), 205 (2), 191 (3), 187 (6), 177 (6), 163 (5), 151 (8), 149 (16), 135 (14), 125 (26), 124 (100), 109 (21), 95 (83), 81 (74), 79 (46), 67 (52), 55 (81).

Table 5.9 Elemental analyses of the addition products

Compound	mp (°C)	Molecular formulae	%	C	H
cis-12 [a]	--	$C_{23}H_{24}O_2$	Calcd	83.13	7.23
			Found	82.91	7.37
16 [a]	101 - 102	$C_{23}H_{20}O_3$	Calcd	80.21	5.85
			Found	80.11	5.94
23 [a]	128 - 129	$C_{17}H_{14}O_2$	Calcd	81.58	5.64
			Found	81.32	5.70
28 [a]	--	$C_{21}H_{22}O_3$	Calcd	78.26	6.83
			Found	78.58	6.93
29 [a]	--	$C_{21}H_{22}O_3$	Calcd	78.26	6.83
			Found	77.99	6.86
30 [a]	--	$C_{21}H_{20}O_2$	Calcd	82.89	6.58
			Found	82.74	6.46
32 [a]	113.5 - 114	$C_{20}H_{20}O_4$	Calcd	74.07	6.17
			Found	74.07	6.18
34	--	$C_{21}H_{22}O_4$	Calcd	74.56	6.51
			Found	74.42	6.57
37	98 - 99	$C_{19}H_{17}O_2N$ [b]	Calcd	78.35	5.84
			Found	78.30	5.89
39 [a]	--	$C_{18}H_{15}O_2N$ [c]	Calcd	77.98	5.42
			Found	78.01	5.53
trans-41	--	$C_{20}H_{18}O_3$	Calcd	78.43	5.88
			Found	78.30	6.02
trans-43	--	$C_{21}H_{20}O_3$	Calcd	78.75	6.25
			Found	78.08	6.17
47 [a]	37 - 40	$C_{24}H_{26}O_3$	Calcd	79.56	7.18
			Found	79.19	7.50
51	155 - 157	$C_{27}H_{32}O_3$	Calcd	80.20	7.92
			Found	79.94	8.01

Notes: [a] These compounds were obtained as pure samples, and others were mixtures of stereomers indicated in Tables 5.6 and 5.8;

[b] Calcd for N, 4.81 and found for N, 4.69;

[c] Calcd for N, 5.05 and found for N, 5.17.

216

5.6 Quantum yield determination

5.6.1 General procedure

The quantum yields for the photocycloaddition of DBMBF$_2$ to olefins (Φ_A) and those for the sensitized dimerization of olefins (Φ_D) were determined with the air-cooled Rayonet photoreactor equipped with RPR $^-$ 30 nm lamps. A group of Pyrex test tubes (100 x 13 mm) were loaded with 3 mL solution, purged with dry N$_2$, evenly spaced on the "r. erry-go-round" and irradiated together with the actinometry solution.

The actinometer was a deaerated 3 mL benzene solution of benzophenone (0.05 M) and benzhydrol (0.1 M), which has a quantum yield of 0.74 for benzpinacol formation.[80] Benzophenone consumption was determined by UV absorption at λ_{max} 340 nm using a UV cuvette of 0.1 cm optical path length. Formation of DBMBF$_2$ adducts was analyzed by GC. The conversion of DBMBF$_2$ was controlled to be less than 20%, which could be monitored by GC or based on the recovery of unreacted DBMBF$_2$.

The quantum yields were examined in different solvents and at the different concentrations of DBMBF$_2$ or olefins. They are generalized as four types of measurements in the following sections.

5.6.2 Quantum yields determined in different solvents

A group of four or six Pyrex text tubes, each loaded with 3 mL of a solution of DBMBF$_2$ (0.03 M) and 1,3-cyclohexadiene (0.3 M) in different solvents, was purged with N$_2$ and irradiated for 1 – 2 hours for the samples in acetonitrile, acetone, dichloro-methane, THF, dioxane, THP and ether solvents, and 0.5 hour for those samples in ether, benzene, toluene and p-xylene solvents. After photolysis, a dichloromethane solution of eicosane and dodecane was added as the internal standard in GC analysis

for the addition and the dimerization products. Dimer formation was analyzed at 110 °C on a 15 m OV-1 capillary column. Then the sample solution was concentrated by rotary evaporation and mixed with hexanes : ether (2 : 1) to precipitate DBMBF$_2$. Without the filtration, the supernatant containing the addition products was analyzed by GC at a column temperature of 245 °C. The products formed were calculated on equation 5.3:

$$[P] = f_r \times \frac{A_p}{A_{IS}} \times [IS] \qquad \text{Eq. 5.3}$$

where [P] and [IS] are respectively the molar concentration of the product and the internal standard; A_p is the GC peak area of the product and A_{IS} the area of the internal standard compound; f_r is the response factor of the product relative to the internal standard. The results of [P] were then introduced into equation 5.4 to calculate the quantum yields of DBMBF$_2$ photoreactions:

$$\Phi = \frac{[P] \times V}{I_a \times t} \qquad \text{Eq. 5.4}$$

In Eq. 5.4, V is 0.003 liter for the volume of the sample solution, I_a is the light intensity absorbed by DBMBF$_2$ (Einstein / minute mL) and measured from the actinometer, and t is the irradiation time in minutes. The results of the quantum yield measurements were listed in Chapter two (Table 2.3).

5.6.3 Measurements of adduct quantum yield (Φ_A) as a function of DBMBF$_2$ concentration

The quantum yields of DBMBF$_2$ photocycloaddition with olefins were determined as a function of DBMBF$_2$ concentration (0.01 – 0.2 M) in dioxane, dichloromethane, THF and acetonitrile. A typical run in dioxane is shown below.

Four Pyrex test tubes loaded with 3 mL dioxane solutions of 1,3-cyclohexadiene (0.3 M) and DBMBF$_2$ (0.01 – 0.07 M) were deaerated and then placed in the "merry-go-

round" mounted in a Rayonet photoreactor. Irradiation with a 350 nm light source was conducted for 2 hours. After photolysis, the solutions were treated and analyzed as described in Section 5.6.2. The results are summarized in Table 2.4.

5.6.4 Measurements of adduct quantum yield (Φ_A) as a function of the olefin concentration

The quantum yields of photocycloaddition of $DBMBF_2$ to 1,3-cyclooctadiene were examined as a function of the diene concentration in dioxane, benzene and THF. A typical run in benzene is described below.

Several 2 or 3 mL benzene solutions of $DBMBF_2$ and 1,3-COD were made in Pyrex test tubes. The concentration of $DBMBF_2$ was kept constant at 0.03 M and that of the diene was varied from 0.063 – 1.5 M. Each solution was purged with N_2 for 5 minutes and then irradiated in a Rayonet photoreactor for 40 minutes. After photolysis, the sample was concentrated, mixed with hexanes : ether (2 : 1) to precipitate the unreacted $DBMBF_2$, and GC analysis was carried out for the supernatant. The adduct quantum yields were calculated according to equation 5.4 (Table 2.6).

In another experiment, a 2 mL THF solution of $DBMBF_2$ (0.2 M) and 1,3-COD of different concentrations (0.063 M to 1.50 M) was irradiated for 1 hour. The adduct quantum yields (Φ_A) are listed in Table 5.10.

The quantum yields for the photoreaction of $DBMBF_2$ with PVE were examined as follows: a 3 mL THF solution of $DBMBF_2$ (0.2 M) and PVE (0.054 – 0.57 M) was purged with N_2 for 3 min and then irradiated at 350 nm for 30 min. After photolysis, the solvent was concentrated by rotary evaporation and mixed with ether / hexanes (2 / 1), then the resulting solution was analysed by GC. The quantum yields of adduct formation (Φ_A) were calculated according to Eq. 5.4 and are listed in Table 5.11.

Table 5.10 Quantum yields for photoaddition of DBMBF$_2$
to 1,3-COD in THF

[1,3-COD] M	$10^3 \Phi_A$ of 12	1/[1,3-COD] M^{-1}	$(10\Phi_A)^{-1}$
0.063	1.38	15.9	72.5
0.077	1.54	13.0	64.9
0.10	2.19	10.0	45.7
0.14	2.52	7.14	39.7
0.30	3.08	3.33	32.5
1.5	5.30	0.67	18.9
K_{SV}^{y}		4.2 $\pm$ 0.4 M^{-1}	

Table 5.11 Quantum yields (Φ_A) for photoaddition of DBMBF$_2$
to PVE in THF

[PVE] M	$10^2 \Phi_A$ of 16	1 / [PVE] M^{-1}	1 / Φ_A
0.054	1.25	18.5	80.0
0.10	1.49	10.0	67.1
0.20	1.89	5.0	52.9
0.39	2.61	2.56	38.3
0.57	2.49	1.75	40.2
K_{SV}^{y}		14.6 $\pm$ 2.6 M^{-1}	

5.6.5 Measurements of photoreaction quantum yields in binary solvent mixtures

The quantum yields in binary solvent mixtures were determined as described for the pure solvents (section 5.6.2). Sample preparation is described below:

A solvent mixture containing a known mole fraction of benzene ($x_{BZ} = 0 \sim 1$) was prepared in a 5 mL volumetric flask. A 3 mL aliquot of the solvent was pipetted into a Pyrex test tube, in which $DBMBF_2$ (24.5 mg, 0.09 mmol) and an olefin (0.9 mmol) were added.

The following tables summarize the quantum yields of the $DBMBF_2$ photoreaction with 1,3-cyclohexadiene (CHD) in various benzene solvent mixtures.

Table 5.12   Quantum yields of the $DBMBF_2$ photoreaction with CHD in benzene-ether solvent mixtures (irradiation for 50 min.)

Benzene mole % in ether	$E_T(30)$ (kcal/mole)	$10^3\Phi_A$ of 6	$10^3\Phi_D$	CHD dimer ratio (2 + 3) : (4 + 5)	2 : 3
0	34.50	14.5	5.4	41.1 / 58.9	0.79
33.4	34.43	14.0	3.7	53.4 / 46.6	1.50
54.0	34.39	14.6	4.5	58.4 / 41.6	1.71
73.0	34.35	14.0	4.4	62.5 / 37.5	1.88
91.3	34.32	15.1	4.9	64.3 / 35.7	2.0
100	34.30	15.0	9.5	80.1 / 19.9	2.75

Table 5.13 Quantum yields of the DBMBF$_2$ photoreaction with CHD in benzene-THP solvent mixtures (irradiation for 40 min.)

Benzene mole % in THP	E$_T$(30) (kcal/mole)	10^{3}Φ$_A$ of 6	10^{3}Φ$_D$	CHD dimer ratio (2 + 3) : (4 + 5)	2 : 3
0	36.60	4.52	2.6	33.5 / 66.5	0.42
4.7	36.49	6.10	2.4	34.3 / 65.7	0.47
14.4	36.27	6.54	2.7	35.2 / 64.8	0.52
37.8	35.73	6.37	2.6	39.5 / 60.5	0.73
62.1	35.17	9.11	2.4	46.5 / 53.5	1.12
81.7	34.72	10.3	2.6	52.5 / 47.5	1.38
100	34.30	15.0	9.1	85.6 / 14.4	2.72

Table 5.14 Quantum yields of the DBMBF$_2$ photoreaction with CHD in benzene-dioxane solvent mixtures (irradiation for 45 min.)

Benzene mole % in dioxane	E$_T$(30) (kcal/mole)	10^{3}Φ$_A$ of 6	10^{3}Φ$_D$	CHD dimer ratio (2 + 3) : (4 + 5)	2 : 3
0	36.0	3.11	4.1	33.4 / 66.6	0.53
4.1	35.93	3.38	4.4	32.3 / 67.7	0.52
12.8	35.78	4.24	4.2	35.6 / 64.4	0.65
34.6	35.41	4.72	4.3	39.5 / 60.5	0.81
58.9	35.0	7.47	3.6	46.0 / 54.0	1.13
74.1	34.74	8.93	4.1	50.4 / 49.6	1.34
90.6	34.46	13.8	4.3	59.7 / 40.3	1.75
100	34.30	15.0	12.0	86.0 / 14.0	2.71

Table 5.15 Quantum yields of the $DBMBF_2$ photoreaction with CHD
in benzene-THF solvent mixtures (irradiation for 60 min.)

Benzene mole % in THF	$E_T(30)$ (kcal/mole)	$10^3\Phi_A$ of 6	$10^3\Phi_D$	CHD dimer ratio	
				(2 + 3) : (4 + 5)	2 : 3
0	37.4	1.8	7.3	31.5 / 68.5	0.42
28.0	36.53	2.4	6.2	35.5 / 64.5	0.57
48.0	35.91	3.7	6.6	40.9 / 59.1	0.84
68.0	35.29	5.2	7.2	45.8 / 54.2	1.00
78.5	34.97	7.2	9.1	53.8 / 46.2	1.45
89.0	34.64	10.4	9.5	53.7 / 46.3	1.62
100	34.30	15.0	11.8	75.4 / 24.6	2.62

Table 5.16 Quantum yields of $DBMBF_2$ photoreactions with CHD
in acetonitrile-benzene solvent mixtures [a]

Benzene mole % in CH_3CN	[Benzene] M	$E_T(30)$ (kcal/mole)	$10^3\Phi_A$ (of 6)	$10^3\Phi_D$	CHD dimer ratio	
					(2+3) : (4+5)	2 : 3
0	0.0	45.6	--[b]	29.2	97.4 : 2.6	7.5
1.1	0.2	45.5	--[b]	24.4	97.2 : 2.8	7.5
2.6	0.5	45.3	--[b]	30.4	97.5 : 2.5	7.4
5.5	1.0	45.0	--[b]	35.8	97.6 : 2.4	7.5
8.4	1.5	44.7	--[b]	41.9	97.8 : 2.2	7.5
11.4	2.0	44.3	--[b]	47.4	97.9 : 2.1	7.7
24.3	4.0	42.9	--[b]	36.8	97.2 : 2.8	7.0
40.2	6.0	41.1	--[b]	26.2	93.7 : 6.3	6.4
70.7	9.0	37.6	1.0	5.4	65.6 : 34.4	2.4
100	11.2	34.3	15.8	9.8	74.5 : 25.5	2.5

Notes: [a] Samples of $[DBMBF_2]$ = 0.03 M and [CHD] = 0.3 M were irradiated at 350 nm for 30 minutes; [b] No adduct detected.

REFERENCES

1, Fox, M.A.; Chanon, M., Eds. *Photoinduced Electron Transfer* Elsevier: New York, **1988**, Part A - D.

2, Kavarnos, G.J.; Turro, N. J. *Chem. Rev.* **1986**, *86*, 401 - 449.

3, Turro, N.J. *Modern Molecular Photochemistry*, The Benjamin / Cummings: Menlo Park, California, **1978**.

4, Weller, A. *Z. Phys. Chem. Neue Folge* **1982**, *133*, 93 - 98.

5, Rehm, D.; Weller, A. *Isr. J. Chem.* **1970**, *8*, 259 - 271.

6, Mattay, J.; Gersdorf, J.; Buchkremer, K. *Chem. Ber.* **1987**, *120*, 307 - 318.

7, Taniguchi, Y.; Nishina, Y.; Mataga, N. *Bull. Chem. Soc. Jpn.* **1972**, *45*, 764 - 769.

8, Leonhardt, H.; Weller, A. *Ber. Bunsenges. Phys. Chem.* **1963**, *67*, 791 - 795.

9, (a) Mattes, S.L.; Farid, S. *Acc. Chem. Res.* **1982**, *15*, 80 - 86;
(b) Mattes, S.L.; Farid, S. *Sciences* **1984**, *226*, 917 - 921;
(c) Green, B.S.; Rejtö, M.; Johnson, D.E.; Hyle, C.E.; Simpson, J.T.; Correa, P.E.; Ho, T.I.; Lewis, F.D. *J. Amer. Chem. Soc.* **1979**, *101*, 3325 - 3331;
(d) Lewis, F.D. *Acc. Chem. Res.* **1979**, *12*, 152 - 158;
(e) Kuzmin, M.G.; Soboleva, I.V. *Prog. Reaction Kinetics* **1986**, *14*, 157 - 218;
(f) Davidson, R.S. in *Adv. Phys. Org. Chem.* Vol. *19*, Gold, V.; Bethell, D., ed., Academic Press: New York, **1983**, pp. 1 - 130;
(g) Bhattacharyya, K.; Chowdhury, M. *Chem. Rev.* **1993**, *93*, 507 - 535;

10, Gould, I.R.; Young, R.H.; Mueller, L.J.; Farid, S. *J. Amer. Chem. Soc.* **1994**, *116*, 8176 - 8187.

11 Förster, Th. in *The Exciplex* Gordon, M.; Ware, W.R., Ed.; Academic Press: New York, **1975**, pp. 1 - 21.

12, Lewis, F.D. in *Photoinduced Electron Transfer*, Fox, M.A.; Chanon, M., Eds.; Elsevier: New York, **1988**, Part C, 1 - 69.

13, (a) Mataga, N.; Okada, T.; Yamamoto, N. *Chem. Phys. Lett.* **1967**, *1*, 119 - 121;
(b) Knibbe, H.; Rölling, K.; Schäfer, F.P.; Weller, A. *J. Chem. Phys.*, **1967**, *47*, 1184 - 1185.

14, Chang, S.L.P.; Schuster, D.I. *J. Phys. Chem.* **1987**, *91*, 3644 - 3649.

15, Beens, H.; Knibbe, H.; Weller, A. *J. Chem. Phys.* **1967**, *47*, 1183 - 1184.

16,   (a) Caldwell, R.A. *J. Amer. Chem. Soc.* **1974**, *96*, 2994 - 2996;
        (b) Caldwell, R.A.; Creed, D. *Acc. Chem. Res.* **1980**, *13*, 45 - 50.

17,   (a) Lewis, F.D.; DeVoe, R.J. *Tetrahedron* **1982**, *38*, 1069 - 1077;
        (b) Mizuno, K.; Pac, C.; Sakurai, H. *J. Amer. Chem. Soc.* **1974**, *96*, 2993 - 2994;
        (c) Mattay, J. *Tetrahedron* **1985**, *41*, 2405 - 2417;
        (d) Mazzocchi, P.H.; Minamikawa, S.; Bowen, M.J. *J. Org. Chem.* **1978**, *43*, 3079 - 3080.

18,   (a) McCullough, J.J.; Miller, R.C.; Wu, W.S. *Can. J. Chem.* **1977**, *55*, 2909 - 2915;
        (b) Pac, C.; Yashuda, M.; Shima, K.; Sakurai, H. *Bull. Chem. Soc. Jpn.* **1982**, *55*, 1605 - 1616.

19,   (a) Gould, I.R.; Mueller, L.J.; Farid, S. *Z. Phys. Chem. (Munich)* **1991**, *170*, 143 - 157;
        (b) Gould, I.R.; Farid, S. *J. Phys. Chem.* **1992**, *96*, 7635 - 7640;
        (c) Gould, I.R.; Young, R.H.; Moody, R.E.; Farid, S. *J. Phys. Chem.* **1991**, *95*, 2068 - 2080.

20,   Mattay, J. *Angew. Chem. Int. Ed. Engl.* **1987**, *26*, 825 - 845.

21,   (a) Becker, D.; Haddad, N. in *Organic Photochemistry, Vol 10*, Padwa, A., Ed.; Marcel Dekker, New York, **1989**, pp. 1 - 162;
        (b) Mattay, J. in *CRC Handbook of Organic Photochemistry and Photobiology*, Horspool, W.M.; Song, P.-S., Eds.; CRC Press: New York, **1995**, 618 - 632;
        (c) Weedon, A.C. in *CRC Handbook of Organic Photochemistry and Photobiology*, Horspool, W.M.; Song, P.-S., Eds.; CRC Press: New York, **1995**, 634 - 651 and 670 - 684;
        (d) Schuster, D.I. in *CRC Handbook of Organic Photochemistry and Photobiology*, Horspool, W.M.; Song, P.-S., Eds.; CRC Press: New York, **1995**, 652 - 669.

22,   Schuster, D.I. *Chem. Rev.* **1993**, *93*, 3 - 22.

23,   (a) Gordon, M.; Ware, W.R., eds., *The Exciplex*, Academic Press: New York, **1975**
        (b) Förster, Th.; Kasper, K; *Z. Phys. Chem., N.F.* **1954**, *1*, 275 - 277.

24,   (a) Lewis, F.D. in *Advances in Photochemistry, Vol. 13*, Volman, D.H.; Hammond, G.S.; Gollnick, K. John Wiley & Sons: New York, **1986**, 165 - 235;
        (b) Mattes, S.L.; Farid, S. in *Organic Photochemistry*, Padwa, A.; Ed., Marcel Dekker: New York, **1983**, Vol. 6, pp. 233 - 326;
        (c) Mattay, J.; Müller, F. *Chem. Rev.* **1993**, *93*, 99 - 117.

25,   (a) Klett, M.; Johnson, R.P. *J. Amer. Chem. Soc.*, **1985**, *107*, 6615 - 6620;
        (b) Albini, A.; Arnold, D.R. *Can. J. Chem.* **1978**, *56*, 2985 - 2993;

(c) Maruyama, K.; Kubo, Y. in *CRC Handbook of Organic Photochemistry and Photobiology*, Horspool, W.M.; Song, P.-S., Eds.; CRC Press: New York, 1995, 222 - 228.

26,   (a) Mattay, J.; Vondenhof, M.; Denig, R. *Chem. Ber.* **1989**, *122*, 951 - 958;
        (b) Evans, T.R.; in *The Exciplex* Gordon, M.; Ware, W.R., Ed.; Academic Press: New York, **1975**, pp. 345 -358;
        (c) Farid, S.; Hartman, S.E.; Evans, T.R. *ibid* **1975**, pp. 327 - 343.

27,   (a) Jones, C.; Allman, B.J.; Mooring, A.; Spahic, B. *J. Amer. Chem. Soc.* **1983**, *105*, 653 - 654;
        (b) Gassman, P.G.; Singleton, D.A. *J. Amer. Chem. Soc.* **1984**, *106*, 7993 - 7994;
        (c) Libman, J. *J. Chem. Soc., Chem. Commun.* **1976**, 361 - 362.

28,   (a) Ledwith, A. *Acc. Chem. Res.* **1972**, *5*, 133 - 139;
        (b) Bauld, N.L. *Tetrahedron* **1989**, *45*, 5307 - 5363.

29,   Asanuma, T.; Yamamoto, M.; Nishijima, Y. *J. Chem. Soc., Chem. Commun.* **1975**, 53 - 54.

30,   Ellinger, L.P. *Polymer* **1964**, *5*, 599.

31,   Ledwith, A. in *The Exciplex* Gordon, M.; Ware, W.R., Ed.; Academic Press: New York, **1975**, pp. 209 -245

32,   Kuwata, S.; Shigemitru, Y.; Odaira, Y. *J. Org. Chem.* **1973**, *38*, 3803 - 3805.

33,   Mattes, S.L.; Luss, H.R.; Farid, S. *J. Phys. Chem.* **1983**, *87*, 4779 - 4881.

34,   Roth, H.D.; Schilling, M.L.M. *J. Amer. Chem. Soc.* **1980**, *102*, 4303 - 4310.

35,   (a) Albini, A.; Spreti, S. *J. Chem. Soc., Chem. Commun.* **1986**, 1426 - 1427;
        (b) Inoue, Y.; Okano, T.; Yamasaki, N.; Tai, A. *J. Photochem. Photobiol. A: Chem.* **1992**, *66*, 61 - 68.

36,   (a) Mattay, J.; Trampe, G.; Runsink, J. *Chem. Ber.* **1988**, *121*, 1991 - 2005;
        (b) Mella, M.; Fasani, E.; Albini, A. *Tetrahedron* **1991**, *47*, 3137 - 3154;
        (c) Turro, N.J.; Chung, W.S. *J. Org. Chem.* **1989**, *54*, 4881 - 4887.

37,   (a) Valentine, D.; Turro, N.J.; Hammond, G.S. *J. Amer. Chem. Soc.* **1964**, *86*, 5202 - 5208;
        (b) Bellikle, D.J.; Wirth, D.D.; Bauld, N.L. *J. Amer. Chem. Soc.* **1981**, *103*, 718 - 720;
        (c) Vondenhof, M.; Mattay, J. *Chem. Ber.* **1990**, *123*, 2457 - 2459;
        (d) Schuster, G.B. *J. Amer. Chem. Soc.* **1984**, *106*, 6870 -6871;
        (e) Schenck, G.O.; Mannsfeld, S.-P.; Schomburg, G.; Krauch, C.H. *Z. Naturforsch., B* **1964**, *19*, 18.

38,   (a) Bauld, N.L.; Bellville, D.J.; Harirchian, B.; Lorenz, K.T.; Pabon, R.A.; Jr., Reynolds, W.; Wirth, D.D.; Chiou, H.S.; Marsh, B.K. *Acc. Chem. Res.* **1987**, *20*, 371 - 378;
       (b) Reynolds, D.W.; Lorenz, K.T.; Chiou, H.-S.; Bellville, D.J.; Pabon, R.A.; Bauld, N.L. *J. Amer. Chem. Soc.* **1987**, *109*, 4960 - 4968.

39,   Schutte, R.; Freeman, G.R. *J. Amer. Chem. Soc.* **1969**, *91*, 3715 - 3720.

40,   (a) Mlcoch, J.; Steckhan, E. *Angew. Chem. Int. Ed. Engl.* **1985**, *24*, 412 - 414;
       (b) Martiny, M.; Steckhan, E.; Esch, T. *Chem. Ber.* **1993**, *126*, 1671 - 1682.

41,   Eberson, L.; Olofsson, B. *Acta Chem. Scand.* **1991**, *45*, 316 - 326.

42,   Calhoun, G.C.; Schuster, G.B. *J. Amer. Chem. Soc.* **1986**, *108*, 8021 - 8027.

43,   (a) Yang, N.C.; Srinivasachar, K.; Kim, B.; Libman, J. *J. Amer. Chem. Soc.* **1975**, *97*, 5006 - 5008;
       (b) Yang, N.C.; Gan, H.; Kim, S.S.; Masnovi, J.M. *Tetrahedron Lett.* **1990**, *31*, 3825 - 3828;
       (c) Yang, N.C.; Shold, D.M.; MeVey, J.K. *J. Amer. Chem. Soc.* **1975**, *97*, 5004 - 5005.

44,   (a) Albini, A.; Fasani, E. *Pure Appl. Chem.* **1988**, *60*, 1009 - 1012;
       (b) Albini, A.; Fasani, E.; Giavanni, F. *J. Org. Chem.*; **1988**, *53*, 5601 - 5607.

45,   (a) Mizuno, K.; Pac, C.; Sakurai, H. *J. Org. Chem.* **1977**, *42*, 3313 - 3315;
       (b) Pac, C.; Yasuda, M.; Shima, K.; Sakurai, H. *Bull. Chem. Soc. Jpn.* **1982**, *55*, 1605 - 1616 and references therein.

46,   (a) Mizuno, K.; Hashizume, T.; Otsuji, Y. *J. Chem. Soc., Chem. Commun.* **1983**, 772 - 773;
       (b) Mizuno, K.; Ueda, H.; Otsuji, Y. *Chem. Lett.* **1981**, 1237 - 1240.

47,   Chanon, M.; Eberson, L. in *Photoinduced Electron Transfer*; Fox, M.A.; Chanon, M., Eds.; Elsevier: New York, **1988**, Part A, pp 409 - 597.

48,   (a) Karasev, V.E.; Korotkikh, O.A. *Russ. J. Inorg. Chem. (Engl. Transl.)* **1986**, *31* (4), 493 - 496;
       (b) Ilge, H.-D; Faßler, D.; Hartmann, H. *Z. Chem.* **1984**, *24*, 218 - 219;
       (c) de Mayo, P.; Takeshita, H. *Can. J. Chem.* **1963**, *41*, 440 - 449;
       (d) de Mayo, P. *Acc. Chem. Res.* **1971**, *4*, 41 - 47.

49,   Cheng, X.E. *Ph.D. Dissertation*, Simon Fraser University, **1990**.

50,   (a) Chow, Y.L.; Cheng, X.E. *J. Chem. Soc., Chem. Commun.* **1990**, 1043 - 1045;
       (b) Chow, Y.L.; Cheng, X.E. *Can. J. Chem.* **1991**, *69*, 1331 - 1336;
       (c) Chow, Y.L.; Cheng, X.E. *Can. J. Chem.* **1991**, *69*, 1575 - 1583.

51,   (a) Hawthorne, M.F.; Reintjes, M. *J. Org. Chem.* **1965**, *30*, 3851 - 3853;

(b) Toporcer, L.H.; Dessy, R.E.; Green, S.I.E. *Inorg. Chem.* **1965**, *4*, 1649 - 1655;

(c) Brown, N.M. D.; Bladon, P. *J. Chem. Soc. (A)* **1969**, 526 - 532;

(d) Gerrard, W.; Lappert, M.F.; Shafferman, R. *Chem. & Ind.* **1958**, 722 - 722.

52,   Morgan, G.T.; Tunstall, R.B. *J. Chem. Soc.* **1924**, *125*, 1963 - 1967.

53,   Dilthey, W.; Edwardof, F.; Schumacher, F.J. *Liebigs. Ann. Chem.* **1906**, *344*, 300, 326.

54,   (a) Ilge, H.-D.; Birckner, E.; Fassler, D.; Kozmenko, M.V.; Kuzmin, M.G.; Hartmann, H. *J. Photochem.* **1986**, *32*, 177 - 189;

(b) Schade, W.; Ilge, H.-D.; Hartmann, H. *J. Prakt. Chem.* **1986**, *328*, 941;

(c) Cragg, R.H.; List, H.; Meller, A. *Gmelin Handbuch der Anorganischen Chemie*, New Suppl. Series Vol. *34*, Borverbindungen Teil 9, Niedenzu, K.; Buschbeck, K.-C.; ed.; Springer-Verlag, Berlin, **1976**, p62 and references therein;

(d) Cotton, F.A.; Ilsley, W.H. *Inorg. Chem.* **1982**, *21*, 300 - 302;

(e) Haddon, R.C.; Chichester, S.V.; Marshall, J.H. *Tetrahedron* **1986**, *42*, 6293 - 6300;

(f) Boese, R.; Koester, R.; Yalpani, M. *Chem. Ber.* **1985**, *118*, 670 - 675;

(g) Balaban, A.T.; Bally, I.; Minkin, V.I.; Usachev, A '. *Tetrahedron* **1977**, *33*, 3265 - 3267;

(h) Trestianu, A.; Niculescu-Majewska, H.; Bally, I.; Barabas, A.; Balaban, A.T. *Tetrahedron* **1968**, *24*, 2499 - 2504;

55,   (a) Darst, K.P.; Lukehart, C.M. *J. Organomet. Chem.* **1978**, *161*, 1 - 11.

(b) $DBMBF_2$ ^{13}C NMR (400 MHz, $CDCl_3$): 183.45 (C=O), 135.23, 132.14*, 129.20, 128.94 (phenyl), 93.49 ppm; *Quaternary phenyl carbon.

56,   Hanson, A.W.; Macaulay, E.W. *Acta. Crystallogr. Sect. B* **1972**, *28*, 1961 - 1967.

57,   Buckingham, J.; Donaghy, S.M.; ed., *Dictionary of Organic Compounds*, Chapman & Hall, New York, **1982**, *Vol. 2*, D08067.

58,   (a) Johansson, C.I. *Ph.D. Dissertation*, Simon Fraser University, **1995**;

(b) The experiments were done by C. I. Johansson and the unpublished results can be found in his group reports.

59,   Buchta, R.C.; Evans, D.H. *Anal. Chem.* **1968**, *40*, 2181 - 2186.

60,   (a) ^1H NMR Spectrum #23135M in *The Sadtler Standard NMR Spectra*, Sadtler Research Laboratories, Philadelphia, **1976**;

(b) ^{13}C NMR Spectrum #1721C, *ibid* Sadtler Research Laboratories, Philadelphia, **1976**.

61,   Morantz, D.J.; Wright, A.J.C. *J. Chem. Phys.* **1971**, *54*, 692 - 697.

62, (a) Harju, T.O.; Erostyak, J.; Chow, Y.L.; Korppi-Tommola, J.E.I. *Chem. Phys.* **1994**, *181*, 259 - 270.
(b) The lifetime of DBMBF$_2$ excimer τ_{AA} = 36 ± 2 ns in aerated acetonitrile was determined on Photon Technology International (PTI) LS -1 fluorimeter using a time-correlated single photon counting method, with the assistance of Ms. Li Diao of the University of Victoria.

63, (a) Chow, Y.L.; Wang, S.S.; Liu, Z.L.; Wintgens, V.; Valat, P. Kossanyi, J. *New J. Chem.* **1994**, *18*, 923 - 936.
(b) Chow, Y.L.; Vanossi, M.; Wang, S.S. *J. Photochem. Photobiol. A: Chem.*, **1995**, *88*, 125 - 128.

64, (a) Chow, Y.L.; Cheng, X.E. and Johansson, C.I. *J. Photochem. Photobiol. A: Chem.*, **1991**, *57*, 247 - 255;
(b) Chow, Y.L.; Ouyang, X.X. *Can. J. Chem.* **1991**, *69*, 423 - 431;
(c) Chow, Y.L.; Wu, S.P.; Ouyang, X.X. *J. Org. Chem.* **1994**, *59*, 421 - 428;
(d) Chow, Y.L.; Johansson, C.I. *Chem. Phys. Lett.* **1994**, *231*, 541 - 546.

65, (a) Goliber, T.E.; Perlstein, J.H. *J. Chem. Phys.* **1984**, *80*, 4162 - 4167;
(b) Halm, J.M. *Polym. Mater. Sci. Eng.* **1984**, *51*, 756 - 762, *C.A.* 102: 103409u;
(c) Goliber, T.E.; Perlstein, J.H. *Photogr. Sci. Eng.* **1982**, *26*, 236 - 238, *CA* 97: 172387a;
(d) Halm, J.M. US 4360584, **1982**, *C.A.* 98: p81515v;
(e) Eastman Kodak, Eur. Pat. Appl. EP 76088, **1983**, *C.A.* 99: p113697v.

66, Toullec, J. in *The Chemistry of Enols*, Rappoport, Z.; Ed., Wiley: New York, **1990**, p323.

67, (a) Bassetti, M.; Cerichelli, G.; Floris, B. *Tetrahedron* **1988**, *44*, 2997 - 3004;
(b) Moriyasu, M.; Kato, A.; Hashimoto, Y. *J. Chem. Soc., Perkin Trans. II* **1986**, 515 - 520.

68, Gacoin, P. *J. Chem. Phys.* **1972**, *57*, 1418 - 1425.

69, (a) Yankov, P.; Saltiel, S. *J. Photochem. Photobiol. A: Chem.* **1988**, *41*, 205 - 214;
(b) Yankov, P.; Saltiel, S.; Petkov, I. *Chem. Phys. Lett.* **1986**, *128*, 517 - 520;
(c) Veierov, D.; Bercovici, T.; Fischer, E.; Mazur, Y.; Yogev, A. *J. Amer. Chem. Soc.* **1977**, *99*, 2723 - 2729;
(d) Veierov, D.; Bercovici, T.; Mazur, Y.; Fischer, E. *J. Org. Chem.* **1978**, *43*, 2006 - 2010;
(e) Veierov, D.; Bercovici, T.; Fischer, E.; Mazur, Y.; Yogev, A. *J. Amer. Chem. Soc.* **1973**, *95*, 8173 - 8175;
(f) Markov, P.; Petkov, I. *Tetrahedron* **1977**, *33*, 1013 - 1015.

70, (a) Oreal, S.A. Jpn. Kokai Tokkyo Koho JP 63277615, **1988**, *C.A.* 111: P201386q;
(b) Dai, G.; Liu, L.; Zhang, J.; Wu, S. *Huaxue Xuebao* **1987**, *45*, 564 - 568;
(c) Prando, P. Eur. Pat. Appl. EP 437886, **1991**, *C.A.* 115: P233832f;

(d) Kamitsubara, Y.; Koga, S.; Fukuda, T.; Nagasawa, H. Jpn. Kokai Tokkyo Koho JP 63312329, **1988**, *C.A.* 110: P174833d;
(e) Taimir, L.; Pivcova, H.; Pospisil, J. *J. Polym. Degrad. Stab.* **1986**, *16*, 159 - 162;
(f) Tabayashi, I.; Harada, H.; Inoe, S.; Fukutomi, H. Jpn. Kokai Tokkyo Kogo JP 63193973, **1988**, *C.A.* 110: P9852b;
(g) Takenaka, F.; Ito, M.; Toya, K Jpn Kokai Tokkyo Koho JP 61190330, **1986**, *C.A.* 107: P49574g.

71,   (a) Baldwin, S.W. in *Org. Photochem.* Padwa, A.; ed., Marcel Dekker: New York, **1981**, *Vol. 5*, pp. 123 - 225;
(b) Casals, P.-F.; Ferard, J.; Ropert, R. *Tetrahedron Lett.* **1976**, 3077 - 3080.

72,   (a) Tada, M.; Harada, H.; Miura, K. *Bull. Chem. Soc. Jpn.* **1978**, *51*, 839 - 841;
(b) Nozaki, H.; Kurita, M.; Mori, T.; Noyori, R. *Tetrahedron* **1968**, *24*, 1821 - 1828.

73,   Eberson, L. *Electron Transfer Reactions in Organic Chemistry*, Springer-Verlag: Berlin, **1987**.

74,   (a) Liu, Z.L.; Zhang, M.X.; Yang, L.; Liu, Y.C.; Chow, Y.L.; Johansson, C.I. *J. Chem. Soc. Perkin Trans. 2*, **1994**, 585 - 590;
(b) Yang, L.; Zhang, M.Z.; Liu, Y.C.; Liu, Z.L.; Chow, Y.L. *J. Chem. Soc., Chem. Commun.* **1995**, 1055 - 1056.

75,   (a) Lakowicz, J.R. *Principles of Fluorescence Spectroscopy*, Plenum: New York, **1983**;
(b) Caldwell, R.A.; Creed, D.; Demarco, D.C.; Melton, L.A.; Ohta, H.; Wine, P.H. *J. Amer. Chem. Soc.* **1980**, *102*, 2369 - 2377.

76,   (a) Heineman, W.R.; Kissinger, P.T. in *Laboratory Techniques in Electroanalytical Chemistry*, Kissinger, P.T.; Heineman, W.R.; Eds.; Marcel Dekker: New York, **1984**, pp. 51 - 127;
(b) Mabbott, G.A. *J. Chem. Educ.* **1983**, *60*, 697 - 701;
(c) Kissinger, P.T.; Heineman, W.R. *J. Chem. Educ.* **1983**, *60*, 702 - 706.

77,   (a) Arnold, D.R.; Humphreys, R.W. *J. Amer. Chem. Soc.* **1979**, *101*, 2743 - 2744;
(b) Gersdorf, J.; Mattay, J.; Görner, H. *J. Amer. Chem. Soc.* **1987**, *109*, 1203 - 1209;
(c) Bauld, N.L.; Harirchian, B.; Reynolds, D.W.; White, J.C. *J. Amer. Chem. Soc.* **1988**, *110*, 8111 - 8117;
(d) Kubo, Y.; Suto, M.; Araki, T.; Mazzocchi, P.H.; Klinger, L.; Shook, D.; Somich, C. *J. Org. Chem.* **1986**, *51*, 4404 - 4411.

78,   (a) Silverstein, R.M.; Bassler, G.C.; Morrill, T.C. *Spectrometric Identification of Organic Compounds*, fifth edition, John Wiley & Sons, Inc., New York, **1991**;
(b) Heller, S.R.; Milne, G.W.A. *EPA / NIH Mass Spectral Data Base*, Washington: U.S. Dept. of Commerce, National Bureau of Standards, **1978**

79,   (a) Liu, R.S.H. *J. Amer. Chem. Soc.* **1967**, *89*, 112 - 114;
        (b) Nebe, W.J.; Fonken, G.J. *J. Amer. Chem. Soc.* **1969**, *91*, 1249 - 1251;
        (c) Padwa, A.; Koehn, W.; Masaraechia, J.; Osborn, C.L.; Trecker, D.J. *J. Amer. Chem. Soc.* **1971**, *93*, 3633 - 3638;
        (d) Inoue, Y.; Daino, Y.; Hagiwara, S.; Nakamura, H.; Hakushi, T. *J. Chem. Soc., Chem. Commun.* **1985**, 804 - 805.

80,   Hammond, G.S.; Leermakers, P.A. *J. Phys. Chem.* **1962**, *66*, 1148 - 1150.

81,   (a) Reichardt, C. *Solvents and Solvent Effects in Organic Chemistry*, 2nd ed.; VDH Publishers : Weinheim, **1988**;
        (b) Laurence, C.; Nicolet, P.; Dalati, M.R.; Abboud, J-L. M.; Notario, R. *J. Phys. Chem.* **1994**, *98*, 5807 - 5816;
        (c) Gee, N.; Shinsaka, K.; Dodelet, J.-P.; Freeman, G.R. *J. Chem. Thermodynamics* **1986**, *18*, 221 - 234.

82,   Groizeleau-Miginiac, L. *Ann. Chim* **1961**, *6*, 1071- 1130; C.A. 57: 7290f.

83,   Pretsch, E.; Clerc, T.; Seibl, J.; Simon, W. *Tables of Spectral Data for Structure Determination of Organic Compounds*, Fresenius, W; Huber, J.F.K.; Pungor, E.; Rechnitz, G.A.; Simon, W.; West, Th.S. eds.; Translated by Biemann, K.;   2nd ed., Springer-Verlag, Berlin, **1989**.

84,   Gustav, K.; Storch, M. *Monatshefte für Chemie* **1990**, *121*, 447 - 454.

85,   Breslow, R.; Johnson, R.W *Tetrahedron Lett.* **1975**, *40*, 3443 - 3446.

86,   Reynolds, D.W.; Bauld, N.L. *Tetrahedron Lett.* **1985**, *26*, 2539 - 2542.

87,   Culp, S.J.; Bednar, W.M.; Pienta, N.J. *J. Org. Chem.* **1985**, *50*, 3953 - 3955.

88,   Schomburg, H.; Staerk, H.; Weller, A. *Chem. Phys. Lett.* **1973**, *22*, 1 - 4.

89,   Itoh, K.; Okazaki, K.; Sera, A.; Chow, Y.L. *J. Chem. Soc., Chem. Commun.* **1992**, 1608 - 1609.

90,   Akbulut, N.; Hartsough, D.; Kim, J.I.; Schuster, G.B. *J. Org. Chem.* **1989**, *54*, 2549 - 2556.

91,   (a) Gould, I.R.; Farid, S. *J. Photchem. Photobiol. A: Chem.* **1992**, *65*, 133 - 147;
        (b) Gould, I.R.; Noukakis, D.; Gomez-Jahn, L.; Young, R.H.; Goodman, J.L.; Farid, S. *Chem. Phys.* **1993**, *176*, 439 - 456;
        (c) Gould, I.R.; Farid, S. *J. Amer. Chem. Soc.* **1993**, *115*, 4814 - 4822;
        (d) Gould, I.R.; Young, R.H.; Mueller, L.J.; Albrecht, A.C.; Farid, S. *J. Amer. Chem. Soc.* **1994**, *116*, 8188 - 8199.

92,   (a) Gaweda, E.; Prochorow, J. *Chem. Phys. Lett.* **1975**, *30*, 155 - 159.
        (b) Prochorow, J.; Bernard, E. *J. Luminescence* **1974**, *8*, 471 - 487.

93,   Beens, H.; Weller, A. *Chem. Phys. Lett.* **1968**, *2*, 140 - 142.

94, Saltiel, J.; Townsend, D.E.; Watson, B.D.; Shannon, P. *J. Amer. Chem. Soc.* 1975, *97*, 5688 - 5695.

95, (a) Masaki, Y.; Yanagida, S.; Pac, C. *Chem. Lett.* 1988, 1305 - 1308;
(b) Masaki, Y.; Uehara, Y.; Yanagida, S.; Pac, C. *Chem. Lett.* 1990, 1339 - 1342.

96, Ohta, H.; Creed, D.; Wine, P.H.; Caldwell, R.A.; Melton, L.A. *J. Amer. Chem. Soc.* 1976, *98*, 2002 - 2003.

97, Mataga, N. in *The Exciplex*, Gordon, M.; Ware, W.R., ed., Academic Press: New York, 1975, pp. 113 - 144.

98, (a) Weller, A. *Pure Appl. Chem.* 1982, *54*, 1885 - 1888.
(b) Weller, A. *Z. Phys. Chem. Neue Folge* 1982, *130*, 129 - 138.

99, (a) Masuhara, H.; Mataga, N. *Acc. Chem. Res.* 1981, *14*, 312 - 318.
(b) Masuhara, H.; Hino, T.; Mataga, N. *J. Phys. Chem.* 1975, *79*, 994 - 1000.

100, (a) Reichardt, C. *Chem. Rev.* 1994, *94*, 2319 - 2358.
(b) Dimroth, K.; Reichardt, C.; Siepmann, T.; Bohlmann, F. *Justus Liebigs Ann. Chem.* 1963, *661*, 1 - 37.
(c) Riechardt, C.; Asharin-Fard, S.; Blum, A.; Eschner, M.; Mehranpour, A.; Milart, P.; Niem, T.; Schaefer, G.; Wilk, M. *Pure Appl. Chem.* 1993, *65*, 2593 - 2601.

101, O'Driscoll, E.; Simon, J.D.; Peters, K.S. *J. Amer. Chem. Soc.* 1990, *112*, 7091 - 7098.

102, Michl, J.; Bonacic-Koutecky, V. *Electronic Aspects of Organic Photochemistry*, Wiley, New York, 1990, Chapter 5, pp. 225 - 286.

103, (a) Rao, Y.S.; Filler, R. *J. Org. Chem.* 1971, *36*, 1447 -1448;
(b) Filler, R.; Rao, Y.S.; Biezais, A.; Miller, F.N.; Beaucaire, V.D. *J. Org. Chem.* 1970, *35*, 930 -935;
(c) Sieglitz, A.; Horn, O. *Chem. Ber.* 1951, *84*, 607 - 618.
(d) Erne, D.; Morf, W.E.; Arvanitis, S.; Cimerman, Z.; Ammann, D.; Simon, W. *Helv. Chim. Acta.* 1979, *62*, 994 - 1006;
(e) Anselme, J.P. *J. Org. Chem.* 1967, *32*, 3716 - 3716.

104, Bosch, E.; Roses, M. *J. Chem. Soc., Faraday Trans.* 1992, *88*, 3541 - 3546.

105, Marcus, Y. *J. Chem. Soc. Perkin Trans. 2*, 1994, 1015 - 1021.

106, Rae, I.D.; Woolcock, M.L. *Aust. J. Chem.* 1987, *40*, 1017 - 1021.

107, (a) Cummings, C.A.; Milner, D.J. *J. Chem. Soc., C*, 1971, *9*, 1571 - 1572.
(b) Uemura, S.; Tanaka, S.; Okano, M. *J. Chem. Soc., Perkin I* 1976, 1966 - 1969.

108,   Errede, L.A.; Cassidy, J.P. *J. Amer. Chem. Soc.* **1960**, *82*, 3653 - 3658.

109,   Pasternak, M.; Morduchowitz, A. *Tetrahedron Lett.* **1983**, *24*, 4275 - 4278.

110,   Bobbitt, J.M.; Willis, J.P. *J. Org. Chem.* **1977**, *42*, 2347 - 2348.

111,   Levin, R.D.; Lias, S.G. *Ionization Potential and Appearance Potential Measurements* (1971 - 1981), U.S. Dept. of Commerce, National Bureau of Standards: Washington, D.C., **1982**.

112,   (a) Murov, S.L. *Handbook of Photochemistry*, Marcel Dekker: New York, **1973**;
(b) Murov, S.L.; Carmichael, I.; Hug, G.L. *Handbook of Photochemistry*, 2nd. ed., Marcel Dekker: New York, **1993**.
(c) Rendell, D. *Fluorescence and Phosphorescence Spectroscopy*, Wiley: New York, **1987**.

113,   (a) Chapman, O.L.; Lenz, G. *Organic Photochemistry*, *Vol. 1*, Chapman, O.L.; ed., Marcel Dekker, New York, **1967**, pp. 283 - 322.
(b) Trecker, D.J. *Organic Photochemistry*, *Vol. 2*, Chapman, O.L.; ed., Marcel Dekker, New York, **1969**, pp. 63 - 116.
(c) Chapman, O.L.; Weiss, D.S. *Organic Photochemistry*, *Vol. 3*, Chapman, O.L.; ed.; Marcel Dekker, New York, **1973**, pp. 197 - 288.
(d) Baldwin, S.W. *Organic Photochemistry*, *Vol 5*, Padwa, A.; ed.; Marcel Dekker, New York, **1981**, pp. 123 - 226.

114,   Eaton, P.E. *Acc. Chem. Res.* **1968**, *1*, 50 - 57.

115,   Wagner, P.J.; Bucheck, D.J. *J. Amer. Chem. Soc.* **1969**, *91*, 5090 - 5097.

116,   Lam, E.Y.Y.; Valentine, D.; Hammond, G.S. *J. Amer. Chem. Soc.* **1967**, *89*, 3482 - 3487.

117,   (a) Eaton, P.E. *J. Amer. Chem. Soc.* **1962**, *84*, 2344 - 2348;
(b) Eaton, P.E. *ibid* **1962**, *84*, 2454 - 2455.

118,   Braslavsky, S.E.; Heibel, G.E. *Chem. Rev.* **1992**, *92*, 1381 - 1410.

119,   Schuster, D.I.; Heibel, G.E.; Caldwell, R.A.; Tang, W. *Photochem. Photobiol.* **1990**, *52*, 645 - 648.

120,   (a) Eaton, P.E.; Lin, K. *J. Amer. Chem. Soc.* **1964**, *86*, 2087 - 2088;
(b) Eaton, P.E.; Lin, K. *ibid* **1965**, *87*, 2052 - 2054;
(c) Corey, E.J.; Tada, M.; LaMahieu, R.; Libit, L. *ibid* **1965**, *87*, 2051 - 2052.

121,   (a) House, H.O.; Sieloff, R.F.; Lee, T.V.; DeTar, M.B. *J. Org. Chem.* **1980**, *45*, 1800 - 1806.
(b) Jr. Garbisch, E.W. *J. Org. Chem.* **1965**, *30*, 2109 - 2120.

122. (a) Nakagawa, J.S.; Tonozuka, M.; Obi, M.; Kiuchi, M.; Hino, T.; Ban, Y. *Organic Synthesis* **1977**, *56*, 49 - 52.
(b) Nakagawa, M.; Tonozuka, M.; Obi, M.; Hino, T.; Ban, Y. *Synthesis* **1974**, 510 - 511.

123. (a) Trost, B.M.; Salzmann, T.N.; Hiroi, K. *J. Amer. Chem. Soc.* **1976**, *98*, 4887 - 4902.
(b) Reich, H.J.; Reich, I.L.; Renga, J.M. *J. Amer. Chem. Soc.* **1973**, *95*, 5813 - 5815.
(c) Sharpless, K.B.; Lauer, R.F.; Teranishi, A.Y. *J. Amer. Chem. Soc.* **1973**, *95*, 6137 - 6139.
(d) Fujita, S.; Kawaguti, T.; Nozaki, H. *Bull. Chem. Soc. Jpn.* **1970**, *43*, 2596 - 2598.

124. Fueno, T.; Matsumura, I.; Okuyama, T.; Furukawa, J. *Bull. Chem. Soc. Jpn.* **1968**, *41*, 818 - 823.

125. Ninomiya, I.; Naito, T. *Photochemical Synthesis*, Academic Press: New York, **1989**, Chapter 10, 209 - 223.

126. Bahurel, Y.L.; MacGregor, D.J.; Penner, T.L.; Hammond, G.S. *J. Amer. Chem. Soc.* **1972**, *94*, 637 - 638.

127. Shimitzu, I.; Minami, I.; Tsuji, J. *Tetrahedron Lett.* **1983**, *24*, 1797 - 1800.

The Plots of $ln(1/\Phi_A)$ vs. $1/E_T(30)$ for Photocycloaddition of DBMBF$_2$ to Cyclic Dienes (Table 2.3) and to Vinyl Ethers (Table 2.10)
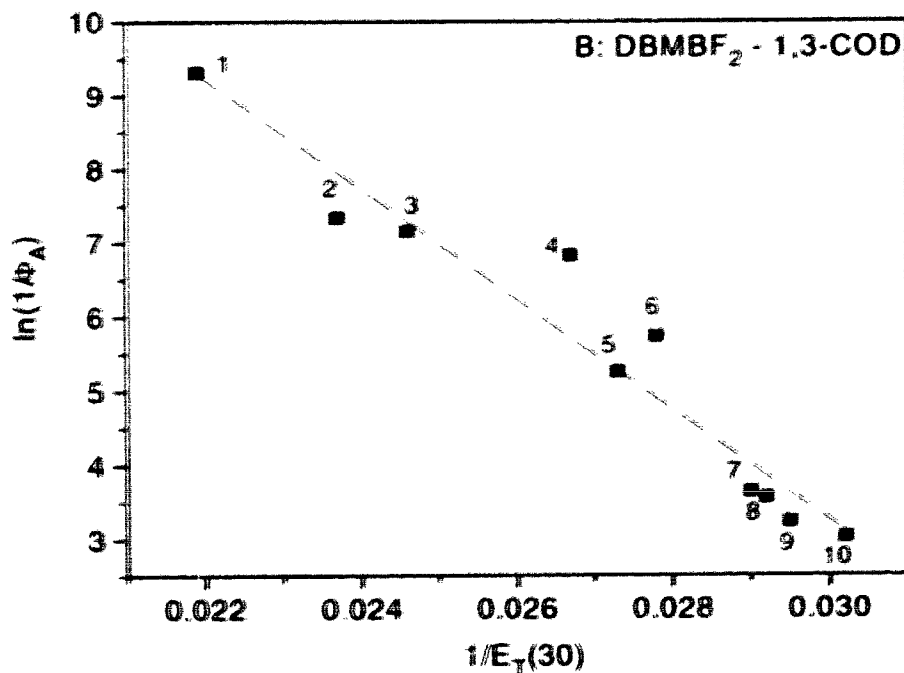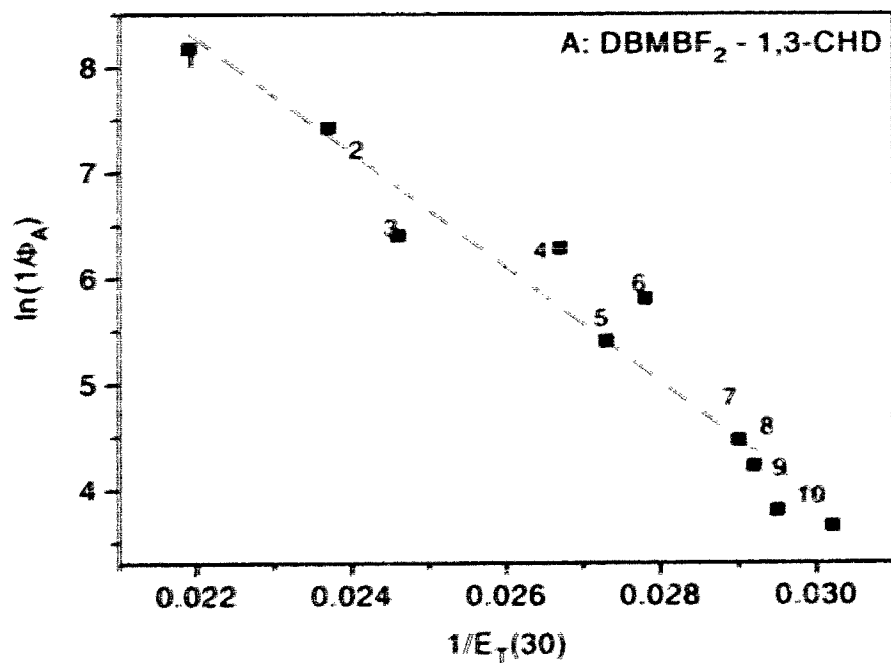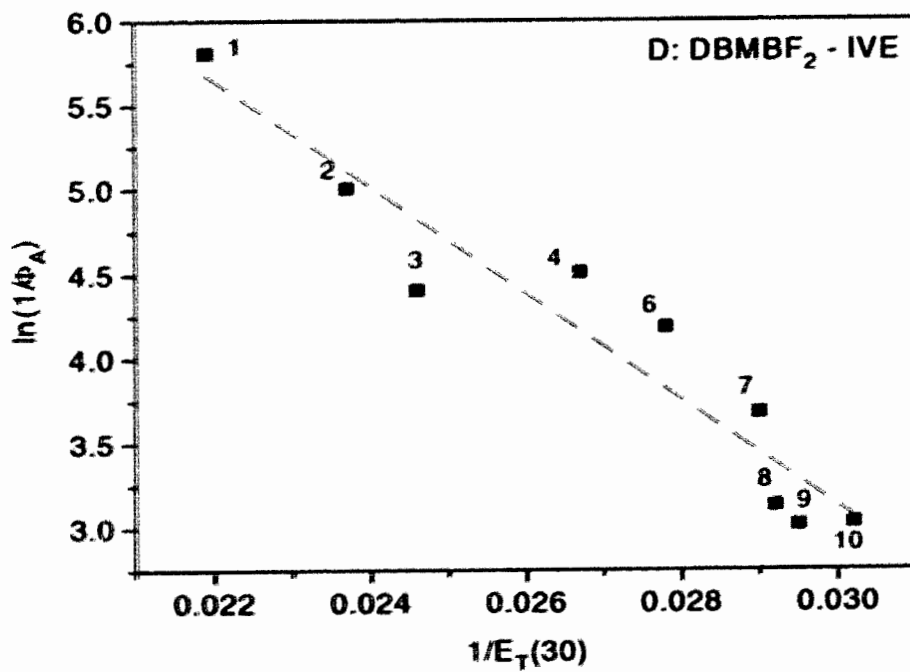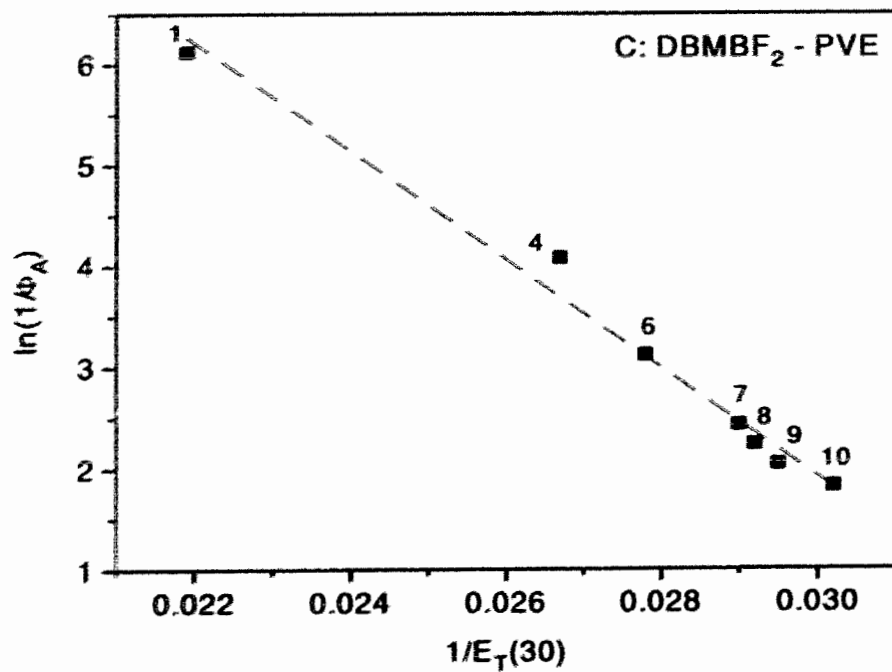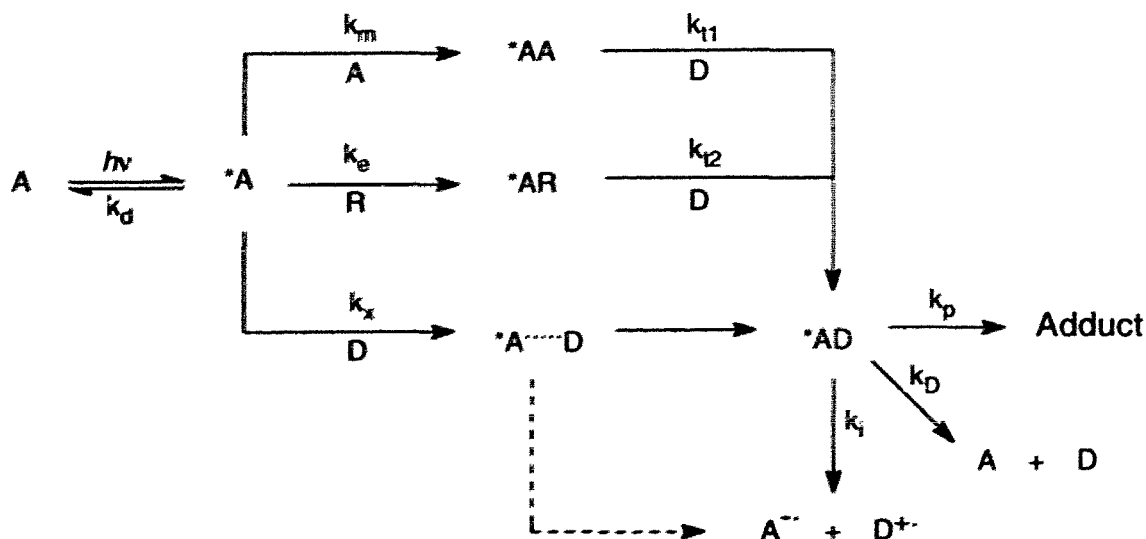
1, acetonitrile; 2, acetone; 3, CH$_2$Cl$_2$; 4, THF; 5, THP; 6, dioxane; 7, ether; 8, benzene; 9, toluene; 10, *p*-xylene.

Derivation of Equation 2.14

Scheme 2.7:

here A = DBMBF$_2$; R = Benzene, Toluene or Xylene; D = Cyclic diene or Vinyl ether.

The rate constants of the above processes are defined as follows:

k_m excimer *AA formation; k_{t1} triplex *AAD formation;

k_e emissive exciplex *AR formation; k_{t2} triplex *ARD formation;

k_x encounter complex *A···D formation; I_a for the absorbed light intensity;

k_p adduct formation from the exciplex *AD;

k_D unimolecular decay of the exciplex *AD;

k_d unimolecular decay of singlet excited DBMBF$_2$ monomer *A;

k_i ionic dissociation of the exciplex *AD.

Under the steady-state assumption, the following relationships can be established based on Scheme 2.7, and note here that the reciprocal of lifetime (τ^{-1}) refers to the rate constant of unimolecular decay of the intermediate proposed:

for the formation and the consumption of *A

$$I_a = (\tau_a^{-1} + k_m[A] + k_e[R] + k_x[D])\,[^*A] \tag{i}$$

for the formation and the consumption of *AA

$$k_m[A][^*A] = (\tau_{AA}^{-1} + k_{t1}[D])\,[^*AA] \tag{ii}$$

for the formation and the consumption of *AR

$$k_e[R][^*A] = (\tau_{AR}^{-1} + k_{t2}[D])\,[^*AR] \tag{iii}$$

for the formation and the consumption of *AD

$$(k_{t1}[^*AA] + k_{t2}[^*AR] + k_x[^*A])\,[D] = (k_i + k_D + k_p)\,[^*AD] \tag{iv}$$

When we introduce Eq. (ii) and (iii) into Eq. (iv) to substitute the terms of [*AA] and [*AR] respectively, Eq. (v) is obtained:

$$(k_{t1}\,\frac{k_m[A]}{\tau_{AA}^{-1}+k_{t1}[D]} + k_{t2}\,\frac{k_e[R]}{\tau_{AR}^{-1}+k_{t2}[D]} + k_x)\,[D]\,[^*A] = (k_i + k_D + k_p)\,[^*AD] \tag{v}$$

then Eq. (i) into Eq. (v) to give Eq. (vi):

$$[^*AD] =$$

$$\frac{I_a}{k_p+k_D+k_i}\,\frac{1}{\tau_a^{-1}+k_m[A]+k_e[R]+k_x[D]}\,(k_{t1}\,\frac{k_m[A]}{\tau_{AA}^{-1}+k_{t1}[D]} + k_{t2}\,\frac{k_e[R]}{\tau_{AR}^{-1}+k_{t2}[D]} + k_x)\,[D] \tag{vi}$$

Since the quantum yield of adduct formation (Φ_A) is defined as:

$$\Phi_A = \frac{k_p[^*AD]}{I_a} \qquad \text{(vii)}$$

if the term of [*AD] is replaced by Eq. (vi), then the adduct quantum yield is expressed as Eq. 2.14:

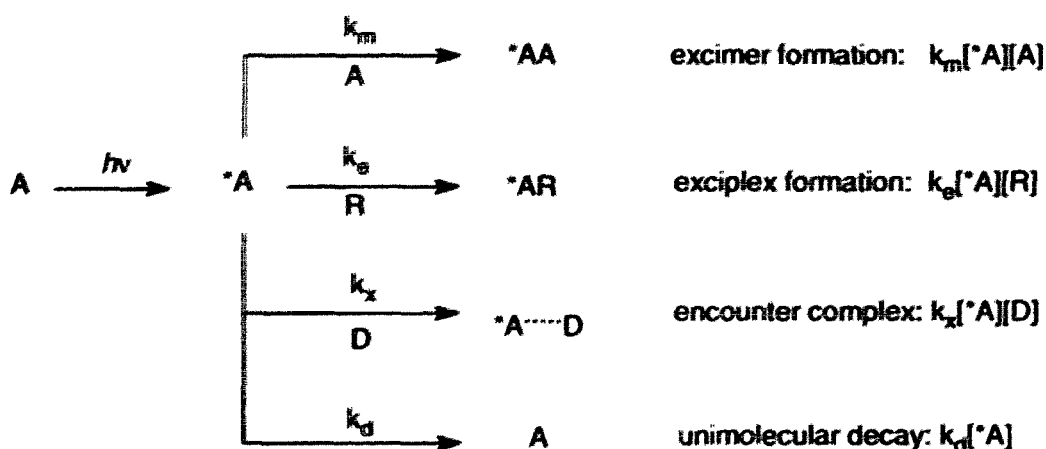$$\Phi_A = \frac{k_p}{k_p+k_D+k_i} \; \frac{1}{\tau_a^{-1}+k_m[A]+k_e[R]+k_x[D]} \left(\frac{k_m[A]\,k_{11}}{\tau_{AA}^{-1}+k_{11}[D]} + \frac{k_e[R]\,k_{12}}{\tau_{AR}^{-1}+k_{12}[D]} + k_x \right)[D]$$

$$\text{(Eq. 2.14)}$$

Calculations of Reaction Probabilities for Singlet Excited DBMBF$_2$ in THF and in Toluene (Table 2.19)

According to Scheme 2.7, singlet excited DBMBF$_2$ (*A) can react with a ground state DBMBF$_2$ molecule (A) to form an excimer (*AA), with an arene (R) to form an emissive exciplex (*AR), or with an electron donor (D) to form an encounter complex (*A --- D), as shown in below:

$\xrightarrow{\underset{A}{k_m}}$ *AA	excimer formation: $k_m[*A][A]$
$\xrightarrow{\underset{R}{k_e}}$ *AR	exciplex formation: $k_e[*A][R]$
$\xrightarrow{\underset{D}{k_x}}$ *A----D	encounter complex: $k_x[*A][D]$
$\xrightarrow{k_d}$ A	unimolecular decay: $k_d[*A]$

The probability of a singlet excited DBMBF$_2$ reaction, among the various pathways, can be calculated as:

the probability of *AA formation (φ_{AA}) =
$$\frac{k_m[A][*A]}{(k_m[A]+k_e[R]+k_x[D]+k_d)[*A]} \qquad (i)$$

the probability of *AR formation (φ_{AR}) =
$$\frac{k_e[R][*A]}{(k_m[A]+k_e[R]+k_x[D]+k_d)[*A]} \qquad (ii)$$

the probability of quenching *A by D (φ_{AD}) =
$$\frac{k_x[D][*A]}{(k_m[A]+k_e[R]+k_x[D]+k_d)[*A]} \qquad (iii)$$

the probability of *A decaying to A (φ_d) =
$$\frac{k_d[*A]}{(k_m[A]+k_e[R]+k_x[D]+k_d)[*A]} \qquad (iv)$$

For the photoreaction of DBMBF$_2$ with 1,3-COD in THF and in toluene, the concentrations of [A], [D] and [R] are given as: [DBMBF$_2$] = 0.03 M, [1,3-COD] = 0.3 M and the neat toluene as [R] = 9.35 M. The four rate constants are chosen below for the probability estimations in both THF and in toluene:

$k_m = 2.7 \times 10^{10}$ M^{-1}s^{-1} is from Fig. 4.9, in acetonitrile;

$k_d = 1/\tau_a = 2.94 \times 10^9$ s^{-1} where $\tau_a = 0.34$ ns is the lifetime of singlet excited DBMBF$_2$ in THF;[62a]

$k_x = 2.5 \times 10^{10}$ M^{-1}s^{-1} is from = 8.1 M^{-1} in Fig. 2.1, in THF;

$k_e = 4 \times 10^9$ M^{-1}s^{-1} from the quenching of DBMBF$_2$ fluorescence by toluene in acetonitrile.[63]

When the above parameters are introduced into equations (i), (ii), (iii) or (iv), the rate of each pathway will be calculated, for example:

$$k_m[A] = 2.7 \times 10^{10} \times 0.03 = 0.81 \times 10^9 \ (Sec^{-1})$$

for the excimer formation, and then this reaction probability (φ_{AA}) is obtained as:

$$\varphi_{AA} = (0.81 \times 10^9) / (11.25 \times 10^9) = 7.2\% \quad \text{as shown in Table A-1.}$$

Table A-1. Calculations of *DBMBF$_2$ reaction probabilities in Table 2.19

	in THF		in Toluene	
	the rate of each reaction	the probability (φ)	the rate of each reaction	the probability (φ)
$k_m[A]$, (Sec^{-1})	0.81×10^9	$\varphi_{AA} = 7.2\%$	0.81×10^9	$\varphi_{AA} = 1.7\%$
$k_e[R]$, (Sec^{-1})	—	—	37.4×10^9	$\varphi_{AR} = 76.9\%$
$k_x[D]$, (Sec^{-1})	7.5×10^9	$\varphi_{AD} = 66.7\%$	7.5×10^9	$\varphi_{AD} = 15.4\%$
k_d, (Sec^{-1})	2.94×10^9	$\varphi_d = 26.1\%$	2.94×10^9	$\varphi_d = 6\%$
total	11.25×10^9	100	48.65×10^9	100